

From the  
Walter-Brendel-Zentrum für Experimentelle Medizin  
At the Biomedical Center of the Ludwig-Maximilians-Universität München  
Interim Director: Prof. Dr. med. Markus Sperandio

---

**Control of Leukocyte Trafficking  
by the Sympathetic Nervous System**

---

Dissertation zum Erwerb des  
**Doctor of Philosophy (PhD) in Medical Research**  
an der Medizinischen Fakultät der Ludwig-Maximilians-Universität München

submitted by

**Jasmin Weber**

from

Hünfeld, Germany

on

06.11.2020



**Supervisor: Prof. Dr. Christoph Scheiermann**

**Second evaluator: Prof. Dr. Martin Kerschensteiner**

**Dean: Prof. Dr. med. dent. Reinhard Hickel**

**Date of oral defense: 22.02.2021**





## Acknowledgements

In the course of the last four years, I have learned a lot about myself. I did not only grow as a scientist, but also as a person. This progress I owe to several people who I would like to say special thanks to.

First of all, I want to thank my supervisor Christoph Scheiermann, who gave me the opportunity to work in this wonderful scientific environment. Although being in another country, he was always there for me with great advice. When he moved to Geneva, he trusted the lab organization in us, which I am really proud of. During my time in his laboratory, I did not only learn about the world of medical research, but also met very special people who I will never forget.

Special thanks go to my colleague Stephan, who started this journey with me. From day one we became good friends that helped each other not only with experiments, but also in our private lives. Although we sometimes failed at a good work-life-balance, we had at least fun in doing so. Without him on my side, the last four years would not have been the same!

I also want to thank Sophia, who was not only my desk neighbor, but also the best travel buddy. I had the best time inside and outside of the lab with her!

It is really hard to describe the gratitude I feel for my lab members. Louise is something between a second supervisor and a good friend. The same music taste brought us together and hopefully will do so in the future! When half of our little family moved to Geneva, Chien-Sin was always there for help, advice and a good laugh. Robert was the one I could bother with technical problems during imaging (which happened basically all the time), while he also performed any seemingly impossible imaging analysis for me.

I also want to thank the Geneva part of the group. Chen did important experiments for me and I really appreciate his effort! It was so much fun to meet Coline, Burak, Stéphane and Chen at our retreat. They are a great team to work with! I also cannot forget to mention my former lab mate Wenyan, who taught me a lot of the techniques that were important for this project. Alba showed me the world of intravital imaging, while listening to the best rock music.

Markus Sperandio made it possible for us to stay and perform our research in Munich, for which I am deeply grateful! As part of his lab I want to mention Sergi in particular, who helped me out so much without any consideration.

Speaking of personal growth, my graduate schools took an essential role in the process. I want to thank the IRTG914 (and especially Verena Kochan) for interesting lectures, seminars and get-togethers as well as the best guidance through the bureaucracy of becoming a PhD. Furthermore, the IMPRS-LS always challenged us to become not only better scientists, but also better people. Thank you Hans-Jörg, Ingrid, Maxi and Marta! I am so proud to be part of this amazing network through which I met special people like Laura, Geri and Drew.

I am also grateful for my TAC members, Julia von Blume and Martin Kerschensteiner, for their great feedback over the years. Whether from Munich or New Haven, they always took the time to give useful input.

Without the support from our excellent core facilities this project would not have been possible. Thus, I want to thank Bastian and Dana from the animal facility, as well as Lisa and Pardis from the flowcytometry core facility.

Importantly, people outside of work were a big part of this journey. I want to thank my best friends (die Allerbesten), who have been on my side for more than twenty years now and had to endure my emotional ups and downs. Without these guys I would have gone insane by now. Kathrin was another very good friend, who went through the same struggle and thus, always had a good advice. I am really glad we found each other again in Munich!

Zum Schluss möchte ich den wichtigsten Menschen danken - meiner Familie. Mama, Papa und Sarah, ihr habt mich auf diesen Weg gebracht und alles Erdenkliche getan, um mir diese Chance zu ermöglichen. Ohne euch wäre ich nicht der Mensch, der ich heute bin. Ich weiß gar nicht, wie ich euch dafür danken soll!

## Abstract

The immune system and nervous system are tightly connected, but this intricate interplay is not yet fully understood. This study aimed to elucidate the influence of the sympathetic nervous system on leukocyte trafficking *in vivo*. Using adoptive transfers combined with flow cytometry as well as intravital imaging, it was demonstrated that adrenergic stimulation – predominantly mediated by  $\beta_2$ -adrenoceptors – affected neutrophils and B cells differently. Neutrophils accumulated in the circulation, due to impaired recruitment. This was accompanied by reduced expression of adhesion molecules on the surface of these cells. Furthermore, it was shown that neutrophil-intrinsic as well as  $\beta_2$ -adrenoceptors of the microenvironment were involved. The  $\beta_3$ -adrenoceptor agonist BRL37344 was found to have rather unspecific effects in blood, whereas in the bone marrow it could be mediating the mobilization of neutrophils. B cell numbers were reduced in blood upon treatment with the  $\beta_2$ -adrenoceptor agonist Clenbuterol, which was ratified as  $\beta_2$ -adrenoceptor specific. It could be shown that B cells were homing slightly better to lymph nodes, where they were retained and thus could not reenter the circulation. This process was likely mediated by integrins, as block of CD62L did not counteract the reduction in blood. Moreover, adrenergic stimulation led to an activated state of B cells, as evidenced by upregulated surface levels of adhesion molecules. For the first time, this study shows an extensive screen of neutrophil and B cell distributions under adrenergic control, perpetuating existing data and confirming that immune cell trafficking is under control of the sympathetic nervous system. This fact will be important for treatment of stress-induced immunological diseases.

# Table of Content

<b>Acknowledgements .....</b>	<b>V</b>
<b>Abstract.....</b>	<b>VII</b>
<b>List of figures.....</b>	<b>XI</b>
<b>List of tables.....</b>	<b>XIII</b>
<b>List of abbreviations.....</b>	<b>XIV</b>
<b>1 Introduction.....</b>	<b>1</b>
<b>1.1 Explanatory statement.....</b>	<b>1</b>
<b>1.2 The immune system requires leukocyte trafficking .....</b>	<b>2</b>
1.2.1 The life cycle of neutrophils .....	3
1.2.2 The life cycle of B cells .....	3
1.2.3 Leukocyte trafficking depends on adhesion molecules.....	4
1.2.4 The conventional leukocyte adhesion cascade .....	8
1.2.5 Organ- and cell type-specific leukocyte trafficking.....	10
<b>1.3 The sympathetic nervous system .....</b>	<b>22</b>
1.3.1 Catecholamines .....	22
1.3.2 Adrenergic receptors.....	23
1.3.3 Sympathomimetic/sympatholytic agents .....	24
1.3.4 Adrenergic signaling pathways.....	25
1.3.5 Sympathetic innervation of peripheral organs .....	28
<b>1.4 Neuro-immune crosstalk .....</b>	<b>30</b>
1.4.1 Leukocyte trafficking under adrenergic control .....	30
<b>1.5 Aim of the study .....</b>	<b>35</b>
<b>2 Methods and Materials .....</b>	<b>37</b>
<b>2.1 Methods.....</b>	<b>37</b>
2.1.1 Animals.....	37
2.1.2 Genotyping .....	37

2.1.3	Primers.....	38
2.1.4	PCR protocols.....	38
2.1.5	Pharmacological adrenergic stimulation and blockade .....	39
2.1.6	Chemical sympathectomy.....	39
2.1.7	Induction of inflammation.....	39
2.1.8	Organ harvest and processing for flow cytometry .....	39
2.1.9	Adoptive transfer experiments.....	41
2.1.10	Flow cytometry.....	42
2.1.11	Functional blocking experiments .....	65
2.1.12	<i>In vitro</i> adrenergic stimulation of B cells and neutrophils and investigation of adhesion molecule expression .....	65
2.1.13	<i>In vivo</i> imaging of B cells in the popliteal lymph node vasculature .....	66
2.1.14	Statistical analysis.....	67
<b>2.2</b>	<b>Materials.....</b>	<b>68</b>
2.2.1	Buffers .....	68
2.2.2	Reagents .....	68
2.2.3	Materials.....	69
2.2.4	Devices .....	69
2.2.5	Software.....	70
2.2.6	Microscope configuration .....	70
<b>3</b>	<b>Results.....</b>	<b>71</b>
<b>3.1</b>	<b>Overview of the experimental design .....</b>	<b>71</b>
<b>3.2</b>	<b>Stimulation of <math>\beta</math>-ARs affects leukocyte numbers in blood .....</b>	<b>72</b>
<b>3.3</b>	<b>Blood leukocyte numbers are controlled by <math>\beta_2</math>- and <math>\beta_3</math>-ARs.....</b>	<b>75</b>
<b>3.4</b>	<b>Neutrophils are redistributed upon adrenergic stimulation .....</b>	<b>78</b>
3.4.1	$\beta_2$ -ARs influence recruitment, $\beta_3$ -ARs influence mobilization of neutrophils.....	78
3.4.2	Neutrophil adhesion molecule levels change upon adrenergic stimulation .....	81
3.4.3	$\beta_2$ -ARs of neutrophils and their environment are targeted .....	83
<b>3.5</b>	<b>B cells are redistributed upon adrenergic stimulation .....</b>	<b>88</b>
3.5.1	Clenbuterol administration might promote B cell homing to LNs.....	88
3.5.2	B cell adhesion molecule levels change upon adrenergic stimulation.....	92
3.5.3	Treatment with Clenbuterol impacts B cell trafficking through lymph nodes .....	93
3.5.4	The adrenergic influence on B cells is $\beta_2$ -AR-specific .....	97

<b>4</b>	<b>Discussion and Conclusion.....</b>	<b>101</b>
4.1	The disparity between stimulation and block.....	101
4.2	The specificity issue with pharmacological agonists.....	103
4.3	Diverse effects on innate and adaptive immune cells .....	105
4.3.1	Are neutrophils mobilized from the BM? .....	105
4.3.2	Is neutrophil recruitment from blood impaired? .....	106
4.3.3	How is neutrophil homing to the BM affected? .....	107
4.3.4	How does the SNS orchestrate neutrophil distributions? .....	108
4.3.5	How does the SNS impact B cell trafficking through LNs? .....	109
4.4	Transferability .....	110
4.5	Concluding remarks.....	112
<b>5</b>	<b>Bibliography.....</b>	<b>i</b>
<b>6</b>	<b>Appendix.....</b>	<b>xix</b>
6.1	The SNS influences other circulating leukocyte subsets .....	xix
6.2	Affidavit.....	xxxii
6.3	List of publications .....	xxxiii
6.4	Confirmation of congruency between printed and electronic version of the doctoral thesis	xxxiv

## List of figures

FIGURE 1-1: THE CONVENTIONAL LEUKOCYTE ADHESION CASCADE.....	10
FIGURE 1-2: LEUKOCYTE TRAFFICKING IN THE BONE MARROW.....	13
FIGURE 1-3: LEUKOCYTE TRAFFICKING IN THE LYMPH NODE AND SPLEEN.....	16
FIGURE 1-4: LEUKOCYTE TRAFFICKING TO THE LIVER. ....	19
FIGURE 1-5: LEUKOCYTE TRAFFICKING IN THE LUNG.....	21
FIGURE 1-6: ACTIVATION AND REGULATION OF $\beta$ -ARS.....	26
FIGURE 1-7: G PROTEIN SWITCH AND NON-CANONICAL SIGNALING.....	27
FIGURE 1-8: ADRENERGIC CONTROL OF LEUKOCYTE TRAFFICKING. ....	34
FIGURE 2-1: GENOTYPING EXAMPLES.....	38
FIGURE 2-2: GATING STRATEGY FOR BLOOD LEUKOCYTE SUBSETS (GALLIOS). ....	44
FIGURE 2-3: GATING STRATEGY FOR BLOOD LEUKOCYTE SUBSETS (FORTESSA). ....	46
FIGURE 2-4: GATING STRATEGY FOR ADOPTIVE TRANSFER WITH $\alpha$ CD45 INJECTION – LYMPHOCYTES – DONOR CELLS (GALLIOS).....	47
FIGURE 2-5: GATING STRATEGY FOR ADOPTIVE TRANSFER WITH $\alpha$ CD45 INJECTION – LYMPHOCYTES – BLOOD (GALLIOS). ....	48
FIGURE 2-6: GATING STRATEGY FOR ADOPTIVE TRANSFER WITH $\alpha$ CD45 INJECTION – LYMPHOCYTES (GALLIOS). ....	49
FIGURE 2-7: GATING STRATEGY FOR ADOPTIVE TRANSFER WITH $\alpha$ CD45 INJECTION – MYELOID CELLS – DONOR CELLS (GALLIOS).....	50
FIGURE 2-8: GATING STRATEGY FOR ADOPTIVE TRANSFER WITH $\alpha$ CD45 INJECTION – MYELOID CELLS – BLOOD (GALLIOS). ....	51
FIGURE 2-9: GATING STRATEGY FOR ADOPTIVE TRANSFER WITH $\alpha$ CD45 INJECTION – MYELOID CELLS (GALLIOS). ....	52
FIGURE 2-10: GATING STRATEGY FOR ADOPTIVE TRANSFER DONOR MIX – DONOR CELLS (FORTESSA). ....	54
FIGURE 2-11: GATING STRATEGY FOR ADOPTIVE TRANSFER DONOR MIX - BLOOD (FORTESSA).....	55
FIGURE 2-12: GATING STRATEGY FOR ADOPTIVE TRANSFER DONOR MIX (FORTESSA). ....	56
FIGURE 2-13: GATING STRATEGY FOR ADOPTIVE TRANSFER KO RECIPIENTS – DONOR CELLS (FORTESSA). ....	57
FIGURE 2-14: GATING STRATEGY FOR ADOPTIVE TRANSFER KO RECIPIENTS - BLOOD (FORTESSA). ....	58
FIGURE 2-15: GATING STRATEGY FOR ADOPTIVE TRANSFER KO RECIPIENTS (FORTESSA). ....	59
FIGURE 2-16: GATING STRATEGY FOR <i>IN VITRO</i> STIMULATION OF B CELLS (FORTESSA).....	60
FIGURE 2-17: GATING STRATEGY FOR <i>IN VITRO</i> STIMULATION OF NEUTROPHILS (FORTESSA). ....	62
FIGURE 2-18: GATING STRATEGY FOR <i>IN VIVO</i> ADHESION MOLECULES (FORTESSA).....	64
FIGURE 3-1: OVERVIEW OF THE SCIENTIFIC QUESTIONS AND THE EXPERIMENTAL DESIGN. ....	71
FIGURE 3-2: EFFECTS OF AGONISM OR ANTAGONISM /ABSENCE OF SYMPATHETIC SIGNALING ON CIRCULATING LEUKOCYTE NUMBERS.....	74
FIGURE 3-3: CHANGES IN BLOOD LEUKOCYTE NUMBERS ARE MEDIATED BY $\beta_2$ - AND $\beta_3$ -ARS.....	77

<b>FIGURE 3-4: NEUTROPHILS ARE REDISTRIBUTED BY ADRENERGIC STIMULATION.</b>	80
<b>FIGURE 3-5: ADHESION MOLECULE LEVELS ON NEUTROPHILS ARE ALTERED UPON ADRENERGIC STIMULATION.</b>	82
<b>FIGURE 3-6: <math>\beta_2</math>-ARS OF NEUTROPHILS AND THEIR ENVIRONMENT ARE TARGETED.</b>	85
<b>FIGURE 3-7: STIMULATION OF <math>\beta_3</math>-ARS COULD AFFECT NEUTROPHIL DISTRIBUTIONS.</b>	87
<b>FIGURE 3-8: ENDOGENOUS B CELL NUMBERS DECREASE IN BLOOD AND ORGANS UPON ADRENERGIC STIMULATION.</b>	89
<b>FIGURE 3-9: B CELL HOMING MIGHT BE AFFECTED BY ADRENERGIC STIMULATION.</b>	91
<b>FIGURE 3-10: ADHESION MOLECULE LEVELS ON B CELLS CHANGE UPON ADRENERGIC STIMULATION.</b>	93
<b>FIGURE 3-11: THE MIGRATORY BEHAVIOR OF B CELLS IS AFFECTED BY ADRENERGIC STIMULATION.</b>	96
<b>FIGURE 3-12: THE ADRENERGIC INFLUENCE ON B CELLS IS <math>\beta_2</math>-AR-SPECIFIC.</b>	98
<b>FIGURE 3-13: <math>\beta_3</math>-ARS ARE NOT INVOLVED IN THE REDUCTION OF CIRCULATING B CELLS.</b>	100
<b>FIGURE 4-1: SUMMARY FIGURE OF THE RESULTS.</b>	113
<b>FIGURE 6-1: EFFECTS OF ABSENCE OF SYMPATHETIC SIGNALING ON CIRCULATING LEUKOCYTE NUMBERS.</b>	XIX
<b>FIGURE 6-2: CHANGES IN BLOOD LEUKOCYTE NUMBERS ARE MEDIATED BY <math>\beta_2</math>- AND <math>\beta_3</math>-ARS.</b>	XX
<b>FIGURE 6-3: LEUKOCYTE COUNTS UPON ADRENERGIC STIMULATION DURING INFLAMMATION.</b>	XXI
<b>FIGURE 6-4: TIME COURSE OF HARVEST TIME AFTER ADRENERGIC STIMULATION.</b>	XXI
<b>FIGURE 6-5: ENDOGENOUS MYELOID CELL NUMBERS IN VARIOUS ORGANS UPON ADRENERGIC STIMULATION.</b>	XXII
<b>FIGURE 6-6: RATIOS OF INTRA- AND EXTRAVASCULAR ENDOGENOUS MYELOID CELLS IN VARIOUS ORGANS UPON ADRENERGIC STIMULATION.</b>	XXIII
<b>FIGURE 6-7: DONOR MYELOID CELL NUMBERS IN VARIOUS ORGANS UPON ADRENERGIC STIMULATION.</b>	XXIV
<b>FIGURE 6-8: RATIOS OF INTRA- AND EXTRAVASCULAR DONOR MYELOID CELLS IN VARIOUS ORGANS UPON ADRENERGIC STIMULATION.</b>	XXV
<b>FIGURE 6-9: ENDOGENOUS LYMPHOID CELL NUMBERS IN VARIOUS ORGANS UPON ADRENERGIC STIMULATION.</b>	XXVI
<b>FIGURE 6-10: RATIOS OF INTRA- AND EXTRAVASCULAR ENDOGENOUS LYMPHOID CELLS IN VARIOUS ORGANS UPON ADRENERGIC STIMULATION.</b>	XXVII
<b>FIGURE 6-11: DONOR LYMPHOID CELL NUMBERS IN VARIOUS ORGANS UPON ADRENERGIC STIMULATION.</b>	XXVIII
<b>FIGURE 6-12: RATIOS OF INTRA- AND EXTRAVASCULAR DONOR LYMPHOID CELLS IN VARIOUS ORGANS UPON ADRENERGIC STIMULATION.</b>	XXIX
<b>FIGURE 6-13: SUMMARY OF CELL DISTRIBUTIONS UPON CLENBUTEROL ADMINISTRATION.</b>	XXX
<b>FIGURE 6-14: LEUKOCYTE NUMBERS IN BLOOD AND LYMPH NODES UPON EGRESS BLOCK.</b>	XXXI

## List of tables

<b>TABLE 1-1: ADHESION MOLECULES INVOLVED IN LEUKOCYTE TRAFFICKING.....</b>	<b>8</b>
<b>TABLE 2-1: PRIMER AND RESPECTIVE SEQUENCES .....</b>	<b>38</b>
<b>TABLE 2-2: PCR PROTOCOLS .....</b>	<b>38</b>
<b>TABLE 2-3: FLOW CYTOMETER CONFIGURATIONS.....</b>	<b>42</b>
<b>TABLE 2-4: STAINING PANEL FOR BLOOD LEUKOCYTE SUBSETS (GALLIOS).....</b>	<b>43</b>
<b>TABLE 2-5: STAINING PANEL FOR BLOOD LEUKOCYTE SUBSETS (FORTESSA).....</b>	<b>45</b>
<b>TABLE 2-6: STAINING PANEL FOR ADOPTIVE TRANSFER (GALLIOS).....</b>	<b>46</b>
<b>TABLE 2-7: STAINING PANEL FOR ADOPTIVE TRANSFER WITH <math>\alpha</math>CD45 INJECTION – LYMPHOCYTES (GALLIOS).....</b>	<b>47</b>
<b>TABLE 2-8: STAINING PANEL FOR ADOPTIVE TRANSFER WITH <math>\alpha</math>CD45 INJECTION – MYELOID CELLS (GALLIOS).....</b>	<b>50</b>
<b>TABLE 2-9: STAINING PANEL FOR ADOPTIVE TRANSFER WITH <math>\alpha</math>CD45 INJECTION – DONOR MIX (FORTESSA) .....</b>	<b>53</b>
<b>TABLE 2-10: STAINING PANEL FOR ADOPTIVE TRANSFER WITH <math>\alpha</math>CD45 INJECTION OF KO RECIPIENTS (FORTESSA).....</b>	<b>56</b>
<b>TABLE 2-11: STAINING PANEL FOR <i>IN VITRO</i> STIMULATION OF B CELLS (FORTESSA) .....</b>	<b>60</b>
<b>TABLE 2-12: STAINING PANEL FOR <i>IN VITRO</i> STIMULATION OF NEUTROPHILS (FORTESSA).....</b>	<b>61</b>
<b>TABLE 2-13: STAINING PANEL FOR <i>IN VIVO</i> ADHESION MOLECULES (FORTESSA).....</b>	<b>63</b>
<b>TABLE 2-14: BLOCKING ANTIBODIES AND REAGENTS .....</b>	<b>65</b>
<b>TABLE 2-15: BUFFER INGREDIENTS .....</b>	<b>68</b>
<b>TABLE 2-16: LIST OF USED REAGENTS WITH RESPECTIVE SUPPLIERS.....</b>	<b>68</b>
<b>TABLE 2-17: LIST OF USED MATERIALS WITH RESPECTIVE SUPPLIERS .....</b>	<b>69</b>
<b>TABLE 2-18: LIST OF USED DEVICES AND RESPECTIVE SUPPLIERS .....</b>	<b>69</b>
<b>TABLE 2-19: LIST OF USED SOFTWARE WITH RESPECTIVE SUPPLIERS .....</b>	<b>70</b>
<b>TABLE 2-20: MICROSCOPE CONFIGURATION.....</b>	<b>70</b>
<b>TABLE 3-1: DONOR NEUTROPHILS AS PERCENTAGE OF INJECTED NEUTROPHILS IN BLOOD AND ORGANS. ....</b>	<b>81</b>
<b>TABLE 3-2: DONOR B CELLS AS PERCENTAGE OF INJECTED B CELLS IN BLOOD AND ORGANS. ....</b>	<b>92</b>

## List of abbreviations

AR	Adrenoceptor
6-OHDA	6-Hydroxydopamine
7-AAD	7-Aminoactinomycin D
AC	Adenylyl Cyclase
ACh	Acetylcholine
Adrb2	$\beta_2$ -Adrenoceptor
Adrb3	$\beta_3$ -Adrenoceptor
AGM	Aorta-Gonad-Mesonephros
AKAP	A-Kinase Anchoring Protein
ATP	Adenosine Triphosphate
$\beta$ ARK	$\beta$ -Adrenoceptor Kinase
BM	Bone Marrow
bp	Base Pairs
BrdU	Bromodeoxyuridine
BRL	BRL37344
Ca <sup>2+</sup>	Calcium ions
cAMP	Cyclic Adenosine Monophosphate
CAR	Coxsackie and Adenovirus Receptor
CFSE	Carboxyfluorescein Succinimidyl Ester
Clen	Clenbuterol
CNS	Central Nervous System
COPD	Chronic Obstructive Pulmonary Disease
DC	Dendritic Cell
Den	Denopamine
DMSO	Dimethyl Sulfoxid
DPBS	Dulbecco's Phosphate-Buffered Saline
E-selectin (CD62E)	Endothelial-selectin
EC	Endothelial Cell
Eos	Eosinophils
EPI	Epinephrine
ERK	Extracellular Signal-Regulated Kinase
ESAM	Endothelial Cell-Selective Adhesion Molecule
ESL-1	E-Selectin Ligand 1
FITC	Fluorescein isothiocyanate
fMLP	N-Formylmethionyl-Leucyl-Phenylalanine
G-CSF	Granulocyte Colony Stimulating Factor
gdLN	Gut-draining Lymph Node
GDP	Guanosine Diphosphate
GPCR	G protein coupled receptor
GRK	G Protein-Coupled Receptor Kinase
GTP	Guanosine Triphosphate
HA	Hyaluronic Acid
HEK	Human Embryonic Kidney
HEV	High Endothelial Venules
HPA	Hypothalamc-Pituitary-Adrenal
hr	Hour
HSC	Hematopoietic Stem Cell
HSPC	Hematopoietic Stem and Progenitor Cell
ICAM-1/2	Intercellular Adhesion Molecule 1/2
IFN	Interferon
IL	Interleukin
iLN	Inguinal Lymph Node
Infl. Monos	Inflammatory Monocytes
IP <sub>3</sub>	Inositol Triphosphate
Iso	Isoproterenol
JAM	Junctional Adhesion Molecule
KO	Knockout
L-selectin (CD62L)	Leukocyte-selectin
LABA	Long Acting $\beta$ -Adrenoceptor Agonist
LFA-1	Lymphocyte Function-Associated Antigen 1
LN	Lymph Node

LPAM	Lymphocyte Peyer's Patch Adhesion Molecule
LPS	Lipopolysaccharide
LSEC	Liver Sinusoidal Endothelial Cell
Mac-1	Macrophage-1
MADCAM-1	Mucosal Addressin Cell Adhesion Molecule
MCP-1	Monocyte Chemoattractant Protein 1
MFI	Mean Fluorescence Intensity
min	Minute
mLN	Mesenteric Lymph Node
NE	Norepinephrine
NET	Neutrophil Extracellular Trap
NK cell	Natural Killer cell
NKT cell	Natural Killer T cell
Non-Infl. Monos	Non-Inflammatory Monocytes
P-selectin (CD62P)	Platelet-selectin
PBS	Phosphate-Buffered Saline
PCR	Polymerase Chain Reaction
PEB	Protein Extraction Buffer
PECAM-1 (CD31)	Platelet-Endothelial Cell Adhesion Molecule
PKA	Protein Kinase A
PKC	Protein Kinase C
PLC	Protein Lipase C
PNAd	Peripheral Nodal Addressin
PNS	Peripheral Nervous System
popLN	Popliteal Lymph Node
Prop	Propranolol
PSGL-1 (CD162)	P-Selectin Glycoprotein Ligand 1
Ras	Rat Sarcoma
RBC	Red Blood Cell
ROS	Reactive Oxygen Species
S1P	Sphingosine 1 Phosphate
S1PR1	Sphingosine 1 Phosphate Receptor 1
SABA	Short Acting $\beta$ -Adrenoceptor Agonist
sdLN	Skin-Draining Lymph Node
sec	Second
sLe <sup>x</sup>	Sialyl Lewis x
SNS	Sympathetic Nervous System
spLN	Superficial Parotid Lymph Node
TH	Tyrosine Hydroxylase
Th cell	T helper cell
TLR	Toll-Like Receptor
TNF $\alpha$	Tumor Necrosis Factor $\alpha$
VAP-1	Vascular Adhesion Protein-1
VCAM-1	Vascular Adhesion Molecule 1
VE-Cadherin	Vascular Endothelial Cadherin
VLA-4	Very Late Antigen 4
vs.	Versus
WBC	White Blood Cell
WT	Wild Type



# 1 Introduction

## 1.1 Explanatory statement

An organism only functions properly when its constituting components are working together in harmony. Two of these major key players are the nervous system and the immune system. Functioning consciously as well as unconsciously, the nervous system senses, interprets and responds to proceedings in the environment. The immune system is not only responsible for host protection against foreign pathogens by initiation of inflammation, but also for the maintenance of its equilibrium by regulating processes like tissue regeneration. The immune system and nervous system are tightly interconnected during inflammation and homeostasis, in which the sympathetic nervous system plays a decisive role (Elenkov et al., 2000). To understand the intricate neuro-immune interplay, the migratory behavior of immune cells under stress is a fascinating aspect to investigate. Immune cell trafficking is crucial for development, immune-surveillance and effector function and takes place between lymphoid organs, the circulation and peripheral tissues. Therefore, it is essential that circulating cell numbers are tightly regulated, as malfunctions can lead to severe diseases.

Despite a plethora of studies investigating the complex interactions between the sympathetic nervous system and the immune system (Jakob et al., 2020; Nance and Sanders, 2007), they are only partly understood. Thus, the focus of this thesis lies on adrenergic effects on leukocyte migration *in vivo* under steady-state conditions. Only after understanding when and where leukocytes are located under physiological stress signals, therapies can effectively target dysfunctions of these processes. Based on previous findings regarding the influence of adrenergic stimuli on the distribution of immune cells in the mouse (Scheiermann et al., 2012), this thesis is about the migratory behavior of murine neutrophils and B cells – as representatives of innate and adaptive immunity, respectively – upon stimulation with sympathomimetic agents.

## 1.2 The immune system requires leukocyte trafficking

Every organism is constantly exposed to pathogens and hence, had to develop an efficient defense machinery – the immune system. It is subdivided into innate and adaptive immunity, of which both depend on the activity of white blood cells, the leukocytes. These immune cells develop and differentiate from progenitors in primary lymphoid organs, travel through the circulation and enter secondary lymphoid tissues where they encounter antigens and are activated. Fetal immune cell differentiation starts in the aorta-gonad-mesonephros (AGM) region (Medvinsky and Dzierzak, 1996; Müller et al., 1994) followed by the fetal liver and is shifted to the bone marrow (BM) and thymus around birth, making these the most important primary lymphoid organs. Secondary lymphoid organs comprise lymph nodes (LNs), the spleen and Peyer’s patches, the latter associated with the small intestine. However, immune cells do not exclusively patrol these organs since every tissue has to be equipped with protective mechanisms against intrinsic and extrinsic hazards as well as maintenance of homeostatic processes.

Innate immunity builds the first, relatively unspecific line of defense against inflammatory insults. It comprises granulocytes (neutrophils, eosinophils, basophils), monocytes, dendritic cells (DCs), natural killer (NK) and natural killer T (NKT) cells, that scan the body for multiple endogenous and exogenous factors, eliminate pathogens, take up foreign antigen and present it to cells of the adaptive immune system. Additionally, invariant T cells interlink innate and adaptive immunity as unique innate-like cells (Toubal et al., 2019). Adaptive immunity creates the immunological memory to effectively fight re-occurring threats with the help of B and T lymphocytes. Thus, for cell interactions as well as exertion of effector function cell types of both arms of immunity have to travel to peripheral organs, where they adhere and migrate across the vascular endothelium – a process called leukocyte trafficking.

Leukocyte trafficking is orchestrated by various factors, such as endothelial architecture, chemokine composition and blood flow rate. Another aspect gaining in importance is the time of day. Peripheral blood leukocyte counts oscillate throughout the day, showing a peak during the behavioral resting phase (Druzd et al., 2017; He et al., 2018; Scheiermann et al., 2012). On the other hand, during the active phase of an organism, leukocytes predominantly immigrate into peripheral tissues, based on changing expression profiles of adhesion molecules on leukocytes as well as endothelial cells (ECs) (He et al., 2018). Depending on their functions, leukocyte subsets circulate the body following specific patterns. In this thesis, I focus on the trafficking of neutrophils and B cells upon adrenergic

stimulation, thus conventional migratory routes during the life time of these cell types are outlined in the following paragraphs.

### **1.2.1 The life cycle of neutrophils**

Neutrophils are the most abundant leukocyte subset in the human circulation, whereas they only make up 30% of the leukocyte composition in murine blood. These granulocytes are an important cell type of the innate immune system, as they fight pathogens via phagocytosis (Lee et al., 2003), the release of neutrophil extracellular traps (NETs) (Papayannopoulos, 2018), reactive oxygen species (ROS) formation (Babior et al., 1973), and the release of granules (Yin and Heit, 2018). Moreover, they aid in tissue repair after an injury while they can also cause tissue damage (Wang, 2018). Due to their crucial role in these processes, the regulation of their circulating numbers is essential. Neutrophils develop from a myeloid progenitor in the BM as primary production site, in which premature cells reside in specialized niches (Birbrair and Frenette, 2016). Rhythmically during homeostasis or as response to an inflammatory stress, mature cells are released into the circulation (Furze and Rankin, 2008) and migrate to peripheral tissues to fulfill their tasks. Afterwards, cells either undergo apoptosis at the same site and get eliminated by tissue resident macrophages, or they migrate to the marginal pool in the lung, where they upregulate age-related markers, leading them back to the BM for clearance (Hidalgo et al., 2019). After their relatively short life in the circulation (Pillay et al., 2010) neutrophils under non-inflammatory conditions are also cleared in spleen and liver (Furze and Rankin, 2008). Although neutrophils have been seen as homogenous population, increasing evidence hints to multiple existing phenotypes exhibiting various functions in health and disease (Hellebrekers et al., 2018).

### **1.2.2 The life cycle of B cells**

B cells are essential cellular components of the adaptive immunity, since they respond to specific antigenic epitopes by production of antibodies, thereby providing a specialized defense against pathogens. Together with T cells, they account for the main part of murine blood leukocytes. B cell development undergoes multiple phases beginning in primary lymphoid tissues and continuing with functional maturation in secondary lymphoid tissues, which constantly receive antigen through circulating lymph. In the spleen, mature B cells reside within lymphoid follicles, where DCs present the foreign antigen to lymphocytes. Subsequently, B cells start proliferating and differentiating into high-affinity

antibody-secreting plasma cells and memory B cells (Eibel et al., 2014), which migrate to peripheral tissues where they mediate adaptive humoral responses. In addition, naïve B cells home to the BM, where they form perisinusoidal niches in which they undergo T cell-independent maturation processes (Cariappa et al., 2007). Next to their role in host defense, they are responsible for lymphoid tissue organogenesis, wound healing, DC regulation and co-stimulation of as well as antigen presentation to T cells (LeBien and Tedder, 2008).

### **1.2.3 Leukocyte trafficking depends on adhesion molecules**

For leukocyte entry to target tissues, circulating immune cells are captured and roll along the endothelium, where they are activated by chemokines. After firm adhesion, leukocytes can crawl and eventually transmigrate. For this sequence of steps, interaction of specific molecules between the circulating cells and the endothelium is required. These molecules are generally termed adhesion molecules and include numerous protein families, which will be shortly introduced here and are further summarized in **Table 1-1**.

One important family comprises selectins, which are expressed by ECs (E-, P-selectin) and leukocytes (L-selectin). These transmembrane proteins require  $Ca^{2+}$  to bind sialylated carbohydrate structures. L-selectin (CD62L) was first discovered on lymphocytes, but is expressed on basically all circulating leukocytes (Lewinsohn et al., 1987). Although it was long thought that L-selectin is only crucial in lymphocyte binding to high endothelial venules (HEVs), further investigation revealed its additional role in the peripheral microvasculature during homeostasis (Ley et al., 1993; von Andrian et al., 1991). Furthermore, L-selectin was found to take part in neutrophil tethering (Walcheck et al., 1996). Protein kinase C (PKC)-dependent phosphorylation of the cytoplasmic domain of this selectin type is required for leukocyte rolling and adhesion to HEVs (Kansas et al., 1993). Importantly and in contrast to other adhesion molecules, L-selectin is shed upon activation (Chen et al., 1995; Venturi et al., 2003).

Another type of selectins is P-selectin (CD62P), which is constitutively expressed by platelets (Hsu-Lin et al., 1984) and stimulated ECs (McEver et al., 1989). After expression in the latter cell type, P-selectin is internalized and stored in intracellular storage granules, called Weibel-Palade bodies, from where it is transported to the surface upon stimulation. As this process is taking place in only a few minutes, P-selectin contributes to a rapid increase in rolling, which is impaired in P-selectin-deficient mice (Mayadas et al., 1993).

The third member, E-selectin (CD62E), is highly glycosylated and exclusively found on activated ECs (Bevilacqua et al., 1987). Its expression in the majority of organs is regulated by inflammatory mediators like tumor necrosis factor  $\alpha$  (TNF $\alpha$ ), except for skin where it is constitutively expressed (Hwang et al., 2004). In several models of inflammation, neutrophil trafficking was not altered in CD62E-deficient mice until P-selectin was blocked, indicating a functional redundancy of these two adhesion molecules (Frenette et al., 1996; Labow et al., 1994).

Among selectin ligands, P-selectin glycoprotein ligand-1 (PSGL-1, CD162) is an important molecule interacting with all three selectins (Moore, 1998). It plays a crucial role in leukocyte recruitment, as blocking by a monoclonal antibody disables binding of murine myeloid cells to P-selectin and thereby completely abolishes leukocyte rolling (Borges et al., 1997). However, in PSGL-1-deficient mice it was shown that a PSGL-1-independent, E-selectin-dependent rolling occurs (Yang et al., 1999), which seems to be supported by  $\alpha$ 2,3-sLe<sup>x</sup> glycosphingolipids (Burdick et al., 2001).

In blood vessels, adhesive processes of cells are predominantly mediated by the protein class of integrins. These adhesion molecules reside in a low-affinity state, whereas ligand binding leads to a high affinity confirmation (Takagi et al., 2002). On leukocytes, members belonging to the  $\beta_2$  and  $\beta_7$  subfamilies are expressed, which bind to endothelial adhesion molecules.  $\beta_2$ -integrins are built of two subunits constituting four different heterodimers, namely  $\alpha_L\beta_2$  (LFA-1, CD11a/CD18),  $\alpha_M\beta_2$  (Mac-1, CD11b/CD18),  $\alpha_X\beta_2$  (CD11c/CD18) and  $\alpha_D\beta_2$  (CD11d/CD18). They play a major role in the firm adhesion between leukocytes and endothelium as well as among leukocytes (Luo et al., 2007). LFA-1 is ubiquitously expressed on immunocompetent cells, whereas Mac-1 is predominantly expressed on cells of the myeloid lineage. The  $\alpha_4\beta_1$ -integrin very late antigen 4 (VLA-4) can mediate rolling and adhesion of leukocytes, thus acting independently of selectins (Alon et al., 1995).

Another crucial family of cell surface proteins comprises intercellular cell adhesion molecule (ICAM) 1 and 2, which are involved in every step of neutrophil extravasation and can have redundant, but also specific functions. ICAM-1 is constitutively expressed on every blood vessel endothelium as well as in low amounts on leukocytes. The surface location of ICAM-1 and ICAM-2 differs in that ICAM-1 is more uniformly expressed, whereas ICAM-2 is clustered at cell junctions of ECs. Furthermore, during inflammation, ICAM-1 levels increase while ICAM-2 is downregulated (Dustin et al., 1986). Both adhesion molecules bind to LFA-1 and Mac-1 on leukocytes (Diamond et al., 1990; Staunton et al., 1989).

Vascular cell adhesion molecule (VCAM)-1 expression on ECs is inducible by several factors, e.g. pro-inflammatory cytokines and shear stress. Its ligands are the integrins VLA-4 ( $\alpha_4\beta_1$ ) and CD49d ( $\alpha_4\beta_7$ ) (Kong et al., 2018).

CD44 is a cell surface adhesion molecule with multiple isoforms of differing molecular sizes. On leukocytes the 'standard' isoform is expressed and transiently upregulated upon cell activation. The major binding partner is hyaluronic acid (HA), which is part of the extracellular matrix and can only be bound following activation of the endothelium (Mohamadzadeh et al., 1998). CD44 exhibits various functions, amongst others it is involved in chemokine presentation and LN homing (Naor et al., 1997).

Junctional adhesion molecules (JAMs) belong to the immunoglobulin family that is important for maintenance of endothelial tight junctions. The first member discovered in platelets was JAM-A. Since then, JAM-B and JAM-C were found to be expressed on a variety of cell types, including leukocytes and ECs (Kummer and Ebnet, 2018). Non-classical family members are ESAM, CAR, JAM-4, and JAM-L. They can interact in *cis* and *trans*: *cis* meaning they interact with other surface proteins on the same cell and *trans* describes their interaction with molecules of adjacent cells. During inflammation, proteins of the JAM family interact with integrins regulating cell adhesion and signaling pathways. Binding of JAM-A to its ligand LFA-1 mediates leukocyte adhesion and transmigration *in vitro* (Ostermann et al., 2002). In *trans*, JAM-B interacts with VLA-4, whereas the major ligand of JAM-C is Mac-1 (Kummer and Ebnet, 2018).

Platelet endothelial cell adhesion molecule 1 (PECAM-1, CD31) is highly expressed at endothelial borders and shows lower levels on leukocytes. It can form homophilic interactions, thereby mediating diapedesis (Muller, 2017).

Like PECAM-1, the heavily O-glycosylated type I transmembrane protein CD99 is expressed on both, leukocytes and ECs and is also required for transendothelial migration, as the inhibition of its homophilic interactions almost completely halts the process (Schenkel et al., 2002).

Vascular endothelial (VE)-cadherin belongs to the family of type II classical cadherin cell adhesion proteins and is expressed by a specific subset of human hematopoietic stem cells (HSCs) and stromal cells (Oberlin et al., 2010) as well as ECs, where it maintains their adhesive state via homophilic interactions (Harris and Nelson, 2010).

Chemokines present another important class of molecules in leukocyte trafficking. This family of small cytokines is released by various cell types in steady state as well as in response to inflammatory stimuli and binds to G protein-coupled receptors (GPCRs) on the surface of immune cells, thus regulating chemotaxis via integrin activation. Four structural chemokine classes exist (C, CC, CXC, CX3X) of which three are involved in

leukocyte trafficking (Olson and Ley, 2002). Close to their amino terminus, CC chemokines harbor two adjacent cysteine residues, CXC chemokines contain one variable and CX3C chemokines contain three variable amino acids between two cysteines (nomenclature, 2001). CCR7, CXCR2, CXCR4 and CXCR5 are crucial for migration of neutrophils and B cells to specific organs, which will be explained in more detail in chapter 1.2.5.

The expression patterns of adhesion molecules vary between vascular beds as well as in the course of a day (He et al., 2018), with higher leukocyte migration capacity during the night in mice due to upregulation of e.g. ICAM-1 and VCAM-1 on ECs and CD11a, CXCR4 and CD49d on leukocytes. Furthermore, every organ shows a specific rhythmic pattern of molecules required to enter the tissue under homeostasis and inflammation (Pick et al., 2019; Yuan et al., 2020).

**Table 1-1: Adhesion molecules involved in leukocyte trafficking.**

Molecule	Synonym	Expressed by	Interaction partner	References
L-selectin	CD62L	Leukocytes	PSGL-1	Lewinsohn <i>et al.</i> , 1987
P-selectin	CD62P	Platelets, stimulated ECs	PSGL-1	Hsu-Lin <i>et al.</i> , 1984 McEver <i>et al.</i> , 1989
E-selectin	CD62E	Activated ECs	PSGL-1	Bevilacqua <i>et al.</i> , 1987
PSGL-1	CD162	Leukocytes	CD62L/P/E	Moore, 1998
LFA-1	$\alpha_L\beta_2$ , CD11a/CD18	Leukocytes (all)	ICAM-1/2	Luo <i>et al.</i> , 2007
Mac-1	$\alpha_M\beta_2$ , CD11b/CD18	Leukocytes (myeloid cells)	ICAM-1/2	Luo <i>et al.</i> , 2007
VLA-4	$\alpha_4\beta_1$	Leukocytes	VCAM-1	Alon <i>et al.</i> , 1995
ICAM-1/2	CD54/CD102	ECs (constitutively), Leukocyte (low)	LFA-1, Mac-1	Dustin <i>et al.</i> , 1986
VCAM-1	CD106	ECs (inducible)	VLA-4	Kong <i>et al.</i> , 2018
CD44	P-glycoprotein 1	Leukocytes	Hyaluronic acid (HA)	Mohammadzadeh <i>et al.</i> , 1998
JAM-A	CD321	Leukocytes, ECs	<i>cis/trans</i> : LFA-1 JAM-A	Ostermann <i>et al.</i> , 2002
JAM-B	CD322	Leukocytes, ECs	<i>cis/trans</i> : VLA-4 JAM-B	Kummer and Ebnet, 2018
JAM-C	CD323	ECs	<i>cis/trans</i> : Mac-1 JAM-C	Kummer and Ebnet, 2018
PECAM-1	CD31	ECs (high), leukocytes (low)	PECAM-1	Muller, 2017
CD99	MIC2	Leukocytes, ECs	CD99	Schenkel <i>et al.</i> , 2002
VE-cadherin	CD144	ECs, HSCs and stromal cells	VE-cadherin	Harris and Nelson, 2010 Oberlin <i>et al.</i> , 2010
Chemokines	CC, CXC, CX3C	Various cell types	Chemokine receptors	Olson and Ley, 2002

#### 1.2.4 The conventional leukocyte adhesion cascade

The infiltration of vascular beds under homeostatic and inflammatory conditions is highly regulated and consists of a series of adhesive steps described as the leukocyte adhesion cascade (Ley *et al.*, 2007; Nourshargh and Alon, 2014) (**Figure 1-1**). It is mediated by an interplay of the molecules described in chapter 1.2.3 and starts with the reversible capture of leukocytes on the endothelium of postcapillary venules, mediated by PSGL-1 interactions with endothelial E- and P-selectin. Next to PSGL-1, E-selectin ligand (ESL)-1 on neutrophils also binds to CD44 (Hidalgo *et al.*, 2007). More circulating leukocytes can interact with already attached cells by binding of L-selectin to PSGL-1 (Walcheck *et al.*,

1996). In contrast to fast rolling occurring without cytokine stimulation, L-selectin-mediated slow rolling, facilitated by ICAM-1 and partly activated LFA-1 as well as the formation of leukocyte microvilli, increases the time for ligand presentation to chemokine receptors and integrins (Chen and Springer, 1999). The crucial integrins LFA-1 and Mac-1 bind to ICAM-1 and ICAM-2, resulting in loose adhesion (Hogg et al., 2002). The subsequent strengthening of adhesion requires activation of LFA-1, a process depending on talin-1 and kindlin-3 as well as chemokines and chemoattractants (such as IL-8), induced by inflammatory mediators (Lefort et al., 2012). On the other hand, VCAM-1 is recognized by monocytes and lymphocytes expressing VLA-4 (Elices et al., 1990). After arrest, leukocytes either reorganize their cytoskeleton (Hyun et al., 2012) to crawl along the EC barrier in search for exit signals, a process depending on integrins (Phillipson et al., 2009), or they pass through the endothelium directly. It was long thought that, unlike the preceding steps, diapedesis was the only non-reversible process. However, recent studies demonstrated reverse migration processes of leukocytes (Nourshargh et al., 2016). Penetration of the endothelial barrier can occur through the body of ECs (transcellular), but is mostly observed through junctions between adjacent cells (paracellular), where proteins like JAM-A and -C are concentrated (Muller, 2011). PECAM-1 plays an essential role in an early step of transmigration, as antibodies almost completely block this process (Muller et al., 1993). In a later step, homophilic interactions of CD99 on both sides are required for transmigration of neutrophils (Lou et al., 2007). VE-cadherin negatively regulates transmigration and has to relocate from the junctions where leukocytes migrate through (Shaw et al., 2001). Presumably, numerous other proteins are involved in diapedesis, probably acting in a sequential manner (Muller, 2011).

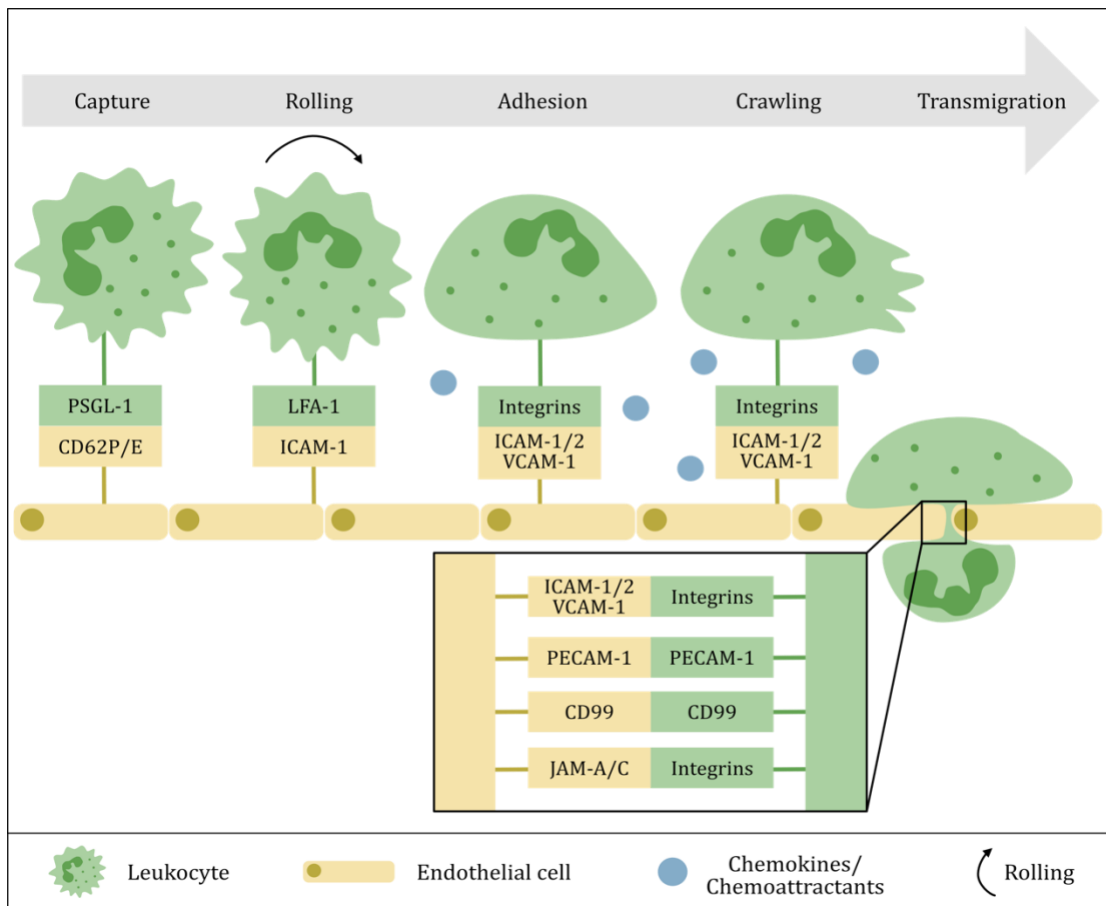


**Figure 1-1: The conventional leukocyte adhesion cascade.**

Circulating leukocytes are captured by interaction of PSGL-1 with CD62P/E on the endothelium. By interaction of LFA-1 and ICAM-1 leukocytes roll along the endothelial layer until they adhere, again mediated by integrins and endothelial ICAM-1/2 or VCAM-1. With the help of chemokines and chemoattractants such as IL-8, leukocytes are activated and adhere more firmly. Afterwards, they crawl along the endothelium in search for a suitable exit site, where they transmigrate. This process is mediated by homophilic interactions of PECAM-1 and CD99, as well as interactions between integrins and endothelial adhesion molecules such as JAM-A.

### 1.2.5 Organ- and cell type-specific leukocyte trafficking

The cascade paradigm described in chapter 1.2.4 has been studied mostly in the cremaster muscle, but is not applicable to every tissue in the body. The tissue environment and leukocyte subset define which adhesion molecules are involved in the interaction between leukocytes and the endothelium. Notably, every organ harbors specialized tissue resident cells that express various factors, thereby regulating leukocyte trafficking in an organ-specific manner.

Here, I will focus on trafficking of B cells and neutrophils, which are mostly recruited to the BM, LNs, lung, liver, and spleen (He et al., 2018). Thus, trafficking mechanisms in these tissues will be covered in detail. Whereas in secondary lymphoid organs like LNs immune

cell trafficking is a continual process, little is known about homeostatic mechanisms for leukocyte migration in the lung and liver, as these were predominantly investigated in the context of inflammation or injury. Thus, although the experimental focus of this study lies on processes under non-inflammatory conditions, adhesive mechanisms during inflammation are also introduced.

#### **1.2.5.1 Bone marrow**

As a major component of innate immunity, numbers of short-lived neutrophils have to be constantly replenished by release from the BM, which is their production site. On the other hand, senescent cells have to be removed from the circulation. Thus, the BM vasculature has to fulfill two distinct roles, maintenance of hematopoietic stem and progenitor cells (HSPCs) and their release into the circulation as well as leukocyte homing for the degradation of neutrophils. A recent study could show that the architecture of specialized BM blood vessels meets the criteria for both processes, which are taking place at distinct sites (Itkin et al., 2016). Arterial blood vessels show lower permeability as well as ROS levels, thereby maintaining HSPC quiescence (Kunisaki et al., 2013). On the contrary, the more permeable sinusoids are the exclusive gateway of the BM. Using mixed BM chimeras, it could be shown that egress and homing of neutrophils are counteractively regulated by the chemokine receptors CXCR2 and CXCR4 (Eash et al., 2010). Furthermore, both processes are governed by circadian rhythms (Casanova-Acebes et al., 2013; Mendez-Ferrer et al., 2008). The major ligand of CXCR4, CXCL12, is constitutively expressed by BM stromal cells and is the most important retention factor for neutrophils in mouse and human (Martin et al., 2003). Its expression is downregulated by the granulocyte colony-stimulating factor (G-CSF) (Semerad et al., 2005), which also regulates neutrophil mobilization through CXCR2 signaling (Semerad et al., 2002). The hematopoietic cytokine augments CXCL1 production by ECs (Eash et al., 2010) and enhances CXCL1 release from BM-resident megakaryocytes, which are located in close proximity to sinusoidal vessels (Köhler et al., 2011).

After about one day in the circulation, murine neutrophils upregulate ICAM-1, CD11b and CXCR4 levels, whereas L-selectin is progressively shed, creating a signal for these neutrophils to get eliminated in the BM, spleen and liver (Furze and Rankin, 2008; Martin et al., 2003). Importantly, oscillations in endothelial selectins and VCAM-1 expression influence leukocyte recruitment to the BM (Scheiermann et al., 2012), but also fluctuating expression levels of CXCR4 on murine neutrophils regulate their recruitment during the onset of the behavioral active phase (Adrover et al., 2019; He et al., 2018). In addition, the

same study demonstrated a role for the previously neglected molecules L-selectin and ICAM-1 in BM homing of various subsets, including neutrophils and B cells (He et al., 2018).

The BM is also the production site for B cells. In specialized niches, immature B cells reside until they transit into sinusoids to be released into the blood stream, a process regulated by the sphingosine-1-phosphate (S1P) receptor (Allende et al., 2010). Similar to neutrophil retention, CXCL12-CXCR4 signaling was identified to be equally essential for B cell development (Nagasawa et al., 1996) and their retention in the BM (Ma et al., 1999). For homing to their tissue of origin, B cells require VCAM-1 (Koni et al., 2001), which is specifically involved in their adhesion and extravasation (He et al., 2018). Taken together, the BM is a crucial organ for homeostasis of immune cells by regulating not only their production, maturation and release, but also their disposal (**Figure 1-2**).

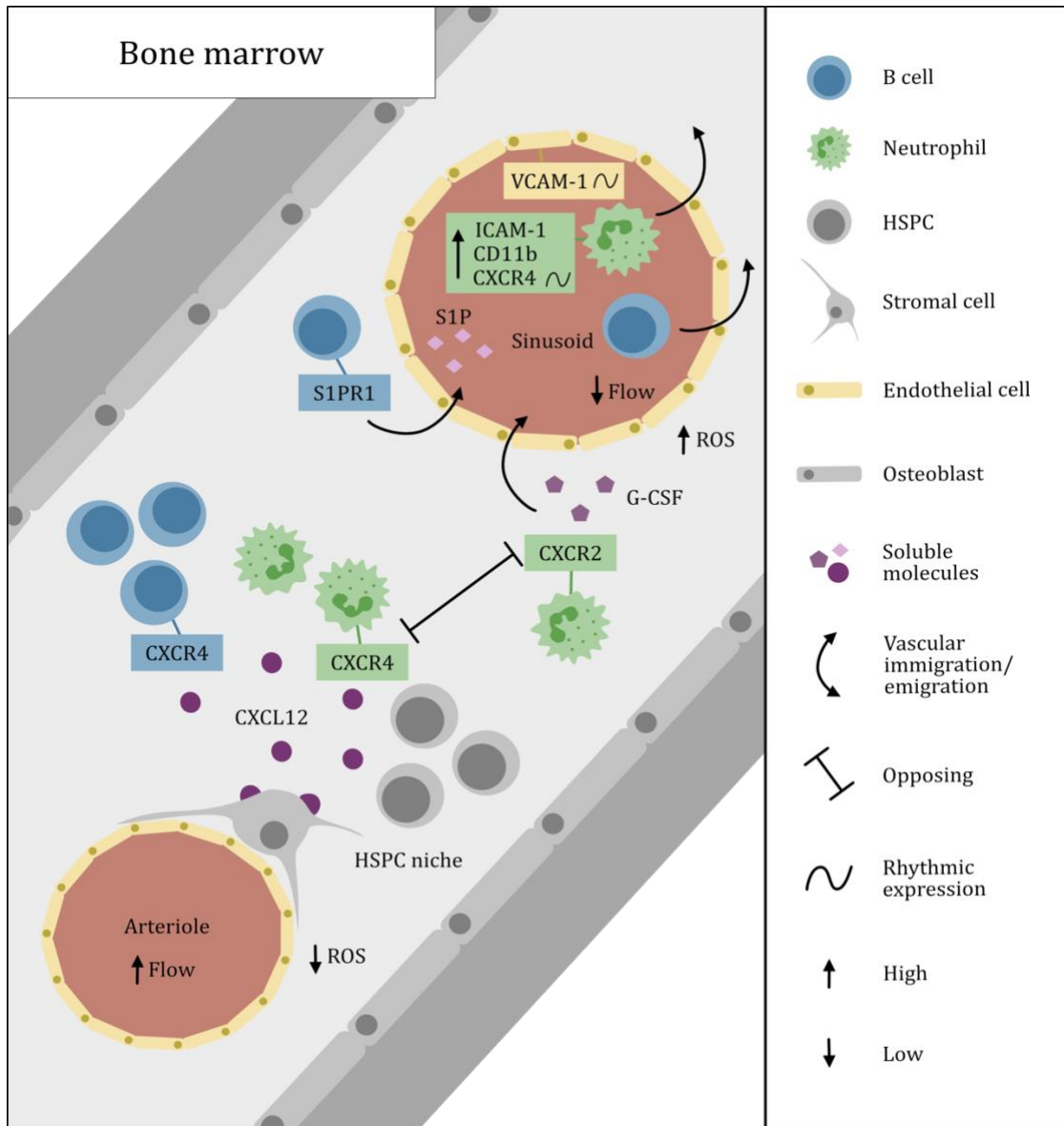


**Figure 1-2: Leukocyte trafficking in the bone marrow.**

The high blood flow in and low reactive oxygen species (ROS) levels around arterioles maintain the proximal niche for hematopoietic stem and progenitor cells (HSPCs), whereas the more permeable sinusoids are the gateway for leukocyte trafficking. Retention of HSPCs and leukocytes is mediated by the CXCR4 ligand CXCL12, which is expressed by stromal cells. CXCR2 counteracts CXCR4 and is activated by G-CSF, resulting in cell egress. B cells leave the BM utilizing interaction of S1P and S1PR1. Leukocyte homing to this tissue is regulated by rhythmic expression of VCAM-1, E-selectin and P-selectin on sinusoidal endothelial cells, as well as upregulated adhesion molecules on neutrophils.

### 1.2.5.2 Lymph nodes

To generate adaptive immune responses, lymphocytes circulate throughout the body, migrate to lymph nodes where they encounter antigen conveyed by antigen presenting cells like DCs, enter lymphatics and eventually return to the circulation. Whereas memory and effector T cells enter LNs via afferent lymph, naïve lymphocytes enter LNs via

specialized blood vessels, called HEVs (Mackay et al., 1990). HEVs are equipped with peripheral nodal addressins (PNAd) that are heavily modified. L-selectin recognizes the carbohydrate ligand 6-sulfo sialyl Lewis X (6-sulfo sLe<sup>x</sup>) (Rosen, 2004) leading to leukocyte rolling along the endothelium. In addition, in human LNs it was shown that vascular adhesion protein 1 (VAP-1) mediates a lymphocyte subtype-specific, selectin-independent interaction with the endothelium, since this monoamine oxidase binds and deaminates an amino group on the surface of lymphocytes, resulting in a covalent bond between lymphocytes and the endothelium (Salmi et al., 1997; Salmi et al., 2001). During rolling, lymphocytes are activated via binding of the chemokine receptors CXCR4 and CCR7 to their constitutively expressed ligands CXCL12 and CCL19/CCL21, respectively (Gunn et al., 1998; Okada et al., 2002). In contrast to T cells, B cells additionally express the receptor for CXCL13, CXCR5, which guides them to their target localization within the tissue (Girard et al., 2012). In mice, CXCL12 and CXCL13 are synthesized by LN stromal cells, whereas CCL21 is expressed by HEVs. Upon activation, leukocyte CD11a (LFA-1) interacts with endothelial ICAM-1 and ICAM-2, resulting in the successful entry into the LN parenchyma (Girard et al., 2012). In mesenteric LNs, the interaction of  $\alpha_4\beta_7$  integrins (VLA-4) with mucosal addressin cell adhesion molecule 1 (MADCAM-1) was found to play an important role in lymphocyte arrest (Gorfu et al., 2009). Lymphocytes crawl along the endothelium of HEVs until they enter the LN interstitium, whereby B cells crawl and transmigrate slower than T cells (Park et al., 2012). Using intravital microscopy, a recent study demonstrated that sialic acid regulates lymphocyte entry into LNs, as its loss affects the expression of L-selectin, integrins, CXCR4, CXCR5, and CCR7, thereby downregulating chemokine responsiveness (Zeng et al., 2020). Once transmigrated, T cells migrate into T cell follicles. B cells, on the other hand, remain in close proximity to HEVs for several hours, scanning adjacent DCs. Afterwards, B cells move along a network of stromal cells and enter B cell follicles, a process depending on CXCR5-CXCL13 interaction (Girard et al., 2012). If lymphocytes do not encounter their cognate antigen in the LN, they egress rhythmically through medullary lymphatic sinuses (Druzd et al., 2017; Suzuki et al., 2016), a process regulated by S1P signals from lymphatic ECs (Matloubian et al., 2004). Although lymphatic sinuses are close to HEVs, B cells do not leave the LN directly, which might be explained by the fact that B cells gradually retrieve the receptor for S1P (S1PR1) during their way through the tissue (Park et al., 2012).

Not only lymphocytes, but also neutrophils circulate through LNs, since this cell type was recently detected in human and murine LNs under steady-state conditions (Lok et al., 2019). A recent study could show that LN entry of neutrophils through HEVs is L-selectin-

dependent and that their egress via efferent lymphatics is, very similar to that of lymphocytes, regulated by S1PR1 (Bogoslowski et al., 2018; Bogoslowski et al., 2020). Next to L-selectin, trafficking of this subset is dependent on CD11a, CXCR4, ICAM-1, and CD49d and alike other organs under circadian control, resulting in preferential homing at the beginning of the behavioral active phase (He et al., 2018). The molecular interactions during leukocyte trafficking in LNs are illustrated in **Figure 1-3**.

### 1.2.5.3 Spleen

Regarding leukocyte migration, the spleen is very similar to LNs, although it lacks HEVs and afferent lymphatics. The spleen receives its blood supply from the splenic artery, and is drained by the splenic vein, which are both emerging from the hilum. The organ structure is organized into the red and white pulp. Lymphocytes reside in the latter, which is located centrally and further divided into inner T cell zones and outer B cell follicles. B cell attraction to the spleen depends on endothelial CXCL13 and Clever-1 (Tadayon et al., 2019), whereupon CXCR5-CXCL13 interactions also orchestrate their interstitial migration (Lewis et al., 2019). The marginal zone between the red and white pulp comprises B cells, macrophages and reticular cells (Mebius and Kraal, 2005). In mice, specialized marginal zone B cells reside in this area via interaction of LFA-1 and  $\alpha_4\beta_7$  (LPAM) with ICAM-1 and VCAM-1 (Lewis et al., 2019). Due to open arterioles, the red pulp is freely accessible via the blood flow. In particular, block of CD11a and ICAM-1 impaired B cell extravasation from the blood into the tissue in a time-of-day-dependent manner (He et al., 2018). For entry of the white pulp signaling through LFA-1 and VLA-4 seems to be necessary (Lo et al., 2003). In contrast, other studies using blocking antibodies in combination with adoptive cell transfer found no role for LFA-1 in lymphocyte migration to the white pulp (Nolte et al., 2002).

In healthy humans and mice, a large pool of neutrophils with a distinct phenotype (CD62L<sup>low</sup> CD11b<sup>high</sup> ICAM-1<sup>high</sup>) is located close to B cells in the marginal zone, aiding in their activation (Puga et al., 2011). In addition, aged neutrophils migrate to the spleen, which are removed from the circulation under physiological conditions (Hyun and Hong, 2017). Moreover, L-selectin was found to be required for rhythmic homing of neutrophils and B cells to the spleen (He et al., 2018), whereas the egress of both cell types is dependent on S1P-S1PR1 interaction (Blaho and Hla, 2014). Together with the LN, leukocyte trafficking in the spleen is summarized in **Figure 1-3**.

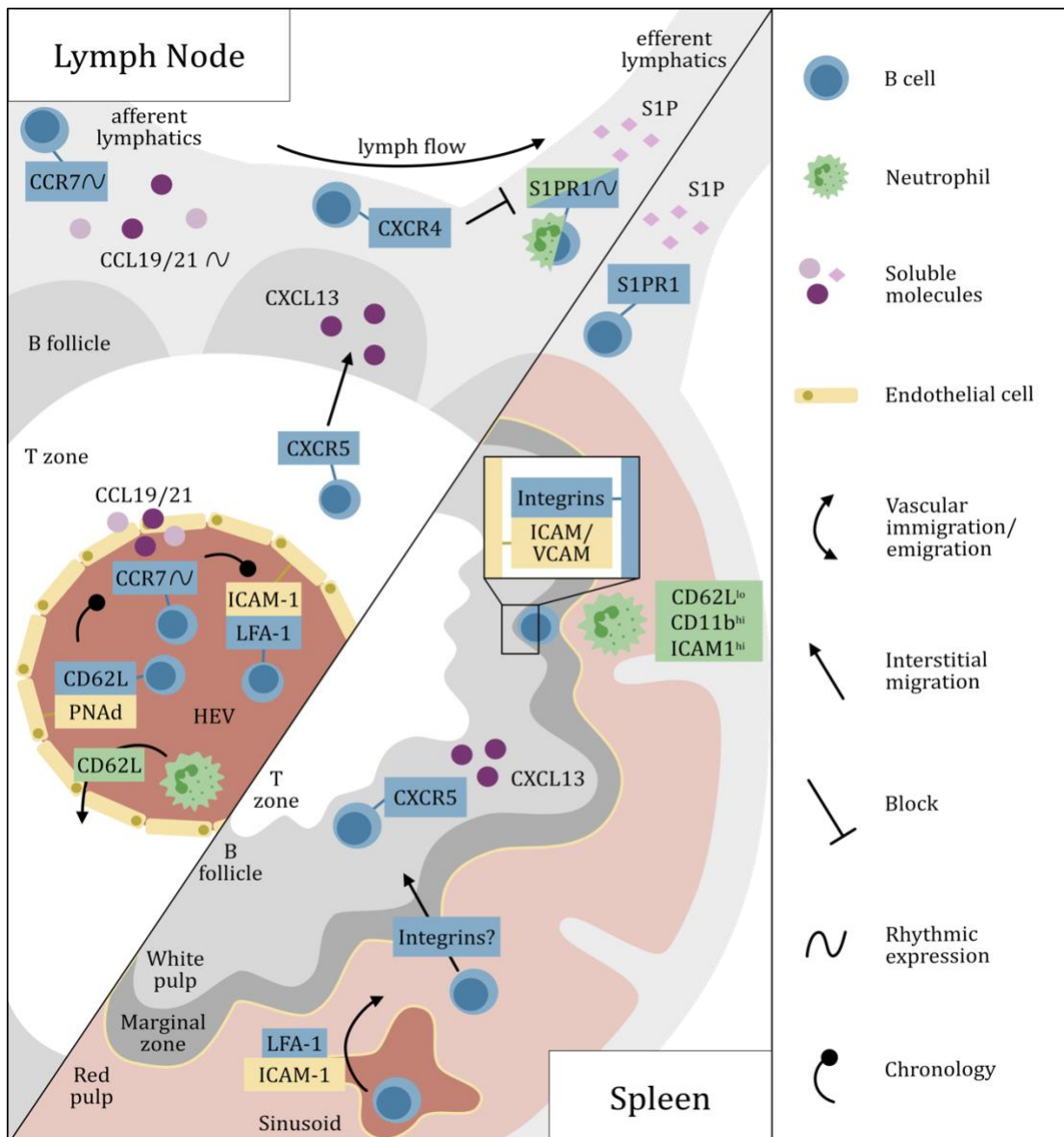


**Figure 1-3: Leukocyte trafficking in the lymph node and spleen.**

In the LN, some lymphocytes enter through afferent lymphatics, guided by CCR7-CCL19/CCL21 interaction. However, naïve B cells enter through HEVs in a sequential process of interaction of CD62L and PNA, followed by activation of CCR7 via its ligands CCL19/CCL21 and LFA-1 with ICAM-1. Transmigrated B cells enter B follicles guided by CXCR5-CXCL13 interaction. B cells leave the LN via S1P-S1PR1 binding, as S1P levels are higher in efferent lymphatics. This process is opposed by CXCR4 and CCR7. Neutrophils circulate through the LN as well, for which they require CD62L and S1PR1. In the spleen, leukocytes enter the red pulp through blood sinusoids, mediated by LFA-1 interactions with endothelial ICAM-1. From the red pulp, B cells migrate to the white pulp, which probably requires integrin signaling. In the B cell follicle, B cells migrate via CXCR5-CXCL13 interaction. Marginal zone B cells are captured via integrin binding to endothelial ICAM-1 and VCAM-1. Neutrophils with specific expression profiles are localized close to these lymphocytes.

#### 1.2.5.4 Liver

Besides its metabolic function, the liver constantly encounters antigens from the intestinal tract as it receives the majority of its blood supply from the mesenteric venous circulation. Additionally, systemic antigens reach the liver via the arterial circulation. Hence, to maintain homeostasis the liver contains immune cells including myeloid-derived DCs and Kupffer cells (tissue resident macrophages), as well as conventional (CD4<sup>+</sup> and CD8<sup>+</sup> T cells, B cells, NK cells) and unconventional (NKT cells,  $\gamma\delta$  TCR<sup>+</sup> T cells, CD4<sup>+</sup>CD8<sup>-</sup> T cells) lymphocytes (Nemeth et al., 2009). On the contrary, neutrophils are mostly absent and have to immigrate (Gregory et al., 1996). The large hepatic blood vessels terminate in capillaries lined by fenestrated liver sinusoidal ECs (LSECs) (Wisse, 1972), a cell type important for antigen presentation and interaction with leukocytes. Under homeostatic conditions, LSECs were found to express a different set of adhesion molecules than post-capillary venules, with very low expression of VCAM-1 and E/P-selectins, whereas VAP-1 and ICAM-1 are constitutively expressed (Steinhoff et al., 1993). However, it was shown that VCAM-1 expression increases in mice over the day and is involved in rhythmic neutrophil recruitment to the liver at night (He et al., 2018). These adhesion molecules interact with  $\beta_2$ -integrins expressed on leukocytes, whereby LFA-1 binds with lower affinity than Mac-1 (Tong et al., 2018). Another difference between venules and sinusoids is that leukocyte rolling along sinusoidal endothelium does not require selectins. It was thought that physical trapping of neutrophils alone regulates adhesion in the liver (Wong et al., 1997). However, CD44 could be identified as crucial molecule in neutrophil recruitment following challenge with lipopolysaccharide (LPS). Absence or block of CD44 resulted in reduced neutrophil adhesion in sinusoids and inhibition of the CD44/HA interaction diminished neutrophil entry into the liver parenchyma (McDonald et al., 2008). A study from 2009 identified ESAM, a nonclassical member of the JAM family, as important molecule for hepatic neutrophil transmigration in ischemia-reperfusion, whereas it was not mediating the transmigration of T cells in this injury context (Khandoga et al., 2009).

Regarding lymphocytes, increasing evidence indicates that selective integrin-dependent and -independent recruitment mechanisms to the liver exist under steady-state and inflammatory conditions. Whereas  $\beta_2$ -integrins mediate leukocyte adhesion in post-sinusoidal venules (Li et al., 2004), the majority of leukocytes located in sinusoids does not require the activation of these adhesion molecules, as TNF $\alpha$ -induced adhesion was not affected by the absence of their ligand ICAM-1 (Patrick et al., 2007). As mentioned above, VAP-1 is highly expressed on endothelium of the human liver and supports

adhesion and transmigration of lymphocytes under physiological shear stress (Lalor et al., 2002). In contrast, murine hepatic ECs express only little amounts of VAP-1 under steady state, but upregulate expression under inflammatory conditions (Bonder et al., 2005). Important for hepatic immune cell trafficking is the chemokine receptor CXCR3 and its ligands CXCL9, CXCL10 and CXCL11. However, their function seems to be redundant, since block of individual molecules only partially affected leukocyte migration (Curbishley et al., 2005). Infiltrating lymphocytes bind VCAM-1 on hepatic ECs via CXCL16 mediated integrin activation (Heydtmann et al., 2005). In contrast, blocking of the VCAM-1 binding partner VLA-4 led to increased B cell numbers in the liver (He et al., 2018). Similar to the LN, B cell homing to the liver was affected in mice deficient for Cosmc, an endoplasmatic molecular chaperone that is required for successful formation of extended O-glycans (Zeng et al., 2020). Summarized, leukocyte trafficking in the liver is highly dependent on the anatomical location as well as the stimulus, although underlying processes are not fully understood yet (**Figure 1-4**).

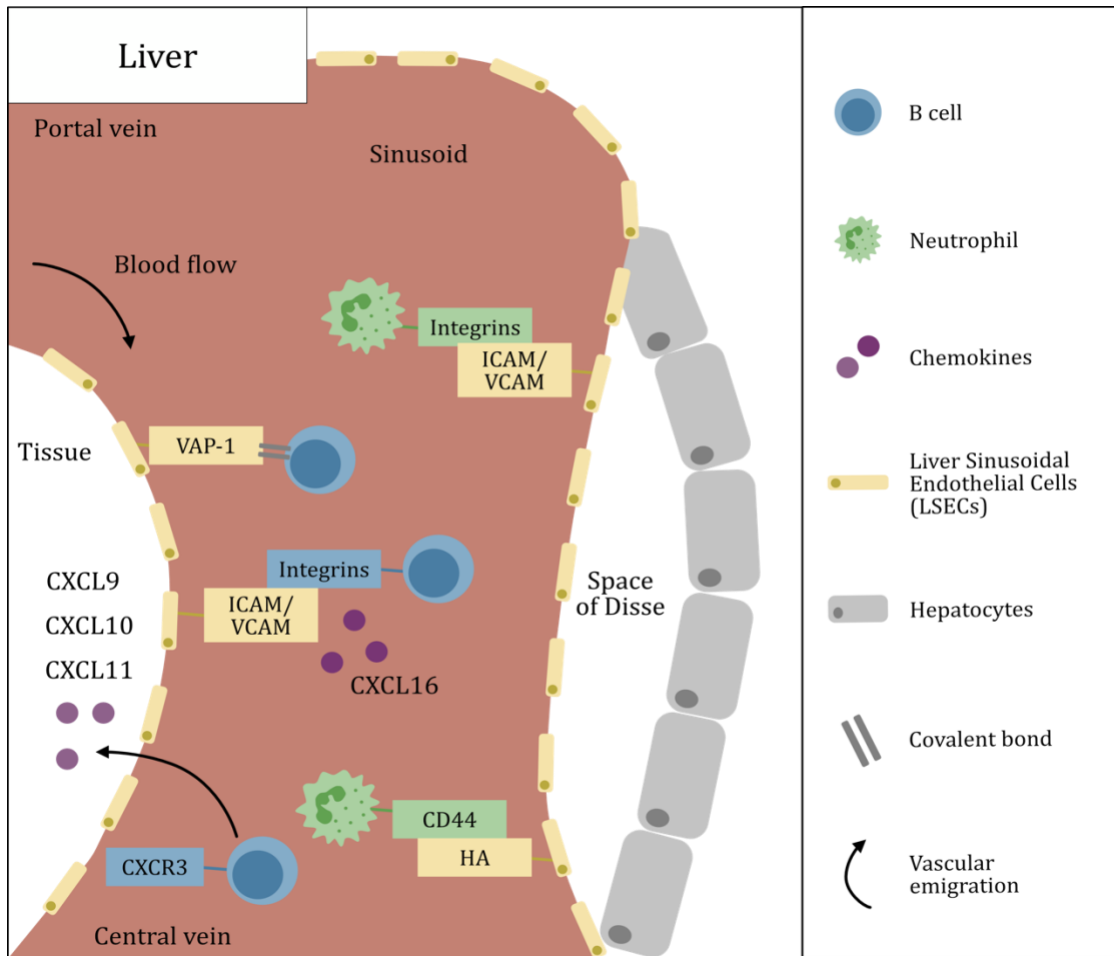


**Figure 1-4: Leukocyte trafficking to the liver.**

Leukocyte trafficking takes place in sinusoids, which are lined by a fenestrated layer of liver sinusoidal endothelial cells (LSECs). Neutrophils interact with these cells via integrins, which bind to ICAM-1 and VCAM-1. Moreover, CD44 binding to hyaluronic acid (HA) facilitates neutrophil migration in the liver. B cells can interact with LSECs via covalent bonds generated by VAP-1, which is highly expressed in the human liver. Their adhesion is mediated by integrin binding to ICAM-1 and VCAM-1 and regulated by the chemokine CXCL16. B cell transmigration into the tissue requires CXCR3 binding to its ligands CXCL9, CXCL10 and CXCL11.

#### 1.2.5.5 Lung

The lung is constantly exposed to airborne pathogens and thus has to assure an effective host defense. Similar to the liver, it receives blood from two circulatory pathways, one transporting oxygen under high pressure to the bronchial tree, the other responsible for gas exchange under low pressure (Aird, 2007). The alveolus represents the smallest functional unit and is separated by a thin membrane from a vast network of capillaries. In comparison to systemic circulation, the majority of leukocyte trafficking does not occur in post-capillary venules but in these pulmonary capillaries, which exhibit a continuous EC layer. Under steady-state conditions, their vascular bed harbors a large pool of leukocytes, including neutrophils, monocytes, and lymphocytes.

Due to the fact that the diameter of capillaries (2-14  $\mu\text{m}$ ) is smaller than that of a neutrophil (13.7  $\mu\text{m}$ ) and most other leukocyte subsets, leukocytes cannot roll along the endothelium, but have to deform to search for a suitable transmigration site (Doerschuk et al., 1993). In combination with the low blood flow prolonging the time of transit as well as CXCR4-CXCL12 interactions (Devi et al., 2013), neutrophils are highly enriched in the lung, called 'marginated pool' (Wiggs et al., 1994), from which they can detach quickly in response to an inflammatory challenge (Yipp et al., 2017). In addition, a recent study showed that after sterile liver injury, neutrophils reenter the circulation from the liver and migrate to marginated pools in the lung, where they increase expression of CXCR4 and home back to the BM for clearance (Wang et al., 2017). B cell recruitment to the lung under steady state can be blocked by inhibition of ICAM-1, CXCR4, CD49d, and CD11a (He et al., 2018).

In general, and in contrast to the steady state, leukocyte recruitment to the lung differs between various disease models. Mechanisms can involve L- and E-selectin, e.g. during an LPS challenge, but they have also been shown to be  $\beta_2$ -integrin-independent, e.g. in a lung injury followed by *Escherichia coli* administration (Maas et al., 2018), suggesting a compensatory mechanism. Classical adhesion molecules for leukocyte capture are not involved in lung recruitment, but once neutrophils are in contact with the stimulated endothelium, L-selectin and integrins are necessary to hold the cells inside the capillaries (Kubo et al., 1999). Furthermore, a critical role for ICAM-1 and LFA-1 for neutrophil recruitment during LPS-induced inflammation was demonstrated using mice deficient for these molecules (Basit et al., 2006). Monocytes are recruited to the lung in a CCR2-dependent manner, whereas neutrophils intravasate independently of CCR2. However, CCR2<sup>+</sup> monocytes were found to augment a neutrophil accumulation (Maus et al., 2003). In mice, endothelial and leukocyte-expressed CXCR2 is the most important chemokine receptor mediating LPS-induced neutrophil recruitment (Reutershan et al., 2006; Strieter et al., 2005). A visual summary of leukocyte trafficking in the lung is presented in **Figure 1-5**.

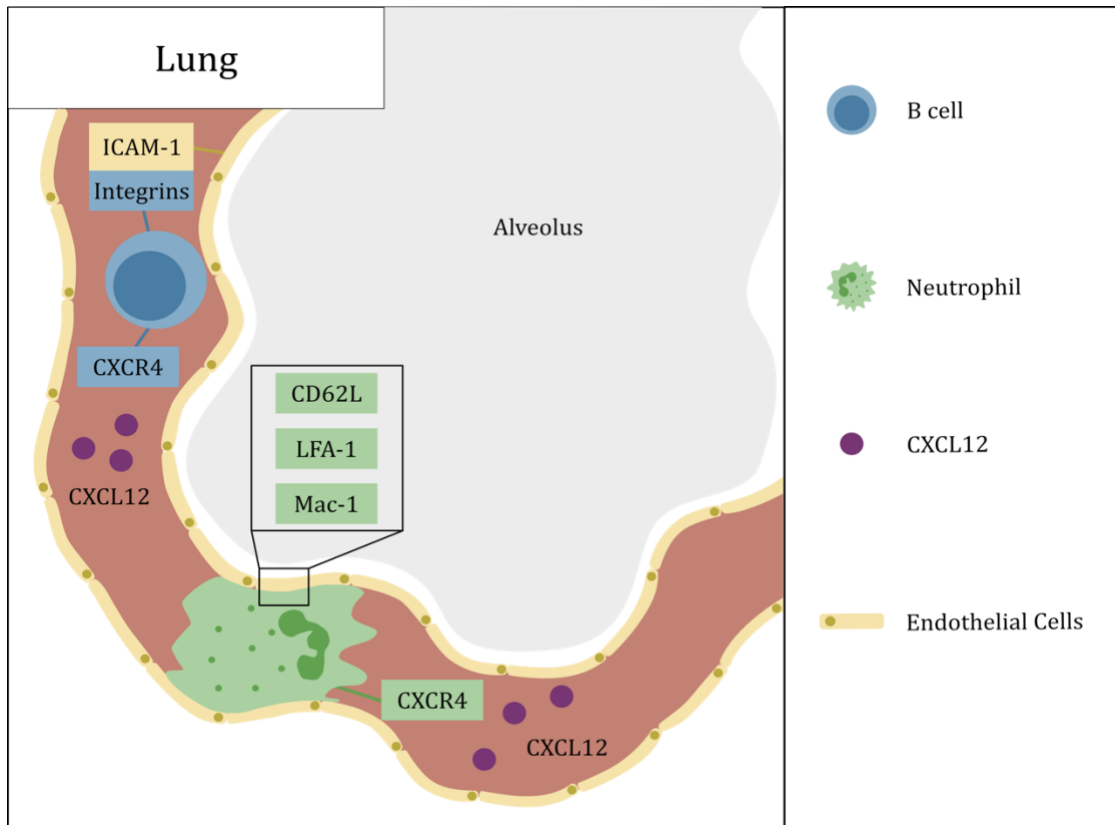


**Figure 1-5: Leukocyte trafficking in the lung.**

Due to the constricted vessel size of sinusoids, neutrophils have to deform and crawl through the vessel, mediated by CXCR4 and CXCL12. To reside in the pulmonary vasculature, the adhesion molecules CD62L, LFA-1 and Mac-1 are important. Lymphocytes require this receptor-ligand-axis as well and interact with lung endothelial cells via integrin binding to ICAM-1.

Combined, these data illustrate the intricacy of leukocyte trafficking to various organs. Besides immune cell type-specificity, anatomical properties of the respective organ play an important role. To add another level of complexity, the tissue microenvironment is under influence of the sympathetic nervous system. In the next section, features of the sympathetic nervous system, as well as its innervation of the investigated organs is presented, followed by current knowledge about its control of leukocyte trafficking.

## 1.3 The sympathetic nervous system

Similar to the immune system, the nervous system comprises a complex network of various cell types interacting with each other as well as numerous other components in the body. The nervous system of vertebrates is classified into the central nervous system (CNS) and the peripheral nervous system, which further subdivides into the somatic, sensory and autonomic nervous system. The autonomic nervous system is not under conscious control and consists of the interconnected sympathetic (SNS) and parasympathetic nervous system (PNS). The SNS emerges from the thoracolumbar spinal cord and is responsible for the so-called “fight-or-flight” response by controlling the activation of cardio-vascular organs. Its counterpart, the PNS, is derived from the cranial nerves and the sacral spinal cord and drives digestive processes during the resting state. The SNS consists of preganglionic neurons acting via acetylcholine (ACh) on postganglionic neurons, which innervate peripheral target tissues such as lymphoid organs (Bellinger et al., 2008; Felten et al., 1987; Nance and Sanders, 2007).

### 1.3.1 Catecholamines

From its nerve varicosities the SNS mainly releases the catecholamine norepinephrine (noradrenaline, NE) with the exception of some cholinergic sympathetic nerves releasing ACh (Zeisel et al., 2018) or dopamine, such as in sweat glands and the periosteum (Apostolova and Dechant, 2009). Additionally, the SNS innervates the adrenal gland, thus triggering the systemic release of epinephrine (adrenaline, EPI) and glucocorticoids into the blood. Catecholamines contain a catechol or 3,4-dihydroxyphenyl group as well as a side chain amine and act in the body as hormones and neurotransmitters. The synthesis of NE starts with the transformation of the amino acid tyrosine into levodopa through tyrosine hydroxylase (TH). Levodopa is decarboxylated into dopamine by DOPA decarboxylase. NE is synthesized from dopamine by dopamine  $\beta$ -hydroxylase and can be converted to EPI by phenylethanolamine N-methyltransferases in the adrenal medulla (Kuhar et al., 1999). Production and release of these catecholamines into the blood stream follows a time-of-day-dependent rhythm, which is reciprocal in mice and humans (De Boer and Van der Gugten, 1987; Linsell et al., 1985; Sauerbier and von Mayersbach, 1977). However, conditions of these rhythms differ between NE and EPI. Whereas EPI exhibits self-sustained rhythmicity, NE oscillations only persisted in the presence of external cues,

such as food uptake, and thus cannot be termed truly circadian (Leach and Suzuki, 2020; Stanley et al., 1989).

Moreover, their levels differ between tissues as well as between tissue compartments, as shown for LNs (Felten et al., 1985) and although EPI and NE bind to the same receptors, EPI shows a higher affinity for e.g.  $\beta_2$ -adrenoceptors than NE (Liapakis et al., 2004).

These neurohormones influence multiple activities in the body as rapid responses to environmental changes, such as blood pressure increase and bronchial relaxation, which are part of the “fight-or-flight” response. Thus, these mechanisms are considered as prerequisite for survival. However, prolonged increase of catecholamines can lead to pathological conditions, like hypertension and heart failure (Tank and Wong, 2015).

### 1.3.2 Adrenergic receptors

The cell surface receptors to which catecholamines bind are called adrenergic receptors (AR). ARs belong to the guanine nucleotide-binding GPCR superfamily of seven-transmembrane proteins. The GPCRs are classified into  $\alpha_1$ -,  $\alpha_2$ - and  $\beta$ -ARs, which can be further subdivided into  $\alpha_{1A}$ -,  $\alpha_{1B}$ -,  $\alpha_{1C}$ -,  $\alpha_{2A}$ -,  $\alpha_{2B}$ -,  $\alpha_{2C}$ -, as well as  $\beta_1$ -,  $\beta_2$ -, and  $\beta_3$ -ARs. Depending on the interconnected G protein of the receptor, different signaling pathways can be initiated upon ligand binding. The heterotrimeric G protein complex consists of an  $\alpha$  subunit, which can be stimulatory ( $G_s$ ), inhibitory ( $G_i$ ) or activate phospholipase C enzymes ( $G_q$ ), and a  $\beta\gamma$  complex (Pierce et al., 2002).  $\alpha_1$  is  $G_q$ -coupled,  $\alpha_2$  is  $G_i$ -coupled, and  $\beta$ -ARs are predominantly  $G_s$ -coupled, but can switch to  $G_i$  (**Figure 1-7**). GPCRs exhibit diverging affinities for different catecholamines and vary in expression levels on target cells. Since  $\beta$ -ARs are the predominant receptor type expressed on leukocytes (Elenkov et al., 2000), they were used as targets for pharmacological modulation in this study.

The first member of the  $\beta$ -AR family is the predominant receptor in the heart, where it regulates myocardial contractility. Thus, antagonists of the  $\beta_1$ -AR are commonly used as therapeutics for cardiovascular diseases like hypertension. In humans, it is also expressed in the kidney and fat cells, regulating renin release and lipolysis, respectively (Alhayek and Preiss, updated 2020 Aug 11).

The  $\beta_2$ -AR was the first GPCR to be cloned (Dixon et al., 1986) and characterized based on its physiological properties. It was thought to predominantly inhibit the immune system via cyclic adenosine monophosphate (cAMP) and protein kinase A (PKA). Importantly, to current knowledge signaling pathways of this receptor subtype are much more complex. It is regulated by G protein-coupled receptor kinases (GRKs) and  $\beta$ -arrestins (**Figure 1-6**).

$\beta_2$ -ARs are expressed by every immune cell type, exhibiting varying expression levels, which could explain a differential cell responsiveness to adrenergic stimuli. NK cells show the highest number of receptors per cell, B cells and monocytes have intermediate numbers and T helper (Th) cells show the lowest numbers of receptors on their surface (Elenkov et al., 2000). Eosinophils express about 7,166 receptors per cell (Yukawa et al., 1990) and on neutrophils receptor binding assays revealed approximately 900 receptors (Galant and Allred, 1981). Interestingly, Th1 cells express  $\beta_2$ -ARs, whereas Th2 cells do not (Sanders et al., 1997). Expression levels also vary during maturation and aging (Radojicic et al., 1991). Furthermore, responsiveness to stimuli does not necessarily depend on receptor density, as coupling of GPCRs and adenylyl cyclase (AC) plays a role as well (Maisel et al., 1989).

The human *Adrb3* gene was first cloned in 1989 (Emorine et al., 1989). Since then, it was identified in several other species like mouse, where two tissue-specific splice variants were characterized (Evans et al., 1999). In comparison to the other two subtypes, the  $\beta_3$ -AR lacks the phosphorylation sites for PKA and  $\beta$ -AR kinase ( $\beta$ ARK), protecting it from desensitization (Nantel et al., 1993), whereas a similar process can occur downstream in the signaling cascade by reduction of AC function (Michel-Reher and Michel, 2013). However, data in this regard are not always consistent and have to be interpreted carefully (Okeke et al., 2019). The human  $\beta_3$ -AR has been detected in blood vessels, brain, urinary bladder, adipose tissue, myocardium, and several other tissues (Skena and Caplan, 2019). The murine receptor is most abundant in white and brown adipose tissue where it mediates thermogenesis and lipolysis (Nahmias et al., 1991), but is also expressed by stromal cells in the BM (Mendez-Ferrer et al., 2008). Mice lacking  $\beta_3$ -ARs show a modest increase in fat stores with females being more affected than males. Furthermore, *Adrb1* mRNA is upregulated in adipose tissues of these mice, suggesting a crosstalk between these receptor subtypes (Susulic et al., 1995).

### **1.3.3 Sympathomimetic/sympatholytic agents**

Due to the crucial role of catecholamines in diverse physiological processes, drugs for clinical use have been developed. These drugs are classified as sympathomimetic when mimicking the action of catecholamines, and as sympatholytic when blocking the binding of catecholamines to their receptors. These reagents can be administered via various routes and are able to act directly by binding to the respective ARs, or indirectly by regulating endogenous catecholamine levels (Westfall, 2009). Short acting  $\beta$ -AR agonists

(SABA) like Salbutamol are used for resolution of acute bronchoconstriction and are therefore the frontline therapy of asthma. They start acting within a few minutes and last for about four to six hours. Long acting  $\beta$ -AR agonists (LABA) like Salmeterol and Formoterol are used as first treatment of chronic obstructive pulmonary disease (COPD). Maintenance treatment of patients with COPD requires ultra-long acting  $\beta$ -AR agonists (Ultra-LABA) like Indacaterol. It is rapidly absorbed and functions for about 24 hours (Billington et al., 2017).

Sympathomimetic and sympatholytic agents can either target the whole family of receptors, like the pan- $\beta$ -AR agonist Isoproterenol and the pan- $\beta$ -AR antagonist Propranolol, or they can exhibit selectivity for distinct subtypes.

Denopamine is a selective agonist of  $\beta_1$ -ARs and exhibits, like all agonists, dose-dependent effects (Masanori et al., 1987). As selective  $\beta_2$ -AR agonist, long-acting Clenbuterol was used in this study (Hall et al., 1980). It shows similar properties as Salbutamol and is utilized as bronchodilator in diseases like asthma (Al-Majed et al., 2017b). Several  $\beta_3$ -AR agonists have been tested in clinical trials, such as Mirabegron for treatment of overactive bladder syndrome (Takasu et al., 2007). In this thesis, the  $\beta_3$ -AR agonist BRL37344 was used, which belongs to the first-generation compounds and was developed in 1990. It displays a higher affinity and potency for rodent over human receptors (Nahmias et al., 1991). Although it shows higher selectivity for  $\beta_3$ - compared to  $\beta_1$ - and  $\beta_2$ -ARs, evidence exists that also other ARs are stimulated by this agonist (Mori et al., 2010; Pott et al., 2003).

#### 1.3.4 Adrenergic signaling pathways

To understand how adrenergic signaling influences immune cell trafficking, it is important to understand the different molecular mechanisms that can be triggered by stimulation of  $\beta$ -ARs (**Figure 1-6**). Attachment of an agonist to the  $\beta$ -AR leads to its conformational change facilitating the binding of the  $G_s$  heterotrimer (consisting of  $\alpha$ ,  $\beta$  and  $\gamma$  subunits) to the receptor. Subsequently, guanosine diphosphate (GDP) in the  $\alpha$ -subunit is replaced by guanosine triphosphate (GTP), resulting in the dissociation of the  $\alpha$ - and  $\beta\gamma$ -subunits from the GPCR. After recruitment of the  $\alpha$ -subunit to the membrane-associated lipid raft, it activates AC, whereas the  $\beta\gamma$ -subunit regulates  $Ca^{2+}$  channels. AC facilitates the hydrolysis of adenosine triphosphate (ATP) to cyclic adenosine monophosphate (cAMP). PKA is activated by binding of cAMP to its regulatory subunit and subsequent release of the catalytic subunit. With the help of A-kinase anchor proteins (AKAPs), PKA is localized in proximity to its various substrates, while one isoform of PKA localizes to the cell

membrane and the other remains intracellular where it mediates gene transcription (Lorton and Bellinger, 2015). Afterwards, different mechanisms can lead to a downregulation of cAMP levels (Vandamme et al., 2012) and the  $G_s$  heterotrimer reassembles by conversion of GTP back to GDP (Rasmussen et al., 2011).

$\beta$ -AR concentrations on cell surfaces are dynamically regulated by neurotransmitter concentrations. In a multistep process, high levels lead to a decreased responsiveness and following downregulation, which results from GPCR phosphorylation by GRKs (Choi et al., 2018). After  $\beta$ -arrestin-1 induced receptor internalization, GPCRs are either degraded or recycled.

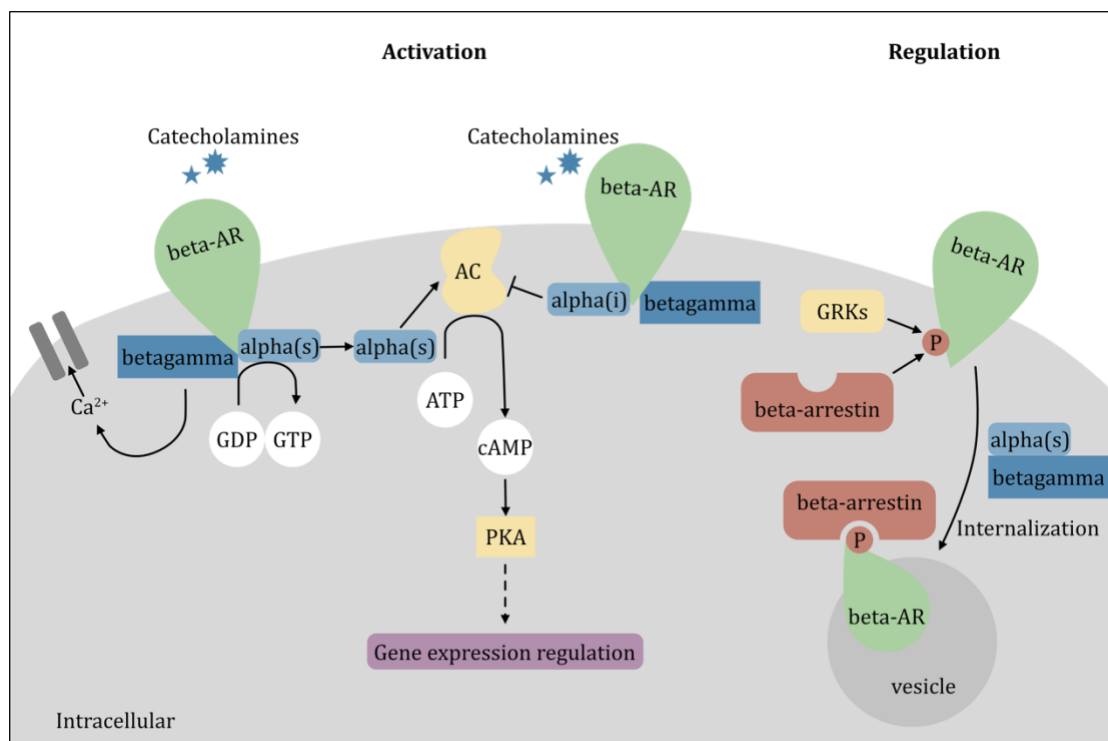


**Figure 1-6: Activation and regulation of  $\beta$ -ARs.**

After binding of catecholamines to  $\beta$ -ARs the heterotrimeric G protein is recruited to the receptor (step not shown). When GDP on the  $\alpha(s)$  subunit is converted to GTP, the G protein dissociates. While the  $\beta\gamma$ -subunit regulates  $Ca^{2+}$  channels, the  $\alpha(s)$ -subunit relocates to the lipid raft, where it activates adenylyl cyclase (AC). This enzyme catalyzes the conversion from ATP to cAMP, which activates the protein kinase A (PKA). This enzyme is responsible for GPCR-regulated changes in gene expression. If the heterotrimeric G protein consists of an inhibitory  $\alpha$ -subunit ( $\alpha(i)$ ), the activity of AC is blocked. To regulate the signaling through  $\beta$ -ARs, G protein-coupled receptor kinases (GRKs) phosphorylate the receptor, to which  $\beta$ -arrestin binds, leading to receptor internalization.

Extensive investigation of the  $\beta_2$ -AR revealed alternative routes without AC and cAMP involvement, called non-canonical pathways (Figure 1-7). Although its signaling is mainly

regulated by  $G_s$ , GPCR phosphorylation by PKA decreases the binding affinity for  $G_s$ , resulting in a switch from  $G_s$  to  $G_i$  (Daaka et al., 1997). This pathway leads to the activation of extracellular signal-regulated kinase (ERK) via the  $\beta\gamma$ -subunit. In addition, the  $\alpha$ -subunit was shown to activate ERK in a cascade involving the non-receptor tyrosine kinase c-Src and the G protein Rat Sarcomer (Ras) (Daaka et al., 1997). Other more recent studies also demonstrated a mechanism independent of G proteins (Shenoy et al., 2006) and evidence for a  $\beta$ -arrestin independent pathway of ERK activation via  $\beta_2$ -AR signaling (O’Hayre et al., 2017). In HEK-293 cells, activation of this AR subtype led to intracellular  $Ca^{2+}$  flux via activation of phospholipase C (PLC) and inositol triphosphate ( $IP_3$ ), independently of cAMP (Galaz-Montoya et al., 2017).

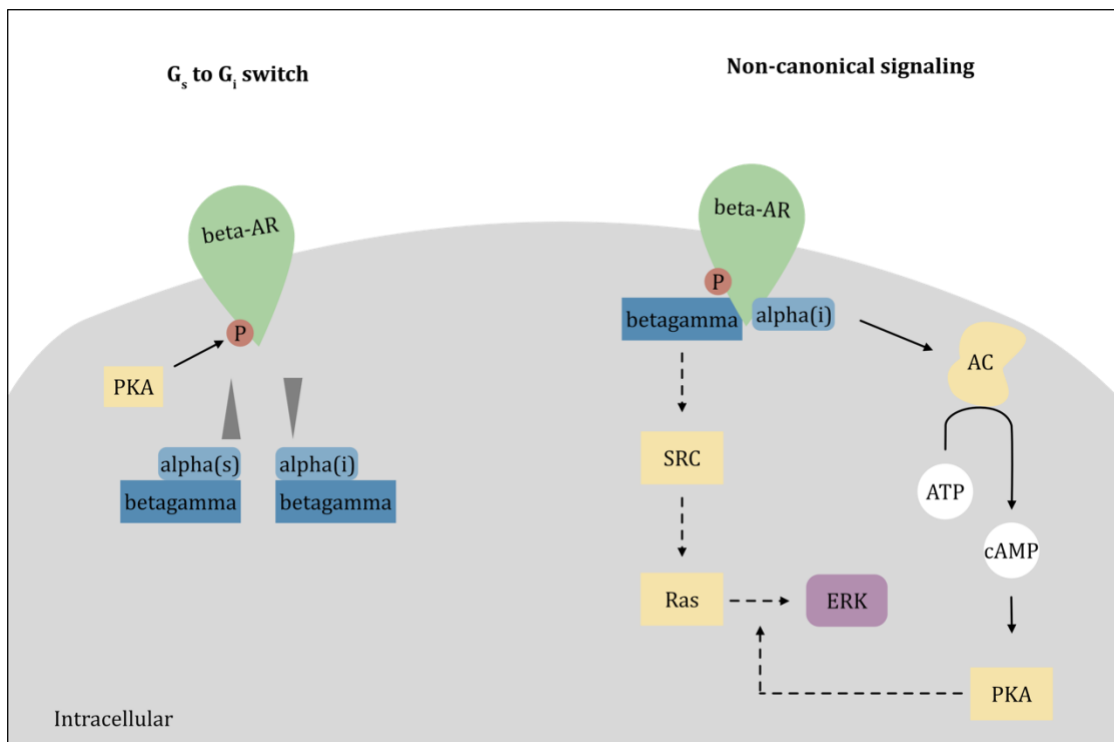


**Figure 1-7: G protein switch and non-canonical signaling.**

When protein kinase A (PKA) phosphorylates  $\beta$ -ARs, the affinity for  $\alpha(s)$  is reduced, while the affinity for  $\alpha(i)$  is increased, leading to a switch of G proteins associated with the receptor. During non-canonical signaling, the  $\beta\gamma$ -subunit activates the extracellular signal-regulated kinase (ERK) via SRC and Ras activation. Meanwhile, the  $\alpha(i)$ -subunit activates AC, resulting in higher cAMP levels. This second messenger activates PKA, which in turn activates other molecules in the signaling cascade leading to ERK activation.

### **1.3.5 Sympathetic innervation of peripheral organs**

As in this thesis the influence of adrenergic stimulation on leukocyte trafficking in selected organs was investigated, it is necessary to understand how these tissues are innervated by the SNS. In the following, sympathetic innervation of the BM, LNs, spleen, liver, and lung are described.

#### **1.3.5.1 Bone marrow**

To reach the BM, efferent sympathetic nerves enter small tunnels of the cortex (nutrient foramina) of long bones and run along the vasculature in microscopic channels of the cortical bone (Haversian and Volkmann's canals) (Calvo, 1968). There, nerves positive for TH, the rate limiting enzyme in NE production, are more abundant than nerves containing neuropeptide Y and vasoactive intestinal peptide (Tabarowski et al., 1996). The BM vasculature consists of evenly distributed sinusoids and arterioles, thus bringing SNS varicosities in close proximity to immune cells. Previous studies showed that adrenergic signals regulate bone formation (Takeda et al., 2002) and HSC release from the BM (Katayama et al., 2006), the latter in a rhythmic manner (Mendez-Ferrer et al., 2008; Scheiermann et al., 2012).

#### **1.3.5.2 Lymph nodes**

In LNs adrenergic fibers enter at the hilar region along with blood vessels, distributing into a subcapsular nerve plexus or into the medulla through the medullary cords (Felten et al., 1984). Sympathetic nerve fibers in rodents surround germinal centers and extend into paracortical and cortical regions, where they end among lymphocytes (Felten et al., 1985). The innervation of human LNs is similar, which is mostly associated with blood vessels (Panuncio et al., 2002).

#### **1.3.5.3 Spleen**

Sympathetic nerve fibers arising from the celiac-mesenteric ganglia enter the spleen at the hilum together with the splenic artery (Felten et al., 1987). In close proximity to the vasculature, they continue along the trabeculae into the trabecular plexuses (Williams and Felten, 1981). A dense nerve fiber network was found in multiple splenic compartments, including the periarteriolar lymphatic sheath (containing T cells), the marginal zones, the capsule, splenic nodules (B cell follicles), and red pulp, suggesting that B cell

differentiation and maturation in the splenic nodules as well as antigen presentation in the marginal zones is regulated by adrenergic innervation (Hu et al., 2020). Importantly, the microanatomy of rodent spleens differs from the one of human spleens, as e.g. the marginal zone is missing in humans (Steiniger, 2015). Furthermore, sympathetic innervation in murine spleens changes in the course of aging, since catecholamine-containing fibers as well as NE levels increase with rising age (Madden et al., 1997).

#### **1.3.5.4 Liver**

The sympathetic branch innervating the liver originates in the celiac and superior mesenteric ganglia receiving pre-ganglionic neurons from the intermediolateral column of the spinal cord (Yi et al., 2010). Nerve distribution differs between species, but in general sympathetic markers were detected in the hepatic artery, the portal vein region and in the area around bile ducts. In comparison to the human liver, rodent nerve fibers do not reach parenchymal cells (Fukuda et al., 1996). Nonetheless, this does not alter the parenchymal response to sympathetic innervation, probably due to the presence of cell-cell connecting gap junctions (Seseke et al., 1992). First, only  $\alpha$ -ARs could be identified in the hepatic arterioles and portal vein (Green et al., 1959), but the presence of  $\beta$ -ARs was demonstrated in the canine liver as well (Geumei and Mahfouz, 1968).

#### **1.3.5.5 Lung**

In the lung, sympathetic innervation mainly targets the vasculature. In contrast to other organs, nerve fiber density decreases from large vessels towards the periphery, but the density differs between species. Sympathetic and parasympathetic perivascular axons of rodents barely reach beyond the lung hilum, while in humans the innervation also reaches small vessels. The smallest intra-acinar arteries are not innervated. Pulmonary vascular resistance is predominantly regulated via  $\alpha_1$ -ARs. In this organ, nerve endings contain large and small vesicles with different neurotransmitter cocktails, which are released depending on the frequency of stimuli (Cifuentes et al., 2008). Hence, more than one transmitter is released, a phenomenon called purinergic co-transmission (Burnstock, 2009). Airway smooth muscle cells and other cell types in the lung, like immune cells including mast cells, macrophages and eosinophils, express  $\beta_2$ -ARs (Barnes, 2004). Hence, in humans, the lung is a common target for  $\beta_2$ -AR agonists to treat airway diseases like asthma and COPD.

## 1.4 Neuro-immune crosstalk

To maintain homeostasis as well as fight pathogens, cross-talk between the immune system and the nervous system is essential. Two regulatory pathways are responsible for signal transduction, the hypothalamic-pituitary-adrenal axis (HPA) and the SNS. The latter communicates with immune cells via synaptic varicosities releasing NE or by the systemic adrenal hormone EPI, which are both recognized by ARs expressed on a variety of cell types in target organs. Under homeostatic conditions the SNS leads to recovery after an injury or immune challenge, which involves the regulation of cell differentiation, expansion and effector functions (Lorton and Bellinger, 2015; Nance and Sanders, 2007). Observed effects of catecholamines on various aspects of immunity depend on the microenvironmental and inflammatory context as well as catecholamine levels. Moreover, catecholamines can affect leukocyte function and migration on multiple levels, controlling mechanical cell properties, cytokine release, and expression of adhesion molecules. Importantly, these catecholamines do not necessarily have to originate from nerve endings since they can also be produced and released by immune cells like macrophages (Flierl et al., 2007) or T cells (Rosas-Ballina et al., 2011). Stimulation of  $\beta_2$ -ARs has various effects on immune cell function, such as inhibition of NET formation (Marino et al., 2018). *In vitro* treatment of neutrophils with NE also impaired neutrophil chemotaxis, phagocytosis, and activation via suppressed production of  $\text{IFN}\gamma$  and IL-10 (Nicholls et al., 2018). In this study, the influence of adrenergic stimulation – in particular  $\beta$ -AR stimulation – on leukocyte trafficking was investigated. Hence, a short summary of the current knowledge about the complex effects of adrenergic signals on leukocyte mobilization and recruitment to tissues is given.

### 1.4.1 Leukocyte trafficking under adrenergic control

The life time of many immune cells in the body is severely limited, thus their numbers have to be regularly replenished to maintain homeostasis. Cells capable of self-renewal, proliferation and differentiation, called HSCs, and partially lineage-committed HSPCs, leave their niches in the BM and circulate through blood and lymph to reach peripheral tissues (Massberg et al., 2007). Under steady-state conditions in mice, egress of HSPCs from the BM is regulated by catecholamines targeting  $\beta_3$ -ARs on stromal cells, leading to a downregulation of the retention factor CXCL12 (Mendez-Ferrer et al., 2008). Additionally, the mobilization factor G-CSF is cooperating with  $\beta$ -ARs, since abolishment

or block of sympathetic signaling reduced G-CSF-dependent HSPC mobilization (Katayama et al., 2006). On the other hand, circadian oscillations in adhesion to the BM vasculature are abolished upon loss of local innervation due to a leveled rhythmic expression pattern of endothelial ICAM-1 (Scheiermann et al., 2012). Using adoptive transfers of wild-type (WT) cells into mice lacking  $\beta_2$ - or  $\beta_3$ -ARs, this study also demonstrated the influence of both  $\beta$ -ARs on this process, since mice deficient for each receptor type exhibited reduced oscillations in recruitment as well as no circadian differences in adhesion molecule expression. A recent study unraveled the paradox of mobilization and homing being regulated by the same signals in a time-of-day-dependent context. They showed that during the day, the cholinergic neurotransmitter ACh inhibits adhesion, while noradrenergic signals facilitate cell mobilization via  $\beta_3$ -ARs. At night, higher levels of EPI stimulate  $\beta_2$ -ARs while cholinergic signals downregulate  $\beta_3$ -AR expression, favoring the process of homing (Garcia-Garcia et al., 2019). Hence, adrenergic and cholinergic signals function counteractively to regulate circulating leukocyte numbers over the course of a day.

In rats, short-term effects of EPI and NE administration are increased numbers of circulating leukocyte subsets (Dhabhar et al., 2012), suggesting an analogical mobilization effect for leukocytes compared to HSPCs. However, it is not clear whether rising numbers of circulating leukocytes are caused by adrenergic targeting of mobilization or demargination, the latter describing the fast detachment from vascular beds to reenter the circulation. Recently, it was shown for human granulocytes that *in vitro* incubation with catecholamines leads to a reorganization of cellular cortical actin, enabling demargination by reduction of cell stiffness (Fay et al., 2016). Interestingly, most leukocyte subtypes have left the circulation two hours post stimulation, whereas neutrophil numbers continue to increase, indicating a subtype-specific effect of catecholamines. Additionally, NE and EPI affect leukocyte numbers in blood in a different manner, as NE increases numbers of neutrophils and B cells, whereas administration of EPI increases numbers of neutrophils and monocytes, but decreases blood lymphocyte numbers (Dhabhar et al., 2012). Thus, next to the cell type-specificity of the response, also catecholamine-specific effects exist.

Another level of complexity was added by a study that investigated the impact of  $\beta_2$ -AR signaling on leukocyte recruitment between male and female mice. Using a dorsal skin air pouch model combined with LPS administration, they demonstrated that neutrophil

recruitment was higher in females compared to males, but that the presence of  $\beta_2$ -ARs is more important for neutrophil trafficking in males than in females. Moreover, comparison between female and male *Adrb2* deficient mice revealed different numbers of CD11a expressing neutrophils among recruited cells, showing higher numbers in males than females (de Coupade et al., 2007). Taken together, these data indicate a sexual dimorphism in the relationship between the sympathetic and immune system.

Chemokines play an important role in leukocyte trafficking as these molecules activate immune cells leading to a firm adhesion and finally to transendothelial migration through blood vessels. Several studies investigated the influence of the SNS on cytokine production and release. Exposure of neutrophils to EPI results in dose-dependent enhanced production of IL-8, but a suppressed production of IL-1 $\beta$ , IL-8, and monocyte chemoattractant protein 1 (MCP-1) when the treatment is combined with an LPS challenge. Moreover, CD11b expression on neutrophils increases under steady-state conditions, whereas after LPS-stimulation, CD11b and CD18 expression are suppressed (Margaryan et al., 2017). In contrast, another study demonstrated that stimulation with EPI, NE and the agonist Isoproterenol reduced N-formyl-methionyl-leucyl-phenylalanine (fMLP)-induced migration, CD11b/CD18 expression and ROS production, without influencing IL-8 expression of human polymorphonuclear cells (Scanzano et al., 2015). Taking these data together, catecholamines can exhibit differential effects on cytokine production, which seems to be dependent on the AR density on the cell surface (Wahle et al., 2005) as well as catecholamine dose and inflammatory context.

SNS activation is generally believed to have immunosuppressive effects. However, this is dependent on several conditions such as the metabolic state, since in obese mice,  $\beta_2$ -AR stimulation induced a shift towards an anti-inflammatory cytokine profile, whereas in the control group, pro-inflammatory cytokines prevailed (Gálvez et al., 2019). In response to multiple Toll-like receptor (TLR) signals, stimulation with NE blocks the secretion of pro-inflammatory cytokines by rapid induction of IL-10 from innate immune cells (Agac et al., 2018). Dysregulation of cytokine release can lead to a dangerously hyperactivated immune state, called cytokine release syndrome. How catecholamines originating from activated peritoneal macrophages influence these cytokine storms explored a study where LPS in combination with EPI produced an enhanced inflammatory response characterized by higher levels of IL-6, TNF $\alpha$  and CXCL1 as well as increased mortality (Staedtke et al., 2018).

To resolve inflammation or to respond to an injury, immune cells have to enter tissues by diapedesis through the endothelial barrier. In a cremaster muscle model, NE nearly completely stalled fMLP-induced neutrophil adhesion and arrest, as well as transmigration (Nicholls et al., 2018). Also, retention of lymphocytes in secondary lymphoid organs is affected by adrenergic stimulation, leading to enhanced adaptive immune responses due to immune cell accumulation. In LNs, local adrenergic signaling to  $\beta_2$ -ARs on lymphocytes retains the cells in these secondary lymphoid organs, leading to reduced numbers in blood and lymph (Suzuki et al., 2016). Strikingly, the strongest influence of adrenergic stimulation on circulating numbers was observed for B cells, probably due to higher  $\beta_2$ -AR expression on their cell surface compared to T cells. Adrenergic promotion of LN retention was linked to the physical interaction of the AR with CCR7 and CXCR4, both important chemokine receptors involved in lymphocyte trafficking through LNs (Nakai et al., 2014).

Summarized, adrenergic stimulation impacts virtually every step of leukocyte trafficking. Observed effects highly depend on dosage of the adrenergic agonist and its time of exposure, the inflammatory milieu, metabolic state and gender of the host, as well as the target cell type and tissue (**Figure 1-8**). This high level of complexity makes it more difficult to get an overview of the adrenergic influence on leukocyte trafficking. Furthermore, the interconnection of the sympathetic and the immune system was often studied in an inflammatory context, while knowledge about processes under steady-state conditions are still fragmentary.

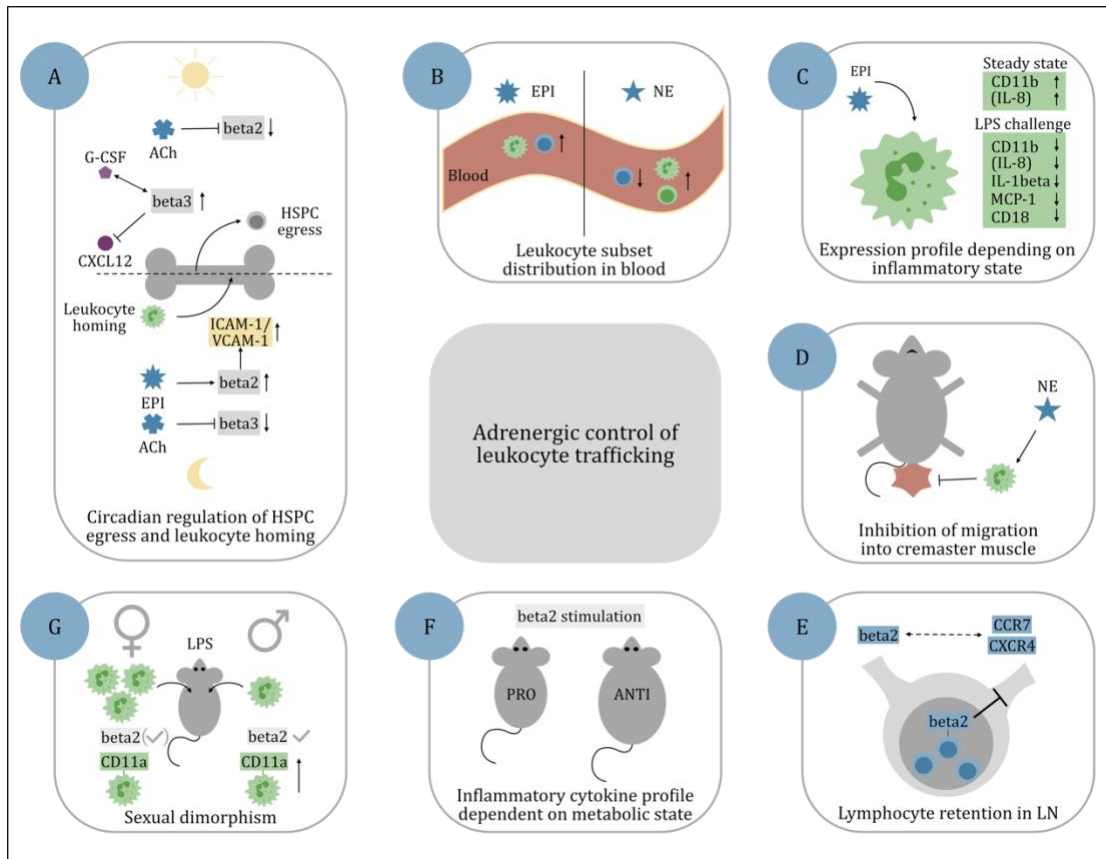


**Figure 1-8: Adrenergic control of leukocyte trafficking.**

Adrenergic signaling has multiple effects. **(A)** In cooperation with cholinergic signals, it regulates the circadian egress of hematopoietic stem and progenitor cells (HSPCs) from and homing of leukocytes to the BM (García-García et al., 2019; Mendez-Ferrer et al., 2008; Scheiermann et al., 2012). **(B)** Stimulation with NE and EPI leads to changes of the blood leukocyte subset composition in rats (Dhabhar et al., 2012). **(C)** Exposure of neutrophils to EPI was shown to alter their expression profile depending on the inflammatory context (Margaryan et al., 2017; Scanzano et al., 2015). **(D)** NE blocks the migration of neutrophils in a cremaster model (Nicholls et al., 2018). **(E)** Activation of  $\beta_2$ -ARs on lymphocytes was shown to cause their retention in LNs, mediated by interactions of  $\beta$ -ARs with chemokine receptors (Nakai et al., 2014; Suzuki et al., 2016). **(F)** The metabolic state plays a role in the interplay, as in obese mice  $\beta_2$ -AR stimulation leads to an anti-inflammatory cytokine profile, compared to wild-type mice, which were shown to exhibit a pro-inflammatory cytokine profile (Gálvez et al., 2019). **(G)** Gender was demonstrated to influence adrenergic leukocyte trafficking, since neutrophil recruitment to a dorsal air pouch was higher in females, while  $\beta_2$ -ARs played a more dominant role in males. Additionally, numbers of CD11a<sup>+</sup> cells infiltrating the pouch differed between females and males (de Coupade et al., 2007).

## 1.5 Aim of the study

Since every living organism encounters stress, it is important to be aware of its effects on the immune system. For proper functioning, immune cells have to migrate through the body and enter target tissues, a process called leukocyte trafficking. The aim of this thesis was to investigate this process specifically for representative of the innate and adaptive arm of immunity – neutrophils and B cells, respectively – upon modulation of adrenergic signaling in several organs. To achieve this,  $\beta$ -ARs of WT mice were pharmacologically stimulated and the distribution of these leukocyte subsets between blood, BM, LNs, liver, lung, and spleen was determined using flow cytometry. Using intravital microscopy of the popliteal LN, their migratory behavior was investigated in more detail. To unravel the role of specific  $\beta$ -ARs, genetically modified mouse strains lacking  $\beta_2$ - or  $\beta_3$ -ARs were examined in adoptive transfer experiments.



## 2 Methods and Materials

### 2.1 Methods

#### 2.1.1 Animals

Seven-weeks old C57BL/6N or J WT mice of both genders were purchased from Janvier Labs (Le Genest-Saint-Isle, France) or Charles River Laboratories (Sulzfeld, Germany) and used for experiments at an age of eight to nine weeks. *Adrb2*<sup>-/-</sup> (*Adrb2* KO) and *Adrb3*<sup>-/-</sup> (*Adrb3* KO) mice were kindly provided from Gerard Karsenty (Columbia University, NYC, USA) and Paul Frenette (Albert Einstein College of Medicine, NYC, USA). Mice were housed under a 12hr:12hr light-dark cycle with food and water *ad libitum*. All animal experimental procedures were performed in accordance with the German Law of Animal Welfare and approved by the Regierung von Oberbayern.

#### 2.1.2 Genotyping

Biopsies obtained from ears were digested at 55°C overnight in 200 µl digestion buffer (**Table 2-14**) supplemented with 1 µl proteinase K (1.5 U/sample). The following day, samples were centrifuged at 18,000 x g and room temperature for 10 min and the supernatant was transferred to a new tube containing 500 µl isopropanol. Precipitated DNA samples were centrifuged at 18,000 x g and room temperature for 10 min and the supernatant was removed. Pellets were dissolved in 100 µl TE buffer (**Table 2-14**) for 1 h at 37°C and either used directly for polymerase chain reaction (PCR) or stored at -20°C. For genotyping PCR, 1 µl of extracted DNA solution was mixed with 8.6 µl nuclease-free water, 10 µl 2x FastGene master mix and 0.5 µl of each, forward and reverse primer (10 µM, **Table 2-1**). DNA was amplified according to protocols in **Table 2-2** on a Mastercycler Eppgradient S (Eppendorf). 10 µl of the PCR product were applied on a 1% agarose gel supplemented with Midori Green (1:25,000, Nippon Genetics). All samples were run for 30 min at 120 V together with the FastGene 100 bp DNA Marker (Nippon Genetics). The gel was imaged under ultraviolet light using an UV Transilluminator (INTAS Science Imaging).

### 2.1.3 Primers

All primer sequences were kindly provided by Paul Frenette and purchased at Eurofins (Munich, Germany). Adrb=  $\beta$ -adrenoceptor, WT= wild type, KO = knockout.

**Table 2-1: Primers and respective sequences.**

Primer	Sequence (5' → 3')
<i>Adrb2</i> forward	AGG GGC ACG TAG AAA GAC AC
<i>Adrb2</i> WT reverse	ACC AAG AAT AAG GCC CGA GT
<i>Adrb2</i> KO reverse	GAG ACT AGT GAG ACG TGC TAC T
<i>Adrb3</i> WT forward	GTT GCG AAC TGT GGA CGT CAG TGG
<i>Adrb3</i> KO forward	GCG ATC GCC TTC TAT CGC CTT CTT G
<i>Adrb3</i> reverse	AAT GCC GTT GGC GCT TAG CCA C

### 2.1.4 PCR protocols

**Table 2-2: PCR protocols.**

Gene	Step	Temperature	Time	Cycles	Product
<i>Adrb2</i> <sup>-/-</sup>	Initial denaturation	94°C	4 min	1x	WT: 220 bp KO: 400 bp
	Denaturation	94°C	30 sec	35x	
	Annealing	55°C	40 sec		
	Extension	72°C	1 min		
	Final extension	72°C	10 min	1x	
<i>Adrb3</i> <sup>-/-</sup>	Initial denaturation	94°C	4 min	1x	WT: 380 bp KO: 650 bp
	Denaturation	94°C	30 sec	35x	
	Annealing	63°C	40 sec		
	Extension	72°C	1 min		
	Final extension	72°C	10 min	1x	

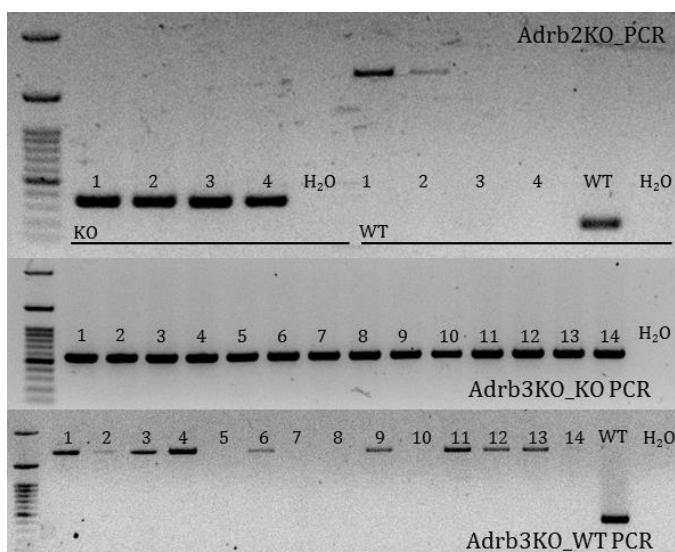


**Figure 2-1: Genotyping examples.**

### **2.1.5 Pharmacological adrenergic stimulation and blockade**

Two hours prior to blood and organ harvest (10 am or 6 pm), mice were injected intraperitoneally with either 100  $\mu$ l PBS or 5 mg/kg Isoproterenol (pan- $\beta$ -AR agonist, Sigma-Aldrich), 5 mg/kg Propranolol (pan- $\beta$ -AR antagonist, Sigma-Aldrich), 2 mg/kg Clenbuterol ( $\beta_2$ -AR agonist, Sigma-Aldrich) or 2 mg/kg BRL37344 ( $\beta_3$ -AR agonist, Sigma-Aldrich) in PBS. 14  $\mu$ g/kg Denopamine ( $\beta_1$ -AR agonist, Sigma-Aldrich) were dissolved in 9% DMSO in PBS, which was used as control for this specific agonist.

### **2.1.6 Chemical sympathectomy**

For complete sympathetic ablation in the periphery, mice were injected intraperitoneally with 100 mg/kg of 6-hydroxydopamine (6-OHDA, with 20 mg/ml ascorbate in saline) on day 0 and 250 mg/kg on day 2 and analyzed from day 5 on.

### **2.1.7 Induction of inflammation**

To investigate the influence of adrenergic stimulation on circulating leukocyte numbers under inflammatory conditions, mice were intraperitoneally injected with 0.5  $\mu$ g TNF $\alpha$ , one hour prior to injection of adrenergic agonists and three hours prior to blood harvest at 12 pm or 8 pm.

### **2.1.8 Organ harvest and processing for flow cytometry**

#### **2.1.8.1 Blood**

During adoptive transfer experiments, blood from anaesthetized mice was collected retro-orbitally into EDTA-coated microhematocrit tubes (VWR). Collecting tubes contained 5  $\mu$ l EDTA (5 mM) to prevent clotting. For experiments without subsequent perfusion, blood from euthanized mice was harvested from the Inferior Vena Cava using a syringe equipped with a 20G-needle containing 50  $\mu$ l EDTA (5 mM). Samples were counted using a ProCyt Dx $\text{\textcircled{R}}$  cell counter (IDEXX Laboratories). Erythrocytes were lysed by incubation in 5 ml RBC lysis buffer (**Table 2-14**) for 5 min, once at room temperature and once on ice. The lysis was stopped with an equal amount of PBS and cells were centrifuged at 300 x g and 22°C for 5 min. Cell pellets were resuspended in 1 ml PEB (**Table 2-14**) and

transferred to 5 ml polystyrene tubes or in 200  $\mu$ l PEB and transferred to wells of a 96-well V-bottom plate for centrifugation and subsequent staining.

#### **2.1.8.2 Bone marrow**

To obtain donor cells for investigation of myeloid cell trafficking, both femora and tibiae were harvested, cleaned and flushed with 1 ml PBS. Cell clusters were disaggregated by pipetting. To investigate cell numbers in the BM of recipients, only one femur was used. Erythrocytes were lysed by incubation in 4 ml RBC lysis buffer (**Table 2-14**) for 5 min at room temperature. The lysis was stopped with an equal amount of PBS and samples were centrifuged at 300 x g and 22°C for 5 min. Cell pellets were resuspended in 1 ml PEB (**Table 2-14**) and 300  $\mu$ l were transferred to 5 ml polystyrene tubes or 100  $\mu$ l to wells of a 96-well V-bottom plate for centrifugation and subsequent staining.

#### **2.1.8.3 Lymph nodes**

To obtain donor cells for investigation of lymphocyte trafficking, both popliteal, inguinal, axillary, brachial, superficial parotid and lumbar lymph nodes, as well as one mesenteric lymph node were harvested. From recipients, eight skin-draining lymph nodes (popliteal, inguinal, axillary and brachial) and one gut-draining lymph node (mesenteric) were harvested. Lymph nodes were processed through a 40  $\mu$ m cell strainer and centrifuged at 300 x g and 22°C for 5 min. Cell pellets were resuspended in 1 ml PEB (**Table 2-14**) and 100  $\mu$ l were transferred to 5 ml polystyrene tubes. For analysis in a 96-well V-bottom plate, 500  $\mu$ l of the pooled skin-draining lymph nodes and the whole sample of the gut-draining lymph node were transferred to each well. Samples were then centrifuged and stained.

#### **2.1.8.4 Liver**

The median lobe of the perfused liver was harvested into DPBS (Life Technologies). For extrapolation to the whole organ the rest of the liver was harvested into an empty collection tube and the weight of both parts was measured. The median lobe was cut into pieces and incubated with 1 mg/ml collagenase IV (C5138, Sigma-Aldrich) and 0.2 mg/ml DNase I (Life Technologies) for one hour rotating at 37°C and subsequently passed through a 40  $\mu$ m cell strainer. Erythrocytes were lysed by incubation in 5 ml RBC lysis buffer (**Table 2-14**) for 5 min at room temperature. The lysis was stopped with an equal amount of PBS and cells were centrifuged at 300 x g and 22°C for 5 min. Cell pellets were resuspended in 1 ml PEB (**Table 2-14**) and 100  $\mu$ l were transferred to 5 ml polystyrene tubes or 40  $\mu$ l to wells of a 96-well V-bottom plate for centrifugation and subsequent staining.

#### **2.1.8.5 Lung**

The left lobe of the perfused lung was harvested into DPBS (Life Technologies). For extrapolation to the whole organ the right lobe was harvested into an empty collection tube and the weight of both lobes was measured. The left lobe was cut into pieces and incubated with 1 mg/ml collagenase IV (C5138, Sigma-Aldrich) and 0.2 mg/ml DNase I (Life Technologies) for one hour rotating at 37°C and subsequently passed through a 40 µm cell strainer. Erythrocytes were lysed by incubation in 5 ml RBC lysis buffer (**Table 2-14**) for 5 min at room temperature. The lysis was stopped with an equal amount of PBS and cells were centrifuged at 300 x g and 22°C for 5 min. Cell pellets were resuspended in 1 ml PEB (**Table 2-14**) and 400 µl were transferred to 5 ml polystyrene tubes or 100 µl to wells of a 96-well V-bottom plate for centrifugation and subsequent staining.

#### **2.1.8.6 Spleen**

The perfused spleen was harvested into PBS and processed through a 40 µm cell strainer. Erythrocytes were lysed by incubation in 5 ml RBC lysis buffer (**Table 2-14**) for 5 min at room temperature. The lysis was stopped with an equal amount of PBS and samples were centrifuged at 300 x g and 22°C for 5 min. Cell pellets were resuspended in 1 ml PEB (**Table 2-14**) and 100 µl were transferred to 5 ml polystyrene tubes or 100 µl to wells of a 96-well V-bottom plate for centrifugation and subsequent staining.

#### **2.1.8.7 Peyer's patches**

The small intestine was harvested and flushed with PBS. Peyer's Patches were carefully cut out, processed through a 40 µm cell strainer and centrifuged at 300 x g and 22°C for 5 min. Cell pellets were resuspended in 1 ml PEB (**Table 2-14**) and the whole sample was transferred to a 5 ml polystyrene tube for centrifugation and subsequent staining.

### **2.1.9 Adoptive transfer experiments**

Donor cells were isolated from the spleen, several lymph nodes and long bones and processed as described in 2.1.8. To investigate trafficking of lymphocytes, cells from spleen and pooled lymph nodes were mixed (70:30 ratio). For the investigation of myeloid cells, splenic and bone marrow cells (50:50 ratio) were used. Cell counts were obtained on a ProCyte Dx® cell counter (IDEXX Laboratories). Donor cells were labeled with 0.1 µM CellTracker Deep Red (Thermo Fisher Scientific) or 1.5 µM carboxyfluorescein succinimidyl ester (CFSE, Thermo Fisher Scientific) in PEB for 20 min at 37°C with subsequent washing for three times. In some experiments, WT and Adrb2 KO or Adrb3 KO cells were mixed

50:50. One hour after adrenergic stimulation (11 am) about  $10 \times 10^6$  cells were injected intravenously. Subset fractions were obtained by flow cytometric analysis of the donor cells. In some experiments, recipient mice were injected intravenously with an antibody against the common leukocyte marker CD45, 5 min before harvest at 12 pm, to label cells in the circulation.

### 2.1.10 Flow cytometry

Single cell suspensions were stained with fluorescence-conjugated antibodies and analyzed by flow cytometry using a Gallios Flow Cytometer (Beckman Coulter) or a LSRFortessa (BD bioscience) (**Table 2-3**). To count the number of cells, 10-15  $\mu$ l CountBright™ Absolute Counting Beads (Molecular Probes) were added to each sample. Data were analyzed with FlowJo software (Tree Star) (**Table 2-18**). Used staining panels and gating strategies are listed below. All used antibodies were specific for mice.

**Table 2-3: Flow cytometer configurations.**

Flow Cytometer	Excitation laser [nm]	Fluorescence channel	Default filter	Filter range
Gallios	405	9	450/50	425-475
		10	550/40	530-570
	488	1	525BP	xxx-550
		2	575BP/26	588-652-
		3	620/30	605-635
		4	695/30	680-710
		5	755LP	>755
	633	6	660BP	650-670
		7	725/20	715-735
8		755LP	>755	
LSRFortessa	355	1	450/50	425-475
		1	380/30	365-395
		2	530/30	515-545
	405	3	450/40	430-470
		4	525/50	500-550
		5	610/20	600-620
		6	660/20	650-670
		7	710/50	685-735
		8	780/60	750-810
	488	9	530/30	515-545
		10	710/20	700-720
	561	11	586/15	579-593
		12	610/20	600-620
		13	670/30	655-685
		14	710/50	685-735
		15	780/60	750-810
	640	16	670/14	663-677
		17	730/45	708-752
18		780/60	750-810	

**Table 2-4: Staining panel for Blood Leukocyte Subsets (Gallios).**

<b>Laser [nm]</b>	<b>Antigen</b>	<b>Fluorochrome</b>	<b>Clone</b>	<b>Dilution</b>	<b>Company</b>	<b>Location</b>
405	Live/Dead	DAPI	-	1:10	Biolegend	London, UK
	CD4	BV570	RM4-5	1:100	Biolegend	London, UK
488	CD115	PE	AFS98	1:100	Biolegend	London, UK
	CD3	PE-DZL594	17A2	1:100	Biolegend	London, UK
	Gr-1	PerCP/Cy5.5	RB6-8C5	1:100	Biolegend	London, UK
	B220	PE/Cy7	RA3-6B2	1:100	Biolegend	London, UK
633	SiglecF	AlexaFluor647	E50-2440RUO	1:100	BD bioscience	Heidelberg, Germany
	NK1.1	AlexaFluor700	PK136	1:100	Life Technologies	Darmstadt, Germany
	CD8a	APC/Cy7	53-6.7	1:100	Biolegend	London, UK

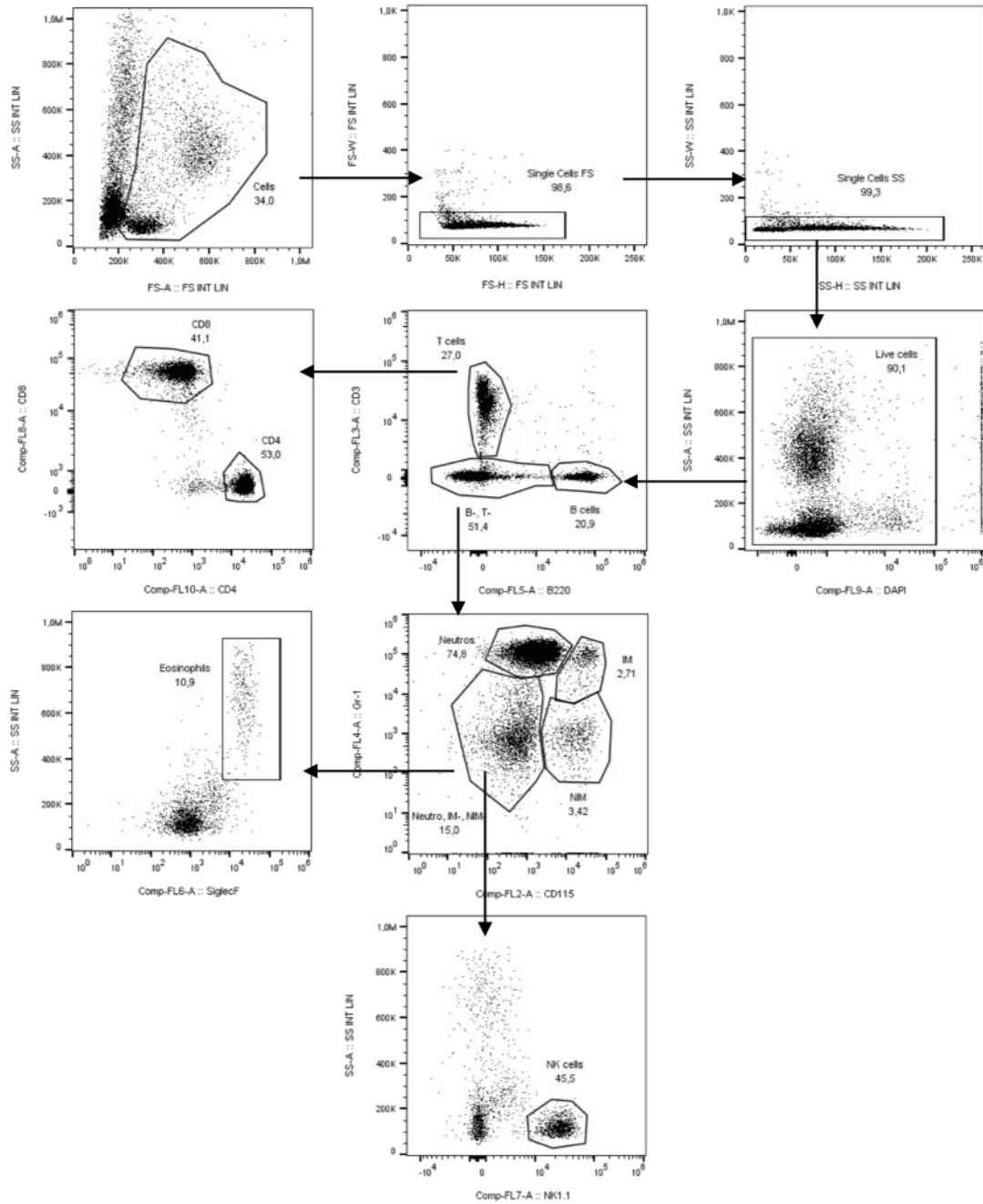


**Figure 2-2: Gating strategy for Blood Leukocyte Subsets (Gallios).**

SS = Side Scatter, FS = Forward Scatter, Neutros = Neutrophils, IM = Inflammatory Monocytes, NIM = Non-Inflammatory Monocytes, NK cells = Natural Killer cells.

**Table 2-5: Staining panel for Blood Leukocyte Subsets (Fortessa).**

<b>Laser [nm]</b>	<b>Antigen</b>	<b>Fluorochrome</b>	<b>Clone</b>	<b>Dilution</b>	<b>Company</b>	<b>Location</b>
355	Live/Dead	DAPI	-	1:10	Biolegend	London, UK
405	CD4	BV605	RM4-5	1:200	Biolegend	London, UK
	B220	SB645	RA3-6B2	1:200	Thermo Fisher Scientific	Munich, Germany
488	Gr-1	FITC	RB6-8C5	1:200	Biolegend	London, UK
	CD8a	PerCP/Cy5.5	53-6.7	1:200	Biolegend	London, UK
561	CD115	PE	AFS98	1:100	Biolegend	London, UK
	CD3	PE-DZL594/610	17A2	1:200	Biolegend	London, UK
640	SiglecF	AlexaFluor647	E50-2440	1:100	BD bioscience	Heidelberg, Germany
	NK1.1	AlexaFluor700	PK136	1:100	Life Technologies	Darmstadt, Germany

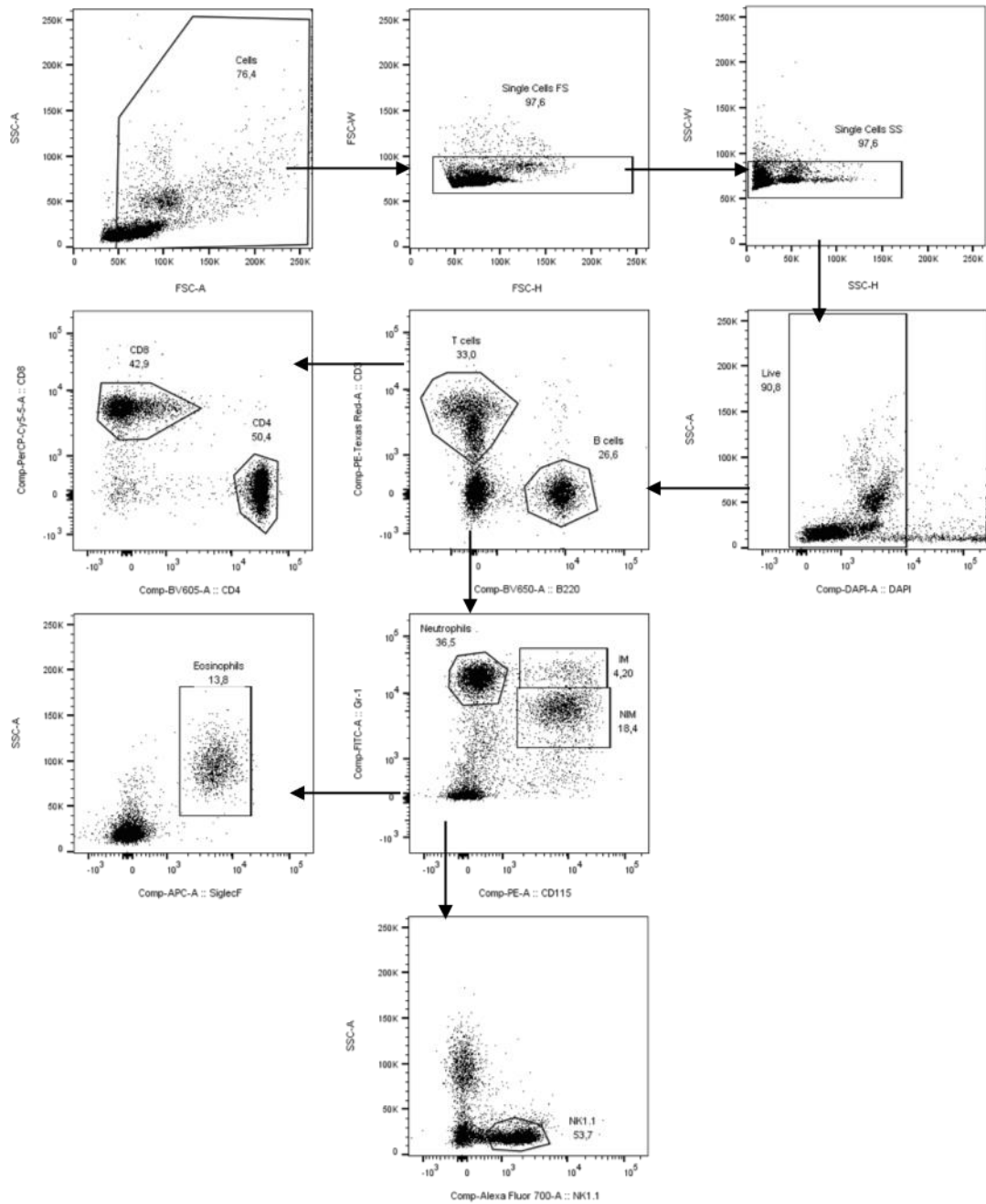


**Figure 2-3: Gating strategy for Blood Leukocyte Subsets (Fortessa).**

SS = Side Scatter, FS = Forward Scatter, IM = Inflammatory Monocytes, NIM = Non-Inflammatory Monocytes, NK cells = Natural Killer cells.

**Table 2-6: Staining panel for Adoptive Transfer with  $\alpha$ CD45 injection - Lymphocytes (Gallios).**

i.v. = intravenous.

Laser [nm]	Antigen	Fluorochrome	Clone	Dilution	Company	Location
405	Live/Dead	DAPI	-	1:10	Biolegend	London, UK
488	CD3	AlexaFluor488	145-2C11	1:100	Biolegend	London, UK
	CD45	PE	30-F11	10 $\mu$ l i.v.	Biolegend	London, UK
	CD8a	PE-CF594	53-6.7RUO	1:200	BD bioscience	Heidelberg, Germany
	CD45	PerCP/Cy5.5	I3/2.3	1:100	Biolegend	London, UK
	B220	PE/Cy7	RA3-6B2	1:100	Biolegend	London, UK
633	Donor cells	CellTracker Deep Red	-	1:20,000	Thermo Fisher Scientific	Munich, Germany
	CD4	APC/Cy7	GK1.5	1:100	Biolegend	London, UK

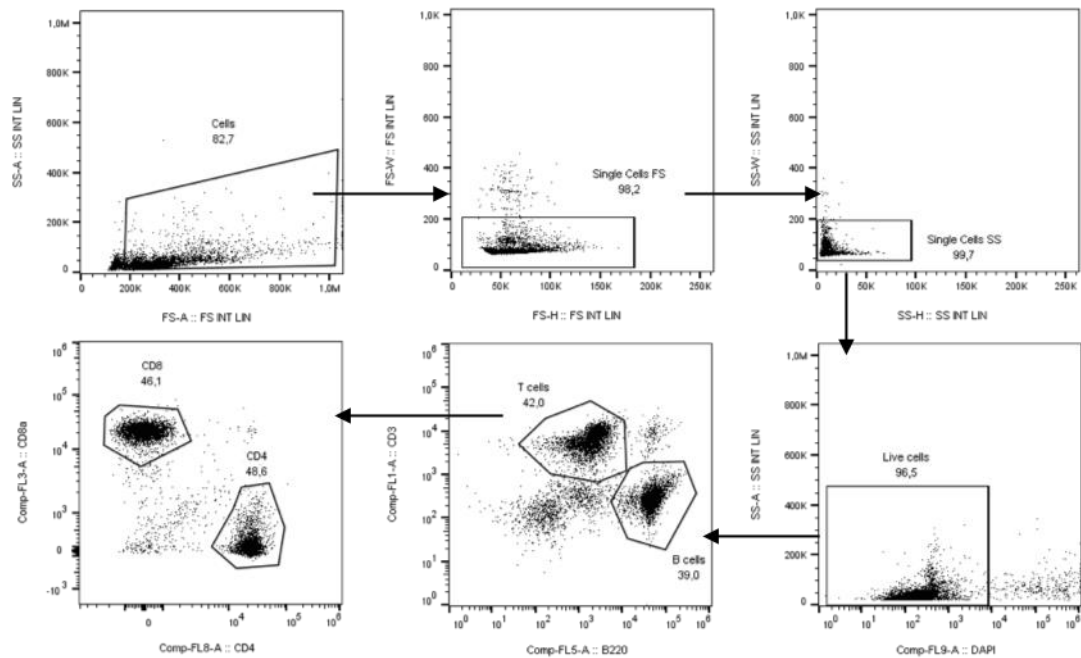


**Figure 2-4: Gating strategy for Adoptive Transfer with  $\alpha$ CD45 injection - Lymphocytes - Donor cells (Gallios).**

SS = Side Scatter, FS = Forward Scatter.

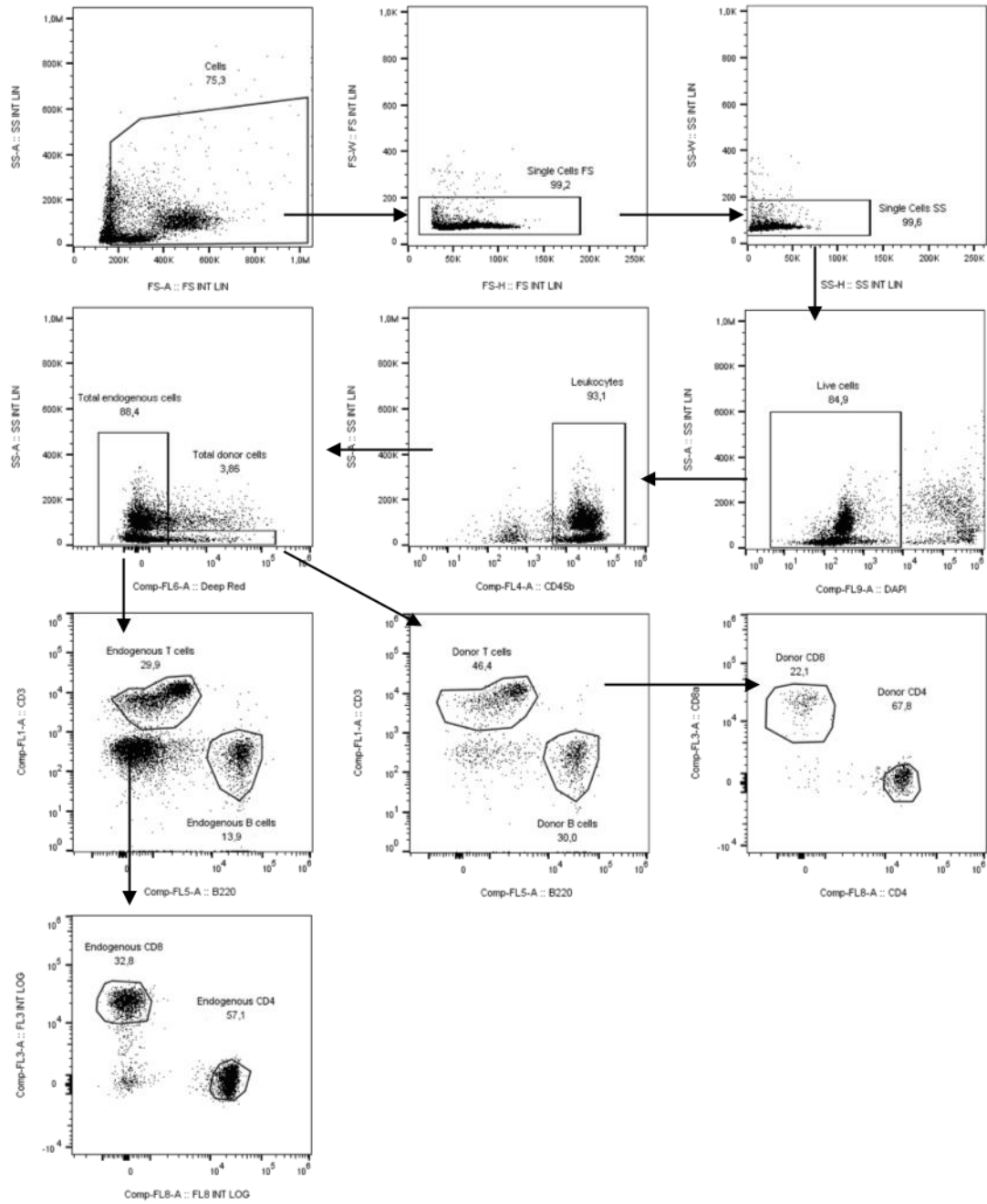


**Figure 2-5: Gating strategy for Adoptive Transfer with  $\alpha$ CD45 injection – Lymphocytes – Blood (Gallios).**  
 SS = Side Scatter, FS = Forward Scatter.

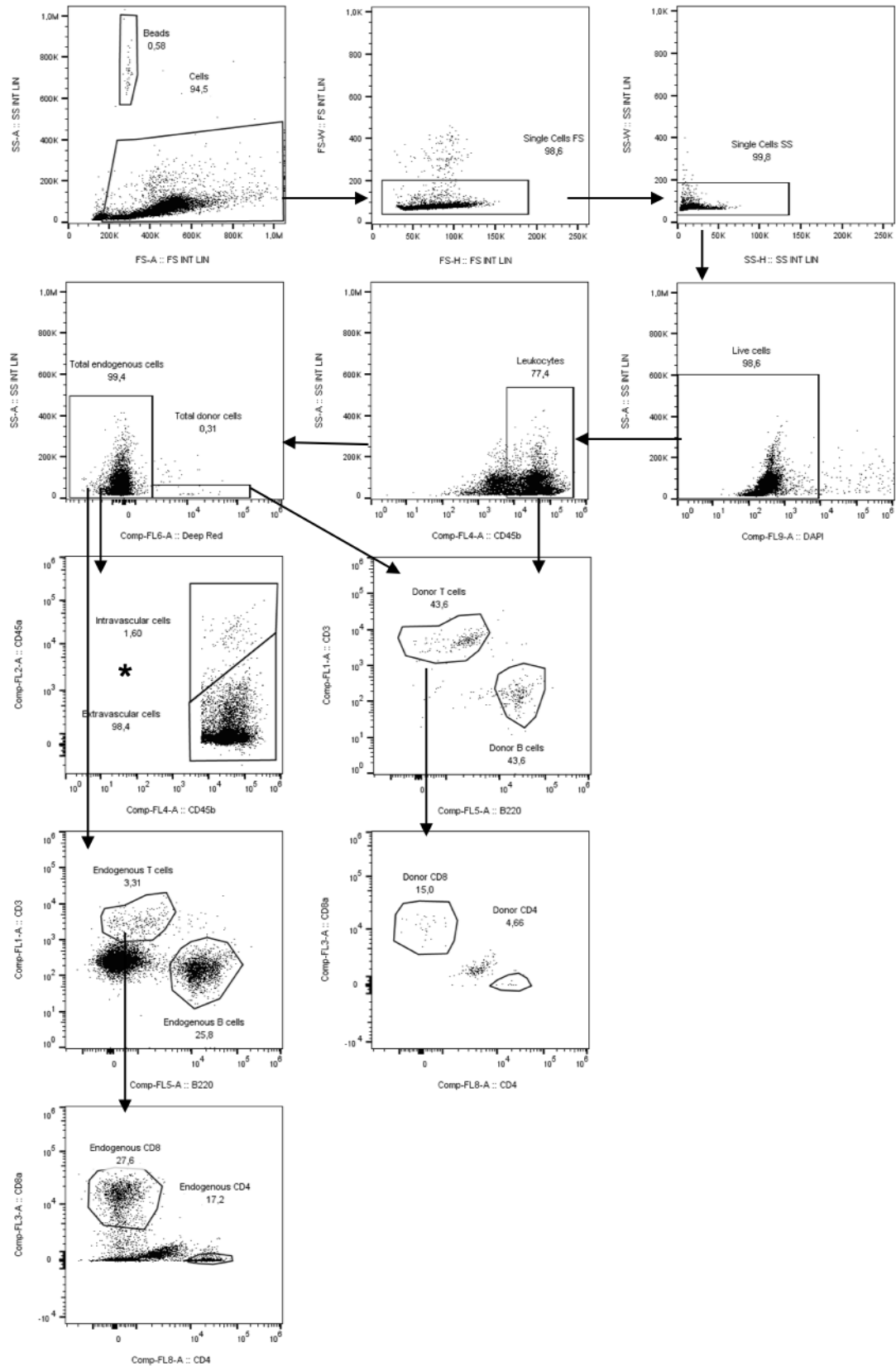


**Figure 2-6: Gating strategy for Adoptive Transfer with  $\alpha$ CD45 injection – Lymphocytes (Gallios).**

The bone marrow was used as example for the gating strategy of recipient organs. The strategy of \* was applied to all subsets. SS = Side Scatter, FS = Forward Scatter.

**Table 2-7: Staining panel for Adoptive Transfer with  $\alpha$ CD45 injection – Myeloid cells (Gallios).**

i.v. = intravenous.

Laser [nm]	Antigen	Fluorochrome	Clone	Dilution	Company	Location
405	Live/Dead	DAPI	-	1:10	Biologend	London, UK
488	Gr-1	FITC	RB6-8C5	1:200	Biologend	London, UK
	CD45	PE	30-F11	10 $\mu$ l i.v.	Biologend	London, UK
	CD115	PE-DZL594	AFS98	1:100	Biologend	London, UK
	CD45	PerCP/Cy5.5	I3/2.3	1:100	Biologend	London, UK
	NK1.1	AlexaFluor700	PK136	1:100	Life Technologies	Darmstadt, Germany
633	Donor cells	CellTracker Deep Red	-	1:20,000	Thermo Fisher Scientific	Munich, Germany
	SiglecF	APC/Cy7	E50-2440RUO	1:100	BD bioscience	Heidelberg, Germany

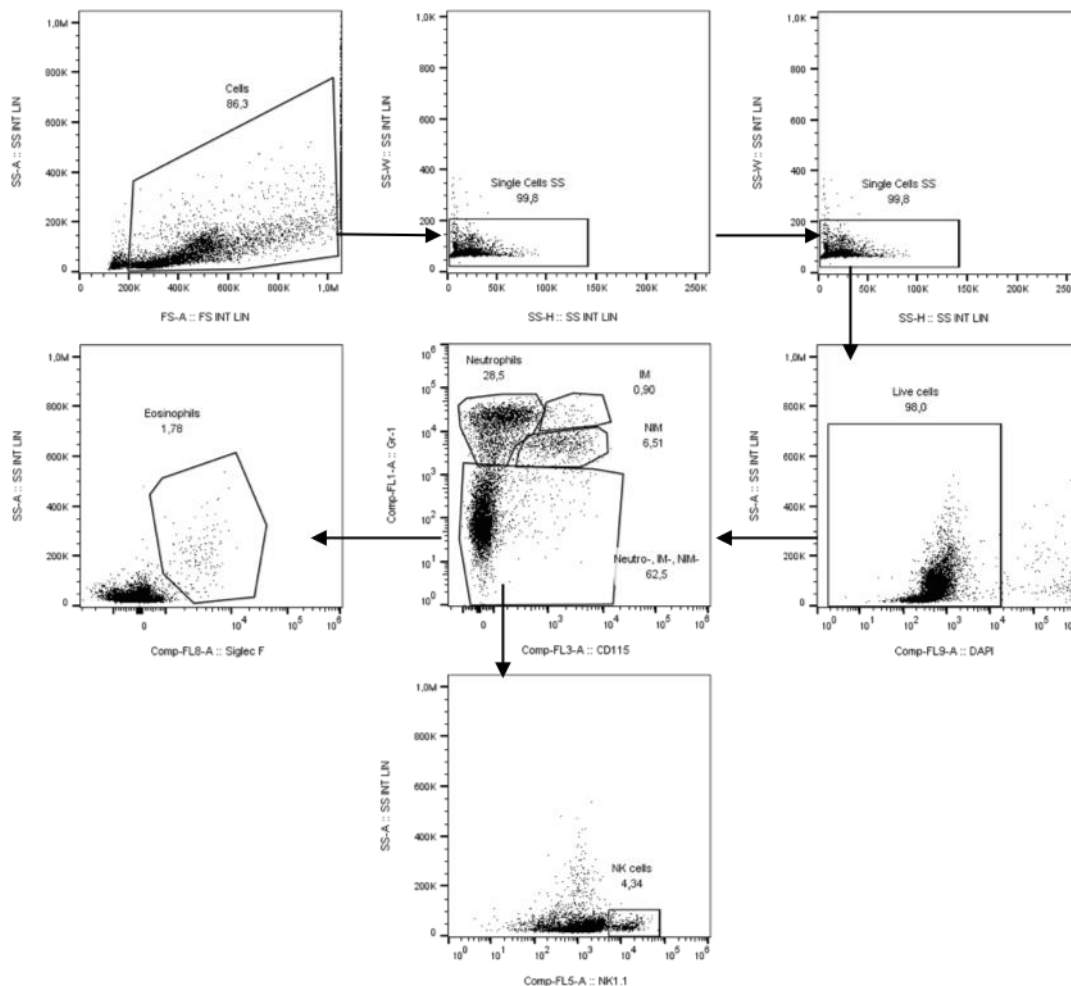


**Figure 2-7: Gating strategy for Adoptive Transfer with  $\alpha$ CD45 injection – Myeloid cells – Donor cells (Gallios).**

SS = Side Scatter, FS = Forward Scatter, IM = Inflammatory Monocytes, NIM = Non-Inflammatory Monocytes, NK cells = Natural Killer cells.

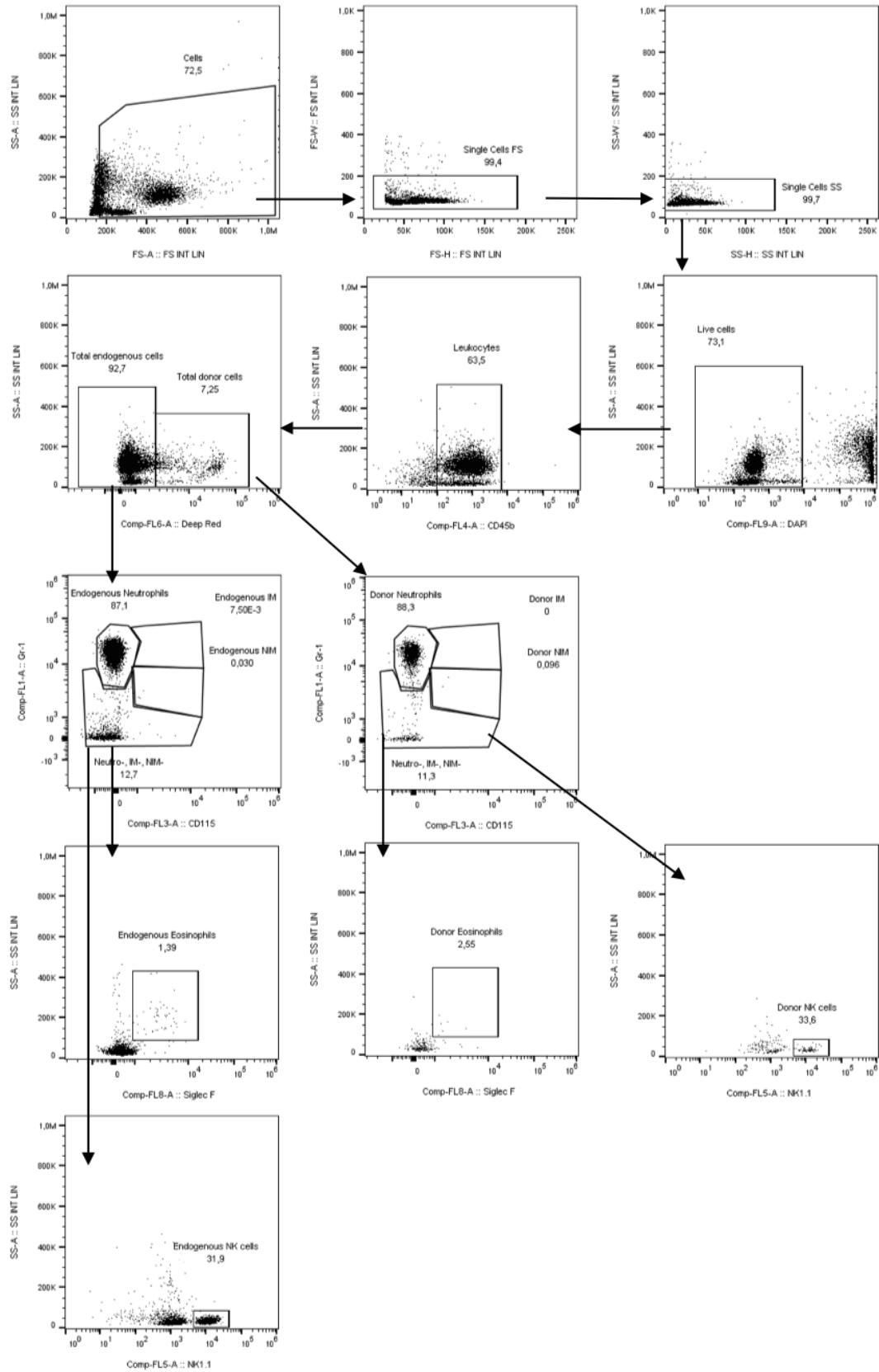


**Figure 2-8: Gating strategy for Adoptive Transfer with  $\alpha$ CD45 injection – Myeloid cells – Blood (Gallios).**

SS = Side Scatter, FS = Forward Scatter, IM = Inflammatory Monocytes, NIM = Non-Inflammatory Monocytes, NK cells = Natural Killer cells.

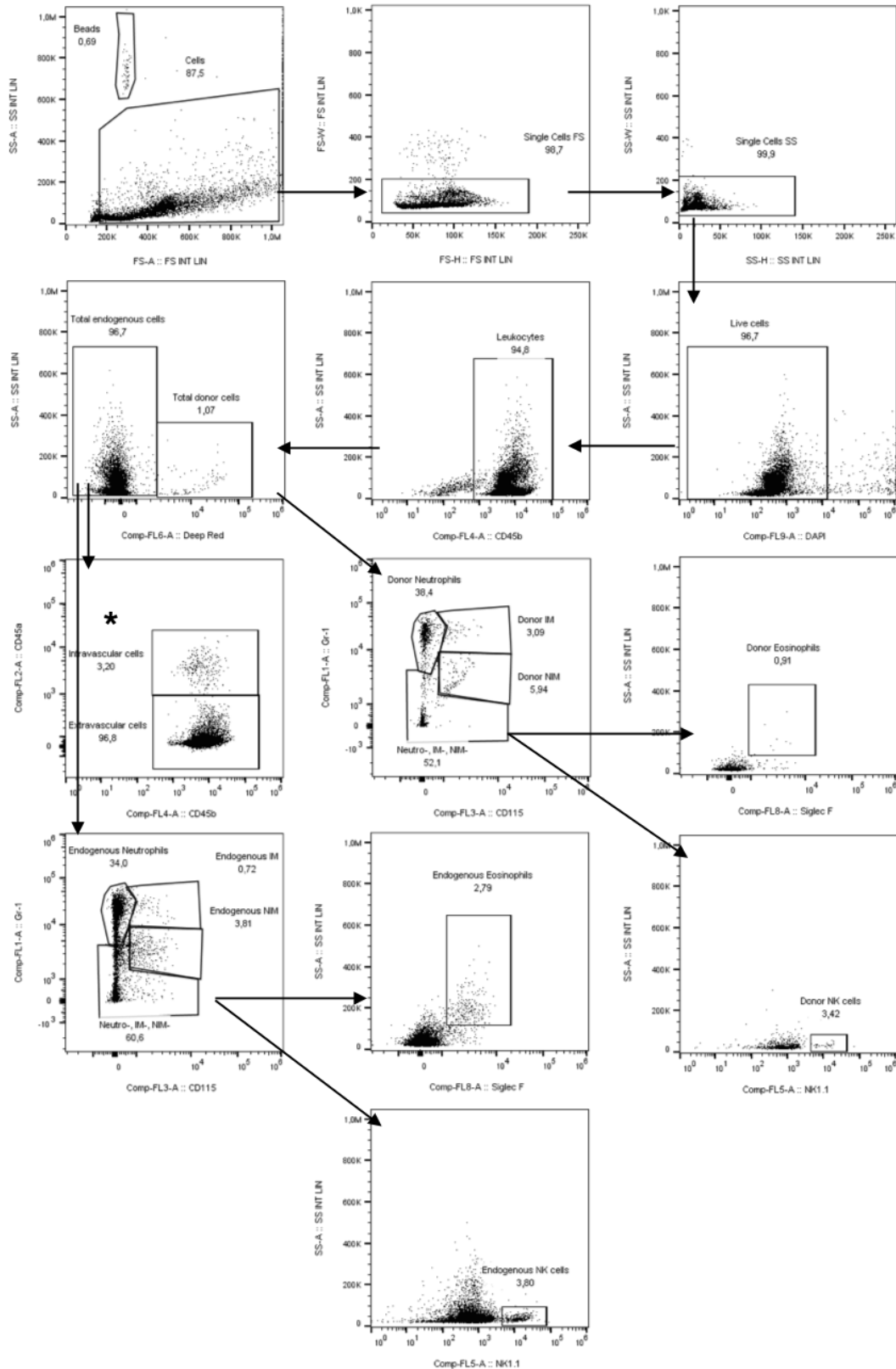


**Figure 2-9: Gating strategy for Adoptive Transfer with  $\alpha$ CD45 injection – Myeloid cells (Gallios).**

The bone marrow was used as example for the gating strategy of recipient organs. The strategy for \* was applied to all subsets. SS = Side Scatter, FS = Forward Scatter, IM = Inflammatory Monocytes, NIM = Non-Inflammatory Monocytes, NK cells = Natural Killer cells.

**Table 2-8: Staining panel for Adoptive Transfer – Donor Mix (Fortessa).**

<b>Laser [nm]</b>	<b>Antigen</b>	<b>Fluorochrome</b>	<b>Clone</b>	<b>Dilution</b>	<b>Company</b>	<b>Location</b>
355	Live/Dead	DAPI	-	1:10	Biolegend	London, UK
405	Ly6G	BV421	1A8	1:400	BD bioscience	Heidelberg, Germany
	CD3	BV711	17A2	1:400	Biolegend	London, UK
488	Donor cells	CFSE	-	1:20,000	Thermo Fisher Scientific	Munich, Germany
	CD45	PerCP/Cy5.5	I3/2.3	1:400	Biolegend	London, UK
561	Ly6C	PE-DZL594/610	HK1.4	1:400	Biolegend	London, UK
	B220	PE/Cy7	RA3-6B2	1:400	Biolegend	London, UK
640	Donor cells	CellTracker Deep Red	-	1:20,000	Thermo Fisher Scientific	Munich, Germany

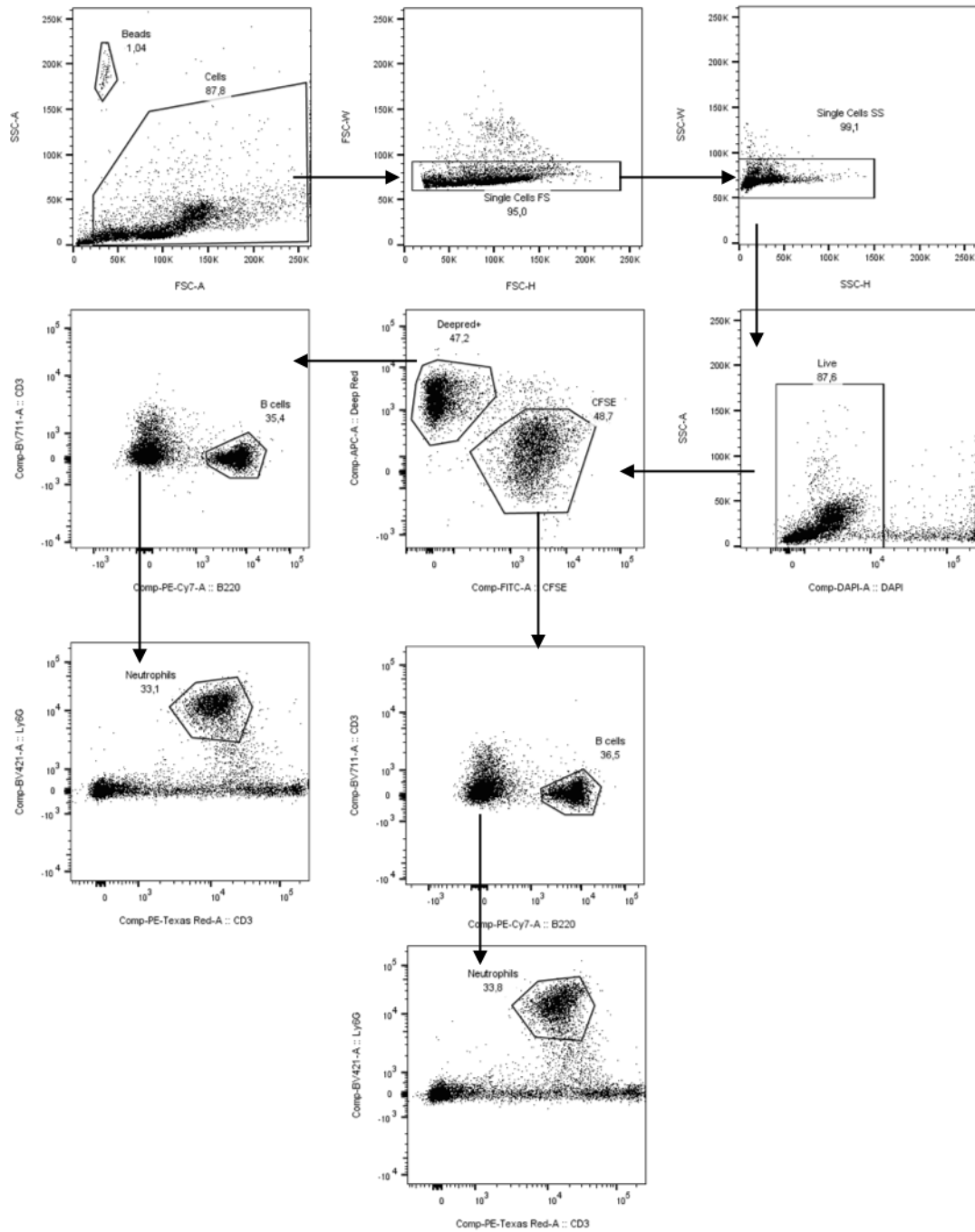


**Figure 2-10: Gating strategy for Adoptive Transfer Donor Mix – Donor cells (Fortessa).**

SS = Side Scatter, FS = Forward Scatter.

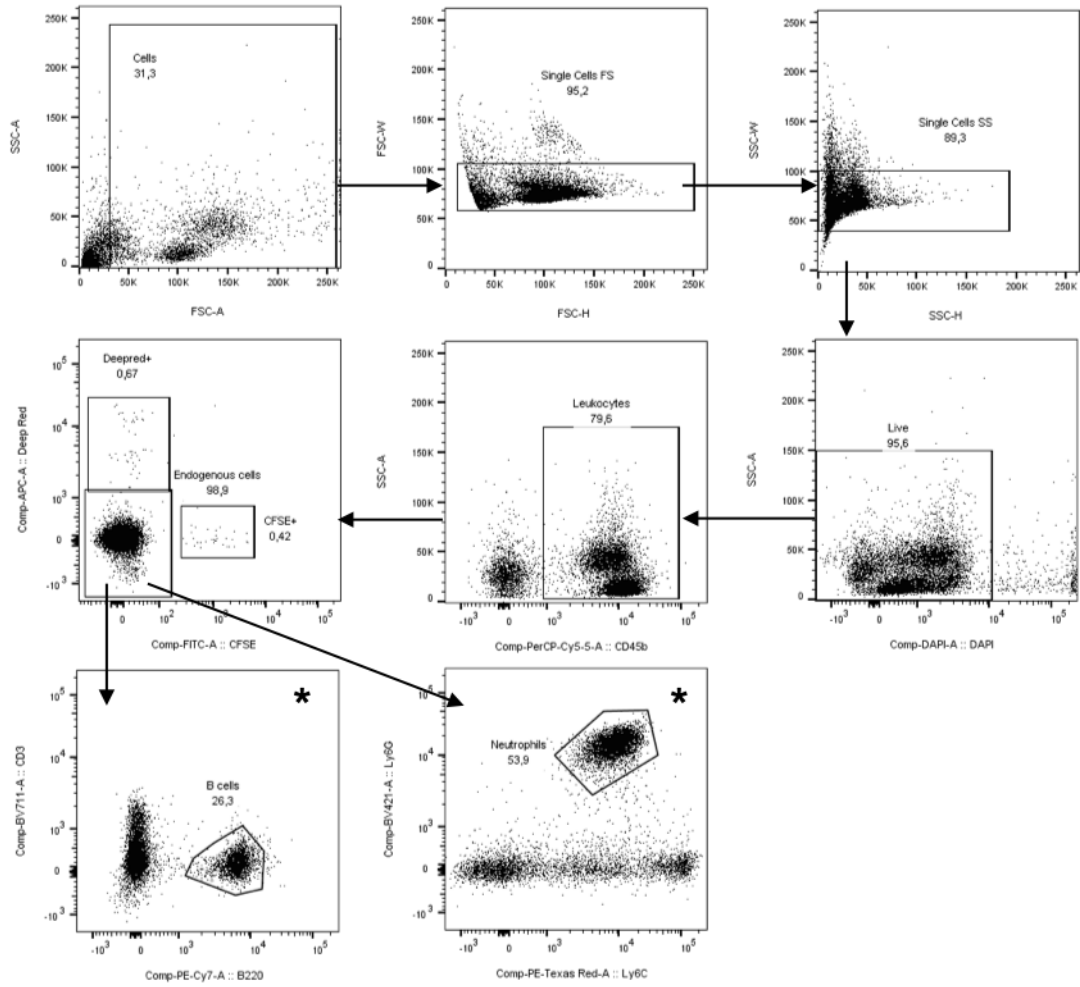


**Figure 2-11: Gating strategy for Adoptive Transfer Donor Mix - Blood (Fortessa).**  
 The strategies of \* were also applied to Deep Red+ and CFSE+ cells. SS = Side Scatter, FS = Forward Scatter.

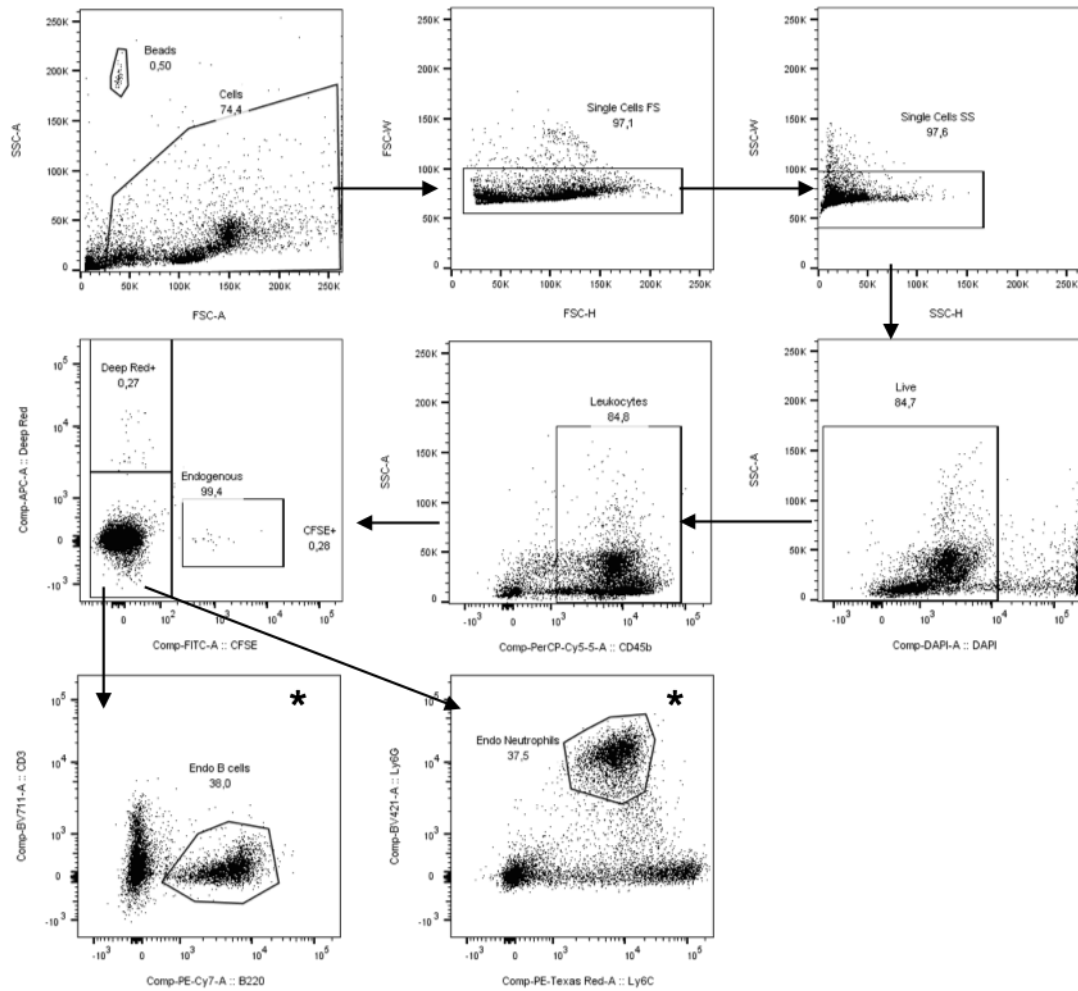


**Figure 2-12: Gating strategy for Adoptive Transfer Donor Mix (Fortessa).**

The bone marrow was used as example for the gating strategy of recipient organs. The strategies of \* were also applied to Deep Red+ and CFSE+ cells. SS = Side Scatter, FS = Forward Scatter, Endo = Endogenous.

**Table 2-9: Staining panel for Adoptive Transfer - KO recipients (Fortessa).**

Laser [nm]	Antigen	Fluorochrome	Clone	Dilution	Company	Location
355	Live/Dead	DAPI	-	1:10	Biologend	London, UK
405	Ly6G	BV421	1A8	1:400	BD bioscience	Heidelberg, Germany
	CD3	BV711	17A2	1:400	Biologend	London, UK
488	CD45	PerCP/Cy5.5	I3/2.3	1:400	Biologend	London, UK
561	Ly6C	PE-DZL594/610	HK1.4	1:400	Biologend	London, UK
	B220	PE/Cy7	Ra3-6B2	1:400	Biologend	London, UK
640	WT Donor cells	CellTracker Deep Red	-	1:20,000	Thermo Fisher Scientific	Munich, Germany

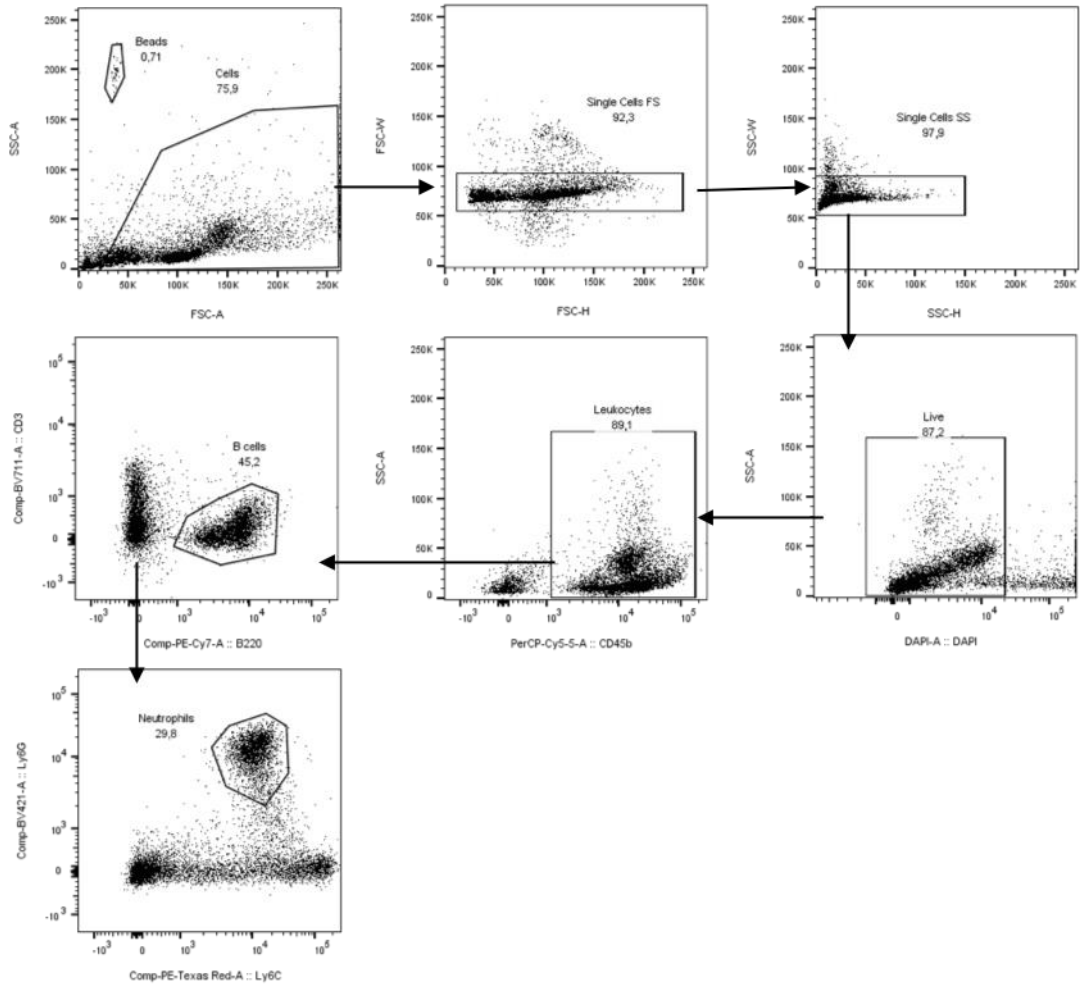


**Figure 2-13: Gating strategy for Adoptive Transfer KO recipients – Donor cells (Fortessa).**

SS = Side Scatter, FS = Forward Scatter.

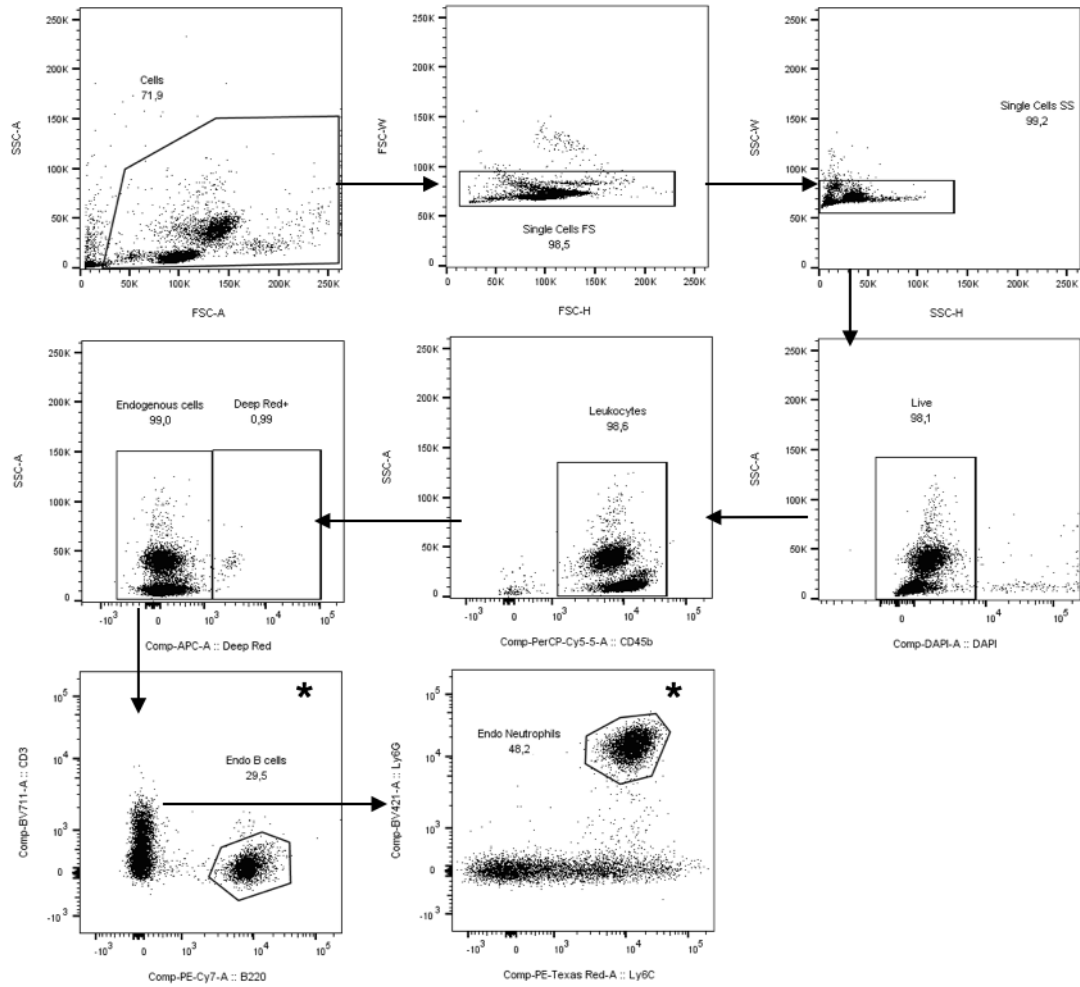


**Figure 2-14: Gating strategy for Adoptive Transfer KO recipients - Blood (Fortessa).**  
 The strategies of \* were also applied to Deep Red+ cells. SS = Side Scatter, FS = Forward Scatter.

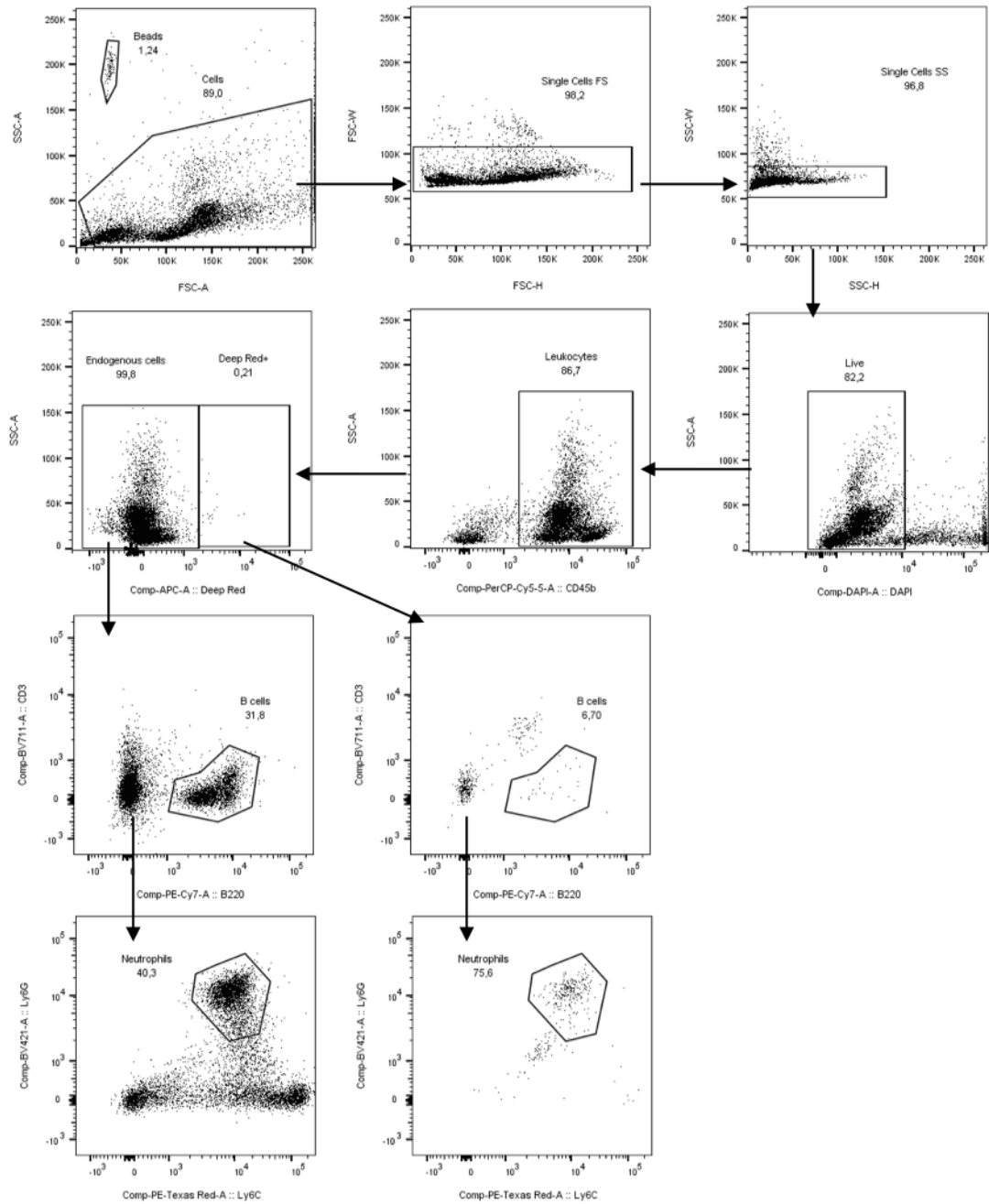


**Figure 2-15: Gating strategy for Adoptive Transfer KO recipients (Fortessa).**  
 The bone marrow was used as an example for the gating strategy of recipient organs. SS = Side Scatter, FS = Forward Scatter.

**Table 2-10: Staining panel for *In vitro* stimulation of B cells (Fortessa).**

Laser [nm]	Antigen	Fluorochrome	Clone	Dilution	Company	Location
355	CD49d	BUV395	R1-2	1:400	BD bioscience	Heidelberg, Germany
	Live/Dead	DAPI	-	1:10	Biolegend	London, UK
405	B220	SB645	RA3-6B2	1:400	Thermo Fisher Scientific	Munich, Germany
488	CD19	FITC	1D3	1:400	Biolegend	London, UK
	CD11a	PerCP-Cy5.5	M17/4	1:400	Biolegend	London, UK
640	CXCR4	APC	L276F12	1:400	Biolegend	London, UK
	CD62L	APC-Cy7	MEL-14	1:400	Biolegend	London, UK

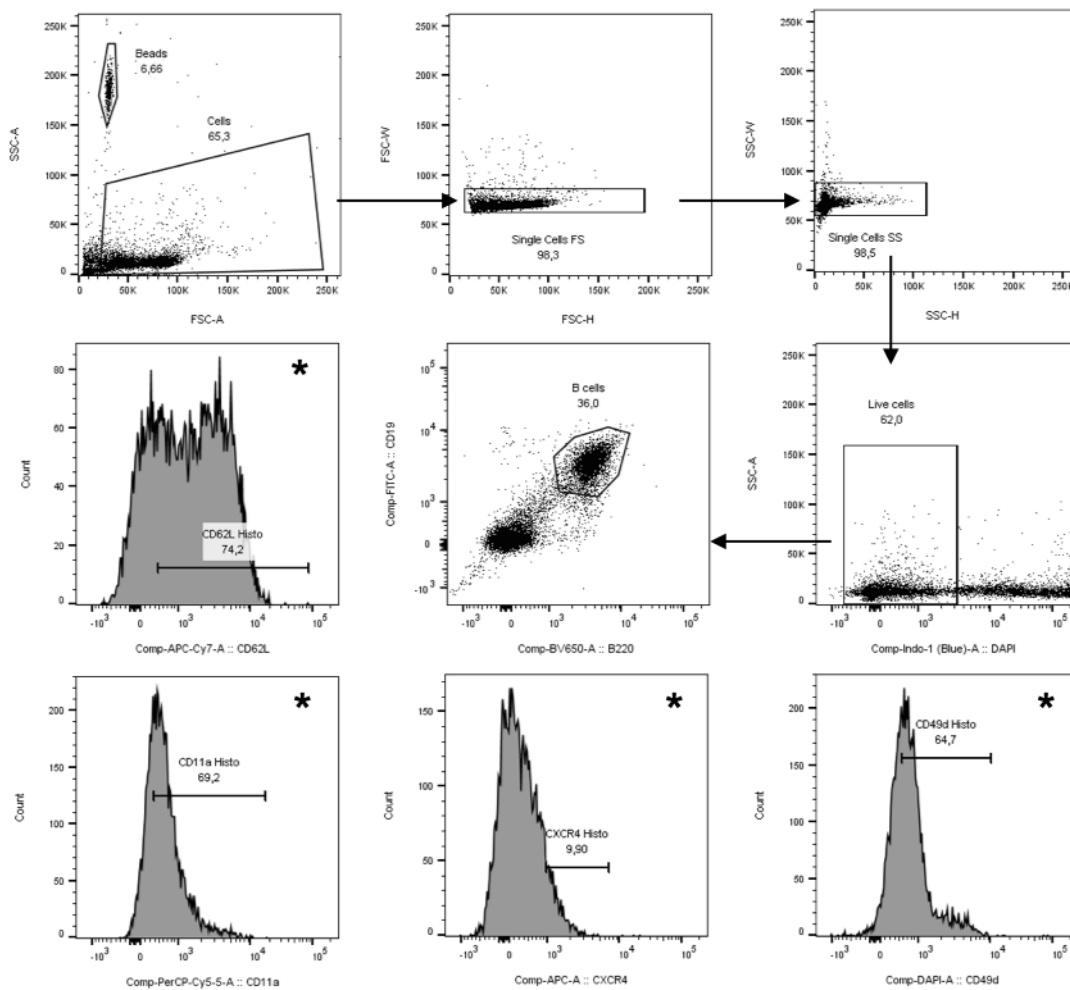


**Figure 2-16: Gating strategy for *In vitro* stimulation of B cells (Fortessa).**

The strategies of \* were applied to B cells. SS = Side Scatter, FS = Forward Scatter.

**Table 2-11: Staining panel for *In vitro* stimulation of neutrophils (Fortessa).**

Laser [nm]	Antigen	Fluorochrome	Clone	Dilution	Company	Location
405	Ly6C	BV421	HK1.4	1:400	Biolegend	London, UK
	CD11b	BV711	M1/70	1:400	Biolegend	London, UK
	Ly6G	BV785	1A8	1:400	Biolegend	London, UK
488	Annexin V	FITC	-	1:200	Biolegend	London, UK
	CXCR4	PerCP/Cy5.5	L276F12	1:400	Biolegend	London, UK
561	PSGL-1	PE	2PH1RUO	1:400	BD bioscience	Heidelberg, Germany
	7-AAD	PE-Cy5	-	1:200	Biolegend	London, UK
640	CD62L	APC/Cy7	MEL-14	1:400	Biolegend	London, UK

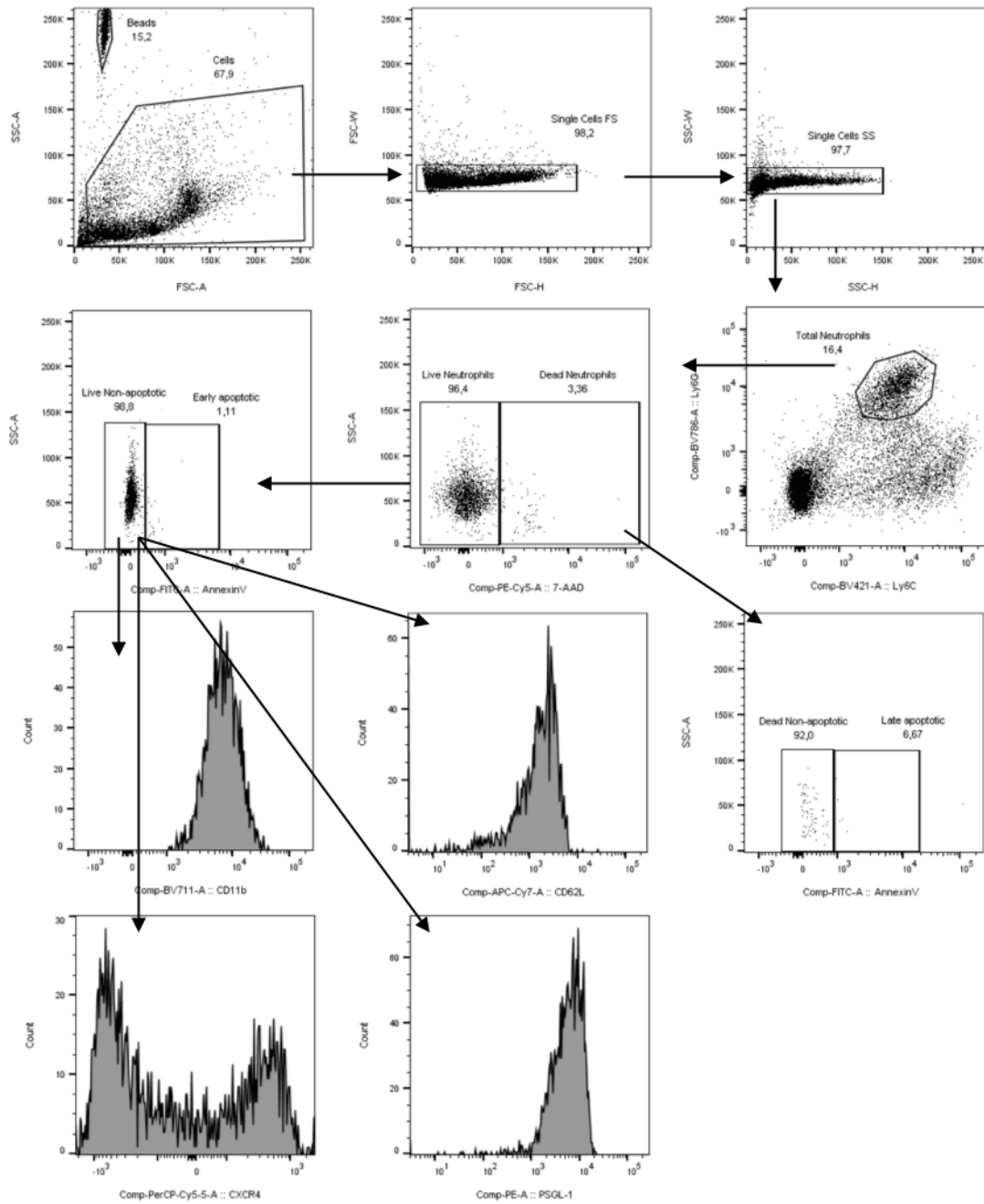


**Figure 2-17: Gating strategy for *In vitro* stimulation of neutrophils (Fortessa).**  
 SS = Side Scatter, FS = Forward Scatter.

**Table 2-12: Staining panel for *In vivo* adhesion molecules (Fortessa).**

Laser [nm]	Antigen	Fluorochrome	Clone	Dilution	Company	Location
355	CD45	BUV395	30-F11	1:200	BD bioscience	Heidelberg, Germany
	CD49d	BUV737	9C10(MFR4.B)	1:200	BD bioscience	Heidelberg, Germany
405	CD3	BV421	145-2C11	1:200	Biolegend	London, UK
	CD11b	BV480	M1/70	1:200	BD bioscience	Heidelberg, Germany
	Ly6G	BV785	1A8	1:200	Biolegend	London, UK
	CD62L	BB515	MEL-14	1:200	BD bioscience	Heidelberg, Germany
	CD19	BB700	1D3	1:200	BD bioscience	Heidelberg, Germany
561	CXCR4	PE/DZL594	L276F12	1:200	Biolegend	London, UK
	CCR7	PE/Cy7	4B12	1:200	Biolegend	London, UK
640	CD162	AlexaFluor647	2PH1	1:200	BD bioscience	Heidelberg, Germany
	Ly6C	AlexaFluor700	HK1.4	1:200	Biolegend	London, UK
	Live/Dead	DRAQ7	-	1:2000	Biolegend	London, UK

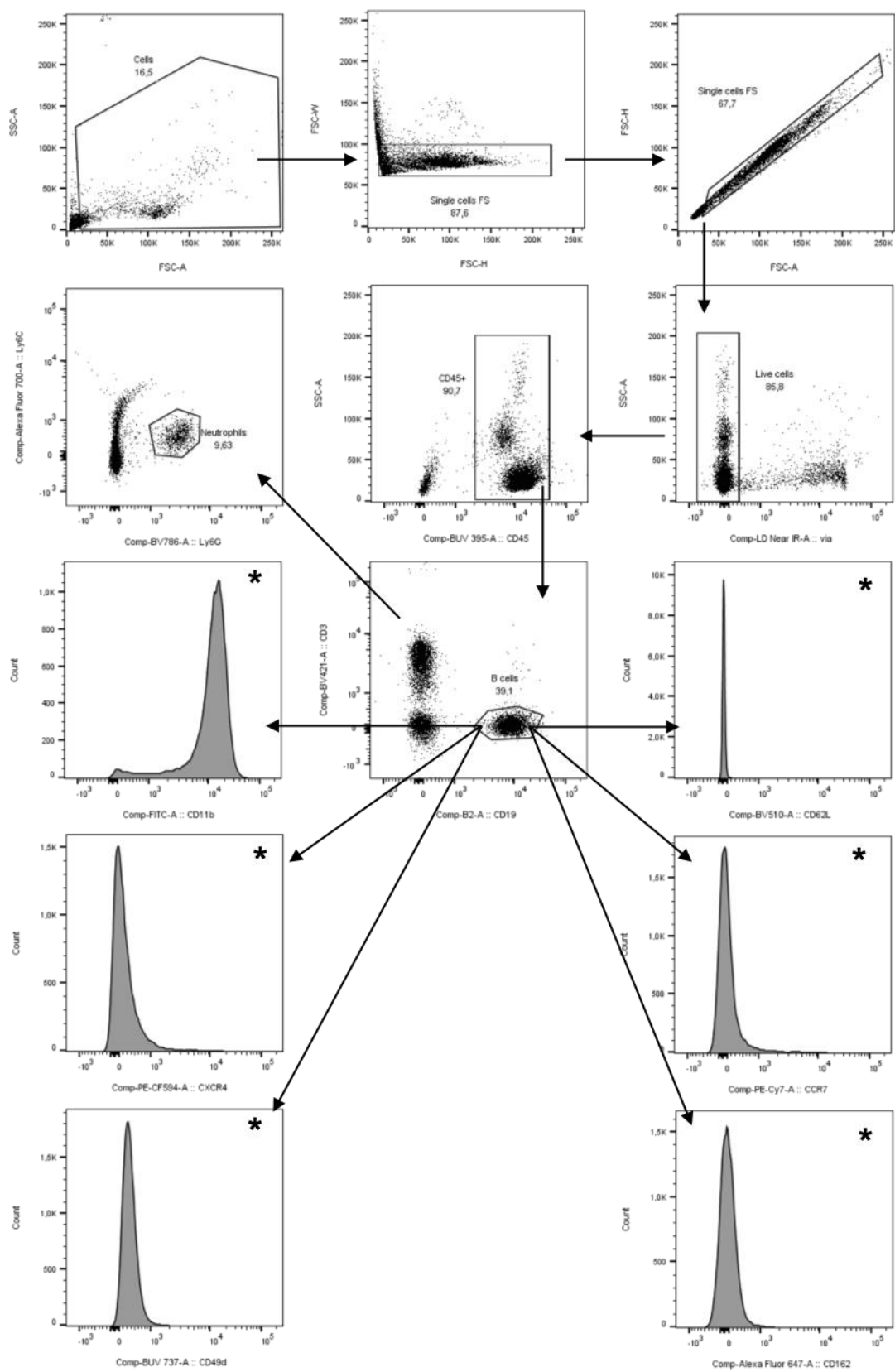


**Figure 2-18: Gating strategy for in vivo adhesion molecules (Fortessa).**  
 The gating strategies for \* were also applied to neutrophils. SS = Side Scatter, FS = Forward Scatter.

### 2.1.11 Functional blocking experiments

To block the entry of lymphocytes to LNs, WT mice were injected intraperitoneally with neutralizing antibodies against the integrins  $\alpha 4$  (CD49d, **Table 2-13**) and  $\alpha L$  (CD11a, **Table 2-13**) (von Andrian and Mempel, 2003). To block lymphocyte egress from LNs, the S1PR1 blocker FTY720 (Mandala et al., 2002) (**Table 2-13**) was injected intraperitoneally. Directly afterwards, mice were injected intraperitoneally with PBS or the specific adrenergic agonists Clenbuterol and BRL37344. Two hours later, at 12 pm, blood and LNs were harvested. As control group, untreated or PBS-treated WT mice were used. For the block of L-selectin (CD62L) a neutralizing antibody (**Table 2-13**) or isotype control were injected intraperitoneally 24 hours prior to adrenergic stimulation.

**Table 2-13: Blocking antibodies and reagents.**

Antigen/compound	Clone	Concentration	Solution	Control	Company
CD11a	M17/4	100 $\mu\text{g}/\text{mouse}$	PBS	-	Hölzel (Cologne, Germany)
CD49d	P/S2	100 $\mu\text{g}/\text{mouse}$	PBS	-	Hölzel (Cologne, Germany)
CD62L	MEL-14	200 $\mu\text{g}/\text{mouse}$	PBS	Rat IgG2a	Hölzel (Cologne, Germany)
FTY720	-	1 mg/kg	PBS	-	Sigma Aldrich (Darmstadt, Germany)

### 2.1.12 *In vitro* adrenergic stimulation of B cells and neutrophils and investigation of adhesion molecule expression

At 12 pm, spleens from WT mice were harvested and processed through a 40  $\mu\text{m}$  cell strainer. After centrifugation at 300 x g and 22°C for 5 min, erythrocytes were lysed by incubation in 4 ml RBC lysis buffer (**Table 2-14**) for 5 min at room temperature. The lysis was stopped with an equal amount of PBS and cells were centrifuged at 300 x g and 22°C for 5 min. The pellet was resuspended in PBS and 4 x 10<sup>5</sup> cells were transferred to each well of a 96-well V-bottom plate. Cell counts were obtained from a 1:10 dilution on a ProCyt Dx® cell counter (IDEXX Laboratories).

Bone marrow was obtained at 12 pm from two femora, processed through a 40  $\mu\text{m}$  cell strainer and centrifuged at 300 x g and 22°C for 5 min. Erythrocytes were lysed by incubation in 4 ml RBC lysis buffer (**Table 2-14**) for 5 min at room temperature. The lysis was stopped with an equal amount of PBS and cells were centrifuged at 300 x g and 22°C for 5 min. The pellet was resuspended in PBS and 4 x 10<sup>5</sup> cells were transferred to each well of a 96-well V-bottom plate. Cell counts were obtained from a 1:10 dilution on a ProCyt Dx® cell counter (IDEXX Laboratories).

Cells were incubated with 100  $\mu$ l PBS or 1 mM of Clenbuterol or BRL37344 for two hours. Subsequently, reagents were washed out once with PBS and once with Annexin V Binding Buffer (Biolegend) and an antibody mixture for identification of subsets and adhesion molecules (**Table 2-10** for B cells and **Table 2-11** for neutrophils) was added and incubated for 30 min at 4°C in darkness. Apoptotic and dead cells were identified using a combination of an Annexin V (Biolegend) antibody and 7-AAD (Biolegend). The plate was washed once with PBS and cells were resuspended in 190  $\mu$ l PBS and 10  $\mu$ l CountBright™ Absolute Counting Beads (Life Technologies).

### **2.1.13 *In vivo* imaging of B cells in the popliteal lymph node vasculature**

WT mice were anaesthetized by intraperitoneal injection of ketamine (100 mg/kg, Medistar) and xylazine (20 mg/kg, Rompun, Bayer vital GmbH). Hindlegs were shaved using a trimmer (Aesculap, GT415, BRAUN) and remaining hair was removed with depilation creme (Veet). A catheter consisting of fine tubing filled with isotonic saline and attached to the tip of a 30G-needle was inserted into the peritoneum to inject PBS or Clenbuterol during imaging. Mice were ventrally secured in an imaging chamber with integrated heating pad. After a skin incision above the knee, connective and fat tissue were torn to expose the popLN. Using sharp forceps, a small hole was carefully created beneath the LN and filled with PBS-soaked tissue pieces to lift the LN slightly out of the tissue. The tissue was kept moist by draping wet tissue paper around the skin incision. A cover glass (35 mm) was placed on top of the exposed LN and fixed in the imaging stage. Blood vessels were visualized by intravenous injection of FITC-Dextran (20  $\mu$ l, average molecular weight 150,000; Sigma-Aldrich) and B cells were visualized by intravenous injection of a fluorescence-labeled antibody (B220-PE, 5  $\mu$ l, clone RA3-6B2, Biolegend) 5 min prior to imaging with a Zeiss Axio Examiner.Z1 confocal spinning disk microscope (**Table 2-19**) equipped with 405, 488, 561, and 640 nm laser sources. After a control video of about 15 min, 100  $\mu$ l of either PBS or Clenbuterol (2 mg/kg) were administered through the peritoneal catheter and B cells in the superficial vasculature were imaged for about one hour until 12 pm. Analysis of the 4D intravital imaging was performed using ImageJ (version 1.51n) and Slidebook (version 6, Intelligent Imaging Innovations, 3i) (**Table 2-18**). To measure the time-dependent change in adhesion, videos were sum projected and subsequently the mean fluorescence intensity (MFI) of adherent cells within individual vessels was measured. Relative adhesion was calculated as percent increase (ratio) between the MFIs, which were detected shortly before the injection of Clenbuterol

and the MFIs of individual time points upon treatment (n(mice) = 2 (PBS/Clenbuterol); n(vessels) = 3-5).

#### **2.1.14 Statistical analysis**

Collective data sets were obtained by pooling data from the same experimental setups. Statistical analyses were performed using GraphPad Prism 6 or 8 software (**Table 2-18**). All data are represented as mean  $\pm$  SEM. An unpaired student's t-test was used for comparison between two groups. For comparison of three or more groups with one variable, one-way ANOVAs followed by Tukey's, Dunnett's or Mann-Whitney's post hoc test were performed. For comparison of three or more groups with two variables, two-way ANOVAs with Dunnett's or Sidak's post hoc test were used. Statistical significance was assessed as \* $p < 0.05$ , \*\* $p < 0.01$ , \*\*\* $p < 0.001$  and \*\*\*\* $p < 0.0001$ .

## 2.2 Materials

### 2.2.1 Buffers

**Table 2-14: Buffer ingredients.**

Buffer	Supplements
Genotyping digestion buffer	0.5 mM EDTA, 0.1 M Tris, 0.2% SDS, 0.2 M NaCl (pH 8.5)
PEB	PBS, 2 mM EDTA, 20% FCS
RBC lysis buffer	0.154 mM NH <sub>4</sub> Cl, 0.05 mM EDTA, 10 mM KHCO <sub>3</sub> (pH 7.25)
Tris-Acetate-EDTA (TAE) buffer	2 M Tris, 50 mM EDTA, 1 M acetic acid
Tris-EDTA (TE) buffer	2 M Tris, 50 mM EDTA

### 2.2.2 Reagents

**Table 2-15: List of used reagents with respective suppliers.**

Reagent	Company	Location
Agarose	Biozym Scientific	Oldendorf, Germany
Ammonium chloride (NH <sub>4</sub> Cl)	Merck	Darmstadt, Germany
Annexin V Binding Buffer	Biologend	London, UK
BRL37344	Sigma-Aldrich	Munich, Germany
CellTrace™ CFSE	Thermo Fisher Scientific	Munich, Germany
CellTracker™ Deep Red	Thermo Fisher Scientific	Munich, Germany
Clenbuterol	Sigma-Aldrich	Munich, Germany
Collagenase IV	Sigma-Aldrich	Taufkirchen, Germany
CountBright™ Absolute Counting Beads	Life Technologies	Darmstadt, Germany
4',6-diamidino-2-phenylindole (DAPI)	Biologend	London, UK
Denopamine	Sigma-Aldrich	Munich, Germany
Dimethyl sulfoxide (DMSO)	Sigma-Aldrich	Munich, Germany
DNase I Ambion™	Life Technologies	Darmstadt, Germany
DPBS	Life Technologies	Darmstadt, Germany
Ethylenediaminetetraacetic acid (EDTA)	Life Technologies	Darmstadt, Germany
FastGene 100 bp DNA Marker	Nippon Genetics	Düren, Germany
FastGene Optima PCR HotStart	Nippon Genetics	Düren, Germany
Fetal Calf Serum (FCS)	Life Technologies	Darmstadt, Germany
Fluorescein isothiocyanate (FITC)-Dextran (150,000)	Sigma-Aldrich	Munich, Germany
FTY720 (Fingolimod)	Sigma-Aldrich	Darmstadt, Germany
Histoacryl glue	B. Braun AG	Puchheim, Germany
HyPure™ Molecular Biology Grad Water (nuclease-free)	GE Healthcare LifeSciences	South Logan, Utah, USA
Isoflurane	CP-Pharma	Burgdorf, Germany
Isopropanol (Propan-2-ol)	AppliChem	Darmstadt, Germany
Isoproterenol	Sigma-Aldrich	Munich, Germany
Ketamine	Medistar	Munich, Germany
Midori Green Advance	Nippon Genetics	Düren, Germany
Phosphate-buffered saline (PBS)	Apotheke Klinikum München	Munich, Germany
Potassium hydrogen carbonate (KHCO <sub>3</sub> )	Merck	Darmstadt, Germany
Propranolol	Sigma-Aldrich	Munich, Germany
Proteinase K	Life Technologies	Darmstadt, Germany

Reagent	Company	Location
Sodium chloride (NaCl)	Sigma-Aldrich	Taufkirchen, Germany
Sodium dodecyl sulfate (SDS) 10%	Sigma-Aldrich	Taufkirchen, Germany
Tris	AppliChem	Darmstadt, Germany
UltraComp eBeads™ Compensation Beads	Thermo Fisher Scientific	Munich, Germany
Veet Depilation Creme	Reckitt Benckiser Deutschland GmbH	Heidelberg, Germany
Xylazine (Rompun™)	Bayer vital GmbH	Leverkusen, Germany

### 2.2.3 Materials

**Table 2-16: List of used materials with respective suppliers.**

Material	Company	Location
Cell strainer (40 µm)	Thermo Fisher Scientific	Darmstadt, Germany
Cover glass (35 mm)	Thermo Fisher Scientific	Darmstadt, Germany
Microhematocrit tubes	VWR	Darmstadt, Germany
Polyethylene tubing	Smiths Medical Deutschland GmbH	Grasbrunn, Germany
PopLN imaging stage	Built in-house	Munich, Germany

### 2.2.4 Devices

**Table 2-17: List of used devices and respective suppliers.**

Device	Company	Location
Aesculap Exacta Cordless Dog Grooming Trimmer	Aesculap AG, BRAUN	Tuttlingen, Germany
Electrophoresis Chamber	BioRad	Munich, Germany
Gallios Flow Cytometer	Beckman Coulter	Krefeld, Germany
Heraeus Multifuge X3R	Thermo Fisher Scientific	Munich, Germany
Isoflurane Chamber	Groppler Medizintechnik	Deggendorf, Germany
LSRFortessa Flow Cytometer (Munich)	BD bioscience	Heidelberg, Germany
Mastercycler Eppgradient S	Eppendorf	Munich, Germany
Mastercycler Nexus	Eppendorf	Munich, Germany
Minicentrifuge	Eppendorf	Munich, Germany
PowerPac Basic	BioRad	Munich, Germany
ProCytex Dx®	IDEXX Laboratories	Hoofddorp, Netherlands
Spinning Disk Microscope	Zeiss	Jena, Germany
ThermoMixer F1.5	Eppendorf	Munich, Germany
UV Transilluminator Gel Imaging Chamber	INTAS Science Imaging	Göttingen, Germany
UVP Minidizer Oven	Analytik Jena	Jena, Germany
Vortex Genie 2	Scientific Industries	Munich, Germany

## 2.2.5 Software

**Table 2-18: List of used software with respective suppliers.**

Software	Company	Location
Excel	Microsoft	USA
GraphPad Prism 6&8	GraphPad Software	La Jolla, CA, USA
FlowJo™ V10.6.2	Becton Dickinson GmbH	Heidelberg, Germany
Fiji Version 1.51n	Open-Source	USA
SlideBook Version 6	Intelligent Imaging Innovations, 3i	Göttingen, Germany

## 2.2.6 Microscope configuration

**Table 2-19: Microscope configuration.**

Microscope	Objectives	Numerical Aperture	Excitation laser [nm]	Default filter	Filter range [nm]
Upright Zeiss Axio Examiner.Z1 confocal spinning disk microscope	5x (n-plan)	0.15	405	387/11	382-391
	10x (w-plan)	0.3	488	485/20	475-495
	20x (w-plan)	1.0	561	560/25	552-572
	63x (w-plan)	1.0	640	650/13	644-656
Magnification = 10x ocular x objective					

## 3 Results

### 3.1 Overview of the experimental design

As an overview, the scientific questions and respective experiments are summarized in **Figure 3-1**.

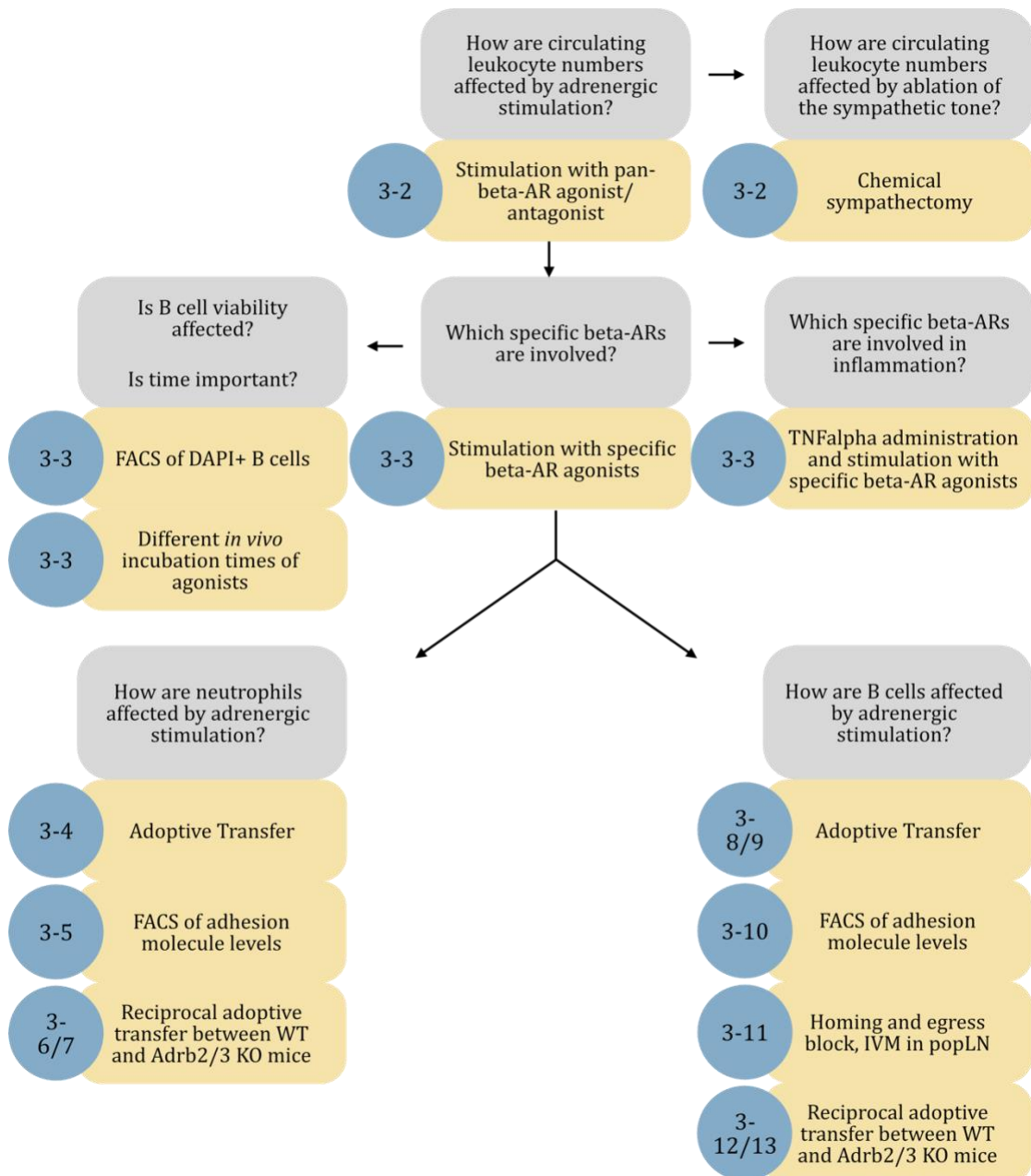


**Figure 3-1: Overview of the scientific questions and the experimental design.**

Scientific questions in gray boxes were approached with respective experiments in yellow boxes. Figure numbers showing respective data are indicated in blue circles. AR = adrenoceptor, Adrb2/3 KO =  $\beta_2/\beta_3$ -adrenoceptor knockout, IVM = intravital microscopy, popLN = popliteal lymph node.

## 3.2 Stimulation of $\beta$ -ARs affects leukocyte numbers in blood

In a first experiment, WT mice were intraperitoneally injected with PBS, the pan- $\beta$ -AR agonist Isoproterenol (Iso) or the pan- $\beta$ -AR antagonist Propranolol (Prop) two hours prior to blood harvest (see 2.1.5). Total leukocyte as well as subset counts were obtained using flow cytometry. As numbers of leukocytes in blood oscillate throughout the day, peaking at 12 pm and troughing at 8 pm in mice (Druzd et al., 2017; He et al., 2018; Scheiermann et al., 2012), samples were harvested at these two time points. Time-of-day differences were verified for white blood cell (WBC), B cell, CD8+ T cell, inflammatory monocyte (Infl. Monos) and eosinophil counts in the PBS control, whereas differences in other subset counts were not significant, but exhibited a trend to decreased circulating numbers at night. At 12 pm, no differences were detectable in WBC counts between the treatments, whereas at 8 pm, leukocyte numbers were increased after injection of the pan- $\beta$ -AR agonist Iso. The pan- $\beta$ -AR antagonist Prop showed a small effect in the evening compared to the control (**Figure 3-2A**). Neutrophil numbers showed similar results during day and night, with significantly elevated numbers in blood upon pharmacological stimulation of  $\beta$ -ARs. Prop injection had a small, but not significant effect at both time points, in that neutrophil numbers were slightly reduced compared to the PBS control. B cell numbers, on the other hand, showed inversed effects. Circulating numbers were drastically reduced upon activation of  $\beta$ -ARs. However, effects were only visible during the day, as numbers in blood were low at night already. Injection of the antagonist Prop led to slightly increased, but again not significantly changed numbers of B cells at both time points (**Figure 3-2A**). Other lymphocyte subsets (CD4+ and CD8+ T cells) were not significantly affected by Iso and Prop administration, although Prop slightly increased numbers during both time points. Additionally, CD8+ T cell numbers were marginally higher upon agonism at night (**Figure 3-2A**). Monocytes and NK cells were not affected by either pharmacological agent. Eosinophil numbers were reduced during the day upon  $\beta$ -AR stimulation, while circulating numbers at night were already low (**Figure 3-2A**). Due to the fact that neutrophils and B cells exhibited the most distinctive – and opposite – results, in the following only these two subsets will be highlighted.

Since antagonism of  $\beta$ -AR signaling by Prop injection did not strongly influence circulating leukocyte numbers, the impact of a chemical sympathectomy was tested. Therefore, mice received the neurotoxin 6-hydroxydopamine (6-OHDA) intraperitoneally over two consecutive days, resulting in abolishment of the sympathetic tone (Glinka et al., 1997).

On day five of the experiment, blood was harvested at 12 pm and leukocyte counts were obtained using flow cytometry (see 2.1.6). Neither for total leukocyte counts, nor for neutrophils and B cells was a difference detected between control and sympathectomized mice (**Figure 3-2B**, for other subsets see **Figure 6-1**). Taken together, these data suggest a role for  $\beta$ -AR signaling in the regulation of circulating leukocyte numbers, whereas blocking showed minor effects and absence of the sympathetic tone affected their numbers not at all.

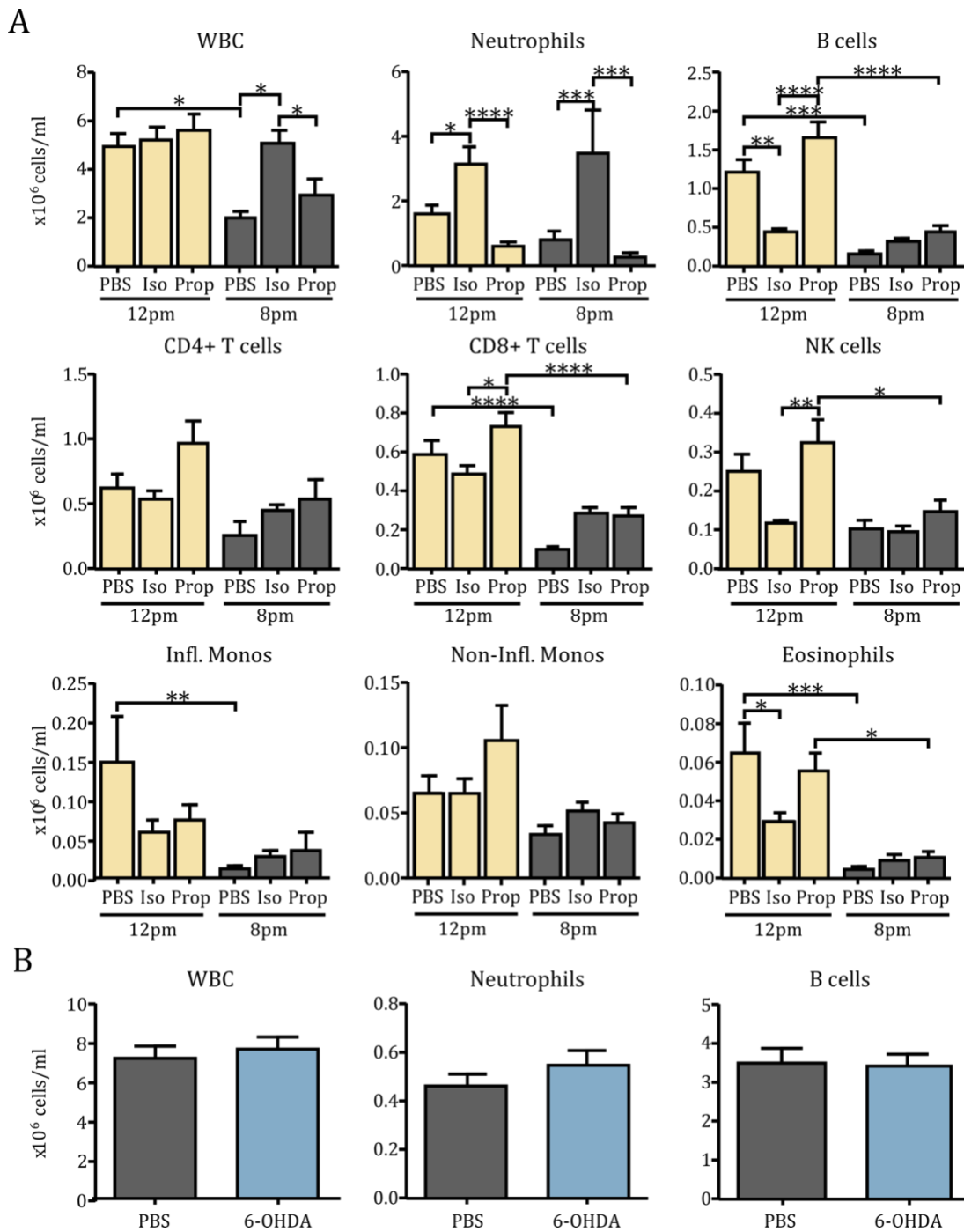


**Figure 3-2: Effects of agonism or antagonism/absence of sympathetic signaling on circulating leukocyte numbers.**

**(A)** Leukocyte numbers in blood after agonism or antagonism of  $\beta$ -ARs during day and night. WT mice were injected with PBS, the pan- $\beta$ -AR agonist Isoproterenol (Iso) or the pan- $\beta$ -AR antagonist Propranolol (Prop) 2hrs prior to blood harvest at 12 pm (yellow) or 8 pm (gray). Cell counts were obtained using flow cytometry.  $n = 6-10$ , two-way ANOVA, Tukey's test. **(B)** WBC, neutrophil and B cell numbers in blood after ablation of the sympathetic tone during the day. WT mice were injected with PBS (gray) or 6-hydroxydopamine (6-OHDA, blue) on day zero and day two, blood was harvested at 12 pm on day five of the treatment.  $n = 5$ , student's t-test. WBC = White blood cells, NK cells = Natural Killer cells, Infl. Monos = Inflammatory Monocytes, Non-Infl. Monos = Non-Inflammatory Monocytes.

### 3.3 Blood leukocyte numbers are controlled by $\beta_2$ - and $\beta_3$ -ARs

To investigate which of the three family members of  $\beta$ -ARs were involved in the regulation of blood leukocyte numbers, specific pharmacological agonists were used.  $\beta_1$ -ARs were stimulated by injection of Denopamine (Den),  $\beta_2$ -ARs by Clenbuterol (Clen) and  $\beta_3$ -ARs by BRL37344 (BRL) two hours prior to blood harvest at 12 pm or 8 pm (see 2.1.5).

Cell counts in DMSO and Den-treated mice did not differ from each other, neither at 12 pm nor at 8 pm (**Figure 3-3A**). Thus,  $\beta_1$ -ARs were not involved in the observed phenotypes in **Figure 3-2A**.

Upon injection of Clen and BRL, similar results to stimulation with Iso (**Figure 3-2A**) were observed. WBC counts between treatments were not altered at 12 pm, due to increased neutrophil and decreased B cell numbers at this time point, which might cancel each other out (**Figure 3-3B**). Effects were even more dramatic for neutrophils at night, since murine blood already contains fewer cells at this time of day. Because of the same reason, circulating B cell numbers did not change at 8 pm. As differences in numbers of both leukocyte subsets were observed during the day time point, experiments in the following sections were only performed at 12 pm. Results for other circulating leukocyte subsets can be found in **Figure 6-2**.

To investigate the influence of adrenergic stimulation under inflammatory conditions, WT mice received  $\text{TNF}\alpha$  one hour before they were injected with PBS or the specific agonists (see 2.1.7). Under inflammatory conditions, the time-of-day difference in PBS-treated mice was gone (except for B cells) and WBC counts were slightly reduced (**Figure 3-3C**) in comparison to steady state (**Figure 3-3B**). Neutrophil counts were not significantly altered upon adrenergic stimulation after  $\text{TNF}\alpha$  administration, but showed a similar trend as under steady state, in that numbers increased upon Clen injection. The dramatic differences in B cell numbers were annihilated, predominantly due to lower numbers after  $\text{TNF}\alpha$  administration ( $0.5 \times 10^6$  cells/ml vs.  $1.5 \times 10^6$  cells/ml under steady state), suggesting that in an inflammatory scenario, adrenergic stimulation does not affect circulating leukocyte numbers to the same extent as under homeostasis.

Since B cell numbers in blood decreased upon adrenergic stimulation, it was tested whether administration of the agonists leads to augmented cell death. Using flow cytometry, B cells positive for the live/dead staining DAPI were identified (**Figure 3-3D**). Depicted as percentage of total B cells, it was demonstrated that administration of Clen and BRL did not increase numbers of dead cells, indicating that B cells were redistributed upon adrenergic stimulation. Additionally, it was tested in an *in vitro* approach whether

direct contact between cells and agonists causes cell death. For this, B cells isolated from the spleen were incubated with the agonists for two hours. As shown in **Figure 3-3E**, the ratio of dead B cells was not higher in treated samples. Taken together, these data demonstrate that treatment with Clen and BRL increased circulating neutrophil numbers while decreasing circulating B cell numbers by redistribution of these leukocyte subsets. So far, blood was harvested two hours after intraperitoneal administration of the pharmacological agonists. To evaluate the temporal profile of the effects on leukocyte numbers in blood, an experimental time course was performed, where blood was harvested 10 min, 60 min, 120 min and 360 min after injection. As shown in **Figure 3-3F**, two hours between treatment and harvest were effectual to alter circulating leukocyte numbers, exemplarily shown for B cells (see other subsets in **Figure 6-4**).

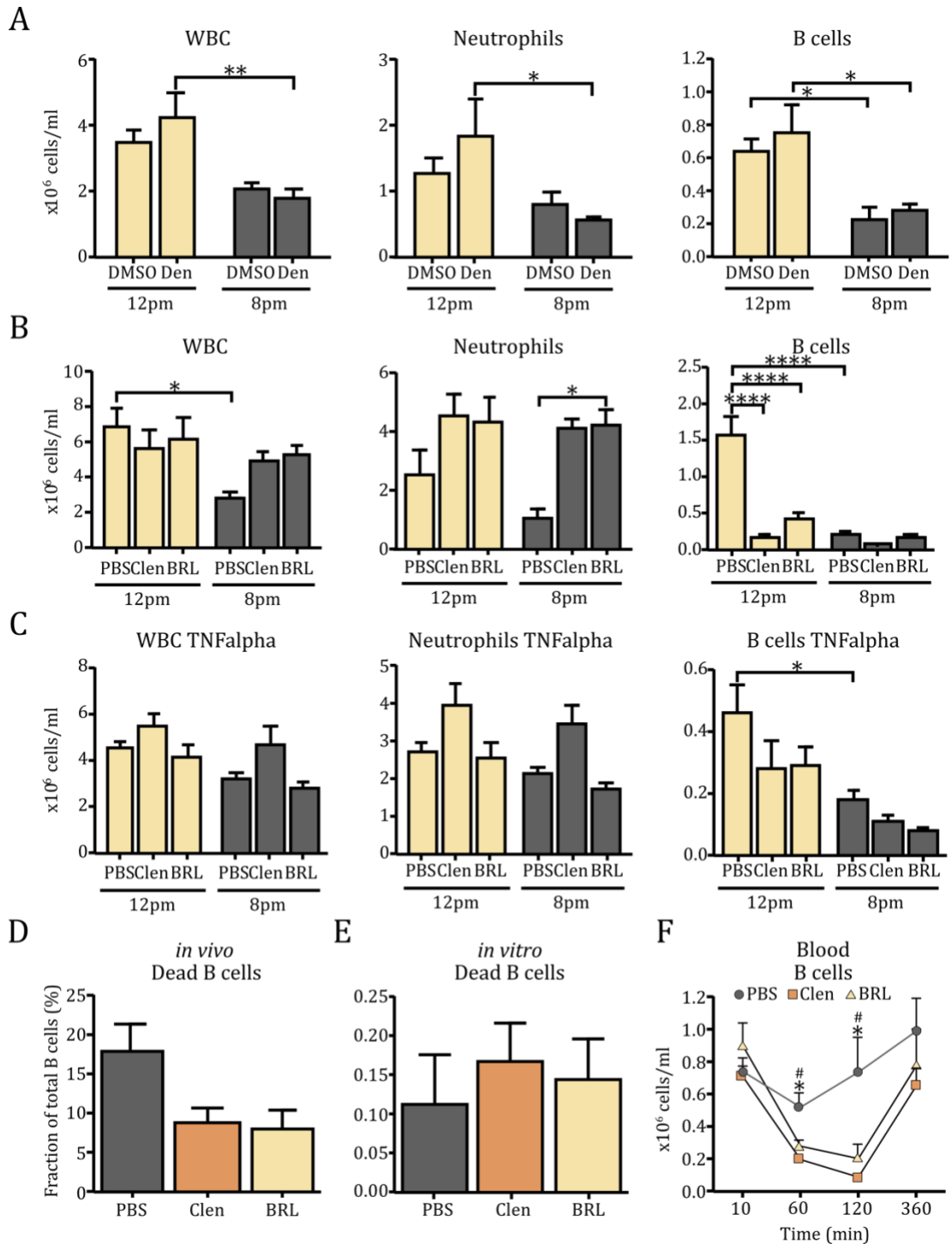


**Figure 3-3: Changes in blood leukocyte numbers are mediated by  $\beta_2$ - and  $\beta_3$ -ARs.**

**(A)** Cell counts in blood upon stimulation of  $\beta_1$ -ARs. WT mice were injected with DMSO or Denopamine (Den) 2hrs prior to harvest at 12 pm (yellow) or 8 pm (gray). n = 6, two-way ANOVA, Tukey's test. **(B)** Cell counts in blood upon stimulation of  $\beta_2$ - and  $\beta_3$ -ARs. WT mice were injected with PBS, Clenbuterol (Clen) or BRL37344 (BRL) 2hrs prior to harvest at 12 pm (yellow) or 8 pm (gray). n = 5-6, two-way ANOVA, Tukey's test. **(C)** Cell counts in blood upon stimulation of  $\beta_2$ - and  $\beta_3$ -ARs under inflammation. WT mice received TNF $\alpha$  and PBS or the adrenergic agonists. Blood was harvested at 12 pm (yellow) or 8 pm (gray). n = 5-6, two-way ANOVA, Tukey's test. **(D)** Fractions of dead B cells after *in vivo* stimulation for 2hrs. n = 3, one-way ANOVA, Dunnett's test. **(E)** Fraction of dead B cells after *in vitro* stimulation for 2hrs. n = 6, one-way ANOVA, Dunnett's test. **(F)** Time course of harvest time. Cell counts in blood after different times between injection and harvest. n = 3, one-way ANOVA, Dunnett's test. WBC = White blood cells.

## 3.4 Neutrophils are redistributed upon adrenergic stimulation

### 3.4.1 $\beta_2$ -ARs influence recruitment, $\beta_3$ -ARs influence mobilization of neutrophils

To investigate whether increased circulating neutrophil numbers were attributed to enhanced mobilization into blood and/or impaired recruitment from blood, an adoptive transfer of donor cells into stimulated recipients was performed (see 2.1.9) with subsequent analysis of donor and endogenous cells in various organs. Cells extracted from spleen and BM were mixed and stained to allow tracing after injection. Recipients were intraperitoneally injected with PBS or the adrenergic agonists Clen ( $\beta_2$ -AR) or BRL ( $\beta_3$ -AR) and one hour later received the donor cells intravenously. After another hour, in which donor cells circulated through the system, mice were intravenously injected with a fluorescently labeled antibody against the common leukocyte marker CD45. Five minutes later, at 12 pm, blood was harvested and mice were perfused to remove non-adherent cells from the circulation. Subsequently, the femur, spleen, liver, and lung were harvested (**Figure 3-4A**). Together with blood, organs were processed for flow cytometry and stained for leukocyte subsets. Using another clone and fluorescent label of a CD45 targeting antibody during processing, leukocytes within the circulation (double positive) could be distinguished from extravascular cells that immigrated into the tissue (single positive). Where sampling of the whole organ was not practical (as for the liver and lung), leukocyte numbers were extrapolated for the whole organ. The same applied for the blood, which was estimated to be 2 ml per mouse.

Endogenous neutrophil numbers in blood were elevated upon injection of either  $\beta$ -AR agonist (**Figure 3-4B**), confirming the results in **Figure 3-3B**. Interestingly, in the BM (represented by two femora), administration of BRL led to a reduction of neutrophil numbers by about five million cells, suggesting that these cells could be mobilized from the BM (**Figure 3-4B**). Numbers were increased in the liver, in which the  $\beta_3$ -AR agonist showed a more dramatic effect (six-fold). In the lung, both agonists increased neutrophil numbers to the same extent. The spleen exhibited more endogenous neutrophils upon treatment with BRL. The distribution of other endogenous myeloid subsets is displayed in **Figure 6-5**.

Detected endogenous neutrophils in each organ were then subdivided into CD45-single positive extravascular cells and CD45-double positive intravascular cells, shown as percentage of the overall detected cells (**Figure 3-4C**). Supporting the suggestion that neutrophils might be mobilized from the BM upon stimulation of  $\beta_3$ -ARs, injection of BRL shifted the ratio of intra- versus extravascular cells to a higher percentage of intravascular

cells in this tissue. The opposite was the case in the liver, where more extravascular neutrophils could be detected upon BRL injection. In the lung and spleen, adrenergic stimulation did not change the localization of neutrophils. Localization data obtained for other endogenous myeloid subsets can be found in **Figure 6-6**.

To examine whether neutrophil homing was impaired by adrenergic stimulation, the percentage of injected donor neutrophils in blood and each organ was calculated (**Figure 3-4D**). Upon injection of the  $\beta_2$ -AR agonist Clen, the percentage of donor neutrophils in blood was significantly increased, suggesting a reduced recruitment to tissues. Stimulation of  $\beta_3$ -ARs did not show an effect, supporting the hypothesis of higher blood counts due to enhanced mobilization from the BM. Additionally, in BM no effect in neutrophil homing could be observed. Taken together, these data suggest that  $\beta_3$ -ARs might be involved in mobilization rather than homing of neutrophils, whereas for  $\beta_2$ -ARs the opposite could be the case. Similar to endogenous neutrophils, pharmacological stimulation of  $\beta_3$ -ARs also increased the percentage of donor neutrophils in the liver, whereas in the lung,  $\beta_2$ -ARs could be involved in neutrophil homing, as the percentage of detected neutrophils showed almost a two-fold increase upon injection of Clen. Neutrophil homing to the spleen was not affected by any of the agonists. The distribution of other adoptively transferred myeloid cells is illustrated in **Figure 6-7**.

Although adrenergic stimulation of the recipients did not have an impact on donor neutrophil numbers in the BM, their localization within the organ was altered, in that slightly more (4%) intravascular cells were detected upon  $\beta_2$ -AR stimulation by Clen (**Figure 3-4E**), indicating that adoptively transferred neutrophils adhered to the vasculature as a first step of homing to the BM. In the liver, very similar results were obtained for donor neutrophils as for endogenous cells, manifesting a 25% higher extravascular fraction upon BRL injection. The localization of injected neutrophils in the lung and spleen was not affected. In general, a relatively high percentage of injected neutrophils could be detected in the tested organs (**Table 3-1**), predominantly due to retention of the majority of cells in the blood. Taken together, presented data suggest a dual role of adrenergic signaling in the redistribution of neutrophils, as  $\beta_2$ -ARs influenced homing and  $\beta_3$ -ARs impacted mobilization of this leukocyte subset. The intra- and extravascular localization of other donor myeloid cells is illustrated in **Figure 6-8**.

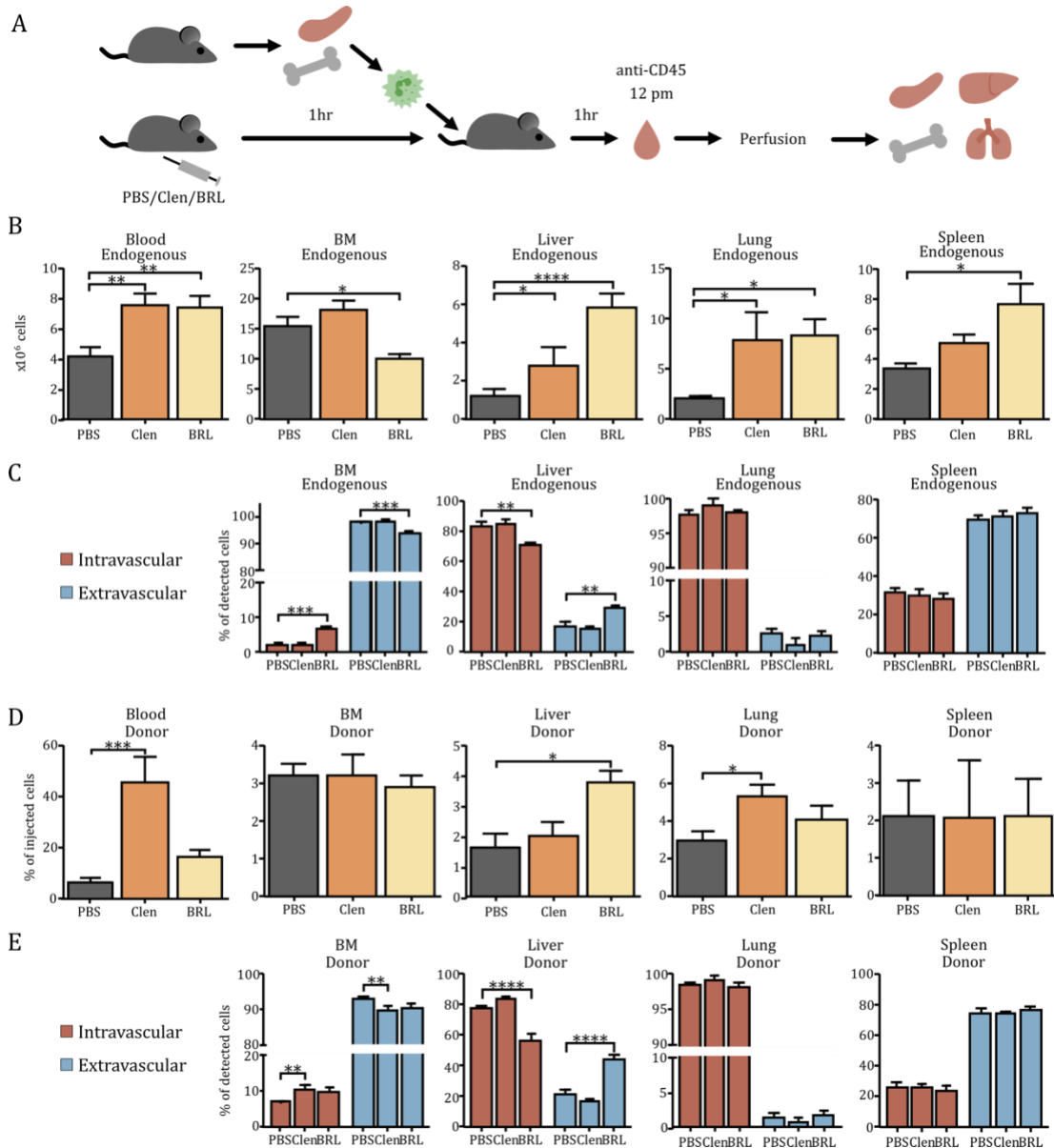


**Figure 3-4: Neutrophils are redistributed by adrenergic stimulation.**

**(A)** Illustration of the experimental design. Recipient mice were intraperitoneally injected with PBS, Clenbuterol (Clen) or BRL37344 (BRL) and received 1hr later the stained donor cells. At 12 pm, a CD45 labeling antibody was injected and blood was harvested 5 min later. Mice were perfused and organs were harvested and processed for flow cytometry. **(B)** Endogenous neutrophil numbers in blood and organs after injection of PBS or the specific agonists, extrapolated to 2 ml of blood or the whole organ, respectively.  $n = 5-39$ , one-way ANOVA, Dunnett's test. **(C)** Intravascular (red) and extravascular (blue) endogenous neutrophils as percentage of the detected cells in the respective organs.  $n = 5-6$ , two-way ANOVA, Dunnett's test. **(D)** Detected donor neutrophils in blood and organs as percentage of the injected cells.  $n = 5-6$ , one-way ANOVA, Dunnett's test. **(E)** Intravascular (red) and extravascular (blue) donor neutrophils as percentage of the detected cells in the respective organs.  $n = 5-6$ , two-way ANOVA, Dunnett's test.

**Table 3-1: Donor neutrophils as percentage of injected neutrophils in blood and organs.**

Data are presented as mean  $\pm$  SEM. BM = bone marrow.

	<b>Blood</b>	<b>BM</b>	<b>Spleen</b>	<b>Liver</b>	<b>Lung</b>	<b>Total</b>
<b>PBS</b>	6.33 $\pm$ 2.00	3.20 $\pm$ 0.30	2.11 $\pm$ 0.97	1.67 $\pm$ 0.45	2.88 $\pm$ 0.54	16.19 $\pm$ 4.26
<b>Clen</b>	44.92 $\pm$ 10.91	3.18 $\pm$ 0.57	2.09 $\pm$ 1.52	2.12 $\pm$ 0.51	5.32 $\pm$ 0.58	57.63 $\pm$ 14.09
<b>BRL</b>	16.51 $\pm$ 2.50	2.86 $\pm$ 0.33	2.13 $\pm$ 0.97	3.77 $\pm$ 0.46	4.06 $\pm$ 0.69	29.33 $\pm$ 4.95

### 3.4.2 Neutrophil adhesion molecule levels change upon adrenergic stimulation

To shuttle between blood and tissues, leukocytes utilize specific sets of adhesion molecules and chemokine receptors that interact with their binding partners on endothelial cells of the respective vascular beds. After observing a redistribution of neutrophils between blood and organs, a putative effect of adrenergic stimulation on adhesion molecule and chemokine receptor levels on the surface of this leukocyte subset was investigated. In an *in vivo* approach (performed by Chen Wang), mice were injected intraperitoneally with PBS, Clen or BRL. Two hours later, at 12 pm, blood was harvested and processed for flow cytometry, where mean fluorescence intensities (MFIs) of CD11b (part of Mac-1), CXCR4, CD162 (PSGL-1), CD62L (L-selectin) and CD49d (part of VLA-4) were recorded (**Table 2-12**).

On circulating neutrophils, which accumulated in blood upon adrenergic stimulation (**Figure 3-4B**), injection of Clen led to decreased surface levels of the adhesion molecule CD11b, which is part of the Mac-1 integrin complex. In contrast, levels of CXCR4 were increased upon administration of both, Clen and BRL. Levels of CD162 were not altered. Although not significantly, CD62L levels were increased when mice were injected with Clen. CD49d levels were downregulated upon Clen-injection (**Figure 3-5A**). As CD62L is shed upon activation, its upregulation upon stimulation of  $\beta_2$ -ARs confirmed the assumption from adoptive transfer experiments (**Figure 3-4D**) in that cells could be hindered to leave the blood due to impaired recruitment. Downregulation of the integrin CD11b supported this hypothesis whereas upregulation of CXCR4 indicated that neutrophils might home back to the BM, for which this chemokine receptor is crucial. However, expression levels of CXCR4 and CD49d were generally low.

To ascertain direct effects of the adrenergic agonists on adhesion molecule levels of neutrophils, cells obtained from BM were seeded in a 96-well plate and incubated *in vitro* with Clen or BRL for two hours. Using flow cytometry, MFIs of CD11b, CXCR4, CD162 and CD62L were measured and are shown in **Figure 3-5B**. Although CXCR4 levels exhibit the same trend as *in vivo*, no significant changes in surface molecule levels were detected. The

same applied for the other tested adhesion molecules and chemokine receptors. Taken together, these data present evidence that adhesion molecule levels on neutrophils are altered, leading to a less activated state of the cells, which could explain why neutrophil numbers in blood were increased, as cells could not leave the circulation. Furthermore, direct stimulation of neutrophils did not show effects on molecule levels, hinting to an environmentally mediated effect of adrenergic stimulation.

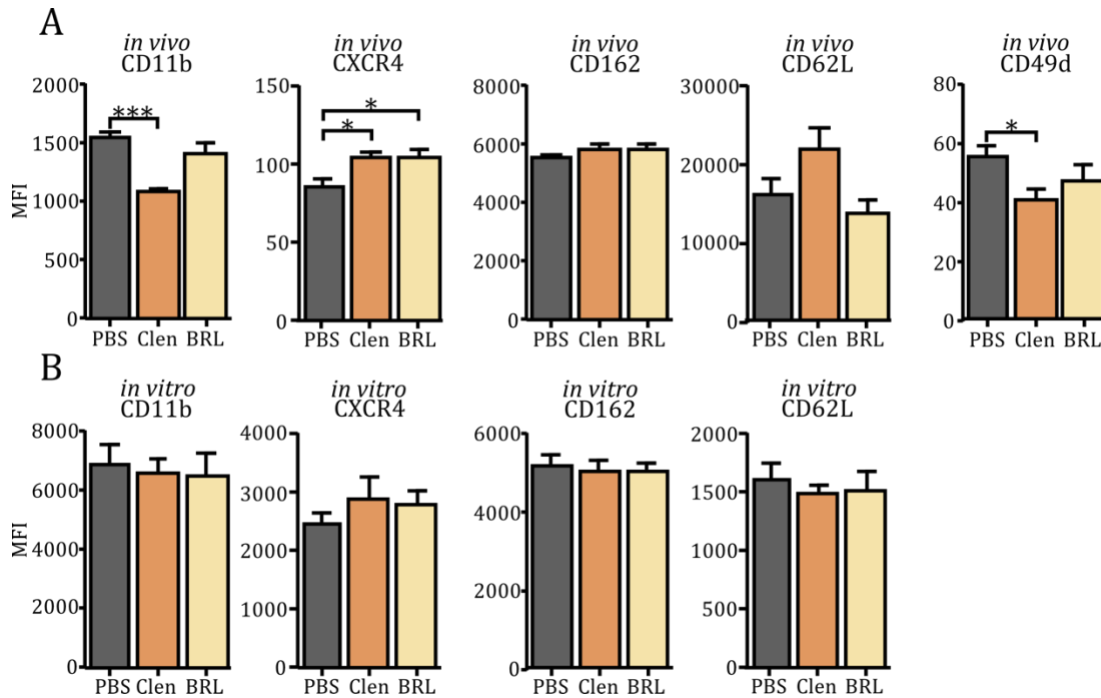


**Figure 3-5: Adhesion molecule levels on neutrophils are altered upon adrenergic stimulation.**

**(A)** MFI of several molecules on circulating neutrophils after *in vivo* adrenergic stimulation. WT mice were intraperitoneally injected with PBS (gray), Clenbuterol (Clen, orange) or BRL37344 (BRL, yellow) 2hrs prior to blood harvest at 12 pm. n = 6, one-way ANOVA, Dunnett's test. Experiment was performed by Chen Wang. **(B)** MFI of several molecules on neutrophils after *in vitro* adrenergic stimulation. BM from WT mice was harvested and processed. Cells were seeded into 96-well plates and stimulated *in vitro* with PBS, Clen or BRL for 2hrs. n = 3, one-way ANOVA, Dunnett's test. MFI = Mean fluorescence intensity.

### 3.4.3 $\beta_2$ -ARs of neutrophils and their environment are targeted

Since *in vivo* stimulation with adrenergic agonists affected adhesion molecule levels on neutrophils differently than stimulation *in vitro* (**Figure 3-5**), it was further investigated whether this leukocyte subset was directly targeted or whether cells in the microenvironment were responsible for their redistribution. Therefore, reciprocal adoptive transfers between WT mice and mice lacking  $\beta_2$ -ARs (Adrb2 KO) were performed (see 2.1.9). WT or KO cells were intravenously injected into stimulated WT recipients, or WT donor cells were injected into stimulated WT or KO recipients. After one hour of circulation, blood from recipients was harvested at 12 pm, mice were perfused and the femur, spleen, liver, and lung were harvested and together with blood processed for flow cytometry (**Figure 3-6A**).

First, endogenous neutrophil numbers in WT and Adrb2 KO mice were screened after PBS- or Clen-injection (**Figure 3-6B**). Although not significant, WT recipients possessed more endogenous neutrophils in their blood after Clen injection, reproducing previous experiments (**Figure 3-4B**). This effect was not observable in blood of mice lacking  $\beta_2$ -ARs, confirming that Clen-induced augmentation of circulating neutrophils was mediated by  $\beta_2$ -ARs. As expected, no effect of  $\beta_2$ -AR stimulation in the BM was observed. No significant changes were detectable in the spleen either, especially due to the high deviation in Clen-stimulated WT mice. In the liver and lung, neutrophil numbers in Clen-stimulated WT mice should have been increased, which was slightly the case in the liver, but not in the lung. This shows that neutrophil homing to these organs under adrenergic stimulation is not robust and could be therefore unspecific. Taken together, no effects of Clen-treatment on neutrophil numbers in organs of Adrb2 KO mice were observed, confirming that neutrophil redistribution was  $\beta_2$ -AR specific. Interestingly however, the lung of Adrb2 KO mice harbored more than three times as much endogenous neutrophils than WT mice, indicating that the pulmonary marginated pool might require the presence of  $\beta_2$ -ARs (**Figure 3-6B**).

In a next step, it was examined whether cell-intrinsic  $\beta_2$ -ARs were involved in the observed phenotype of neutrophil redistribution. For this, WT or Adrb2 KO donor cells were injected into PBS- or Clen-treated WT recipients (**Figure 3-6C**). Data are presented as fraction normalized to WT donor cells in the PBS-treated control group. In blood, WT donor neutrophils were accumulated, reproducing the results shown in **Figure 3-4D**. This change was observed to a lesser extent when Adrb2 KO donor neutrophils were injected into pharmacologically stimulated WT mice, indicating that  $\beta_2$ -ARs on neutrophils were partially involved in impaired neutrophil recruitment from the blood. No significant

changes were expected and assessed in the BM, spleen and liver, although the latter exhibited elevated WT donor neutrophils upon Clen injection. Increased homing of WT donor neutrophils to the lung was anticipated, but not detected, supporting the assumption that homing to this tissue might have been unspecific.

Adrenoceptors are not only expressed by leukocytes, but also by a wide variety of stromal cells. Thus, it was investigated whether  $\beta_2$ -ARs on these microenvironmental cells play a role in the adrenergic redistribution of neutrophils. **Figure 3-6D** depicts the fraction of WT donor neutrophils in PBS- or Clen-treated WT or *Adrb2* KO recipients, normalized to donor cells in the PBS-treated control. In blood of WT recipients treated with Clen, WT donor neutrophils exhibited the expected significant increase in cell numbers, which did not hold true for WT neutrophils in mice lacking  $\beta_2$ -ARs (**Figure 3-6D**). Due to lower differences in a KO environment compared to differences in numbers of KO donor neutrophils in a WT environment (**Figure 3-6C**), it can be assumed that the involvement of  $\beta_2$ -ARs on stromal cells is greater than that of receptors on neutrophils. In BM, no changes of WT donor cell homing to Clen-stimulated WT mice were registered in previous experiments (**Figure 3-4C**), but in this experimental setting less WT donor neutrophils homed to the BM, which was not the case for cells lacking  $\beta_2$ -ARs (**Figure 3-6D**). No significant changes were detectable in the other tested organs. Summed up, reciprocal adoptive transfers between WT and *Adrb2* KO mice revealed that  $\beta_2$ -ARs primarily on stromal cells, but also on neutrophils influenced the distribution of neutrophils between blood and organs.

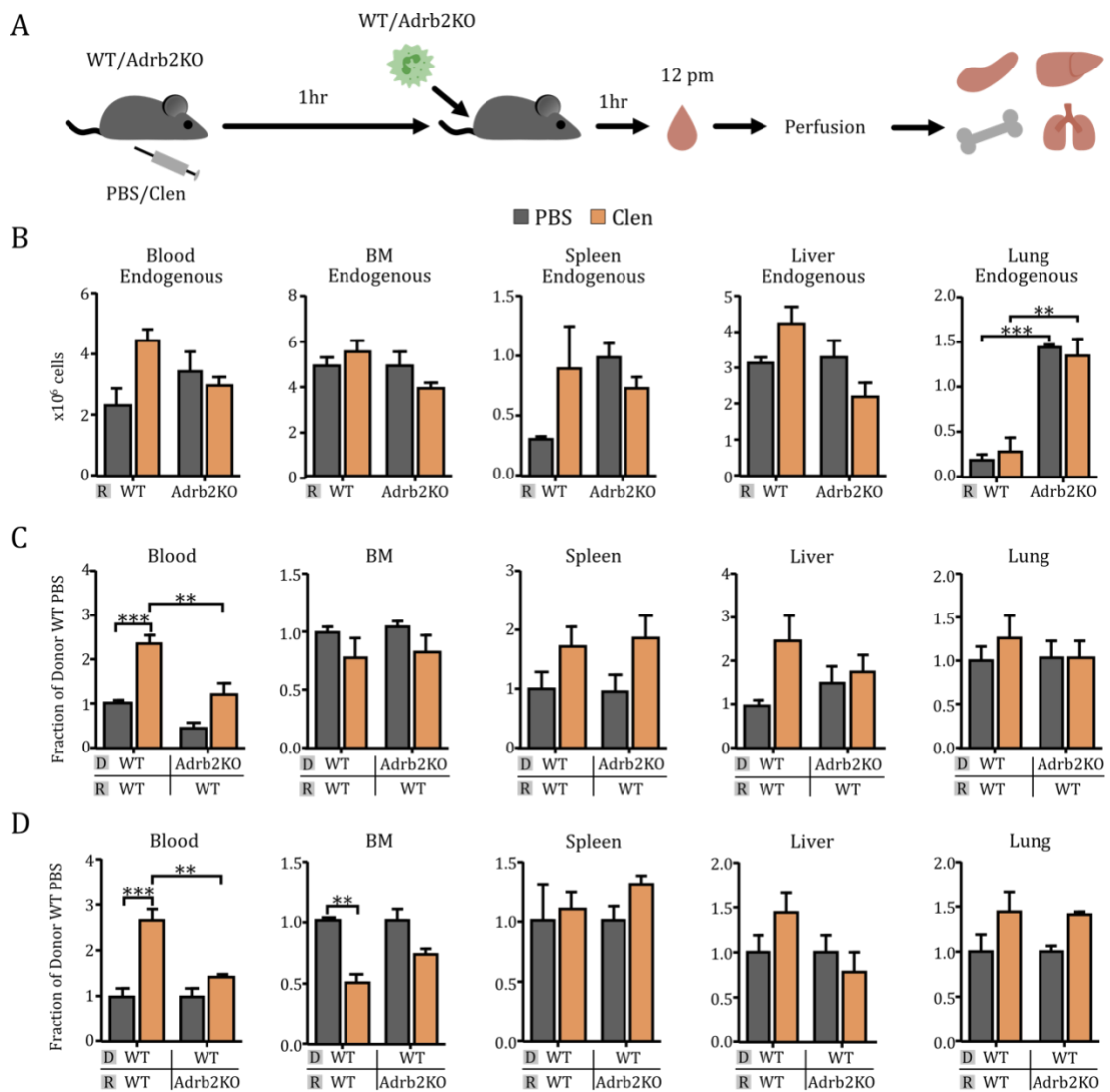


**Figure 3-6:  $\beta_2$ -ARs of neutrophils and their environment are targeted.**

**(A)** Illustration of the experimental design. WT or Adrb2 KO mice were injected with PBS (gray) or Clenbuterol (Clen, orange) and received 1hr later mixed WT and Adrb2KO donor cells. Another hour later, at 12 pm, blood was harvested, mice were perfused and organs were harvested for flow cytometry. **(B)** Endogenous neutrophil numbers in blood and organs of PBS- or Clen-injected recipients. Cell counts were extrapolated to 2 ml of blood or the whole organ.  $n = 6$ , two-way ANOVA, Sidak's test. **(C)** Fraction of WT or Adrb2KO donor neutrophils in blood and organs of WT recipients, normalized to WT donor cells in the PBS-injected control.  $n = 6$ , two-way ANOVA, Sidak's test. **(D)** Fraction of WT donor neutrophils in PBS- or Clen-treated WT or Adrb2KO recipients.  $n = 6$ , two-way ANOVA, Sidak's test. WT = Wild type, Adrb2KO =  $\beta_2$ -adrenoceptor knockout, D = Donor, R = Recipient.

To ascertain the contribution of cell-intrinsic and microenvironmental  $\beta_3$ -ARs in the observed effects, the same approach was performed with mice systemically lacking  $\beta_3$ -ARs (Adrb3 KO). WT or Adrb3 KO cells were injected into PBS- or BRL-treated WT recipients and WT donor cells were injected into stimulated WT or Adrb3 KO recipients. At 12 pm, blood was harvested and mice were perfused. A femur, the spleen as well as the liver and lung were harvested and processed for flow cytometry (**Figure 3-7A**).

To test whether effects observed by BRL injection were intrinsically mediated by  $\beta_3$ -ARs, endogenous neutrophil numbers in blood and organs of stimulated WT and ADRB3 KO mice were investigated (**Figure 3-7B**). In blood of WT mice, injection of BRL was expected to raise endogenous neutrophil numbers, as shown in **Figure 3-4B**. However, this was not the case here, making an interpretation more difficult. In previous experiments, endogenous neutrophils left the BM upon  $\beta_3$ -AR stimulation (**Figure 3-4B**), of which a tendency was detected in this experiment as well. Interestingly, endogenous neutrophil numbers were generally higher in ADRB3 KO mice, again pointing to a role of  $\beta_3$ -ARs in the mobilization of these cells from the BM. No significant changes were observed in endogenous cell numbers in the other tested organs, although increased endogenous neutrophil numbers in liver and lung of BRL-stimulated WT mice were expected.

Next, the involvement of neutrophil-intrinsic  $\beta_3$ -ARs was investigated. Therefore, WT or ADRB3 KO donor cells were injected into PBS- or BRL-treated WT recipients (**Figure 3-7C**). In agreement with the outcome in **Figure 3-4D**, no changes of WT donor neutrophil numbers in blood of PBS- or BRL-treated WT mice were assessed. Interestingly, more donor neutrophils lacking  $\beta_3$ -ARs remained in the circulation, but as mentioned for endogenous numbers in blood it is difficult to interpret the data. Donor cells of both genotypes exhibited the same phenotype in BM, namely reduced homing to the tissue upon treatment with BRL. This suggests that  $\beta_3$ -ARs on neutrophils do not play a role in enhanced mobilization from the BM. In general, no significant differences were found between WT and ADRB3 KO donor cells in the spleen, liver and lung, indicating that  $\beta_3$ -ARs on neutrophils were not involved in the observed redistribution to these organs.

Hence, it was assumed that receptors on cells of the neutrophil environment played a major role in the observed phenomena. To investigate this, WT donor cells were injected into PBS- or BRL-treated WT or ADRB3 KO recipients (**Figure 3-7D**). Whereas no effects were observed in the blood, spleen, liver and lung, fractions of donor cells significantly differed between BM samples from PBS-treated and BRL-treated WT recipients. Since the effect in BRL-stimulated WT mice was not observed in BRL-stimulated ADRB3 KO mice, it can be assumed that in the BM, BRL specifically targeted  $\beta_3$ -ARs. Thus, data collected in the reciprocal adoptive transfer with ADRB3 KO mice are difficult to interpret, but in BM BRL might actually target  $\beta_3$ -ARs on stromal cells rather than receptors on neutrophils.

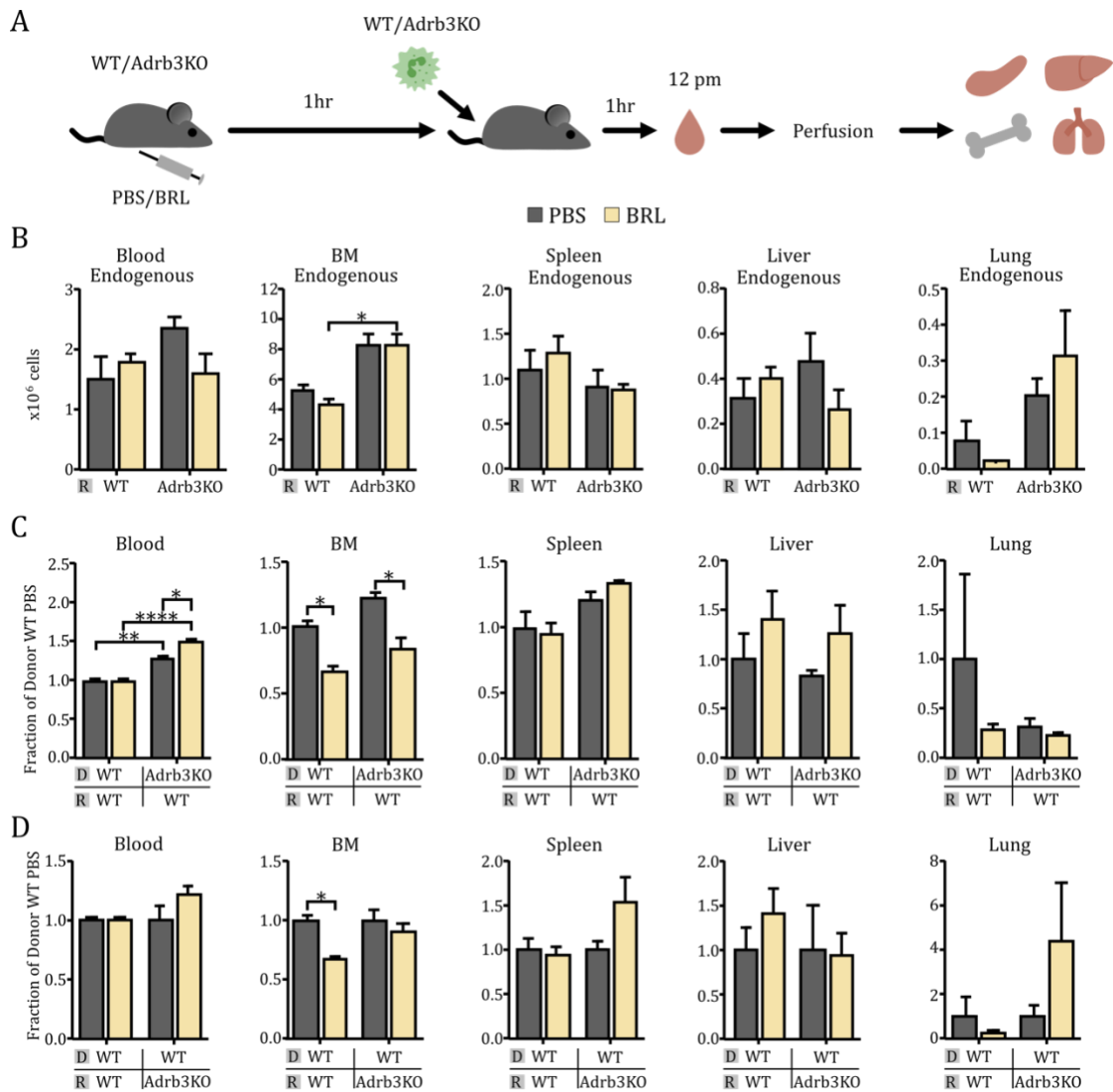


**Figure 3-7: Stimulation of  $\beta_3$ -ARs could affect neutrophil distributions.**

**(A)** Illustration of the experimental design. WT or Adrb3KO mice were injected with PBS (gray) or BRL37344 (BRL, yellow) and received 1hr later mixed WT and Adrb3KO donor cells. Another hour later, at 12 pm, blood was harvested, mice were perfused and organs were harvested for flow cytometry. **(B)** Endogenous neutrophil numbers in blood and organs of PBS- or BRL-injected recipients. Cell counts were extrapolated to 2 ml of blood or the whole organ.  $n = 6$ , two-way ANOVA, Sidak's test. **(C)** Fraction of WT or Adrb3KO donor neutrophils in blood and organs of WT recipients, normalized to WT donor cells in the PBS-injected control.  $n = 6$ , two-way ANOVA, Sidak's test. **(D)** Fraction of WT donor neutrophils in PBS- or BRL-treated WT or Adrb3KO recipients.  $n = 6$ , two-way ANOVA, Sidak's test. WT = Wild type, Adrb3KO =  $\beta_3$ -adrenoceptor knockout, D = Donor, R = Recipient.

## 3.5 B cells are redistributed upon adrenergic stimulation

### 3.5.1 Clenbuterol administration might promote B cell homing to LNs

As shown in **Figure 3-3B**, endogenous B cells left the blood stream after injection of the adrenergic agonists Clen ( $\beta_2$ -AR) and BRL ( $\beta_3$ -AR). To investigate their destination, multiple organs were examined. PBS or the adrenergic agonists were administered two hours prior to the injection of a CD45 labeling antibody and blood harvest at 12 pm. After perfusion, the femur, liver, lung and spleen were harvested. Since B cells mainly circulate through lymphoid organs, LNs draining different areas were included in the analysis (**Figure 3-8A**).

Reduced endogenous B cell numbers in blood from previous experiments (**Figure 3-3B**) were confirmed, as injection of both agonists mitigated circulating B cell numbers by three-fold (**Figure 3-8B**). Administration of BRL led to decreased B cell numbers in the BM, which – similar to neutrophils – indicates a role of  $\beta_3$ -ARs in the mobilization of B cells. In the liver and lung,  $\beta$ -AR stimulation reduced endogenous numbers as well. Thus, the investigated organs were not target of B cells leaving the circulation due to treatment with the adrenergic agonists. Since B cells mainly circulate through the spleen and LNs it was expected that cells might migrate to these secondary lymphoid organs. To explore this, two head/ear/neck-draining superficial parotid LNs (spLNs), an abdomen-draining mesenteric LN (mLN) and both skin-draining inguinal LNs (iLNs) were harvested to allow the examination of different body compartments. However, endogenous B cell numbers in these tissues were not significantly raised by Clen and BRL administration (**Figure 3-8B**), probably due to already high amounts of B cells. Distributions of endogenous CD4+ and CD8+ T cells are presented in **Figure 6-9**.

Investigation of the localization inside (CD45 double positive) or outside (CD45 single positive) of blood vessels (**Figure 3-8C**) revealed that stimulation of both  $\beta$ -ARs led to a higher percentage of extravascular endogenous B cells in the liver (~15%), spleen (~10%) and spLNs (<1%), whereas only  $\beta_2$ -AR stimulation had the same effect in the mLN (<1%). Their localization was not altered in the BM, lung and iLNs. Intra- and extravascular percentages of other endogenous lymphoid cells can be found in **Figure 6-10**.

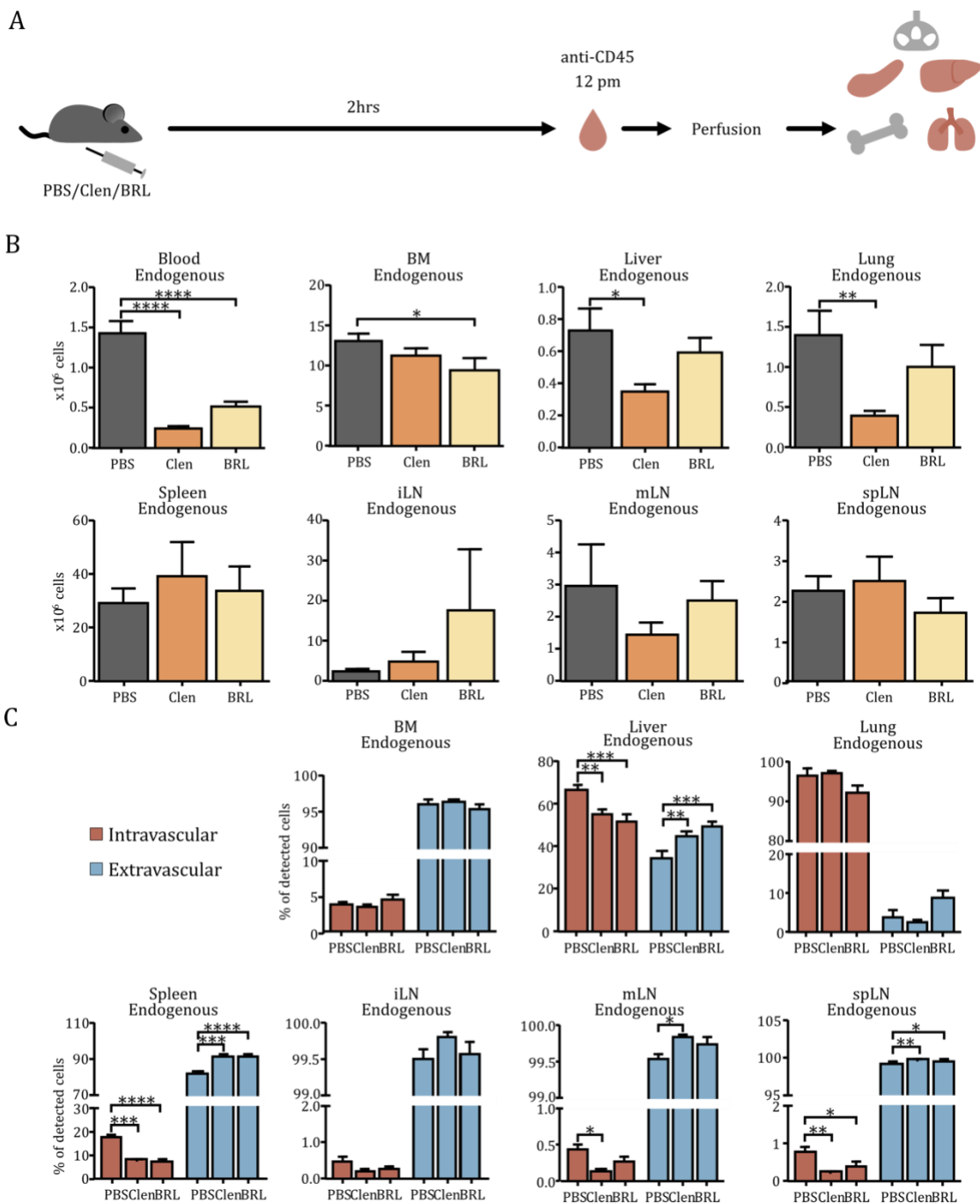


**Figure 3-8: Endogenous B cell numbers decrease in blood and organs upon adrenergic stimulation.**

**(A)** Illustration of the experimental design. Recipient mice were intraperitoneally injected with PBS, Clenbuterol (Clen) or BRL37344 (BRL). At 12 pm, a CD45 labeling antibody was injected and blood was harvested 5 min later. Mice were perfused and organs were harvested and processed for flow cytometry. **(B)** Endogenous B cell numbers in blood and organs after injection of PBS or the specific agonists, extrapolated to 2 ml of blood or the whole organ, respectively.  $n = 5-39$ , one-way ANOVA, Dunnett's test. **(C)** Intravascular (red) and extravascular (blue) endogenous B cells as percentage of the detected cells in the respective organs.  $n = 5-6$ , two-way ANOVA, Dunnett's test. iLN = inguinal lymph node, mLN = mesenteric lymph node, splLN = superficial parotid lymph node.

Since endogenous B cell numbers were not significantly elevated in LNs, adoptively transferred donor B cells were investigated to focus on the impact of adrenergic stimulation on homing (**Figure 3-9**). Cells from the spleen and LNs were mixed and intravenously injected into WT mice that have received either PBS or the agonists at 10 am. After one hour of circulation (at 12 pm), an antibody against CD45 was injected intravenously and blood was harvested five minutes later. Mice were perfused and one femur, the spleen, lung, liver and three LNs draining different areas were harvested. Data are presented as percentages of in total injected B cells. The fraction of donor B cells in blood was significantly reduced after BRL injection compared to PBS-treated mice, whereas after Clen injection cell percentages only showed a trend similar to endogenous cells (**Figure 3-9B**). Homing to the BM was not altered, while a higher percentage of transferred cells was found in the liver upon BRL treatment. Injection of Clen led to a decreased portion of donor B cells in the lung, indicating that B cell homing to the lung might be impaired. As mentioned above, endogenous B cell numbers were not significantly elevated in LNs and the spleen (**Figure 3-9B**). One possible reason could be that these tissues contain a massive amount of B cells already and about one million cells entering from the blood hardly made a significant difference. B cell homing to most of the tested secondary lymphoid organs was not affected by adrenergic stimulation (**Figure 3-9B**). However, in the mLN, the percentage of donor B cells was significantly increased upon injection of Clen (~1%), suggesting an effect of adrenergic stimulation on B cell homing to LNs. Strikingly, other lymphoid cells were even more efficiently homing to the mLN (CD4<sup>+</sup> T cells ~18% and CD8<sup>+</sup> T cells ~23%, **Figure 6-11**). In general, it is important to mention that only a small fraction of the overall injected donor B cells (~15%) could be detected in the tested organs (**Table 3-2**), indicating that they either accumulated at the injection site or that the majority died. The distribution of other lymphoid donor cells is depicted in **Figure 6-11**.

Regarding their localization inside or outside of blood vessels, 20% more donor B cells emigrated into the liver upon BRL treatment, therefore exhibiting the same behavior as endogenous cells in **Figure 3-8C**. This suggests preferred homing of endogenous as well as donor B cells to the liver upon administration of BRL. Compared to the control group, mLNs of Clen-stimulated mice possessed ~3.5% more intravascular donor B cells, indicating that these cells adhered to the vasculature in order to home to the tissue. Ratios of intra- and extravascular donor CD4<sup>+</sup> and CD8<sup>+</sup> T cells can be found in **Figure 6-12**. Summarized, B cells robustly left the circulation upon adrenergic stimulation and a small fraction was found to home to the gut-draining mLN upon stimulation of  $\beta_2$ -ARs.

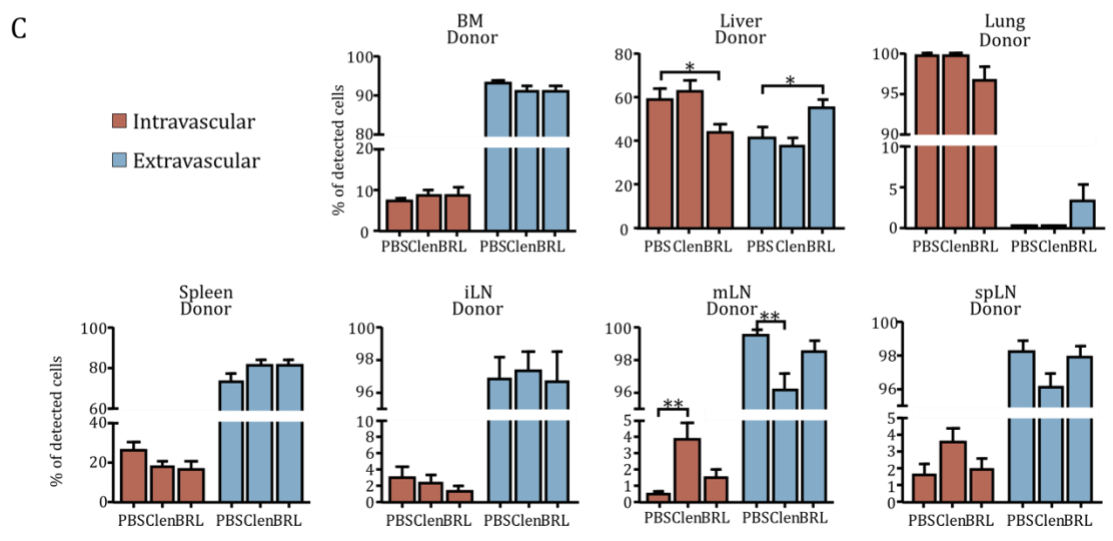
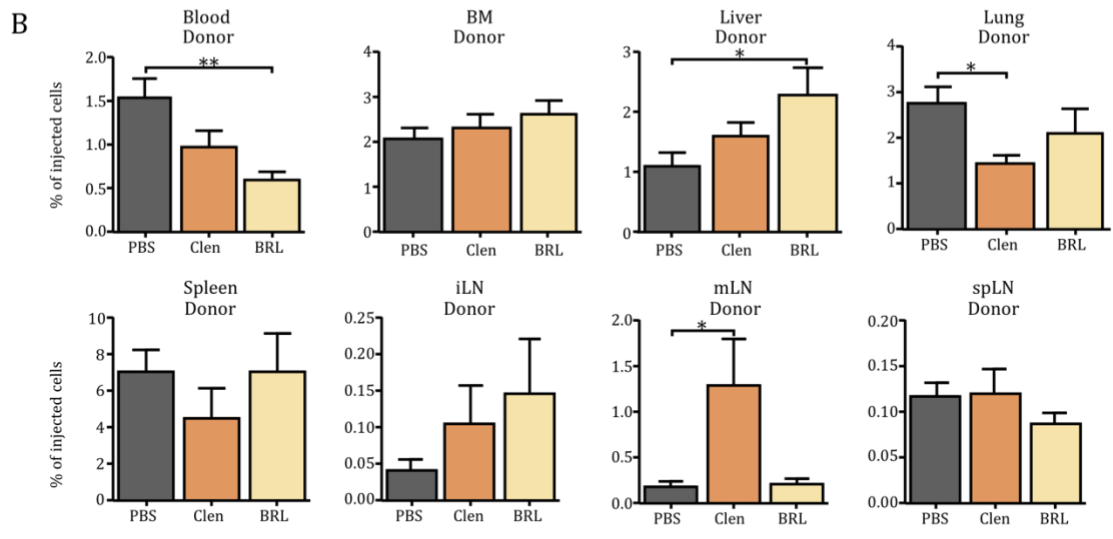
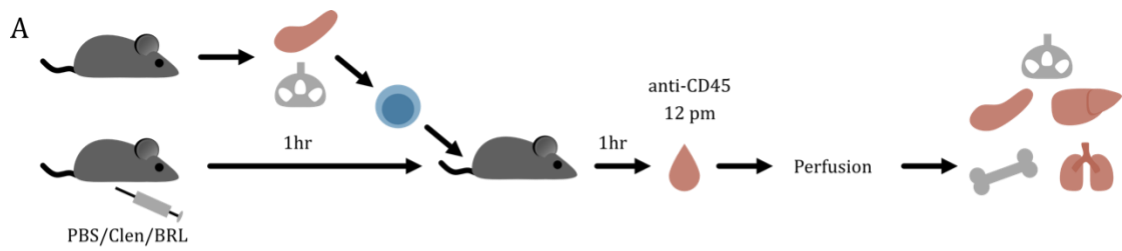


**Figure 3-9: B cell homing might be affected by adrenergic stimulation.** **(A)** Illustration of the experimental design. Recipient mice were intraperitoneally injected with PBS, Clenbuterol (Clen) or BRL37344 (BRL) and received 1hr later stained donor cells. At 12 pm, a CD45 labeling antibody was injected and blood was harvested 5 min later. Mice were perfused and organs were harvested and processed for flow cytometry. **(B)** Percentage of donor B cell from total injected B cells in blood and organs after injection of PBS or the specific agonists, extrapolated to 2 ml of blood or the whole organ, respectively. n = 5-18, one-way ANOVA, Dunnett's test. **(C)** Intravascular (red) and extravascular (blue) donor B cells as percentage of the detected cells in the respective organs. n = 5-6, two-way ANOVA, Dunnett's test. iLN = inguinal lymph node, mLN = mesenteric lymph node, splLN = superficial parotid lymph node.

**Table 3-2: Donor B cells as percentage of injected B cells in blood and organs.**

Data are presented as mean  $\pm$  SEM. BM = bone marrow, iLN = inguinal lymph node, mLN = mesenteric lymph node, spLN = superficial parotid lymph node.

	Blood	BM	Spleen	Liver	Lung	iLN	mLN	spLN	Total
<b>PBS</b>	1.51 $\pm$	2.06 $\pm$	7.17 $\pm$	1.09 $\pm$	2.76 $\pm$	0.04 $\pm$	0.18 $\pm$	0.12 $\pm$	14.94 $\pm$
	0.22	0.22	1.10	0.23	0.39	0.01	0.05	0.02	2.24
<b>Clen</b>	0.97 $\pm$	2.33 $\pm$	4.58 $\pm$	1.60 $\pm$	1.41 $\pm$	0.10 $\pm$	1.28 $\pm$	0.12 $\pm$	12.39 $\pm$
	0.20	0.26	1.60	0.20	0.18	0.05	0.52	0.03	3.04
<b>BRL</b>	0.59 $\pm$	2.62 $\pm$	7.09 $\pm$	2.25 $\pm$	2.13 $\pm$	0.15 $\pm$	0.21 $\pm$	0.09 $\pm$	15.13 $\pm$
	0.11	0.30	2.14	0.47	0.54	0.08	0.05	0.01	3.70

### 3.5.2 B cell adhesion molecule levels change upon adrenergic stimulation

To home to LNs, B cells require activation of various adhesion molecules and chemokine receptors, which interact with complementary receptors on ECs lining tissue blood vessels. To examine if surface levels of these molecules were altered upon adrenergic stimulation, mice were injected with PBS, Clen or BRL. Two hours later, at 12 pm, blood was harvested and MFIs of CXCR4, CD49d, CD62L, CD162 and CCR7 on B cells were recorded using flow cytometry (performed by Chen Wang).

Compared to neutrophils, surface levels of more B cell intrinsic molecules were affected upon *in vivo* pharmacological stimulation. Treatment with both  $\beta$ -AR agonists increased levels of CXCR4 and CD162 (two-fold) on circulating B cells, while CCR7 levels were significantly elevated only after Clen injection. CXCR4 and CCR7 are important chemokine receptors for lymphocyte homing to LNs, thus their upregulation supports the hypothesis of enhanced homing upon adrenergic stimulation, whereas CXCR4 also regulates B cell retention in the BM. Levels of CD62L were downregulated (two-fold) upon injection of Clen and BRL (**Figure 3-10A**), designating an activated state of B cells, as this adhesion molecule is shed upon activation and important for rolling of lymphocytes along HEVs in LNs.

To test whether changes in surface molecule levels were caused by direct effects of adrenergic agonists on B cells, an *in vitro* assay was performed. Therefore, the spleen of WT mice was harvested at 12 pm, isolated cells were seeded into 96-well plates and stimulated with 1 mM of each agonist for two hours. In this approach, MFIs of CXCR4, CD49d, CD62L and CD11a were recorded.

**Figure 3-10B** depicts a reduction of CD62L levels on B cells after *in vitro* incubation with Clen. In contrast to the *in vivo* approach, no changes were detected for the other tested molecules. Taken together, these data demonstrate that *in vivo* treatment with pharmacological agonists changed levels of adhesion molecules on the surface of B cells, corroborating an enhanced homing phenotype, whereby binding of agonists seemed to have a direct impact merely on CD62L levels.

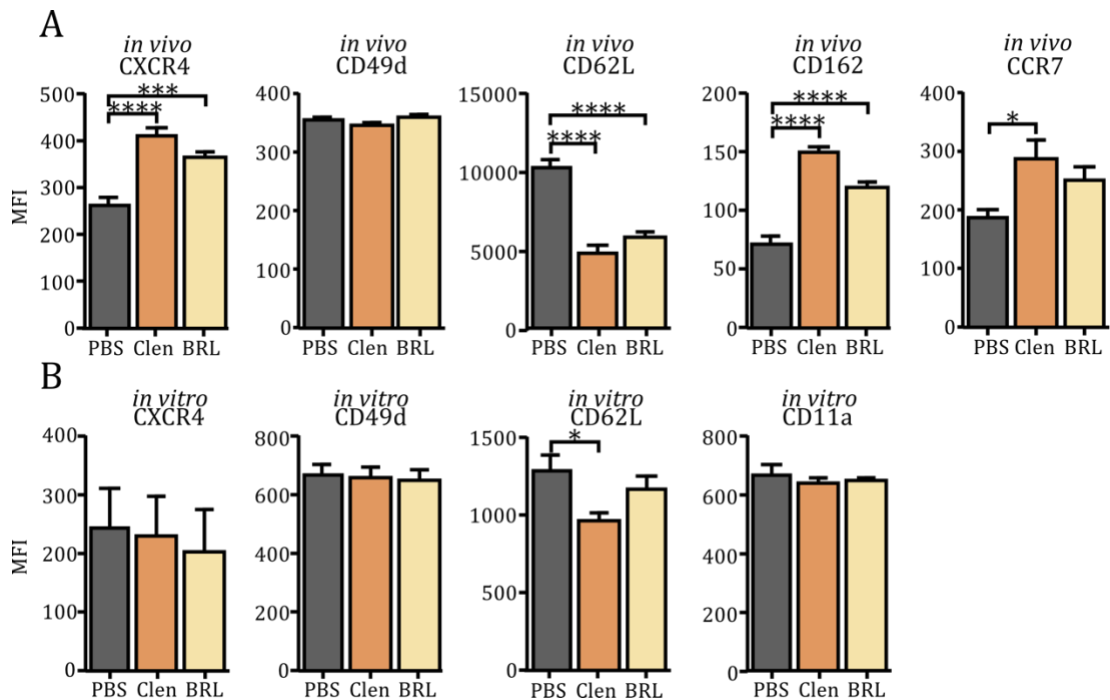


**Figure 3-10: Adhesion molecule levels on B cells change upon adrenergic stimulation.**

**(A)** MFI of several molecules on circulating B cells after *in vivo* adrenergic stimulation. WT mice were intraperitoneally injected with PBS (gray), Clenbuterol (Clen, orange) or BRL37344 (BRL, yellow) 2hrs prior to blood harvest at 12 pm. n = 6, one-way ANOVA, Dunnett's test. Experiment was performed by Chen Wang. **(B)** MFI of several molecules on B cells after *in vitro* adrenergic stimulation. Splens from WT mice were harvested and processed. Cells were seeded into 96-well plates and stimulated *in vitro* with PBS, Clen or BRL for 2hrs. n = 3, one-way ANOVA, Dunnett's test. MFI = Mean fluorescence intensity.

### 3.5.3 Treatment with Clenbuterol impacts B cell trafficking through lymph nodes

Since adrenergic stimulation altered levels of adhesion molecules mainly being involved in trafficking of B cells through LNs (**Figure 3-10**), it was investigated whether block of homing to these tissues attenuated or even abolished the phenotype observed in blood. First, LN homing was blocked using antibodies against the integrins CD49d and CD11a (see 2.1.11) with subsequent injection of PBS, Clen or BRL. Two hours later, at 12 pm, blood, skin-draining LNs (axillary, brachial, inguinal and popliteal) as well as one gut-draining LN (mesenteric) were harvested and processed for flow cytometry. Data were normalized to untreated mice, which did not receive any stimulus (indicated by a black line).

Shown in **Figure 3-11A**, B cell numbers in blood were elevated up to five-fold compared to the untreated group, confirming a malfunction of B cell homing to LNs. Although not

significant, Clen- and BRL-treated mice still exhibited slightly lower cell numbers in blood after the block. Besides a putative integrin-independent homing mechanism, reduced circulating numbers could also be attributed to the inability to re-enter the circulation. Indeed, enhanced retention was confirmed in pooled skin-draining LNs (sdLNs), where the fraction of B cells upon Clen administration was similar to the untreated group and increased (two-fold) compared to the PBS control. In the gut-draining mesenteric LN (gdLN), cell numbers were decreased compared to the untreated control, but there was no difference between PBS-treated and stimulated mice.

Another molecule that was downregulated – or shed – by *in vivo* stimulation with adrenergic agonists was CD62L. As mentioned before, this molecule is important for rolling along HEVs in LNs. Thus, a blocking antibody was used (see 2.1.11), which was intraperitoneally injected 24 hours prior to harvest. As control, an isotype instead of the blocking antibody was administered. On the next day, mice received PBS or the  $\beta_2$ - and  $\beta_3$ -AR agonist at 10 am. Two hours later, at 12 pm, blood was harvested and processed for flow cytometry. B cell numbers were normalized to the isotype control. LNs were not investigated in this experimental setup.

Although B cell numbers in blood upon CD62L block of PBS-injected mice exhibited an almost ten-fold increase compared to the isotype control (black line), B cells of blocked and Clen- or BRL-stimulated mice still left the blood, ruling out the involvement of CD62L in the adrenergic-driven migratory behavior of B cells through LNs (**Figure 3-11B**).

Previous studies demonstrated that stimulation of  $\beta_2$ -ARs on lymphocytes leads to their retention in LNs (Nakai et al., 2014) and similar mechanisms could be assumed from homing block by inhibition of the integrins CD11a and CD49d (**Figure 3-11A**). Therefore, it was assessed whether block of LN egress by injection of FTY720 had a similar effect on B cell numbers in blood and LNs as adrenergic stimulation. FTY720 is a functional antagonist of S1PR1, a receptor crucial for lymphocyte egress from LNs (Mandala et al., 2002). WT mice were first injected intraperitoneally with PBS or FTY720 (see 2.1.11) and directly afterwards with PBS, Clen or BRL. Two hours later, at 12 pm, blood, sdLNs and one gdLN were harvested and processed for flow cytometry. Data are shown as normalized to the group that received two consecutive injections of PBS (PBS+PBS).

Blood of the PBS-injected control group showed the usual effects of adrenergic stimulation, namely decreased B cell numbers in the circulation upon injection of Clen and BRL (**Figure 3-11C**). Injection of FTY720 also resulted in decreased B cell numbers in blood, confirming the efficiency of egress block, although lymph was not tested. In sdLNs,

Clen- and BRL-treated samples with preceding PBS injection (PBS+Clen and PBS+BRL) exhibited slightly reduced, but not significantly altered numbers. No additive effects were observed in the cohort receiving the egress blocker FTY720 prior to PBS or agonist administration. Egress block (FTY+PBS) should have led to increased lymphocyte numbers in LNs, however, the treatment was performed just shortly before the harvest (two hours), so this time frame was possibly not sufficient for B cells to accumulate to a measurable extent in the investigated LNs. In the gdLN, FTY720 treatment in combination with PBS administration (FTY+PBS) showed slightly increased cell numbers, whereas there was no difference detectable to the stimulated groups (FTY+Clen and FTY+BRL). Thus, it is not clear whether FTY720 and pharmacological agonists have similar effects on B cell retention in the LN. Further experiments will be necessary to elucidate the effect of adrenergic stimulation on homing and egress of B cells. The impact of egress block on other leukocyte subsets can be found in **Figure 6-14**.

To investigate the influence of adrenergic stimulation, particularly mediated by  $\beta_2$ -ARs, on the migration behavior of B cells *in vivo*, intravital imaging of B cells in the vasculature of the popliteal LN (popLN) was performed. After surgical exposure of the popLN of anaesthetized mice, unstimulated B cells in superficial blood vessels were imaged for about 15 minutes to ensure altered adhesion profiles were not trauma-induced. At 10 am (the usual time for *in vivo* treatments), either PBS or Clen were injected intraperitoneally and the same vessels were imaged (see 2.1.13). The MFI inside of blood vessels was measured and normalized to the MFI of control videos. In the sum projection of the imaged z-stacks over time, rolling or circulating cells were excluded (analysis by Dr. Robert Pick). The graph in **Figure 3-11D** depicts the relative adhesion of B cells for a time frame of three minutes after injection of PBS or Clen. Initial adhesion in vessels of the popLN was slightly higher in Clen-treated mice, rising steeper after two minutes. Afterwards, relative adhesion decreased again. This behavior indicates that B cell adhesion, if only transiently, could be controlled by the adrenergic tone.

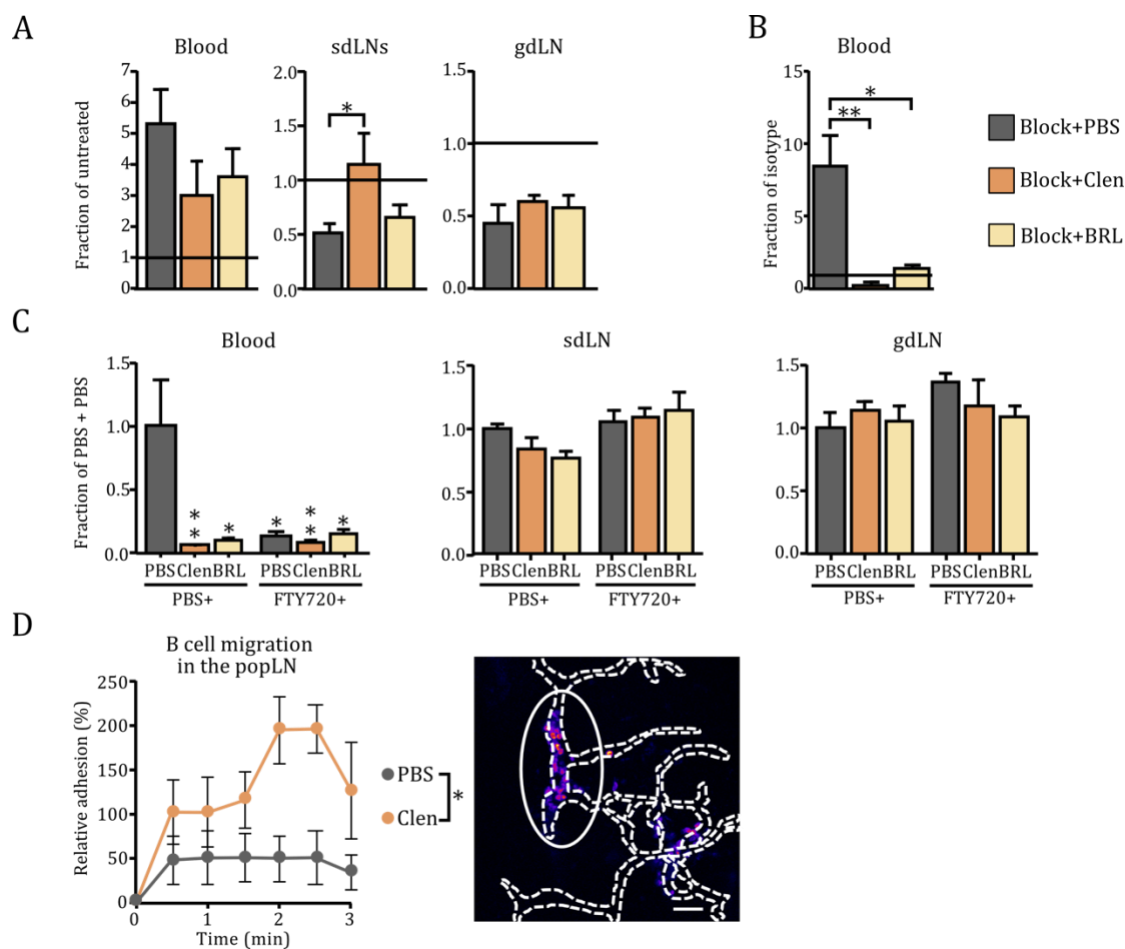


**Figure 3-11: The migratory behavior of B cells is affected by adrenergic stimulation.** **(A)** Fraction of B cells in blood and LNs after neutralization of CD49d and CD11a combined with adrenergic stimulation. WT mice were intraperitoneally injected with blocking antibodies and directly afterwards with PBS, Clenbuterol (Clen) or BRL37344 (BRL). At 12 pm, blood and LNs were harvested and processed for flow cytometry. Data are shown as normalized to the untreated group not receiving any stimulus (black line).  $n = 6$ , one-way ANOVA, Dunnett's test. **(B)** Fraction of B cells after CD62L block combined with adrenergic stimulation. WT mice were either intraperitoneally injected with a blocking antibody against CD62L or the respective isotype 24hrs prior to injection of PBS, Clen or BRL at 10 am. Blood was harvested at 12 pm. Data are shown as normalized to the isotype control (black line).  $n = 3$ , one-way ANOVA, Dunnett's test. **(C)** Fraction of B cells in blood and LNs after egress block and adrenergic stimulation. At 10 am, WT mice were intraperitoneally injected with PBS or FTY720 and directly afterwards with PBS, Clen or BRL. At 12 pm blood and LNs were harvested and processed for flow cytometry.  $n = 3$ , two-way ANOVA, Tukey's test, stars indicate comparison to PBS+PBS group. **(D)** Relative adhesion of B cells in the superficial vasculature of the popLN after PBS or Clen injection and representative image. B cells in LN vessels were imaged for 15 min before PBS or Clen were injected and the same vessels were imaged. Relative adhesion over time is shown as percentage normalized to the control video (analysis by Dr. Robert Pick). Scale bar = 50  $\mu\text{m}$ ,  $n = 2$ , unpaired t-test, Mann-Whitney's test. sdLN = skin-draining lymph node, gdLN = gut-draining lymph node, popLN = popliteal lymph node.

### 3.5.4 The adrenergic influence on B cells is $\beta_2$ -AR-specific

So far, adrenergic stimulation led to a reduction of endogenous B cell numbers in blood, BM, liver and lung. To investigate whether B cell-intrinsic or -extrinsic  $\beta_2$ -ARs were responsible for the phenotype in the majority of tested organs, a reciprocal adoptive transfer was performed with this leukocyte subset. WT or *Adrb2* KO donor cells were transferred to PBS- or Clen-treated WT recipients, or WT donor cells were transferred to treated WT or *Adrb2* KO mice. After one hour of circulation, blood was harvested at 12 pm. Mice were perfused and organs were harvested for flow cytometric analysis (**Figure 3-12A**).

First, endogenous B cell numbers in WT and *Adrb2* KO mice stimulated with PBS or Clen were examined (**Figure 3-12B**). In blood of WT mice, results from previous experiments (**Figure 3-8B**) could be reproduced, showing a two-fold decrease in cell numbers upon Clen administration. As this was not the case in Clen-stimulated mice lacking the target receptors, effects observed in blood were confirmed to be specific for  $\beta_2$ -ARs. No changes were expected and assessed for endogenous B cell numbers in BM and spleen of WT mice. Interestingly, B cells were accumulated in the spleen of *Adrb2* KO recipients, indicating that  $\beta_2$ -ARs might play a role in B cell homing to or retention in this organ. Upon Clen injection in previous experiments, B cells left the liver (**Figure 3-8B**), and the same trend was observed in WT recipients (**Figure 3-12B**). In the lung, lower numbers were expected as well, but could not be confirmed, indicating that – similar to neutrophils – the B cell phenotype in this organ was unspecific. Similar to the spleen, endogenous cell numbers in the lung of *Adrb2* KO mice were higher than in WT controls. Thus, this experiment demonstrated that effects of Clen on endogenous B cells were  $\beta_2$ -AR specific.

After confirming its specificity, it was tested which cell type was the main target of Clen or if, alike neutrophils, leukocytes and their microenvironment were involved. Therefore, WT or *Adrb2* KO donor cells were transferred to PBS- or Clen-treated WT recipients (**Figure 3-12C**). In general, no significant changes between WT and *Adrb2* KO donor B cells were detected, indicating that B cell intrinsic  $\beta_2$ -ARs did not play a major role in the changed migration behavior. According to previous results (**Figure 3-9B**), reduced homing of WT donor cells to WT lungs was expected, which could not be reproduced.

The same applied for the fraction of WT donor B cells in PBS- or Clen-stimulated WT or *Adrb2* KO recipients (**Figure 3-12D**). Taken together, B cells left the blood stream upon specific stimulation of  $\beta_2$ -ARs, but, despite the robust phenotype, lack of  $\beta_2$ -ARs on either cell type did not affect numbers in blood. Thus, it remains unclear whether receptors on

B cells or their microenvironment – or both – are targets of pharmacological stimulation and further experiments will be necessary for clarification.

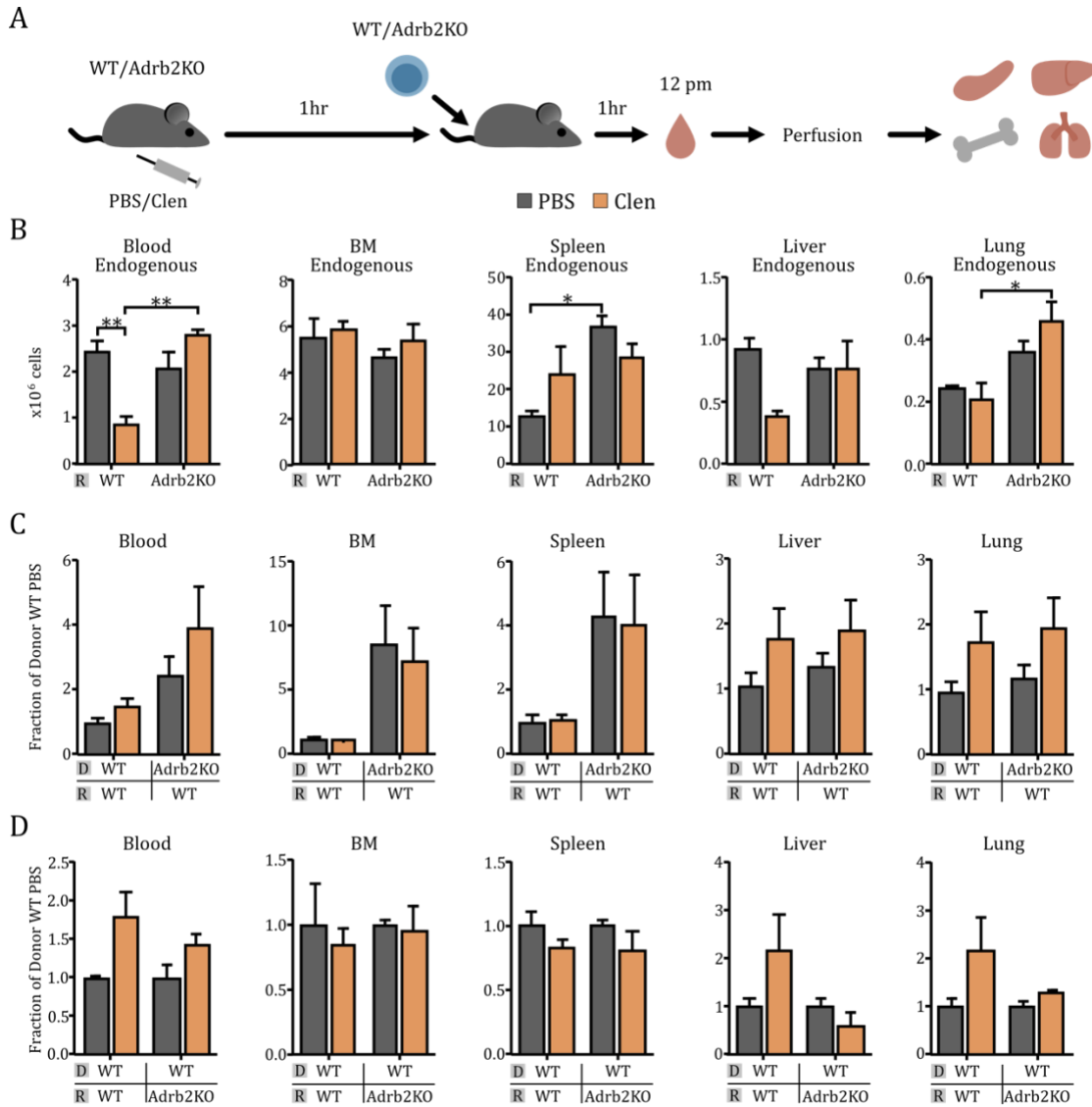


**Figure 3-12: The adrenergic influence on B cells is  $\beta_2$ -AR-specific.**

**(A)** Illustration of the experimental design. WT or Adrb2KO mice were injected with PBS (gray) or Clenbuterol (Clen, orange) and received 1hr later mixed WT and Adrb2KO donor cells. Another hour later, at 12 pm, blood was harvested, mice were perfused and organs were harvested for flow cytometry. **(B)** Endogenous B cell numbers in blood and organs of PBS- or Clen-injected recipients. Cell counts were extrapolated to 2 ml of blood or the whole organ.  $n = 6$ , two-way ANOVA, Sidak's test. **(C)** Fraction of WT or Adrb2KO donor B cells in blood and organs of WT recipients, normalized to WT donor cells in the PBS-injected control.  $n = 6$ , two-way ANOVA, Sidak's test. **(D)** Fraction of WT donor B cells in PBS- or Clen-treated WT or Adrb2KO recipients.  $n = 6$ , two-way ANOVA, Sidak's test. WT = Wild type, Adrb2KO =  $\beta_2$ -adrenoceptor knockout, D = Donor, R = Recipient.

For neutrophils it was difficult to interpret whether the pharmacological agonist BRL targeted  $\beta_3$ -ARs specifically (**Figure 3-7D**). The same approach was performed for B cells, which were examined in a reciprocal adoptive transfer between WT and Adrb3 KO mice. WT or Adrb3 KO donor cells were injected into PBS- or BRL-treated WT recipients, or WT donor cells were transferred to treated WT or Adrb3 KO recipients. At 12 pm, blood was harvested and recipients were perfused. Subsequently, four organs were harvested and processed together with blood for flow cytometry (**Figure 3-13A**).

For endogenous B cell numbers in blood of WT recipients, a dramatic reduction was expected upon BRL injection, according to previous results (**Figure 3-8B**). This held true for WT recipients, but also for recipients lacking  $\beta_3$ -ARs (**Figure 3-13B**), corroborating that the observed effects in blood were most likely not mediated through  $\beta_3$ -ARs, but due to unspecific effects of BRL, potentially due to binding to other  $\beta$ -ARs (Mori et al., 2010). In BM, only BRL showed an effect for endogenous B cell numbers in **Figure 3-8B**, which could indicate that in this organ BRL acted specifically. Slightly reduced numbers were found in BRL-injected WT recipients, with higher numbers of B cells in the BM of Adrb3 KO mice (**Figure 3-13B**), suggesting that  $\beta_3$ -ARs could be involved in B cell mobilization from this tissue. In contrast to results in **Figure 3-8B**, changes in B cell numbers in the liver were detected, however, this could have been caused by unspecific binding. In the lung, results were difficult to interpret due to the high deviation in the PBS-treated controls.

WT and Adrb3 KO donor B cells exhibited extreme differences in their distribution to blood, BM and the spleen of WT mice (**Figure 3-13C**). Donor B cells lacking  $\beta_3$ -ARs did not leave the blood, but homed more efficiently to the BM (15-fold) and spleen (ten-fold) as well, indicating that  $\beta_3$ -ARs could be important in these tissue-specific processes. In contrast, no significant changes were observable in the liver and lung (because of a high deviation between samples). Moreover, no differences were detected between PBS- and BRL-treated Adrb3 KO mice.

After transferring WT donor B cells into stimulated WT or Adrb3 KO mice, no significant differences were discovered (**Figure 3-13D**), although donor numbers in blood of both recipients were slightly reduced upon BRL administration.

Summarized, the role of  $\beta_3$ -ARs in altered B cell migration behavior remains elusive, especially since BRL obviously had off-target effects, potentially on  $\beta_2$ -ARs (Mori et al., 2010). Hence, the reduction of B cells in the circulation was probably mediated by  $\beta_2$ -ARs rather than  $\beta_3$ -ARs.

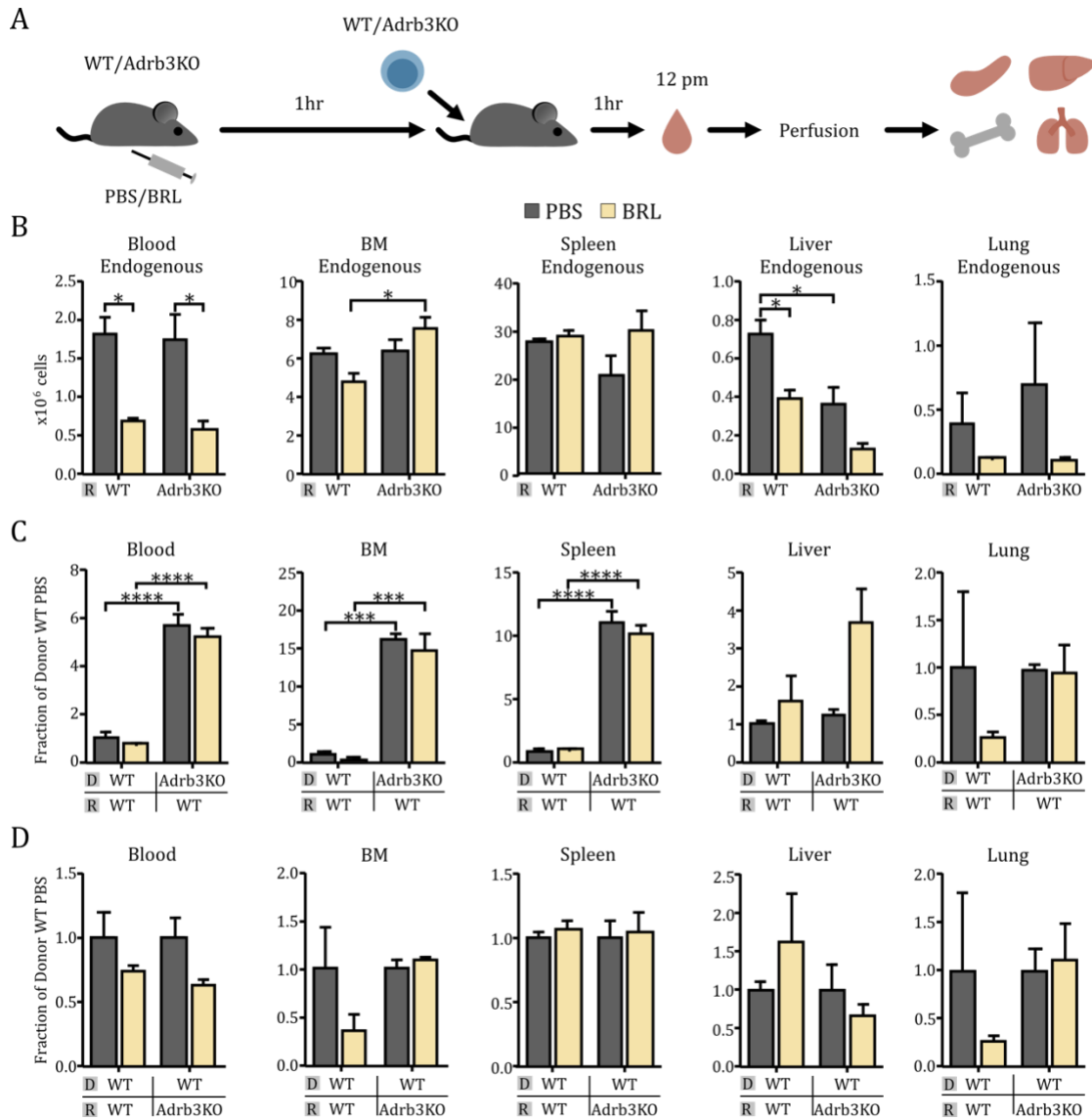


**Figure 3-13:  $\beta_3$ -ARs are not involved in the reduction of circulating B cells.**

**(A)** illustration of the experimental design. WT or Adrb3KO mice were injected with PBS (gray) or BRL37344 (BRL, yellow) and received 1hr later mixed WT and Adrb3KO donor cells. Another hour later, at 12 pm, blood was harvested, mice were perfused and organs were harvested for flow cytometry. **(B)** Endogenous B cell numbers in blood and organs of PBS- or BRL-injected recipients. Cell counts were extrapolated to 2 ml of blood or the whole organ.  $n = 6$ , two-way ANOVA, Sidak's test. **(C)** Fraction of WT or Adrb3KO donor B cells in blood and organs of WT recipients, normalized to WT donor B cells in the PBS-injected control.  $n = 6$ , two-way ANOVA, Sidak's test. **(D)** Fraction of WT donor B cells in PBS- or BRL-treated WT or Adrb3KO recipients.  $n = 6$ , two-way ANOVA, Sidak's test. WT = Wild type, Adrb3KO =  $\beta_3$ -adrenoceptor knockout, D = Donor, R = Recipient.

## 4 Discussion and Conclusion

Interactions between the immune system and the nervous system have been a topic of interest for several decades. However, despite a plethora of publications, the intricate interplay between these two crucial systems remains elusive. This is due to the difficult dissection of complex dynamics between multiple cellular and molecular elements in various organs. In this study, I focused on the influence of  $\beta$ -AR activation on the *in vivo* distribution of neutrophils and B cells. Adoptive transfer experiments and flow cytometric analyses demonstrated differing effects of  $\beta_2$ -AR stimulation on both leukocyte subsets. In the course of this chapter, findings will be discussed and integrated into the current knowledge about adrenergic control of leukocyte trafficking.

### 4.1 The disparity between stimulation and block

The agonist Isoproterenol unselectively binds to  $\beta$ -ARs and activates the same pathways as endogenous ligands such as norepinephrine. Thus, it was hypothesized that enhanced activation of these receptors could trigger intracellular signaling pathways resulting in modulation of the migratory properties of leukocytes. As a matter of fact, neutrophil numbers in blood robustly increased, whereas B cell numbers were diminished, and this occurred already after a short-term incubation time of two hours. However, it is important to keep in mind that Isoproterenol acts in addition to the already existing catecholamines in blood. Their levels vary over the course of a day, according to phases of activity and rest. For mice, the night equals the phase of activity and catecholamine levels in plasma are higher compared to the rest phase during the day (De Boer and Van der Gugten, 1987). In contrast, for humans whose active phase is during the day, plasma levels are inversed (Linsell et al., 1985). Hence, exogenous stimulants can have varying effects depending on the time point of administration and sensitivity of the system to stimulation. In this study, 12 pm and 8 pm were chosen for harvest, as these times reflect the peak and trough of leukocyte concentrations in murine blood (Druzd et al., 2017; He et al., 2018; Scheiermann et al., 2012). The fact that neutrophil numbers were increased after Isoproterenol administration at both time points suggests that enhancement of  $\beta$ -AR stimulation with the used dosage has the same effect, regardless of endogenous plasma catecholamine levels. Circulating B cell numbers were only decreased after Isoproterenol injection during the day. However, due to already low numbers in blood at night in the PBS control,

it is unclear whether this is due to different endogenous catecholamine levels. To date, knowledge on concentration of catecholamines in various tissues is limited. In order to elucidate effects of neurotransmitters on the migratory behavior of immune cells, a detailed map is necessary, stating concentrations of substances such as norepinephrine in various body parts, ideally under both steady state and different inflammatory scenarios. While quantification of catecholamine levels in body fluids is commonly performed, tests in organs are more challenging, since structural features of catecholamines are present in a variety of other biomolecules as well. Detection methods in living cells have been established (Tong et al., 2019), but are difficult to use in complex biological environments. Thus, sophisticated detection methods are required such as it was used to measure norepinephrine levels in different compartments of the rat heart (Novotny et al., 2007).

Administration of the pan- $\beta$ -AR antagonist Propranolol blocks signaling cascades by competitive binding of the substance to  $\beta$ -ARs (Al-Majed et al., 2017a). Hence, endogenous ligands of adrenergic receptors are hindered to bind, leading to the hypothesis that circulating leukocyte numbers might change compared to the PBS control. However, only slight effects of the unselective antagonist were observed for both subsets, regardless of the time of administration. The fact that injection of Propranolol did not show dramatic effects could have multiple reasons. Effects could be dose dependent; thus, it would be useful to test different concentrations of the blocker.  $\beta$ -AR density also changes depending on desensitization processes (at least for  $\beta_1$ - and  $\beta_2$ -ARs (Nantel et al., 1993)), which is difficult to test *in vivo*. Furthermore, levels of  $\beta$ -ARs on the cell surface vary in a cell type-specific and maturation-dependent manner (Elenkov et al., 2000). Importantly, it was shown that Propranolol exhibits a much lower affinity for  $\beta_3$ -ARs in comparison to  $\beta_1$ - and  $\beta_2$ -ARs (Cernecka et al., 2014), which could explain the weaker phenotype compared to agonism targeting all  $\beta$ -AR subtypes. Although Propranolol does not show sympathomimetic effects (Al-Majed et al., 2017a), it is also not known whether other intracellular mechanisms are activated (called partial agonism). To elucidate this, it would be necessary to perform phospho-proteomic analyses of cells stimulated with the pan- $\beta$ -AR agonist and antagonist. Since Propranolol only blocks  $\beta$ -ARs, signaling of  $\alpha$ -ARs is unaffected and could therefore exhibit influences on leukocyte distributions as well, such as it was shown for long-term stimulation with respective agonists (Stevenson et al., 2001).

To investigate whether absence of sympathetic tone influenced circulating leukocyte numbers, chemical sympathectomy using the neurotoxin 6-OHDA was performed. This drug structurally resembles norepinephrine and dopamine leading to its uptake into

peripheral nerve terminals, where it damages these structures via generation of ROS and interactions with the mitochondrial respiratory chain (Rodriguez-Pallares et al., 2007). Thus, signals from peripheral nerves are ablated upon repeated administration of 6-OHDA. However, the absence of peripheral nerve signals did not alter circulating neutrophil and B cell numbers. This could be explained by a putative compensatory effect of epinephrine, which is derived from the adrenal cortex to be systemically released into the blood stream and correspondingly was not target of the chemical sympathectomy. Therefore, it will be useful to test the impact of epinephrine absence on circulating leukocyte numbers, for which mice can be adrenalectomized. In addition, it could be tested whether exogenous norepinephrine and epinephrine can rescue effects of combined sympathetic ablation and adrenalectomy on circulating leukocyte numbers. Furthermore, use of 6-OHDA systemically ablates neural signals. Knowing that loss of local adrenergic innervation leads to defects of circadian leukocyte adhesion and emigration in the BM and cremaster muscle in a time-of-day-dependent manner (Scheiermann et al., 2012), it would be of interest which specific subsets are dependent on locally delivered signals. Removal of the superior cervical ganglion innervating the cranial BM could help to investigate the effects of the local adrenergic tone on neutrophil mobilization from this tissue. However, since the most robust readout in this thesis is the blood, it will be difficult to investigate local blood compartments. Further sources for catecholamines should also be regarded, such as the leukocyte subsets T cells (Rosas-Ballina et al., 2011) and macrophages (Flierl et al., 2007), which might have an impact on the local catecholamine milieu, depending on e.g. their activation mechanisms (Fischer et al., 2017).

## **4.2 The specificity issue with pharmacological agonists**

Next, it was tested which specific  $\beta$ -ARs were involved in the effects of adrenergic stimulation by Isoproterenol. For this, the  $\beta_1$ -AR targeting agonist Denopamine, the  $\beta_2$ -AR agonist Clenbuterol and the  $\beta_3$ -AR agonist BRL37344 were injected. Whereas Denopamine did not alter leukocyte subset numbers in blood, Clenbuterol and BRL37344 reproduced the effects of Isoproterenol, which led to the conclusion that  $\beta_2$ - and  $\beta_3$ -ARs are involved in the control of leukocyte trafficking. Later in this study, use of mice lacking  $\beta_3$ -ARs revealed, however, that BRL37344-induced effects were not specific for this particular receptor type, suggesting that other adrenoceptors such as  $\beta_2$ -ARs were targeted (Mori et al., 2010; Pott et al., 2003). As a consequence, the same effects should have been detected for both agonists. This was the case in blood, indicating that these

observations are most likely mediated by  $\beta_2$ -ARs. In contrast, in other organs such as the BM, only BRL37344 administration affected neutrophil and B cell numbers. Using *Adrb3* KO mice, a previous study reported that non-hematopoietic  $\beta_3$ -ARs in the BM are involved in the circadian leukocyte recruitment to this tissue (Scheiermann et al., 2012). Hence, BRL37344 could target  $\beta_3$ -ARs specifically in this tissue, potentially as a function of surface receptor density, which is relatively high in the BM during the day, whereas at night  $\beta_2$ -ARs prevail (Garcia-Garcia et al., 2019). For interpretation of data obtained with this agonist further investigation is required, e.g. by injection of BRL37344 into mice lacking other  $\beta$ -ARs or *in vitro* binding assays, where the compound competes with a standard radioligand with high affinity for available receptor sites on leukocytes and cells of their microenvironment. Taken together, when investigating the interplay between neural signals and immune cells, numerous challenges have to be considered. From a plethora of previous studies, it is clear that this relationship is extremely dynamic, with respect to its dependence on the examined cell types, the maturation and activation state of these cells, the inflammatory milieu as well as evidently trivial aspects such as the time of agonist exposure (Elenkov et al., 2000). Regarding the latter, it was tested what time was best for analysis after administration of the specific agonists. In conformity with previous reports (Nakai et al., 2014), in blood two hours of stimulation showed the greatest differences from leukocyte numbers in the control group (exemplarily shown for B cells), but already after one hour, B cell numbers were reduced. Circulating B cell numbers normalized to initial levels after six hours after injection, suggesting that agonists were metabolized until then. Thus, acute (within two hours) impacts of adrenergic stimulation were examined for more insight into direct effects of leukocyte distributions. Moreover, it was tested whether diminished B cell numbers in the circulation were caused by enhanced cell death, as it was shown for prolonged treatment with  $\alpha$ -AR agonists (Stevenson et al., 2001). This was not the case, neither after *in vivo* nor after *in vitro* treatment of B cells with both  $\beta$ -AR agonists.

It is known that the SNS – together with the hypothalamic pituitary axis (HPA) – plays a role in inflammation, known as the inflammatory reflex. When local inflammation is detected by fibers of sensory and vagal nerves, signals are transmitted to the CNS, which leads to activation of the SNS. Release of neurotransmitters at the site of inflammation can have a complex outcome challenging the previous speculation, that activity of the SNS might be generally anti-inflammatory (Pongratz and Straub, 2014). To investigate the impact of adrenergic stimulation on leukocyte migration in an inflammatory scenario,  $\text{TNF}\alpha$  was injected one hour before mice received the specific  $\beta$ -AR agonists. Although

displaying a similar trend to the steady state – increased neutrophil and decreased B cell numbers in blood – effects were not as profound. This could be explained by lower B cell numbers upon TNF $\alpha$  administration, however, neutrophil numbers were similarly high compared to the steady state. Another possibility could be a putative effect of TNF $\alpha$  on the responsiveness of  $\beta$ -ARs. Whereas  $\beta$ -ARs are capable of regulating LPS-induced TNF $\alpha$  secretion (Elenkov et al., 1995), a potential inverted effect is much more intricate, since expression of adrenoceptors on leukocytes is dynamic and depends on the cellular differentiation and activation state, as well as the regulation by catecholamine levels, which vary during an immune response (Elenkov et al., 2000). Hence, in order to examine and compare effects of adrenergic stimulation on leukocyte trafficking during inflammation, future studies will have to focus on distinct inflammatory models.

### **4.3 Diverse effects on innate and adaptive immune cells**

Trafficking of neutrophils and B cells through a variety of vital organs was investigated. Since these two leukocyte subsets are important representatives of the innate and adaptive immunity, respectively, it is important to understand how they are influenced by adrenergic signals. As shown in multiple experimental setups utilizing pharmacological agonists and KO mice, impacts of adrenergic stimulation on these cell types differed greatly. In blood, neutrophil numbers were elevated, whereas B cell numbers declined, coinciding with other studies (Dhabhar et al., 2012; Nakai et al., 2014). Mechanisms leading to altered circulating numbers are enhanced mobilization or impaired recruitment/homing. On the other hand, decreased numbers result from impaired mobilization, enhanced recruitment/homing or perturbed recirculation. In the following paragraph, a possible adrenergic influence on these parameters will be discussed.

#### **4.3.1 Are neutrophils mobilized from the BM?**

Signals from the SNS were shown to control leukocyte egress from the BM (Mendez-Ferrer et al., 2008), albeit the process being rather complicated due to interaction of various components at specific times of the day. Here, BRL37344 injection led to decreased neutrophil numbers in BM and increased numbers in blood during the day (12 pm). However, – as mentioned above – data obtained with this adrenergic agonist have to be interpreted carefully. Typically, only post-mitotic neutrophils are released into the blood.

BM egress under stress situations could lead to release of premature cells, which can be tested by staining of maturation markers, such as CXCR2 (Evrard et al., 2018). Another marker for neutrophil maturation is CXCR4, which is upregulated on immature neutrophils (Evrard et al., 2018). Examination of molecule levels on neutrophils after *in vivo* stimulation with the  $\beta_2$ -AR agonist revealed slightly upregulated CXCR4 levels, supporting the hypothesis that neutrophils might be prematurely released into the circulation upon adrenergic stimulation. Mobilization of neutrophils from the BM benefits the organism during inflammation, since these cells are ready to be recruited to sites where their presence is required. Thus, this readout is used as diagnostic marker at the onset of various diseases, such as recently shown for severe COVID-19 (Carissimo et al., 2020). If stress persistently upregulates numbers of immature neutrophils in the circulation, this could mark disease-related effects.

To clarify whether neutrophils really are increased due to enhanced mobilization and not other mechanisms such as demargination from the lung (Devi et al., 2013), proliferation assays using the synthetic nucleoside bromodeoxyuridine (BrdU) could be utilized to identify and quantify newly proliferating neutrophils in the circulation after  $\beta_3$ -AR stimulation. Contradicting enhanced demargination, neutrophil numbers were elevated in the perfused liver and lung. Although for human granulocytes it was demonstrated *in vitro* that catecholamine-induced cellular softening leads to demargination (Fay et al., 2016), this might not be the case in the murine *in vivo* experimental procedure used here.

#### **4.3.2 Is neutrophil recruitment from blood impaired?**

Upon  $\beta_2$ -AR stimulation via Clenbuterol administration, neutrophil numbers in blood were elevated at both time points tested (12 pm and 8 pm). After adoptive transfer of exogenous neutrophils, these cells were captured in the circulation, probably due to impeded recruitment from blood, which was found to be mediated by  $\beta_2$ -ARs. In order to be recruited to sites of inflammation or tissue damage, neutrophils utilize certain adhesion molecules and chemokine receptors, whose requirement differs between vascular beds. One of these molecules is CD62L, which mediates neutrophil rolling along the endothelial barrier in the majority of organs. Although not significant, CD62L levels increased upon Clenbuterol administration, indicating a less activated state (since this molecule is shed upon activation) that could explain retention in the circulation. This change in CD62L levels is in contrast to a study where expression on neutrophils decreased when stimulated with the catecholamines norepinephrine and epinephrine,

which are both binding to  $\beta_2$ -ARs, albeit with different affinities (epinephrine binds more potently to  $\beta_2$ -ARs than norepinephrine (Liapakis et al., 2004)). Further evidence for a reduced recruitment is provided by decreased CD49d levels, which is part of the integrin complex VLA-4 facilitating neutrophil adhesion to ECs. However, integrin levels are not as meaningful as their activity state, since binding affinities are able to change without alterations in surface levels of these molecules (Schürpf and Springer, 2011). Moreover, although levels of integrins were not affected by adrenergic stimulation, levels of their binding partners such as ICAM-1 could be altered, which were not tested in the course of this work.

If BRL37344 targeted both adrenoceptors simultaneously (Mori et al., 2010; Pott et al., 2003), circulating neutrophil numbers should have exceeded neutrophil numbers in blood from Clenbuterol-stimulated mice (due to impaired recruitment and additional egress from the BM). This could have been compensated by their migration to other organs, such as the liver, which exhibited six-fold elevated neutrophil numbers upon BRL37344 administration. An already specified possibility to test putative off-target effects is administration of BRL37344 to mice lacking  $\beta_2$ -ARs. Although this approach will not demonstrate the extent to which this compound binds both  $\beta$ -ARs, it will clarify whether  $\beta_2$ -ARs are involved in results obtained with the reputed  $\beta_3$ -AR specific agonist.

#### **4.3.3 How is neutrophil homing to the BM affected?**

Next to BM egress,  $\beta$ -ARs – mainly  $\beta_3$ -ARs of non-hematopoietic origin – were shown to mediate leukocyte homing to the BM at night (Scheiermann et al., 2012). Thus, stimulation of these receptors should have led to decreased neutrophil numbers in blood and increased numbers in BM. In contrast, using adoptively transferred cells, their accumulation in the circulation was demonstrated after recipient injection with Clenbuterol or BRL37344, although experiments were performed during the day. In addition, donor neutrophils did not exhibit enhanced migration to the BM upon Clenbuterol and BRL37344 administration. To investigate if adrenergic stimulation disrupts or promotes neutrophil homing in a time-of-day-dependent manner, adoptive transfers should be performed at night as well – when the magnitude of homing to the BM is greater than during the day.

While CXCR4 is important for leukocyte retention in BM, its upregulation is also a signal for senescent neutrophils to home back to the site of their production (Martin et al., 2003).

Thus, adrenergic signal-mediated upregulation of CXCR4 in the *in vivo* setup indicates neutrophil migration back to the BM. In this case, adrenergic stimulation in the tested time frame was potentially too short to promote homing in the extent of measurable differences in neutrophil numbers in the BM, but the process could have been initialized, i.e. by upregulation of CXCR4 on the surface of neutrophils. Moreover, altered CXCR4 levels can be interpreted one way or the other – as levels are upregulated on immature neutrophils as well as senescent neutrophils – complicating a conclusion of adrenergic effects on neutrophil migration behavior. In this respect, administration of BrdU could help to identify the age of neutrophils under investigation. Hence, more detailed experiments are required to unravel the molecular machinery leading to the observed phenotypes. Besides, only molecules on neutrophils have been tested, but reciprocal adoptive transfers revealed a role for non-hematopoietic cells, in accordance to other studies (Scheiermann et al., 2012). Thus, adhesion molecules on e.g. ECs of organs of interest should be tested after administration of Clenbuterol and a more reliable  $\beta_3$ -AR specific agonist. Provided that a previous work reported enhanced levels of E-selectin, P-selectin and VCAM-1 in BM after stimulation with Isoproterenol at night (Scheiermann et al., 2012), future investigations should focus on these molecules. Generation of EC lineage-specific Adrb KO mice would help to specify the influence of this important environmental component.

#### **4.3.4 How does the SNS orchestrate neutrophil distributions?**

As discussed above, neutrophil migration between several organs at different times of the day is a delicate process. The interplay between adrenergic signal-driven egress and homing to the BM was recently reported to be time-sensitively coordinated by the cholinergic nervous system that downregulates  $\beta_2$ -ARs during the day, resulting in egress via  $\beta_3$ -ARs, while at night,  $\beta_2$ -ARs prevail and facilitate leukocyte homing to the BM (Garcia-Garcia et al., 2019). To add a level of complexity, effects of adrenergic agonists are highly dependent on the cellular maturation and activation state. Thus, discrepancies between different studies could be based on the fact that only cell types were identified rather than other features, such as age or activation state. In the course of their life time in the circulation, neutrophils change their properties following a circadian rhythm (Adrover et al., 2019). Since knowledge about neutrophil heterogeneity is evolving (Ng et al., 2019), it will be important to further phenotype cells of this subset for a more detailed categorization of adrenergic effects on neutrophils. Since reciprocal adoptive transfers

revealed a role of  $\beta_2$ -ARs on the neutrophil as well as the microenvironmental side, lineage-specific *Adrb2* KO mice would give more insight into the interplay between these two components.

#### **4.3.5 How does the SNS impact B cell trafficking through LNs?**

B cells constantly recirculate through secondary lymphoid organs in surveillance of antigen. They enter LNs via HEVs and migrate within these tissues to distinct follicles. If they do not encounter their cognate antigen, they egress into the lymph and back to the blood stream. Egress from LNs is orchestrated by an interplay between exit-promoting factors such as S1PR1 and retention-promoting factors such as the chemokine receptor CCR7 (Pham et al., 2008). Accordingly, examination of CCR7 levels on circulating B cells upon  $\beta_2$ -AR stimulation revealed an increase of this molecule. In addition, B cell numbers in skin-draining LNs were elevated despite homing block, further suggesting a retention-promoting effect of  $\beta_2$ -AR stimulation. These data are in line with other studies, where enhanced retention in LNs was attributed to physical interactions between  $\beta_2$ -ARs and the chemokine receptors CXCR4 and CCR7 (Nakai et al., 2014). However, homing was neglected in that report, whereas adoptively transferred B cells in this study were found to preferentially migrate to the mLN, although they were injected just one hour prior to harvest, indicating a slightly augmented homing of B cells to LNs due to  $\beta_2$ -AR stimulation. Moreover, intravital imaging of B cells in the vasculature of popLNs revealed an altered adhesion capacity upon administration of Clenbuterol. Considering these data, it is possible that integrins are involved in enhanced homing to LNs. Therefore, levels of adhesion molecules on the surface of B cells were tested. Since integrin levels did not change, but blocking of these molecules with antibodies impacted the migratory behavior of B cells, it is hypothesized that integrin affinity might be controlled by  $\beta_2$ -ARs. This could be tested using affinity binding assays with soluble ICAM-1 (the ligand of these integrins).

Whereas homing of adoptively transferred B cells to the mLN was increased upon Clenbuterol administration, homing block demonstrated B cell retention merely in sdLNs and not the gut-draining mLN. What causes this inconsistency? First, cellular contents of LNs are dependent on the tissue size, which differs between LNs as well as between mice. Second, molecular requirements for homing vary between certain LNs. In HEVs of gut-associated lymphoid tissue (GALT) such as the mLN, MADCAM-1 is highly expressed (Streeter et al., 1988). Its binding partner VLA-4 (which partly consists of CD49d) was demonstrated to be crucial for lymphocyte trafficking to GALT (Gorfu et al., 2009;

Habtezion et al., 2016). Since it is hypothesized that integrin affinity might be controlled by  $\beta_2$ -ARs, administration of Clenbuterol could increase CD49d affinity and therefore enhance donor B cell homing to mLNs. This could also explain why block of CD49d and CD11a (homing block) led to lower B cell numbers in the mLN, whereas numbers of B cells were still elevated in sdLNs of Clenbuterol-stimulated mice. Thus, the mLN should be in the center of future investigations addressing adrenergic control of B cell trafficking.

Strikingly, CD62L levels on B cells were dramatically reduced upon adrenergic stimulation – *in vivo* and *in vitro* – pointing to an enhanced activity of the cells, since this molecule is shed upon activation. Similar results were obtained by others, whereby corticosterone outrivalled norepinephrine and epinephrine in its effects (Dhabhar et al., 2012). Given that this molecule is important for lymphocyte homing to LNs (He et al., 2018; Rosen, 2004), it was expected that block of CD62L would increase circulating and diminish B cell numbers in LNs. Surprisingly, no effect was observed in blood, disproving a role of this molecule in adrenergic redistribution of this lymphocyte subset. However, the blocking antibody reacts with CD62L and it is not clear whether there is still a certain capacity to shed the molecule. Mice lacking CD62L will give more insight into its involvement in lymphocyte redistribution. Other affected molecules were CXCR4 and CD162 (PSGL-1). To unravel their importance in the observed phenotype, further blocking experiments are required.

After observing increased CD62L levels upon *in vitro* stimulation of B cells with Clenbuterol, it was hypothesized that cell-intrinsic  $\beta_2$ -ARs are crucial for the observed effects. In addition, others already showed a cell-autonomous effect of adrenergic signals on the trafficking of lymphocytes through LNs (Nakai et al., 2014). However, no interpretation could be provided, since donor cells in the control did not behave as expected. To clarify this issue more elegantly, lineage-specific *Adrb2* KO mice will be of great use.

#### **4.4 Transferability**

Is it possible to transfer effects of adrenergic stimulation on leukocyte trafficking from mouse to human? As catecholamine levels oscillate in both species, but with inverted rhythms (De Boer and Van der Gugten, 1987; Linsell et al., 1985), it seems likely that comparable mechanisms might occur. Of course, several differences have to be considered such as varying receptor densities on leukocytes (Elenkov et al., 2000) as well as altered

affinities of adrenergic agonists between species (Nahmias et al., 1991). Moreover, receptor function on human leukocytes can vary between healthy subjects and subjects suffering from medical conditions such as hypertension (Feldmann et al., 1984). Whereas in mouse models multiple stress situations are experimentally mimicked, by e.g. manipulation of housing temperatures (Hylander et al., 2019), investigations of the interplay between the immune system and nervous system in humans are mostly limited to blood examinations during physical activity or psychological stress situations, such as public speaking (Goebel and Mills, 2000). However, it is important to take into account that different stressors can have different outcomes – in both species (Bowers et al., 2008).

Since leukocyte trafficking is essential for every aspect of a functioning immune system, leukocyte redistribution under control of adrenergic input might be capable of manipulating immune responses. Indeed, it was recently shown that during the active phase of mice, higher responses in LNs are achieved, such as an elevated magnitude of antibody production (Suzuki et al., 2016). If this is transferable to humans, vaccination efficiency might be improved by combination with low doses of adrenergic agonists at the appropriate time of the day. In addition to adaptive immune responses, the innate immune system profits from stimulation of  $\beta$ -ARs, evidenced by improved survival of lethally irradiated mice (Scheiermann et al., 2012). Thus, application of adrenergic agonists could open possibilities to improve BM transplantations, although repeated doses will be necessary and possible side effects have to be monitored frequently.

In this study it was shown that stimulation of  $\beta$ -ARs massively influences circulating leukocyte numbers in mice. Therefore, this system provides certain potential for therapeutic treatments of diseases where the immune system is involved. To date, mostly  $\beta$ -AR blockers such as Propranolol are clinically used to treat cardiovascular diseases (do Vale et al., 2019), whereas adrenergic agonists are predominantly used for acute treatments of e.g. allergic asthma. While their mode of action targets smooth muscle cells of the vasculature to achieve bronchorelaxation, effects on the immune system might have been underestimated in these scenarios, especially in the context of prolonged treatments. Taken together, to reduce negative side effects of currently used and future drugs, it will be important to elucidate possible outcomes of  $\beta$ -AR modulation on leukocyte behavior and function.

## 4.5 Concluding remarks

In this work, first steps have been undertaken to disentangle impacts of the sympathetic nervous system – via  $\beta$ -ARs – on the trafficking of neutrophils and B cells under steady-state conditions. Using experimental procedures such as adoptive transfers and intravital microscopy, it was demonstrated that neutrophil numbers in the circulation are increased by an interplay between enhanced mobilization and impaired recruitment. In contrast, B cells left the blood stream and migrated to LNs, where they were retained and thus hindered to reenter the circulation. Using reciprocal adoptive transfers between WT and genetically modified mice lacking  $\beta_2$ - and  $\beta_3$ -ARs, most of these observations were attributed to stimulation of hematopoietic and non-hematopoietic  $\beta_2$ -ARs, which directly or indirectly altered adhesion molecule levels on leukocytes. Additionally, BRL37344 was identified as nonspecific for  $\beta_3$ -ARs and hence should not be used to examine the role of this adrenoceptor type. Thus, for the first time this study shows the distribution of neutrophils and B cells under adrenergic stimulation in an organism-wide approach.

Despite these novel findings, which are summarized in **Figure 4-1**, this thesis also points out the knowledge gap in current research on this topic, especially regarding molecular mechanisms leading to the observed redistribution of cells *in vivo*. Furthermore, this study demonstrates once more the complexity of this research field, which requires methodology allowing for combined analysis of physiological components such as the immune system, the nervous system and the circadian clock. Distinct cell types such as stromal cells in various organs should be spotlighted for single cell analyses, which will facilitate defining the mechanisms leading to adrenergic-driven reallocation of leukocytes and tissue-specific effects of the sympathetic tone under steady state. Efforts in this respect will be necessary to gain fundamental insight into how the immune system works in tune with intrinsically and extrinsically induced stress which is a constant part of our daily life.

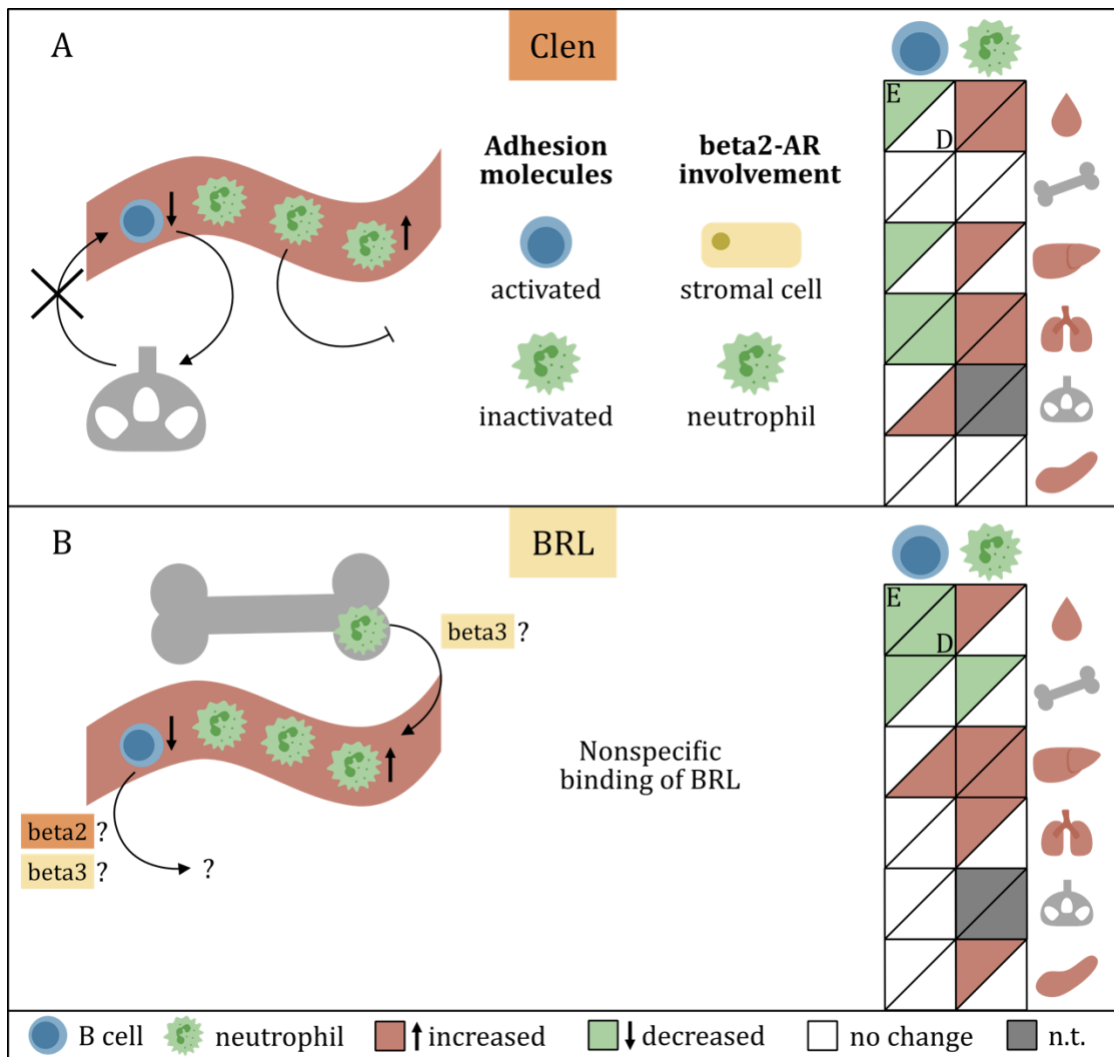


**Figure 4-1: Summary figure of the results.**

**(A)** Administration of the  $\beta_2$ -AR agonist Clenbuterol (Clen) leads to the accumulation of endogenous neutrophils in blood due to impaired recruitment, whereas B cells presumably migrate to lymph nodes where they are retained. Stimulation results in an activated state of B cells and an inactivated state of neutrophils, becoming manifest in altered adhesion molecule levels.  $\beta_2$ -ARs on stromal cells as well as neutrophils are involved in these effects, while for B cells it remains elusive. The matrix on the right-hand side displays altered numbers of endogenous (E) and donor (D) B cells and neutrophils across blood, bone marrow, liver, lung, lymph nodes and spleen under steady state upon Clen administration. **(B)** Although BRL was found to have unspecific effects due to off-target binding, egress of neutrophils into blood could be  $\beta_3$ -AR specific. In blood, the same phenotype as after  $\beta_2$ -AR stimulation was observed, so it remains elusive which receptor type is responsible. The matrix on the right-hand side displays altered numbers of endogenous (E) and donor (D) B cells and neutrophils across blood, bone marrow, liver, lung, lymph nodes and spleen under steady state upon BRL administration. n.t. = not tested.



## 5 Bibliography

Adrover, J.M., Del Fresno, C., Crainiciuc, G., Cuartero, M.I., Casanova-Acebes, M., Weiss, L.A., Huerga-Encabo, H., Silvestre-Roig, C., Roissant, J., Cossío, I., *et al.* (2019). A neutrophil timer coordinates immune defense and vascular protection. *Immunity* 50, 390-402.

Agac, D., Estrada, L.D., Maples, R., Hooper, L.V., and Farrar, J.D. (2018). The beta2-adrenergic receptor controls inflammation by driving rapid IL-10 secretion. *Brain Behav Immun* 74, 176-185.

Aird, W.C. (2007). Phenotypic heterogeneity of the endothelium: II. Representative vascular beds. *Circ Res* 100, 174-190.

Al-Majed, A.A., Bakheit, A.H.H., Abdel Aziz, H.A., Alajimi, F.M., and AlRabiah, H. (2017a). Propranolol. In *Profiles of Drug Substances, Excipients and Related Methodology*, pp. 287-338.

Al-Majed, A.A., Khalil, N.Y., Khbrani, I., and Abdel-Aziz, H.A. (2017b). Clenbuterol Hydrochloride. *Profiles Drug Subst Excip Relat Methodol* 42, 91-123.

Alhayek, S., and Preiss, C.V. (updated 2020 Aug 11). *Beta 1 Receptors* (Treasure Island (FL): StatPearls Publishing).

Allende, M.L., Tuymetova, G., Lee, B.G., Bonifacino, E., Wu, Y.-P., and Proia, R.L. (2010). S1P1 receptor directs the release of immature B cells from bone marrow into blood. *J Exp Med* 207, 1113-1124.

Alon, R., Kassner, P.D., Carr, M.W., Finger, E.B., Hemler, M.E., and Springer, T.A. (1995). The integrin VLA-4 supports tethering and rolling in flow on VCAM-1. *J Cell Biol* 128, 1243-1253.

Apostolova, G., and Dechant, G. (2009). Development of neurotransmitter phenotypes in sympathetic neurons. *Auton Neurosci* 151, 30-38.

Babior, B.M., Kipnes, R.S., and Curnutte, J.T. (1973). Biological defense mechanisms. The production by leukocytes of superoxide, a potential bactericidal agent. *J Clin Invest* 52, 741-744.

Barnes, P.J. (2004). Distribution of receptor targets in the lung. *Proc Am Thorac Soc* 1, 345-351.

Basit, A., Reutershan, J., Morris, M.A., Solga, M., Rose Jr., C.E., and Ley, K. (2006). ICAM-1 and LFA-1 play critical roles in LPS-induced neutrophil recruitment into the alveolar space. *Am J Physiol Lung Cell Mol Physiol* 291, L200-207.

Bellinger, D.L., Millar, B.A., Perez, S., Carter, J., Wood, C., ThyagaRajan, S., Molinaro, C., Lubahn, C., and Lorton, D. (2008). Sympathetic modulation of immunity: relevance to disease. *Cell Immunol* 252, 27-56.

Bevilacqua, M.P., Poher, J.S., Mendrick, D.L., Cotran, R.S., and Gimbrone Jr., M.A. (1987). Identification of an inducible endothelial-leukocyte adhesion molecule. *Proc Natl Acad Sci U S A* *84*, 9238-9242.

Billington, C.K., Penn, R.B., and P., H.I. (2017).  $\beta$ 2-agonists. *Handb Exp Pharmacol* *237*, 23-40.

Birbrair, A., and Frenette, P.S. (2016). Niche heterogeneity in the bone marrow. *Ann N Y Acad Sci* *1370*, 82-96.

Blaho, V.A., and Hla, T. (2014). An update on the biology of sphingosine 1-phosphate receptors. *J Lipid Res* *55*, 1596-1608.

Bogoslowski, A., Butcher, E.C., and Kubes, P. (2018). Neutrophils recruited through high endothelial venules of the lymph nodes via PNA<sub>d</sub> intercept disseminating *Staphylococcus aureus*. *Proc Natl Acad Sci U S A* *115*, 2449-2454.

Bogoslowski, A., Wijeyesinghe, S., Lee, W.-Y., Chen, C.S., Alanani, S., Jenne, C., Steeber, D.A., Scheiermann, C., Butcher, E.C., Masopust, D., *et al.* (2020). Neutrophils recirculate through lymph nodes to survey tissues for pathogens. *J Immunol* *204*, 2552-2561.

Bonder, C.S., Norman, M.U., Swain, M.G., Zbytniuk, L.D., Yamanouchi, J., Santamaria, P., Ajuebor, M., Salmi, M., Jalkanen, S., and Kubes, P. (2005). Rules of recruitment for Th1 and Th2 lymphocytes in inflamed liver: a role for  $\alpha$ -4 integrin and vascular adhesion protein-1. *Immunity* *23*, 153-163.

Borges, E., Eytner, R., Moll, T., Steegmaier, M., Campbell, M.A., Ley, K., Mossmann, H., and Vestweber, D. (1997). The P-selectin glycoprotein ligand-1 is important for recruitment of neutrophils into inflamed mouse peritoneum. *Blood* *90*, 1934-1942.

Bowers, S.L., Bilbo, S.D., Dhabhar, F.S., and Nelson, R.J. (2008). Stressor-specific alterations in corticosterone and immune responses in mice. *Brain Behav Immun* *22*, 105-113.

Burdick, M.M., Bochner, B.S., Collins, B.E., Schnaar, R.L., and Konstantopoulos, K. (2001). Glycolipids support E-selectin-specific strong cell tethering under flow. *Biochem Biophys Res Commun* *284*, 42-49.

Burnstock, G. (2009). Purinergic cotransmission. *Exp Physiol* *94*, 20-24.

Calvo, W. (1968). The innervation of the bone marrow in laboratory animals. *Am J Anat* *123*, 315-328.

Cariappa, A., Chase, C., Liu, H., Russell, P., and Pillai, S. (2007). Naive recirculating B cells mature simultaneously in the spleen and bone marrow. *Blood* *109*, 2339-2345.

Carissimo, G., Xu, W., Kwok, I., Abdad, M.Y., Chan, Y.-H., Fong, S.-W., Puan, K.J., Lee, C.Y.-P., Yeo, N.K.-W., Amrun, S.N., *et al.* (2020). Whole blood immunophenotyping uncovers immature neutrophil-to-VD2 T-cell ratio as an early marker for severe COVID-19. *Nat Commun* *11*.

Casanova-Acebes, M., Pitaval, C., Weiss, L.A., Nombela-Arrieta, C., Chevre, R., N, A.G., Kunisaki, Y., Zhang, D., van Rooijen, N., Silberstein, L.E., *et al.* (2013). Rhythmic modulation of the hematopoietic niche through neutrophil clearance. *Cell* *153*, 1025-1035.

- Cernecka, H., Sand, C., and Michel, M.C. (2014). The odd sibling: features of  $\beta$ 3-adrenoceptor pharmacology. *Mol Pharmacol* *86*, 479-484.
- Chen, A., Engel, P., and Tedder, T.F. (1995). Structural requirements regulate endoproteolytic release of the L-selectin (CD62L) adhesion receptor from the cell surface of leukocytes. *J Exp Med* *182*, 519-530.
- Chen, S., and Springer, T.A. (1999). An automatic braking system that stabilizes leukocyte rolling by an increase in selectin bond number with shear. *J Cell Biol* *144*, 185-200.
- Choi, M., Staus, D.P., Wingler, L.M., Ahn, S., Pani, B., Capel, W.D., and Lefkowitz, R.J. (2018). G protein-coupled receptor kinases (GRKs) orchestrate biased agonism at the beta2-adrenergic receptor. *Sci Signal* *11*.
- Cifuentes, F., Montoya, M., and Morales, M.A. (2008). High-frequency stimuli preferentially release large dense-core vesicles located in the proximity of nonspecialized zones of the presynaptic membrane in sympathetic ganglia. *Dev Neurobiol* *68*, 446-456.
- Curbishley, S.M., Eksteen, B., Gladue, R.P., Lalor, P.F., and Adams, D.H. (2005). CXCR3 activation promotes lymphocyte transendothelial migration across human endothelium under fluid flow. *Am J Pathol* *167*, 887-899.
- Daaka, Y., Luttrell, L.M., and Lefkowitz, R.J. (1997). Switching of the coupling of the beta2-adrenergic receptor to different G proteins by protein kinase A. *Nature* *390*, 88-91.
- De Boer, S.F., and Van der Gugten, J. (1987). Daily variations in plasma noradrenaline, adrenaline and corticosterone concentrations in rats. *Physiol Behav* *40*, 323-328.
- de Coupade, C., Brown, A.S., Dazin, P.F., Levine, J.D., and Green, P.G. (2007).  $\beta$ 2-Adrenergic Receptor-Dependent Sexual Dimorphism For Murine Leukocyte Migration. *J Neuroimmunol* *186*, 54-62.
- Devi, S., Wang, Y., Chew, W.K., Lima, R., González, N.A., Mattar, C.N.Z., Chong, S.Z., Schlitzer, A., Bakocevic, N., Chew, S., *et al.* (2013). Neutrophil mobilization via plerixafor-mediated CXCR4 inhibition arises from lung demargination and blockade of neutrophil homing to the bone marrow. *J Exp Med* *210*, 2321-2336.
- Dhabhar, F.S., Malarkey, W.B., Neri, E., and McEwen, B.S. (2012). Stress-induced redistribution of immune cells--from barracks to boulevards to battlefields: a tale of three hormones--Curt Richter Award winner. *Psychoneuroendocrinology* *37*, 1345-1368.
- Diamond, M.S., Staunton, D.E., de Fougères, A.R., Stacker, S.A., Garcia-Aguilar, J., Hibbs, M.L., and Springer, T.A. (1990). ICAM-1 (CD54): a counter-receptor for Mac-1 (CD11b/CD18). *J Cell Biol* *111*, 3129-3139.
- Dixon, R.A., Kobilka, B.K., Strader, D.J., Benovic, J.L., Dohlman, H.G., Frielle, T., Bolanowski, M.A., Bennett, C.D., Rands, E., Diehl, R.E., *et al.* (1986). Cloning of the gene and cDNA for mammalian beta-adrenergic receptor and homology with rhodopsin. *Nature* *321*, 75-79.
- do Vale, G.T., Ceron, C.S., Gonzaga, N.A., Simplicio, J.A., and Padovan, J.C. (2019). Three Generations of beta-blockers: History, Class Differences and Clinical Applicability. *Curr Hypertens Rev* *15*, 22-31.

Doerschuk, C.M., Beyers, N., Coxson, H.O., Wiggs, B., and Hogg, J.C. (1993). Comparison of neutrophil and capillary diameters and their relation of neutrophil sequestration in the lung. *J Appl Physiol* *74*, 3040-3045.

Druzd, D., Matveeva, O., Ince, L., Harrison, U., He, W., Schmal, C., Herzel, H., Tsang, A.H., Kawakami, N., Leliavski, A., *et al.* (2017). Lymphocyte Circadian Clocks Control Lymph Node Trafficking and Adaptive Immune Responses. *Immunity* *46*, 120-132.

Dustin, M.L., Rothlein, R., Bhan, A.K., Dinarello, C.A., and Springer, T.A. (1986). Induction by IL 1 and interferon- $\gamma$ : tissue distribution, biochemistry, and function of a natural adherence molecule (ICAM-1). *J Immunol* *136*, 5024-5033.

Eash, K.J., Greenbaum, A.M., Gopalan, P.K., and Link, D.C. (2010). CXCR2 and CXCR4 antagonistically regulate neutrophil trafficking from murine bone marrow. *J Clin Invest* *120*, 2423-2431.

Eibel, H., Kraus, K., Sic, H., Kienzler, A.-K., and Rizzi, M. (2014). B cell biology: an overview. *Curr Allergy Asthma Rep* *14*, 434.

Elenkov, I.J., Haskó, G., Kovács, K.J., and Vizi, E.S. (1995). Modulation of lipopolysaccharide-induced tumor necrosis factor- $\alpha$  production by selective  $\alpha$ - and  $\beta$ -adrenergic drugs in mice. *J Neuroimmunol* *61*, 123-131.

Elenkov, I.J., Wilder, R.L., Chrousos, G.P., and Vizi, E.S. (2000). The sympathetic nerve--an integrative interface between two supersystems: the brain and the immune system. *Pharmacol Rev* *52*, 595-638.

Elices, M.J., Osborn, L., Takada, Y., Crouse, C., Luhowskyj, S., Hemler, M.E., and Lobb, R.R. (1990). VCAM-1 on activated endothelium interacts with the leukocyte integrin VLA-4 at a site distinct from the VLA-4/fibronectin binding site. *Cell* *60*, 577-584.

Emorine, L.J., Marullo, S., Briend-Sutren, M.M., Patey, G., Tate, K., Delavier-Klutchko, C., and Strosberg, A.D. (1989). Molecular characterization of the human  $\beta$  3-adrenergic receptor. *Science* *245*, 1118-1121.

Evans, B.A., Papaioannou, M., Hamilton, S., and Summers, R.J. (1999). Alternative splicing generates two isoforms of the  $\beta$ 3-adrenoceptor which are differentially expressed in mouse tissues. *Br J Pharmacol* *127*, 1525-1531.

Evrard, M., Kwok, I.W.H., Chong, S.Z., Teng, K.W.W., Becht, E., Chen, J., Sieow, J.L., Penny, H.L., Ching, G.C., Devi, S., *et al.* (2018). Developmental Analysis of Bone Marrow Neutrophils Reveals Populations Specialized in Expansion, Trafficking, and Effector Functions. *Immunity* *48*, 364-379 e368.

Fay, M.E., Myers, D., Kumar, A., Turbyfield, C.T., Byler, R., Crawford, K., Mannino, R.G., Laohapant, A., Tyburski, E.A., Sakurai, Y., *et al.* (2016). Cellular softening mediates leukocyte demargination and trafficking, thereby increasing clinical blood counts. *Proc Natl Acad Sci U S A* *113*, 1987-1992.

Feldmann, R.D., Limbird, L.E., Nadeau, J., Robertson, D., and Wood, A.J. (1984). Leukocyte  $\beta$ -receptor alterations in hypertensive subjects. *J Clin Invest* *73*, 648-653.

Felten, D.L., Felten, S.Y., Bellinger, D.L., Carlson, S.L., Ackerman, K.D., Madden, K.S., Olschowki, J.A., and Livnat, S. (1987). Noradrenergic sympathetic neural interactions with the immune system: structure and function. *Immunol Rev* 100.

Felten, D.L., Felten, S.Y., Carlson, S.L., Olschowka, J.A., and Livnat, S. (1985). Noradrenergic and peptidergic innervation of lymphoid tissue. *J Immunol* 135, 755s-765s.

Felten, D.L., Livnat, S., Felten, S.Y., Carlson, S.L., Bellinger, D.L., and Yeh, P. (1984). Sympathetic innervation of lymph nodes in mice. *Brain Res Bull* 13, 693-699.

Fischer, K., Ruiz, H.H., Jhun, K., Finan, B., Oberlin, D.J., van der Heide, V., Kalinovich, A.V., Petrovic, N., Wolf, Y., Clemmensen, C., *et al.* (2017). Alternatively activated macrophages do not synthesize catecholamines or contribute to adipose tissue adaptive thermogenesis. *Nat Med* 23, 623-630.

Flierl, M.A., Rittirsch, D., Nadeau, B.A., Chen, A.J., Sarma, J.V., Zetoune, F.S., McGuire, S.R., List, R.P., Day, D.E., Hoesel, L.M., *et al.* (2007). Phagocyte-derived catecholamines enhance acute inflammatory injury. *Nature* 449, 721-725.

Frenette, P.S., Mayadas, T.N., Rayburn, H., Hynes, R.O., and Wagner, D.D. (1996). Susceptibility to infection and altered hematopoiesis in mice deficient in both P- and E-selectins. *Cell* 84, 563-574.

Fukuda, Y., Imoto, M., Koyama, Y., Miyazawa, Y., and Hayakawa, T. (1996). Demonstration of Noradrenaline-Immunoreactive Nerve Fibres in the Liver. *Journal of International Medical Research*.

Furze, R.C., and Rankin, S.M. (2008). The role of the bone marrow in neutrophil clearance under homeostatic conditions in the mouse. *FASEB J* 22, 3111-3119.

Galant, S.P., and Allred, S. (1981). Binding and functional characteristics of beta adrenergic receptors in the intact neutrophil. *J Lab Clin Med* 98, 227-237.

Galaz-Montoya, M., Wright, S.J., Rodriguez, G.J., Lichtarge, O., and Wensel, T.G. (2017). Beta2-Adrenergic receptor activation mobilizes intracellular calcium via a non-canonical cAMP-independent signaling pathway. *J Biol Chem* 292, 9967-9974.

Gálvez, I., Martín-Cordero, L., Hinchado, M.D., Álvarez-Barrientos, A., and Ortega, E. (2019). Anti-inflammatory effect of  $\beta_2$  adrenergic stimulation on circulating monocytes with a pro-inflammatory state in high-fat diet-induced obesity. *Brain Behav Immun* 80, 564-572.

Garcia-Garcia, A., Korn, C., Garcia-Fernandez, M., Domingues, O., Villadiego, J., Martin-Perez, D., Isern, J., Bejarano-Garcia, J.A., Zimmer, J., Perez-Simon, J.A., *et al.* (2019). Dual cholinergic signals regulate daily migration of hematopoietic stem cells and leukocytes. *Blood* 133, 224-236.

Geumei, A., and Mahfouz, M. (1968). The presence of beta-adrenergic receptors in the hepatic vasculature. *Br J Pharmacol Chemother* 32, 466-472.

Girard, J.P., Mousson, C., and Förster, R. (2012). HEVs, lymphatics and homeostatic immune cell trafficking in lymph nodes. *Nat Rev Immunol* 12, 762-773.

Glinka, Y., Gassen, M., and Youdim, M.B. (1997). Mechanisms of 6-hydroxydopamine neurotoxicity. *J Neural Transm Suppl* 50, 55-66.

Goebel, M.U., and Mills, P.J. (2000). Acute psychological stress and exercise and changes in peripheral leukocyte adhesion molecule expression and density. *Psychosom Med* 62, 664-670.

Gorfu, G., Rivera-Nieves, J., and Ley, K. (2009). Role of  $\beta 7$  integrins in intestinal lymphocyte homing and retention. *Curr Mol Med* 9, 836-850.

Green, H.D., Hall, L.S., Sexton, J., and Deal, C.P. (1959). Autonomic vasomotor responses in the canine hepatic arterial and venous beds. *Am J Physiol*.

Gregory, S.H., Sagnimeni, A.J., and Wing, E.J. (1996). Bacteria in the bloodstream are trapped in the liver and killed by immigrating neutrophils. *J Immunol* 157, 2514-2520.

Gunn, M.D., Tangemann, K., Tam, C., Cyster, J.G., Rosen, S.D., and Williams, L.T. (1998). A chemokine expressed in lymphoid high endothelial venules promotes the adhesion and chemotaxis of naive T lymphocytes. *Proc Natl Acad Sci U S A* 95, 258-263.

Habtezion, A., Nguyen, L.P., Hadeiba, H., and Butcher, E.C. (2016). Leukocyte Trafficking to the Small Intestine and Colon. *Gastroenterology* 150, 340-354.

Hall, H., Sällemark, M., and Ross, S.B. (1980). Clenbuterol, a central beta-adrenoceptor agonist. *Acta Pharmacol Toxicol (Copenh)* 47, 159-160.

Harris, E.S., and Nelson, W.J. (2010). VE-Cadherin: At the Front, Center, and Sides of Endothelial Cell Organization and Function. *Curr Opin Cell Biol* 22, 651-658.

He, W., Holtkamp, S., Hergenhan, S.M., Kraus, K., de Juan, A., Weber, J., Bradfield, P., Grenier, J.M.P., Pelletier, J., Druzd, D., *et al.* (2018). Circadian Expression of Migratory Factors Establishes Lineage-Specific Signatures that Guide the Homing of Leukocyte Subsets to Tissues. *Immunity* 49, 1175-1190 e1177.

Hellebrekers, P., Vrisekoop, N., and Koenderman, L. (2018). Neutrophil phenotypes in health and disease. *Eur J Clin Invest* 48, e12943.

Heydtmann, M., Lalor, P.F., Eksteen, J.A., Hübscher, S.G., Briskin, M., and Adams, D.H. (2005). CXC chemokine ligand 16 promotes integrin-mediated adhesion of liver-infiltrating lymphocytes to cholangiocytes and hepatocytes within the inflamed human liver. *J Immunol* 174, 1055-1062.

Hidalgo, A., Chilvers, E.R., Summers, C., and Koenderman, L. (2019). The neutrophil life cycle. *Trends Immunol* 40, 584-597.

Hidalgo, A., Peired, A.J., Wild, M., Vestweber, D., and Frenette, P.S. (2007). Complete identification of E-selectin ligands on neutrophils reveals distinct functions of PSGL-1, ESL-1, and CD44. *Immunity* 26, 477-489.

Hogg, N., Henderson, R., Leitinger, B., McDowall, A., Porter, J., and Stanley, P. (2002). Mechanisms contributing to the activity of integrins on leukocytes. *Immunol Rev* 186, 164-171.

Hsu-Lin, S., Berman, C.L., Furie, B.C., August, D., and Furie, B. (1984). A platelet membrane protein expressed during platelet activation and secretion. Studies using a monoclonal antibody specific for thrombin-activated platelets. *J Biol Chem* 259, 9121-9126.

- Hu, D., Al-Shalan, H.A.M., Shi, Z., Wang, P., Wu, Y., Nicholls, P.K., Greene, W.K., and Ma, B. (2020). Distribution of nerve fibers and nerve-immune cell association in mouse spleen revealed by immunofluorescent staining. *Scientific Reports* 10.
- Hwang, J.M., Yamanouchi, J., Santamaria, P., and Kubes, P. (2004). A critical temporal window for selectin-dependent CD4+ lymphocyte homing and initiation of late-phase inflammation in contact sensitivity. *J Exp Med* 199, 1223-1234.
- Hylander, B.L., Gordon, C.J., and Repasky, E.A. (2019). Manipulation of Ambient Housing Temperature To Study the Impact of Chronic Stress on Immunity and Cancer in Mice. *J Immunol* 202, 631-636.
- Hyun, Y.-M., and Hong, C.-W. (2017). Deep insight into neutrophil trafficking in various organs. *J Leukoc Biol* 102, 617-629.
- Hyun, Y.-M., Sumagin, R., Sarangi, P.P., Lomakina, E., Overstreet, M.G., Baker, C.M., Fowell, D.J., Waugh, R.E., Sarelius, I.H., and Kim, M. (2012). Uropod elongation is a common final step in leukocyte extravasation through inflamed vessels. *J Exp Med* 209.
- Itkin, T., Gur-Cohen, S., Spencer, J.A., Schajnovitz, A., Ramasamy, S.K., Kusumbe, A.P., Ledergor, G., Jung, Y., Milo, I., Poulos, M.G., *et al.* (2016). Distinct bone marrow blood vessels differentially regulate haematopoiesis. *Nature* 532, 232-238.
- Jakob, M.O., Murugan, S., and Klose, C.S.N. (2020). Neuro-immune circuits regulate immune responses in tissues and organ homeostasis. *Front Immunol* 11.
- Kansas, G.S., Ley, K., Munro, J.M., and Tedder, T.F. (1993). Regulation of leukocyte rolling and adhesion to high endothelial venules through the cytoplasmic domain of L-selectin. *J Exp Med* 177, 833-838.
- Katayama, Y., Battista, M., Kao, W.M., Hidalgo, A., Peired, A.J., Thomas, S.A., and Frenette, P.S. (2006). Signals from the sympathetic nervous system regulate hematopoietic stem cell egress from bone marrow. *Cell* 124, 407-421.
- Khandoga, A., Huettinger, S., Khandoga, A.G., Li, G., Butz, S., Lauch, K.-W., Vestweber, D., and Krombach, F. (2009). Leukocyte transmigration in inflamed liver: A role for endothelial cell-selective adhesion molecule. *J Hepatol* 50, 755-765.
- Köhler, A., De Filippo, K., Hasenberg, M., van den Brandt, C., Nye, E., Hosking, M.P., Lane, T.E., Männ, L., Ransohoff, R.M., Hauser, A.E., *et al.* (2011). G-CSF-mediated thrombopoietin release triggers neutrophil motility and mobilization from bone marrow via induction of Cxcr2 ligands. *Blood* 117, 4349-4357.
- Kong, D.-H., Kim, Y.K., Kim, M.R., Jang, J.H., and Lee, S. (2018). Emerging roles of vascular cell adhesion molecule-1 (VCAM-1) in immunological disorders and cancer. *Int J Mol Sci* 19, 1057.
- Koni, P.A., Joshi, S.K., Temann, U.A., Olson, D., Burkley, L., and Flavell, R.A. (2001). Conditional vascular cell adhesion molecule 1 deletion in mice: impaired lymphocyte migration to the bone marrow. *J Exp Med* 193, 741-754.

Kubo, H., Doyle, N.A., Graham, L., Bhagwan, S.D., Quinlan, W.M., and Doerschuk, C.M. (1999). L- and P-selectin and CD11/CD18 in intracapillary neutrophil sequestration in rabbit lungs. *Am J Respir Crit Care Med* 159, 267-274.

Kuhar, M.J., Couceyro, P.R., and Lambert, P.D. (1999). Biosynthesis of Catecholamines. In *Neurochemistry: Molecular, Cellular and Medical Aspects*, G.J. Siegel, B.W. Agranoff, and R.W.e.a. Albers, eds. (Philadelphia: Lippincott-Raven).

Kummer, D., and Ebnet, K. (2018). Junctional Adhesion Molecules (JAMs): The JAM-Integrin Connection. *Cells* 7.

Kunisaki, Y., Bruns, I., Scheiermann, C., Ahmed, J., Pinho, S., Zhang, D., Mizoguchi, T., Wei, Q., Lucas, D., Ito, K., *et al.* (2013). Arteriolar niches maintain haematopoietic stem cell quiescence. *Nature* 502, 637-643.

Labow, M.A., Norton, C.R., Rumberger, J.M., Lombard-Gillooly, K.M., Shuster, D.J., Hubbard, J., R., B., A., K.P., Terry, R.W., and Harbison, M.L. (1994). Characterization of E-selectin-deficient mice: demonstration of overlapping function of the endothelial selectins. *Immunity* 1, 709-720.

Lalor, P.F., Edwards, S., McNab, G., Salmi, M., Jalkanen, S., and Adams, D.H. (2002). Vascular adhesion protein-1 mediates adhesion and transmigration of lymphocytes on human hepatic endothelial cells. *J Immunol* 169, 983-992.

Leach, S., and Suzuki, K. (2020). Adrenergic Signaling in Circadian Control of Immunity. *Front Immunol* 11.

LeBien, T.W., and Tedder, T.F. (2008). B lymphocytes: how they develop and function. *Blood* 112, 1570-1580.

Lee, W.L., Harrison, R.E., and Grinstein, S. (2003). Phagocytosis by neutrophils. *Microbes Infect* 5, 1299-1306.

Lefort, C.T., Rossaint, J., Moser, M., Petrich, B.G., Zarbock, A., Monkley, S.J., Critchley, D.R., Ginsberg, M.H., Fässler, R., and Ley, K. (2012). Distinct roles for talin-1 and kindlin-3 in LFA-1 extension and affinity regulation. *Blood* 119.

Lewinsohn, D.M., Bargatze, R.F., and Butcher, E.C. (1987). Leukocyte-endothelial cell recognition: evidence of a common molecular mechanism shared by neutrophils, lymphocytes, and other leukocytes. *J Immunol* 138, 4313-4321.

Lewis, S.M., Williams, A., and Eisenbarth, S.C. (2019). Structure-function of the immune system in the spleen. *Sci Immunol* 4, eaau6085.

Ley, K., Laudanna, C., Cybulsky, M.I., and Nourshargh, S. (2007). Getting to the side of inflammation: the leukocyte adhesion cascade updated. *Nat Rev Immunol* 7, 678-689.

Ley, K., Tedder, T.F., and Kansas, G.S. (1993). L-selectin can mediate leukocyte rolling in untreated mesenteric venules in vivo independent of E- and P-selectin. *Blood* 82, 1632-1638.

Li, X., Klintman, D., Weitz-Schmidt, G., Schramm, R., and Thorlacius, H. (2004). Lymphocyte function antigen-1 mediates leukocyte adhesion and subsequent liver damage in endotoxemic mice. *Br J Pharmacol* 141, 709-716.

- Liapakis, G., Chan, W.C., Papadokostaki, M., and Javitch, J.A. (2004). Synergistic contributions of the functional groups of epinephrine to its affinity and efficacy at the beta2 adrenergic receptor. *Mol Pharmacol* 65, 1181-1190.
- Linsell, C.R., Lightman, S.L., Mullen, P.E., Brown, M.J., and Causon, R.C. (1985). Circadian rhythms of epinephrine and norepinephrine in man. *J Clin Endocrinol Metab* 60, 1210-1215.
- Lo, C.G., Lu, T.T., and Cyster, J.G. (2003). Integrin-dependence of lymphocyte entry into the splenic white pulp. *J Exp Med* 197, 353-361.
- Lok, L.S.C., Dennison, T.W., Mahbubani, K.M., Saeb-Parsy, K., Chilvers, E.R., and Clatworthy, M.R. (2019). Phenotypically distinct neutrophils patrol uninfected human and mouse lymph nodes. *Proc Natl Acad Sci U S A* 116, 19083-19089.
- Lorton, D., and Bellinger, D.L. (2015). Molecular mechanisms underlying beta-adrenergic receptor-mediated cross-talk between sympathetic neurons and immune cells. *Int J Mol Sci* 16, 5635-5665.
- Lou, O., Alcaide, P., Lusinskas, F.W., and Muller, W. (2007). CD99 is a key mediator of the transendothelial migration of neutrophils. *J Immunol* 178, 1136-1143.
- Luo, B.-H., Carman, C.V., and Springer, T.A. (2007). Structural Basis of Integrin Regulation and Signaling. *Annu Rev Immunol* 25, 619-647.
- Ma, Q., Jones, D., and Springer, T.A. (1999). The Chemokine Receptor CXCR4 Is Required for the Retention of B Lineage and Granulocytic Precursors within the Bone Marrow Microenvironment. *Immunity* 10, 463-471.
- Maas, S.L., Soehnlein, O., and Viola, J.R. (2018). Organ-Specific Mechanisms of Transendothelial Neutrophil Migration in the Lung, Liver, Kidney, and Aorta. *Front Immunol* 9, 2739.
- Mackay, C.R., Marston, W.L., and Dudler, L. (1990). Naive and memory T cells show distinct pathways of lymphocyte recirculation. *J Exp Med* 171, 801-817.
- Madden, K.S., Bellinger, D.L., Felten, S.Y., Snyder, E., Maida, M.E., and Felten, D.L. (1997). Alterations in sympathetic innervation of thymus and spleen in aged mice. *Mech Ageing Dev* 94, 165-175.
- Maisel, A.S., Fowler, P., Rearden, A., Motulsky, H.J., and Michel, M.C. (1989). A new method for isolation of human lymphocyte subsets reveals differential regulation of beta-adrenergic receptors by terbutaline treatment. *Clin Pharmacol Ther* 46, 429-439.
- Mandala, S., Hajdu, R., Bergstrom, J., Quackenbush, E., Xie, J., Milligan, J., Thornton, R., Shei, G.-J., Card, D., Keohane, C., *et al.* (2002). Alteration of lymphocyte trafficking by sphingosine-1-phosphate receptor agonist. *Science* 296, 346-349.
- Margaryan, S., Hyusyan, A., Martirosyan, A., Sargsian, S., and Manukyan, G. (2017). Differential modulation of innate immune response by epinephrine and estradiol. *Horm Mol Biol Clin Investig* 30.
- Marino, F., Scanzano, A., Pulze, L., Pinoli, M., Rasini, E., Luini, A., Bombelli, R., Legnaro, M., de Eguileor, M., and Cosentino, M. (2018).  $\beta$  2 -Adrenoceptors inhibit neutrophil extracellular traps in human polymorphonuclear leukocytes. *J Leukoc Biol* 104, 603-614.

Martin, C.A., Burdon, P.C.E., Bridger, G., Gutierrez-Ramos, J.C., Williams, T.J., and Rankin, S.M. (2003). Chemokines acting via CXCR2 and CXCR4 control the release of neutrophils from the bone marrow and their return following senescence. *Immunity* 19, 583-593.

Masanori, Inamasu, Tetsuya, Totsuka, Tomihiro, Ikeo, Taku, Nagao, Shigeyuki, and Takeyama (1987). Beta1-adrenergic selectivity of the new cardiostimulant denopamine in its stimulating effects on adenylate cyclase. *Biochem Pharmacol* 36, 1947-1954.

Massberg, S., Schaerli, P., Knezevic-Maramica, I., Köllnberger, M., Tubo, N., Moseman, E.A., Huff, I.V., Junt, T., Wagers, A.J., Mazo, I.B., *et al.* (2007). Immunosurveillance by hematopoietic progenitor cells trafficking through blood, lymph, and peripheral tissues. *Cell* 131, 994-1008.

Matloubian, M., Lo, C.G., Cinamon, G., Lesneski, M.J., Xu, Y., Brinkmann, V., Allende, M.L., Proia, R.L., and Cyster, J.G. (2004). Lymphocyte egress from thymus and peripheral lymphoid organs is dependent on S1P receptor 1. *Nature* 427, 355-360.

Maus, U.A., Waelsch, K., Kuziel, W.A., Delbeck, T., Mack, M., Blackwell, T.S., Christman, J.W., Schlöndorff, D., Seeger, W., and Lohmeyer, J. (2003). Monocytes are potent facilitators of alveolar neutrophil emigration during lung inflammation: a role of the CCL2-CCR2 axis. *J Immunol* 170, 3273-3278.

Mayadas, T.N., Johnson, R.C., Rayburn, H., Hynes, R.O., and Wagner, D.D. (1993). Leukocyte rolling and extravasation are severely compromised in P selectin-deficient mice. *Cell* 74, 541-554.

McDonald, B., McAvoy, E.F., Lam, F., Gill, V., de la Motte, C., Savani, R.C., and Kubes, P. (2008). Interaction of CD44 and hyaluronan is the dominant mechanism for neutrophil sequestration in inflamed liver sinusoids. *J Exp Med* 205, 915-927.

McEver, R.P., Beckstead, J.H., Moore, K.L., Marshall-Carlson, L., and Bainton, D.F. (1989). GMP-140, a platelet alpha-granule membrane protein, is also synthesized by vascular endothelial cells and is localized in Weibel-Palade bodies. *J Clin Invest* 84, 92-99.

Mebius, R.E., and Kraal, G. (2005). Structure and function of the spleen. *Nat Rev Immunol* 5, 606-616.

Medvinsky, A., and Dzierzak, E. (1996). Definitive hematopoiesis is autonomously initiated by the AGM region. *Cell* 86, 897-906.

Mendez-Ferrer, S., Lucas, D., Battista, M., and Frenette, P.S. (2008). Haematopoietic stem cell release is regulated by circadian oscillations. *Nature* 452, 442-447.

Michel-Reher, M.B., and Michel, M.C. (2013). Agonist-induced desensitization of human beta3-adrenoceptors expressed in human embryonic kidney cells. *Naunyn Schmiedebergs Arch Pharmacol* 386, 843-851.

Mohamadzadeh, M., DeGrendele, H., Arizpe, H., Estess, P., and Siegelman, M. (1998). Proinflammatory stimuli regulate endothelial hyaluronan expression and CD44/HA-dependent primary adhesion. *J Clin Invest* 101, 97-108.

Moore, K.L. (1998). Structure and function of P-selectin glycoprotein ligand-1. *Leuk Lymphoma* 29, 1-15.

- Mori, A., Miwa, T., Sakamoto, K., Nakahara, T., and Inshii, K. (2010). Pharmacological evidence for the presence of functional beta(3)-adrenoceptors in rat retinal blood vessels. *Naunyn Schmiedebergs Arch Pharmacol* *382*, 119-126.
- Müller, A.M., Medvinsky, A., Strouboulis, J., Grosveld, F., and Dzierzak, E. (1994). Development of hematopoietic stem cell activity in the mouse embryo. *Immunity* *1*, 291-301.
- Muller, W. (2011). Mechanisms of Leukocyte Transendothelial Migration. *Annu Rev Pathol* *6*, 323-344.
- Muller, W., Weigl, S.A., Deng, X., and Phillips, D.M. (1993). PECAM-1 is required for transendothelial migration of leukocytes. *J Exp Med* *178*, 449-460.
- Muller, W.A. (2017). Localized Signals that Regulate Transendothelial Migration. *Curr Opin Immunol* *38*, 24-29.
- Nagasawa, T., Hirota, S., Tachibana, K., Takakura, N., Nishikawa, S., Kitamura, Y., Yoshida, N., Kikutani, H., and Kishimoto, T. (1996). Defects of B-cell lymphopoiesis and bone-marrow myelopoiesis in mice lacking the CXC chemokine PBSF/SDF-1. *Nature* *382*, 635-638.
- Nahmias, C., Blin, N., Elalouf, J.M., Mattei, M.G., Strosberg, A.D., and Emorine, L.J. (1991). Molecular characterization of the mouse beta 3-adrenergic receptor: relationship with the atypical receptor of adipocytes. *The EMBO Journal* *10*, 3721-3727.
- Nakai, A., Hayano, Y., Furuta, F., Noda, M., and Suzuki, K. (2014). Control of lymphocyte egress from lymph nodes through beta2-adrenergic receptors. *J Exp Med* *211*, 2583-2598.
- Nance, D.M., and Sanders, V.M. (2007). Autonomic innervation and regulation of the immune system (1987-2007). *Brain Behav Immun* *21*, 736-745.
- Nantel, F., Bonin, H., Emorine, L.J., Zilberfarb, V., Strosberg, A.D., Bouvier, M., and Marullo, S. (1993). The human beta 3-adrenergic receptor is resistant to short term agonist-promoted desensitization. *Mol Pharmacol* *43*, 548-555.
- Naor, D., Sionov, R.V., and Ish-Shalom, D. (1997). CD44: structure, function, and association with the malignant process. *Adv Cancer Res* *71*, 241-319.
- Nemeth, E., Baird, A.W., and O'Farrelly, C. (2009). Microanatomy of the liver immune system. *Semin Immunopathol* *31*, 333-343.
- Ng, L.G., Ostuni, R., and Hidalgo, A. (2019). Heterogeneity of neutrophils. *Nat Rev Immunol* *19*, 255-265.
- Nicholls, A.J., Wen, S.W., Hall, P., Hickey, M.J., and Wong, C.H.Y. (2018). Activation of the sympathetic nervous system modulates neutrophil function. *J Leukoc Biol* *103*, 295-309.
- Nolte, M.A., Hamann, A., Kraal, G., and Mebius, R.E. (2002). The strict regulation of lymphocyte migration of splenic white pulp does not involve common homing receptors. *Immunology* *106*, 299-307.

nomenclature, I.U.o.I.S.W.H.O.S.o.c. (2001). Chemokine/chemokine receptor nomenclature. *J Leukoc Biol* 70, 465-466.

Nourshargh, S., and Alon, R. (2014). Leukocyte migration into inflamed tissues. *Immunity*.

Nourshargh, S., Renshaw, S.A., and Imhof, B.A. (2016). Reverse migration of neutrophils: Where, when, how, and why? *Trends Immunol* 37, 273-286.

Novotny, M., Quaiserova-Mocko, V., Wehrwein, E.A., Kreulen, D.L., and Swain, G.M. (2007). Determination of Endogenous Norepinephrine Levels in Different Chambers of the Rat Heart by Capillary Electrophoresis Coupled with Amperometric Detection. *J Neurosci Methods* 163, 52-59.

O'Hayre, M., Eichel, K., Avino, S., Zhao, X., Steffen, D.J., Feng, X., Kawakami, K., Aoki, J., Messer, K., Sunahara, R.K., *et al.* (2017). Genetic evidence that  $\beta$ -arrestins are dispensable for the initiation of  $\beta$  2-adrenergic receptor signaling to ERK. *Sci Signal* 10.

Oberlin, E., Fleury, M., Clay, D., Petit-Cocault, L., Candelier, J.-J., Mennesson, B., Jaffredo, T., and Souyri, M. (2010). VE-cadherin expression allows identification of a new class of hematopoietic stem cells within human embryonic liver. *Blood* 116, 4444-4455.

Okada, T., Ngo, V.N., Ekland, E.H., Forster, R., Lipp, M., Littman, D.R., and Cyster, J.G. (2002). Chemokine requirements for B cell entry to lymph nodes and Peyer's patches. *J Exp Med* 196, 65-75.

Okeke, K., Angers, S., Bouvier, M., and Michel, M.C. (2019). Agonist-induced desensitisation of  $\beta$ 3-adrenoceptors: Where, when, and how? *Br J Pharmacol* 176, 2539-2558.

Olson, T.S., and Ley, K. (2002). Chemokines and chemokine receptors in leukocyte trafficking. *Am J Physiol Regul Integr Comp Physiol* 283, R7-28.

Ostermann, G., Weber, K.S.C., Zerneck, A., Schröder, A., and Weber, C. (2002). JAM-1 is a ligand of the  $\beta$ 2 integrin LFA-1 involved in transendothelial migration of leukocytes. *Nature Immunology* 3, 151-158.

Panuncio, A.L., De la Peña, S., Gualco, G., and Reissenweber, N. (2002). Adrenergic innervation in reactive human lymph nodes. *J Anat*.

Papayannopoulos, V. (2018). Neutrophil extracellular traps in immunity and disease. *Nat Rev Immunol* 18, 134-147.

Park, C., Hwang, I.-Y., Sinha, R.K., Kamenyeva, O., Davis, M.D., and Kehrl, J.H. (2012). Lymph node B lymphocyte trafficking is constrained by anatomy and highly dependent upon chemoattractant desensitization. *Blood* 119, 978-989.

Patrick, A.L., Rullo, J., Beaudin, S., Liaw, P., and Fox-Robichaud, A.E. (2007). Hepatic leukocyte recruitment in response to time-limited expression of TNF-alpha and IL-1beta. *Am J Physiol Gastrointest Liver Physiol* 293, G663-672.

Pham, T.H.M., Okada, T., Matloubian, M., Lo, C.G., and Cyster, J.G. (2008). S1P1 receptor signaling overrides retention mediated by G alpha i-coupled receptors to promote T cell egress. *Immunity* 28, 122-133.

- Phillipson, M., Heit, B., Parsons, S.A., Petri, B., Mullaly, S.C., Colarusso, P., Gower, R.M., Neely, G., Simon, S.I., and Kubes, P. (2009). Vav1 is essential for mechanotactic crawling and migration of neutrophils out of the inflamed microvasculature. *J Immunol* *182*, 6870-6878.
- Pick, R., He, W., Chen, C.S., and Scheiermann, C. (2019). Time-of-Day-Dependent Trafficking and Function of Leukocyte Subsets. *Trends Immunol* *40*, 524-537.
- Pierce, K.L., Premont, R.T., and Lefkowitz, R.J. (2002). Seven-transmembrane receptors. *Nat Rev Mol Cell Biol* *3*, 639-650.
- Pillay, J., den Braber, I., Vrisekoop, N., Kwast, L.M., de Boer, R.J., Borghans, A.M., Tesselaar, K., and Koenderman, L. (2010). In vivo labeling with <sup>2</sup>H<sub>2</sub>O reveals a human neutrophil lifespan of 5.4 days. *Blood* *116*, 625-627.
- Pongratz, G., and Straub, R.H. (2014). The sympathetic nervous response in inflammation. *Arthritis Res Ther* *16*.
- Pott, C., Brixius, K., Bundkirchen, A., Bölk, B., Bloch, W., Steinritz, D., Mehlhorn, U., and Schwinger, R.H.G. (2003). The preferential beta3-adrenoceptor agonist BRL 37344 increases force via beta1-/beta2-adrenoceptors and induces endothelial nitric oxide synthase via beta3-adrenoceptors in human atrial myocardium. *Br J Pharmacol* *138*, 521-529.
- Puga, I., Cols, M., Barra, C.M., He, B., Cassis, L., Gentile, M., Comerma, L., Chorny, A., Shan, M., Xu, W., *et al.* (2011). B cell-helper neutrophils stimulate the diversification and production of immunoglobulin in the marginal zone of the spleen. *Nat Immunol* *13*, 170-180.
- Radojcic, T., Baird, S., Darko, D., Smith, D., and Bulloch, K. (1991). Changes in beta-adrenergic receptor distribution on immunocytes during differentiation: an analysis of T cells and macrophages. *J Neurosci Res* *30*, 328-335.
- Rasmussen, S.G., DeVree, B.T., Zou, Y., Kruse, A.C., Chung, K.Y., Kobilka, T.S., Thian, F.S., Chae, P.S., Pardon, E., Calinski, D., *et al.* (2011). Crystal structure of the beta2 adrenergic receptor-Gs protein complex. *Nature* *477*, 549-555.
- Reutershan, J., Morris, M.A., Burcin, T.L., Smith, D.F., Chang, D., Saprito, M.S., and Ley, K. (2006). Critical role of endothelial CXCR2 in LPS-induced neutrophil migration into the lung. *J Clin Invest* *116*, 695-702.
- Rodriguez-Pallares, J., Parga, J.A., Muñoz, A., Guerra, M.J., and Labandeira-Garcia, J.L. (2007). Mechanism of 6-hydroxydopamine neurotoxicity: the role of NADPH oxidase and microglial activation in 6-hydroxydopamine-induced degeneration of dopaminergic neurons. *J Neurochem* *103*, 145-156.
- Rosas-Ballina, M., Olofsson, P.S., Ochani, M., Valdés-Ferrer, S.I., Levine, Y.A., Reardon, C., Tusche, M.W., Pavlov, V.A., Andersson, U., Chavan, S., *et al.* (2011). Acetylcholine-synthesizing T cells relay neural signals in a vagus nerve circuit. *Science* *334*, 98-101.
- Rosen, S.D. (2004). Ligands for L-selectin: homing, inflammation, and beyond. *Annu Rev Immunol* *22*, 129-156.

Salmi, M., Tohka, S., Berg, E.L., Butcher, E.C., and Jalkanen, S. (1997). Vascular adhesion protein 1 (VAP-1) mediates lymphocyte subtype-specific, selectin-independent recognition of vascular endothelium in human lymph nodes. *J Exp Med* *186*, 589-600.

Salmi, M., Yegutkin, G.G., Lehtonen, R., Koskinen, K., Salminen, T., and Jalkanen, S. (2001). A cell surface amine oxidase directly controls lymphocyte migration. *Immunity* *14*, 265-276.

Sanders, V.M., Baker, R.A., Ramer-Quinn, D.S., Kasprovicz, D.J., Fuchs, B.A., and Street, N.E. (1997). Differential expression of the beta2-adrenergic receptor by Th1 and Th2 clones: implications for cytokine production and B cell help. *J Immunol* *158*, 4200-4210.

Sauerbier, I., and von Mayersbach, H. (1977). Circadian variation of catecholamines in human blood. *Horm Metab Res* *9*, 529-530.

Scanzano, A., Schembri, L., Rasini, E., Luini, A., Dallatorre, J., Legnaro, M., Bombelli, R., Congiu, T., Cosentino, M., and Marino, F. (2015). Adrenergic modulation of migration, CD11b and CD18 expression, ROS and interleukin-8 production by human polymorphonuclear leukocytes. *Inflamm Res* *64*, 127-135.

Scheiermann, C., Kunisaki, Y., Lucas, D., Chow, A., Jang, J.E., Zhang, D., Hashimoto, D., Merad, M., and Frenette, P.S. (2012). Adrenergic nerves govern circadian leukocyte recruitment to tissues. *Immunity* *37*, 290-301.

Schena, G., and Caplan, M.J. (2019). Everything You Always Wanted to Know about beta3-AR\* (\*But Were Afraid to Ask). *Cells* *8*.

Schenkel, A.R., Mamdouh, Z., Chen, X., Liebman, R.M., and Muller, W. (2002). CD99 plays a major role in the migration of monocytes through endothelial junctions. *Nat Immunol* *3*, 143-150.

Schürpf, T., and Springer, T.A. (2011). Regulation of integrin affinity on cell surfaces. *EMBO J* *30*, 4712-4727.

Semerad, C.L., Christopher, M.J., Liu, F., Short, B., Simmons, P.J., Winkler, I., Levesque, J.-P., Chappel, J., Ross, F.P., and Link, D.C. (2005). G-CSF potently inhibits osteoblast activity and CXCL12 mRNA expression in the bone marrow. *Blood* *106*, 3020-3027.

Semerad, C.L., Liu, F., Gregory, A.D., Stumpf, K., and Link, D.C. (2002). G-CSF is an essential regulator of neutrophil trafficking from the bone marrow to the blood. *Immunity* *17*, 413-423.

Seseke, F.G., Gardemann, A., and Jungermann, K. (1992). Signal propagation via gap junctions, a key step in the regulation of liver metabolism by the sympathetic hepatic nerves. *FEBS letters* *301*, 265-270.

Shaw, S.K., Bamba, P.S., Perkins, B.N., and Lusinskas, F.W. (2001). Real-time imaging of vascular endothelial-cadherin during leukocyte transmigration across endothelium. *J Immunol* *167*, 2323-2330.

Shenoy, S.K., Drake, M.T., Nelson, C.D., Houtz, D.A., Xiao, K., Madabushi, S., Reiter, E., Premont, R.T., Lichtarge, O., and Lefkowitz, R.J. (2006). beta-arrestin-dependent, G protein-independent ERK1/2 activation by the beta2 adrenergic receptor. *J Biol Chem* *281*, 1261-1273.

Staedtke, V., Bai, R.-Y., Kim, K., Darvas, M., Davila, M.L., Riggins, G.J., Rothman, P.B., Papadopoulos, N., Kinzler, K.W., Vogelstein, B., *et al.* (2018). Disruption of a self-amplifying catecholamine loop reduces cytokine release syndrome. *Nature* 564, 273-277.

Stanley, B.G., Schwartz, D.H., Hernandez, L., Hoebel, B.G., and Leibowitz, S.F. (1989). Patterns of extracellular norepinephrine in the paraventricular hypothalamus: relationship to circadian rhythm and deprivation-induced eating behavior. *Life Sci* 45, 275-282.

Staunton, D.E., Dustin, M.L., and Springer, T.A. (1989). Functional cloning of ICAM-2, a cell adhesion ligand for LFA-1 homologous to ICAM-1. *Nature* 339, 61-64.

Steinhoff, G., Behrend, M., Schrader, B., Duijvestijn, A.M., and Wonigeit, K. (1993). Expression patterns of leukocyte adhesion ligand molecules on human liver endothelia. Lack of ELAM-1 and CD62 inducibility on sinusoidal endothelia and distinct distribution of VCAM-1, ICAM-1, ICAM-2, and LFA-3. *Am J Pathol* 142, 481-488.

Steiniger, B.S. (2015). Human spleen microanatomy: why mice do not suffice. *Immunology* 145, 334-346.

Stevenson, J.R., Westermann, J., Liebmann, P.M., Hortner, M., Rinner, I., Felsner, P., Wolfler, A., and Schauenstein, K. (2001). Prolonged alpha-adrenergic stimulation causes changes in leukocyte distribution and lymphocyte apoptosis in the rat. *J Neuroimmunol* 120, 50-57.

Streeter, P.R., Berg, E.L., Rouse, B.T., Bargatze, R.F., and Butcher, E.C. (1988). A tissue-specific endothelial cell molecule involved in lymphocyte homing. *Nature* 331, 41-46.

Strieter, R.M., Keane, M.P., Burdick, M.D., Sakkour, A., Murray, L.A., and Belperio, J.A. (2005). The role of CXCR2/CXCR2 ligands in acute lung injury. *Curr Drug Targets Inflamm Allergy* 4, 299-303.

Susulic, V.S., Frederich, R.C., KLawitts, J., Tozzo, E., Kahn, B.B., Harper, M.E., Himms-Hagen, J., Flier, J.S., and Lowell, B.B. (1995). Targeted disruption of the beta 3-adrenergic receptor gene. *J Biol Chem* 270, 29483-29492.

Suzuki, K., Hayano, Y., Nakai, A., Furuta, F., and Noda, M. (2016). Adrenergic control of the adaptive immune response by diurnal lymphocyte recirculation through lymph nodes. *J Exp Med* 213, 2567-2574.

Tabarowski, Z., Gibson-Berry, K., and Felten, S.Y. (1996). Noradrenergic and peptidergic innervation of the mouse femur bone marrow. *Acta Histochem* 98, 453-457.

Tadayon, S., Dunkel, J., A., T., Halle, O., Karikoski, M., Gerke, H., Rantakari, P., Virtakoivu, R., Pabst, O., Salmi, M., *et al.* (2019). Clever-1 contributes to lymphocyte entry into the spleen via the red pulp. *Sci Immunol* 4.

Takagi, J., Petre, B.M., Walz, T., and Springer, T.A. (2002). Global conformational rearrangements in integrin extracellular domains in outside-in and inside-out signaling. *Cell* 110, 599-511.

Takasu, T., Ukai, M., Sato, S., Matsui, T., Nagase, I., Maruyama, T., Sasamata, M., Miyata, K., Uchida, H., and Yamaguchi, O. (2007). Effect of (R)-2-(2-aminothiazol-4-yl)-4'-{2-[(2-hydroxy-2-phenylethyl)amino]ethyl} acetanilide (YM178), a novel selective beta3-adrenoceptor agonist, on bladder function. *J Pharmacol Exp Ther* 321, 642-647.

- Takeda, S., Eleftheriou, F., Levasseur, R., Liu, X., Zhao, L., Parker, K.L., Armstrong, D., Ducy, P., and Karsenty, G. (2002). Leptin regulates bone formation via the sympathetic nervous system. *Cell* *111*, 305-317.
- Tank, A.W., and Wong, D.L. (2015). Peripheral and central effects of circulating catecholamines. *Compr Physiol* *5*, 1-15.
- Tong, C.-F., Zhang, Y., Lü, S.-Q., Li, N., Gong, Y.-X., Yang, H., Feng, S.-L., Du, Y., Huang, D.-D., and Long, M. (2018). Binding of intercellular adhesion molecule 1 to  $\beta$  2-integrin regulates distinct cell adhesion processes on hepatic and cerebral endothelium. *Am J Physiol Cell Physiol* *315*, C409-C421.
- Tong, K.Y., Zhao, J., Tse, C.-W., Rong, J., and Au-Yeung, H.Y. (2019). Selective catecholamine detection in living cells by a copper-mediated oxidative bond cleavage. *Chem Sci* *10*, 8519-8526.
- Toubal, A., Nel, I., Lotersztajn, S., and Lehuen, A. (2019). Mucosal-associated invariant T cells and disease. *Nat Rev Immunol* *19*, 643-657.
- Vandamme, J., Castermans, D., and Thevelein, J.M. (2012). Molecular mechanisms of feedback inhibition of protein kinase A on intracellular cAMP accumulation. *Cell Signal* *24*, 1610-1618.
- Venturi, G.M., Tu, L., Kadono, T., Khan, A.I., Fujimoto, Y., Oshel, P., Bock, C.B., Miller, A.S., Albrecht, R.M., Kubes, P., *et al.* (2003). Leukocyte migration is regulated by L-selectin endoproteolytic release. *Immunity* *19*, 713-724.
- von Andrian, U.H., Chambers, J.D., McEnvoy, L.M., Bargatze, R.F., Arfors, K.E., and Butcher, E.C. (1991). Two-step model of leukocyte-endothelial cell interaction in inflammation: distinct roles for LECAM-1 and the leukocyte beta 2 integrins in vivo. *Proc Natl Acad Sci U S A* *88*, 7538-7542.
- von Andrian, U.H., and Mempel, T.R. (2003). Homing and cellular traffic in lymph nodes. *Nat Rev Immunol* *3*, 867-878.
- Wahle, M., Neumann, R.P., Moritz, F., Krause, A., Buttgereit, F., and Baerwald, C.G.O. (2005). Beta2-adrenergic receptors mediate the differential effects of catecholamines on cytokine production of PBMC. *J Interferon Cytokine Res* *25*, 384-394.
- Walcheck, B., Moore, K.L., McEver, R.P., and Kishimoto, T.K. (1996). Neutrophil-neutrophil interactions under hydrodynamic shear stress involve L-selectin and PSGL-1. A mechanism that amplifies initial leukocyte accumulation of P-selectin in vitro. *J Clin Invest* *98*, 1081-1087.
- Wang, J. (2018). Neutrophils in tissue injury and repair. *Cell Tissue Res* *371*, 531-539.
- Wang, J., Hossain, M., Thanabalasuriar, A., Gunzer, M., Meininger, C., and Kubes, P. (2017). Visualizing the function and fate of neutrophils in sterile injury and repair. *Science* *358*, 111-116.
- Westfall, T.C. (2009). Sympathomimetic Drugs and Adrenergic Receptor Antagonists. In *Encyclopedia of Neuroscience* (Academic Press), pp. 685-695.
- Wiggs, B.R., English, D., Quinlan, W.M., Doyle, N.A., Hogg, J.C., and Doerschuk, C.M. (1994). Contributions of capillary pathway size and neutrophil deformability to neutrophil transit through rabbit lungs. *J Appl Physiol* *77*, 463-470.

- Williams, J.M., and Felten, D.L. (1981). Sympathetic innervation of murine thymus and spleen: a comparative histofluorescence study. *Anat Rec* 199, 531-542.
- Wisse, E. (1972). An ultrastructural characterization of the endothelial cell in the rat liver sinusoid under normal and various experimental conditions, as a contribution to the distinction between endothelial and Kupffer cells. *J Ultrastruct Res* 38, 528-562.
- Wong, J., Johnston, B., Lee, S.S., Bullard, D.C., Smith, C.W., Beaudet, A.L., and Kubes, P. (1997). A minimal role for selectins in the recruitment of leukocytes into the inflamed liver microvasculature. *J Clin Invest* 99, 2782-2790.
- Yang, J., Hirata, T., Croce, K., Merrill-Skoloff, G., Tchernychev, B., Williams, E., Flaumenhaft, R., Furie, B.C., and Furie, B. (1999). Targeted gene disruption demonstrates that P-selectin glycoprotein ligand 1 (PSGL-1) is required for P-selectin-mediated but not E-selectin-mediated neutrophil rolling and migration. *J Exp Med* 190, 1769-1782.
- Yi, C.-X., la Fleur, S.E., Fliers, E., and Kalsbeek, A. (2010). The role of the autonomic nervous liver innervation in the control of energy metabolism. *BBA - Molecular Basis of Disease* 1802, 416-431.
- Yin, C., and Heit, B. (2018). Armed for destruction: formation, function and trafficking of neutrophil granules. *Cell Tissue Res* 371, 455-471.
- Yipp, B.G., Kim, J.H., Lima, R., Zbytniuk, L.D., Petri, B., Swanlund, N., Ho, M., Szeto, V.G., Tak, T., Koenderman, L., *et al.* (2017). The lung is a host defense niche for immediate neutrophil-mediated vascular protection. *Sci Immunol* 2.
- Yuan, Y., Wu, S., Li, W., and He, W. (2020). A Tissue-Specific Rhythmic Recruitment Pattern of Leukocyte Subsets. *Front Immunol* 11.
- Yukawa, T., Ukena, D., Kroegel, C., Chanez, P., Dent, G., Chung, K.F., and Barnes, P.J. (1990). Beta 2-adrenergic receptors on eosinophils. Binding and functional studies. *Am Rev Respir Dis* 141, 1446-1452.
- Zeisel, A., Hochgerner, H., Lönnerberg, P., Johnsson, A., Memic, F., van der Zwan, J., Häring, M., Braun, E., Borm, L.E., La Manno, G., *et al.* (2018). Molecular Architecture of the Mouse Nervous System. *Cell* 174, 999-1014.
- Zeng, J., Eljalby, M., Aryal, R.P., Lehoux, S., Stavenhagen, K., Kudelka, M.R., Wang, Y., Wang, J., Ju, T., von Andrian, U.H., *et al.* (2020). Cosmc controls B cell homing. *Nat Commun* 11, 3990.



## 6 Appendix

### 6.1 The SNS influences other circulating leukocyte subsets

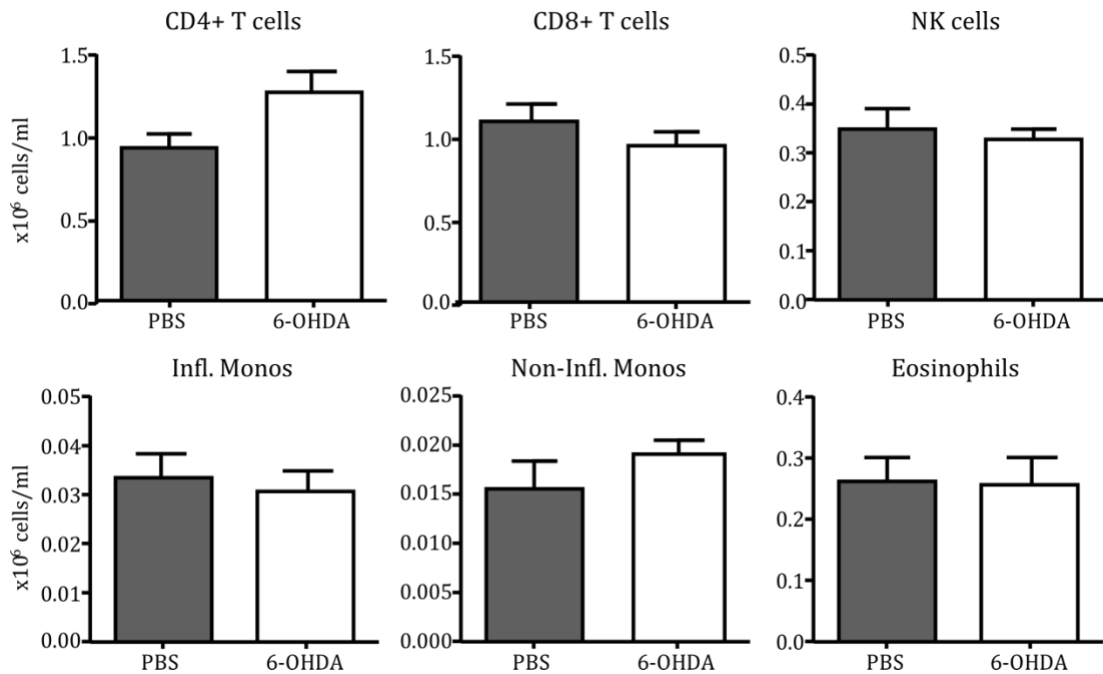


**Figure 6-1: Effects of absence of sympathetic signaling on circulating leukocyte numbers.**

Leukocyte numbers in blood after ablation of the sympathetic tone during the day. WT mice were injected with PBS (gray) or 6-hydroxydopamine (6-OHDA, white) on day zero and day two, blood was harvested at 12 pm on day five of the treatment. n = 5, student's t-test. NK cells = Natural Killer cells, Infl. Monos = Inflammatory Monocytes, Non-Infl. Monos = Non-Inflammatory Monocytes.

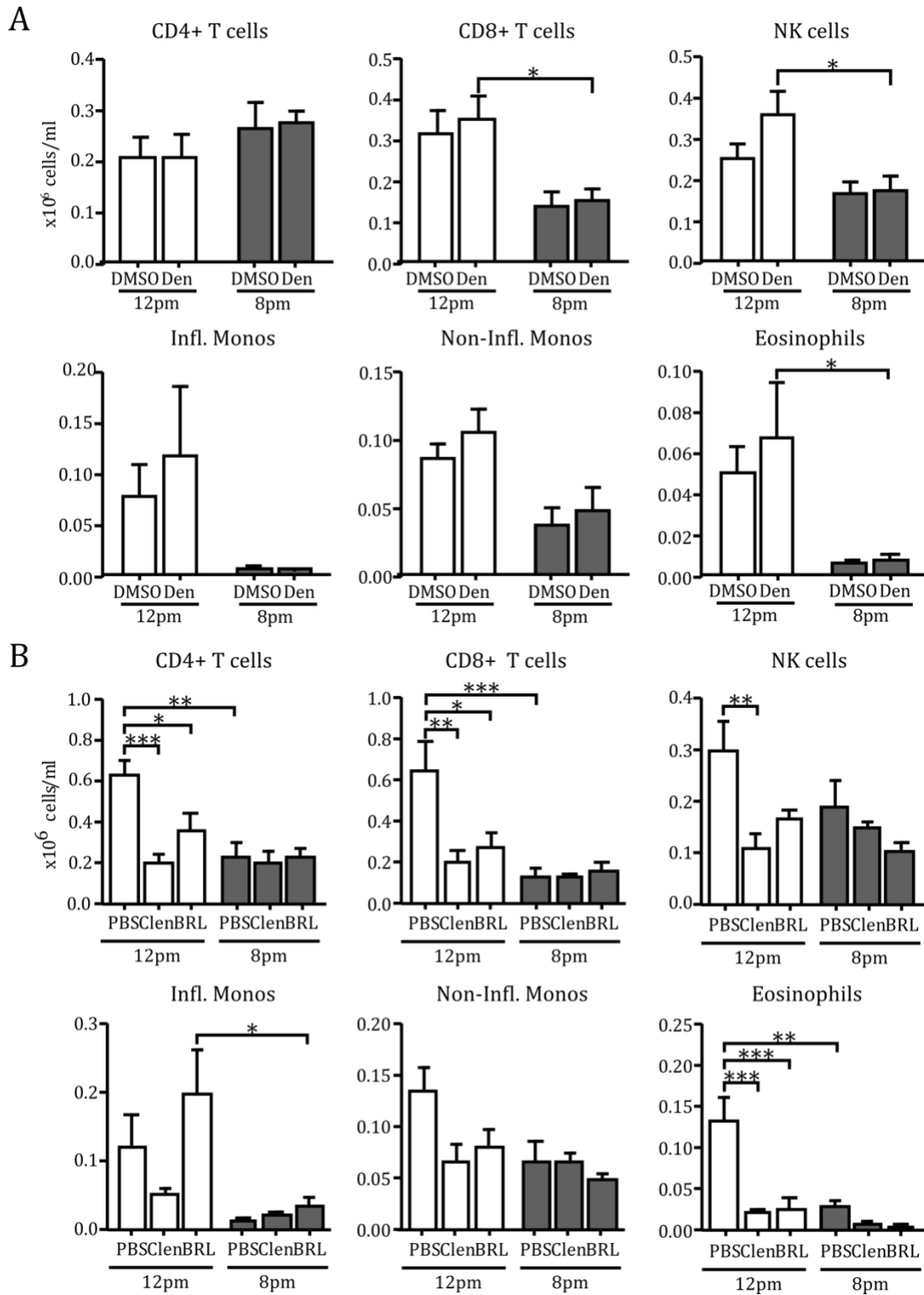


**Figure 6-2: Changes in blood leukocyte numbers are mediated by  $\beta_2$ - and  $\beta_3$ -ARs.** (A) Leukocyte counts in blood upon stimulation of  $\beta_1$ -ARs. WT mice were injected with DMSO or Denopamine (Den) 2hrs prior to harvest at 12 pm (white) or 8 pm (gray). n = 6, two-way ANOVA, Tukey's test. (B) Leukocyte counts in blood upon stimulation of  $\beta_2$ - and  $\beta_3$ -ARs. WT mice were injected with PBS, Clenbuterol (Clen) or BRL37344 (BRL) 2hrs prior to harvest at 12 pm (white) or 8 pm (gray). n = 5-6, two-way ANOVA, Tukey's test. NK cells = Natural Killer cells, Infl. Monos = Inflammatory Monocytes, Non-Infl. Monos = Non-Inflammatory Monocytes.

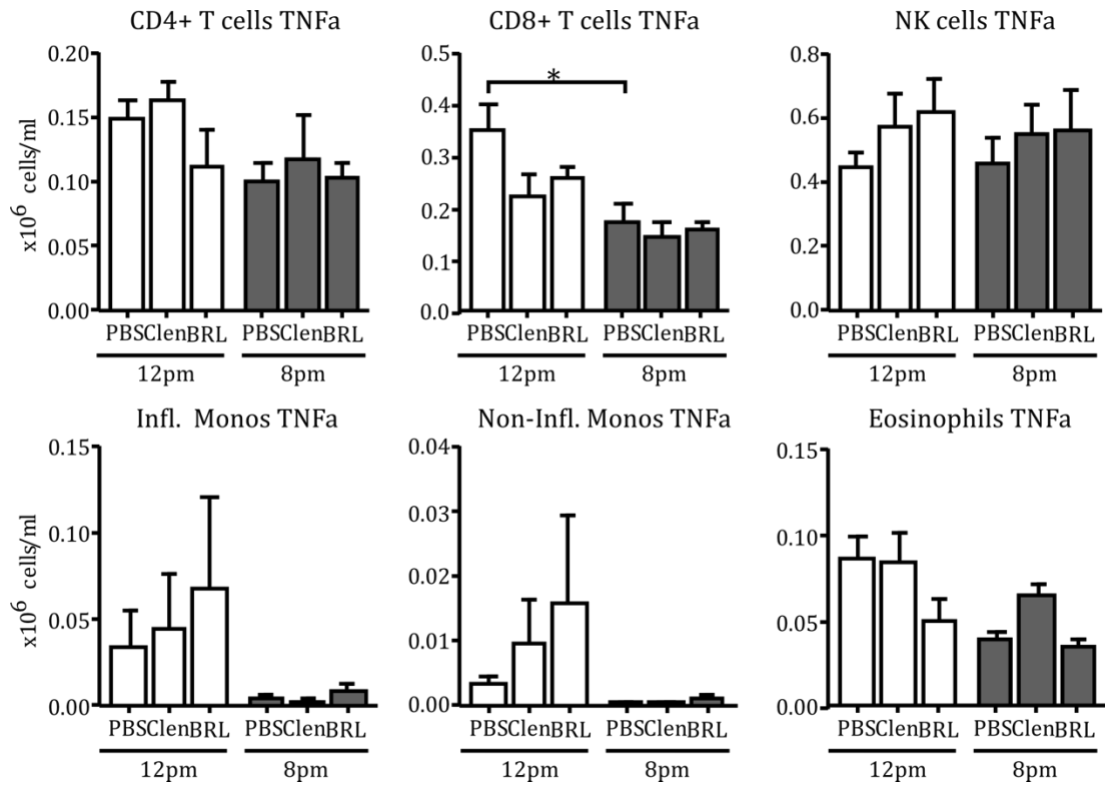


**Figure 6-3: Leukocyte counts upon adrenergic stimulation during inflammation.** Cell counts in blood upon stimulation of  $\beta_2$ - and  $\beta_3$ -ARs under inflammation. WT mice received TNF $\alpha$  and PBS or the adrenergic agonists. Blood was harvested at 12 pm (white) or 8 pm (gray). n = 5-6, two-way ANOVA, Tukey's test. NK cells = Natural Killer cells, Infl. Monos = Inflammatory Monocytes, Non-Infl. Monos = Non-Inflammatory Monocytes.

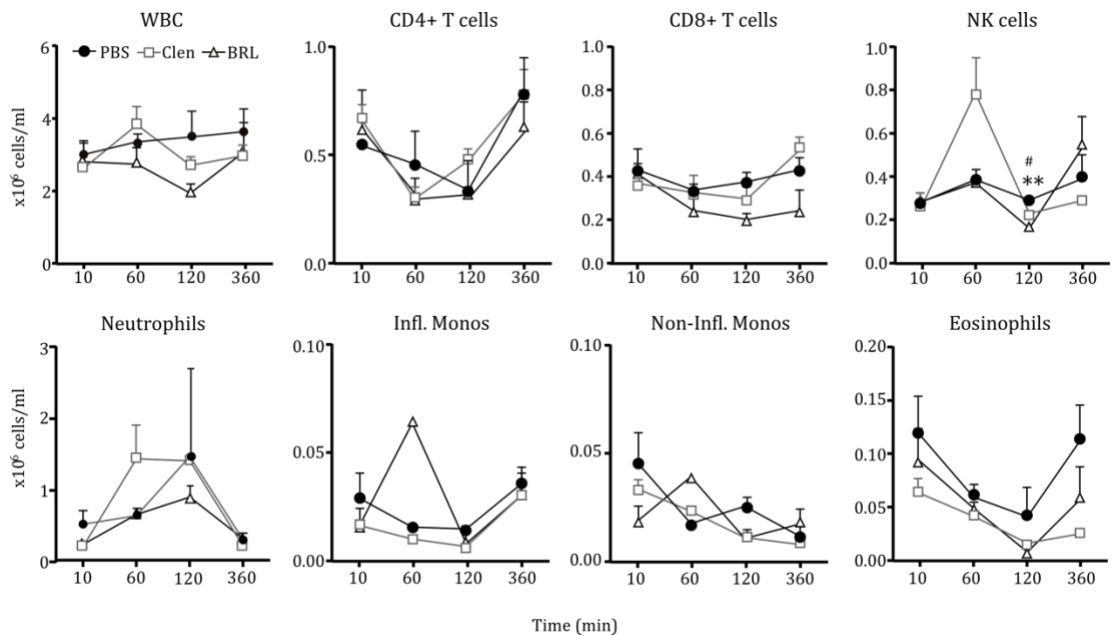


**Figure 6-4: Time course of harvest time after adrenergic stimulation.** Cell counts in blood after different times between injection and harvest. n = 3, one-way ANOVA, Dunnett's test, \* test of Clen against PBS, # test of BRL against PBS. NK cells = Natural Killer cells, Infl. Monos = Inflammatory Monocytes, Non-Infl. Monos = Non-Inflammatory Monocytes.

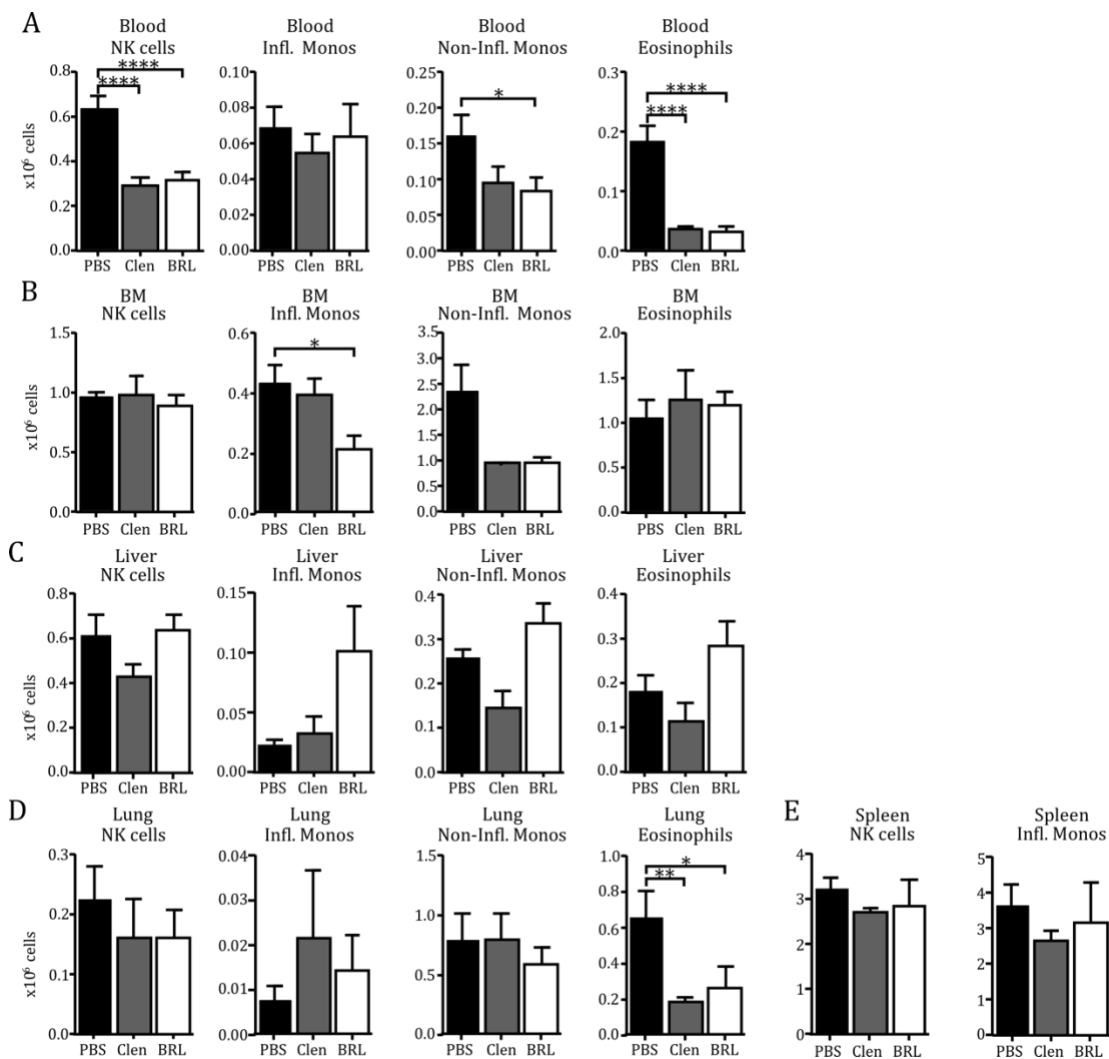


**Figure 6-5: Endogenous myeloid cell numbers in various organs upon adrenergic stimulation.**

**(A)** Endogenous myeloid cell counts in blood, two hours after stimulation with Clenbuterol (Clen) or BRL37344 (BRL). n = 5-39, one-way ANOVA, Dunnett's test. **(B)** Endogenous myeloid cell counts in the bone marrow (BM), 2 hrs after stimulation with Clen or BRL. n = 5-6, one-way ANOVA, Dunnett's test. **(C)** Endogenous myeloid cell counts in the liver, 2 hrs after stimulation with Clen or BRL. n = 5-6, one-way ANOVA, Dunnett's test. **(D)** Endogenous myeloid cell counts in the lung, 2 hrs after stimulation with Clen or BRL. n = 5-6, one-way ANOVA, Dunnett's test. **(E)** Endogenous myeloid cell counts in the spleen, 2 hrs after stimulation with Clen or BRL. n = 5-6, one-way ANOVA, Dunnett's test. NK cells = Natural Killer cells, Infl. Monos = Inflammatory Monocytes, Non-Infl. Monos = Non-Inflammatory Monocytes.

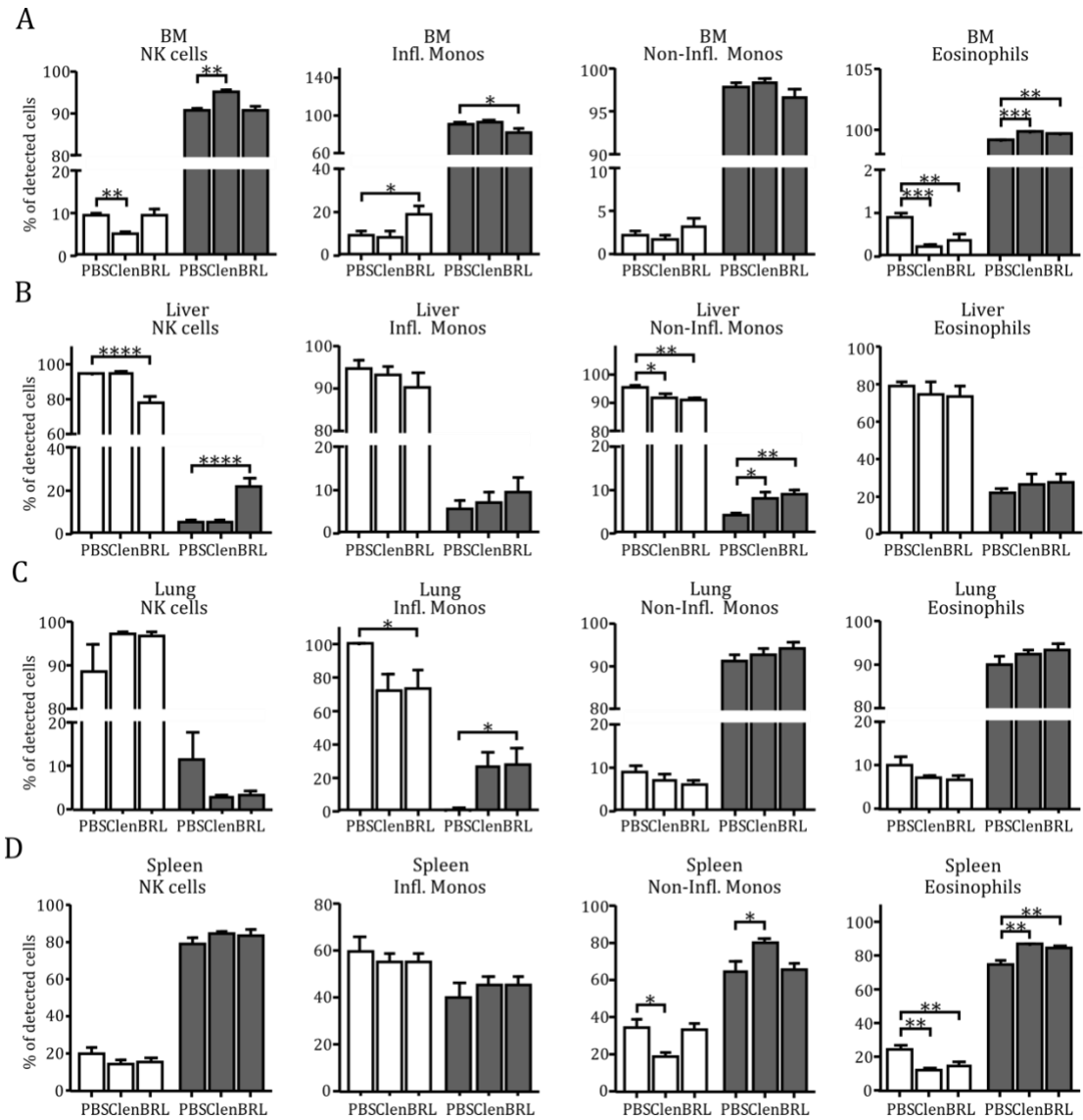


**Figure 6-6: Ratios of intra- and extravascular endogenous myeloid cells in various organs upon adrenergic stimulation.**

**(A)** Intravascular (white) and extravascular (gray) endogenous myeloid cells in the bone marrow (BM) as percentage of the detected cells in this organ.  $n = 5-6$ , two-way ANOVA, Dunnett's test. **(B)** Intravascular (white) and extravascular (gray) endogenous myeloid cells in the liver as percentage of the detected cells in this organ.  $n = 5-6$ , two-way ANOVA, Dunnett's test. **(C)** Intravascular (white) and extravascular (gray) endogenous myeloid cells in the lung as percentage of the detected cells in this organ.  $n = 5-6$ , two-way ANOVA, Dunnett's test. **(D)** Intravascular (white) and extravascular (gray) endogenous myeloid cells in the spleen as percentage of the detected cells in this organ.  $n = 5-6$ , two-way ANOVA, Dunnett's test. NK cells = Natural Killer cells, Infl. Monos = Inflammatory Monocytes, Non-Infl. Monos = Non-Inflammatory Monocytes.

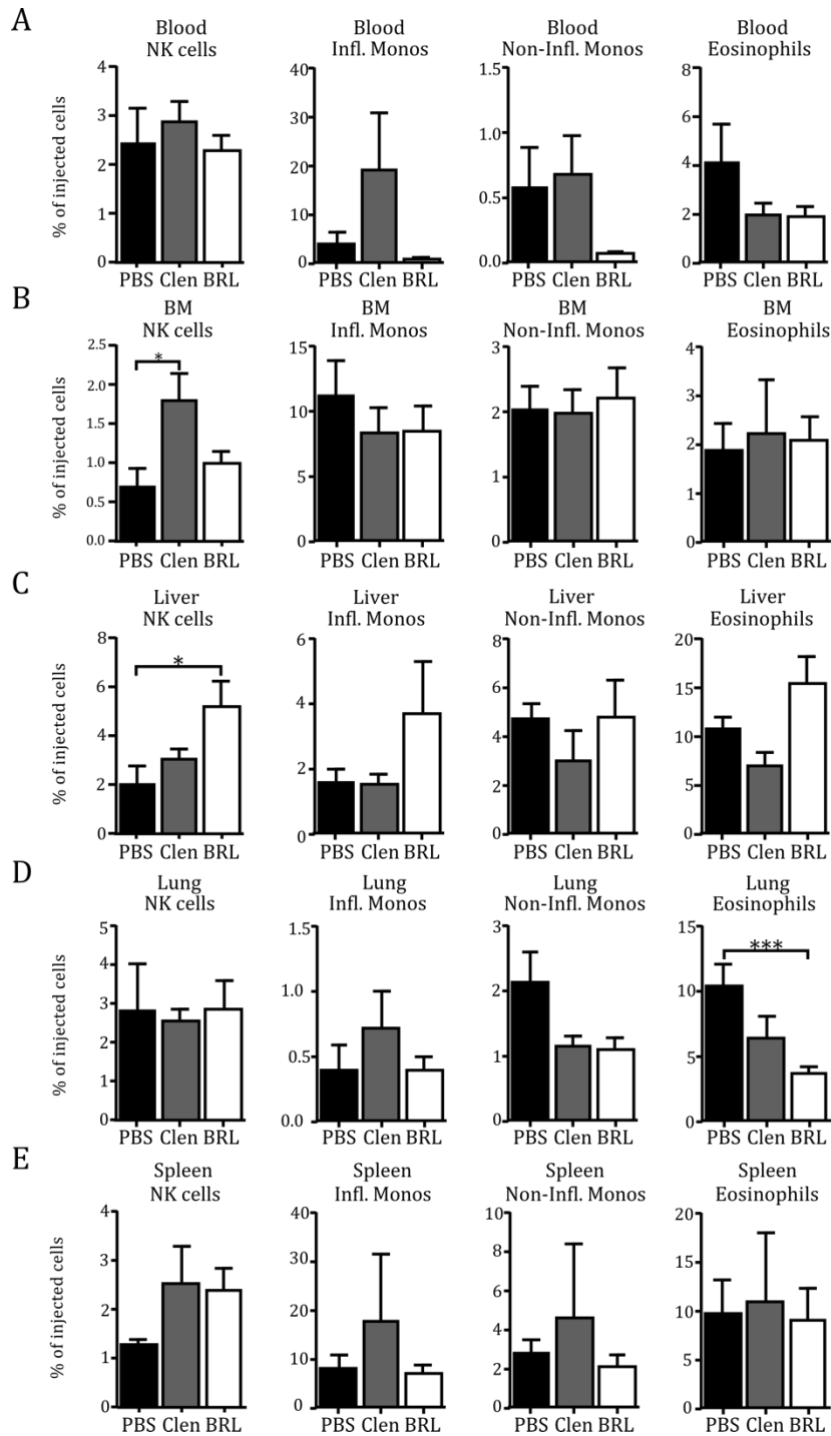


**Figure 6-7: Donor myeloid cell numbers in various organs upon adrenergic stimulation.**

**(A)** Donor myeloid cell counts in blood, 1 hr after transfer and 2 hrs after stimulation with Clenbuterol (Clen) or BRL37344 (BRL). n = 5-6, one-way ANOVA, Dunnett's test. **(B)** Donor myeloid cell counts in the bone marrow (BM), 1 hr after transfer and 2 hrs after stimulation with Clen or BRL. n = 5-6, one-way ANOVA, Dunnett's test. **(C)** Donor myeloid cell counts in the liver, 1 hr after transfer and 2 hrs after stimulation with Clen or BRL. n = 5-6, one-way ANOVA, Dunnett's test. **(D)** Donor myeloid cell counts in the lung, 1 hr after transfer and 2 hrs after stimulation with Clen or BRL. n = 5-6, one-way ANOVA, Dunnett's test. **(E)** Donor myeloid cell counts in the spleen, 1 hr after transfer and 2 hrs after stimulation with Clen or BRL. n = 5-6, one-way ANOVA, Dunnett's test. NK cells = Natural Killer cells, Infl. Monos = Inflammatory Monocytes, Non-Infl. Monos = Non-Inflammatory Monocytes.

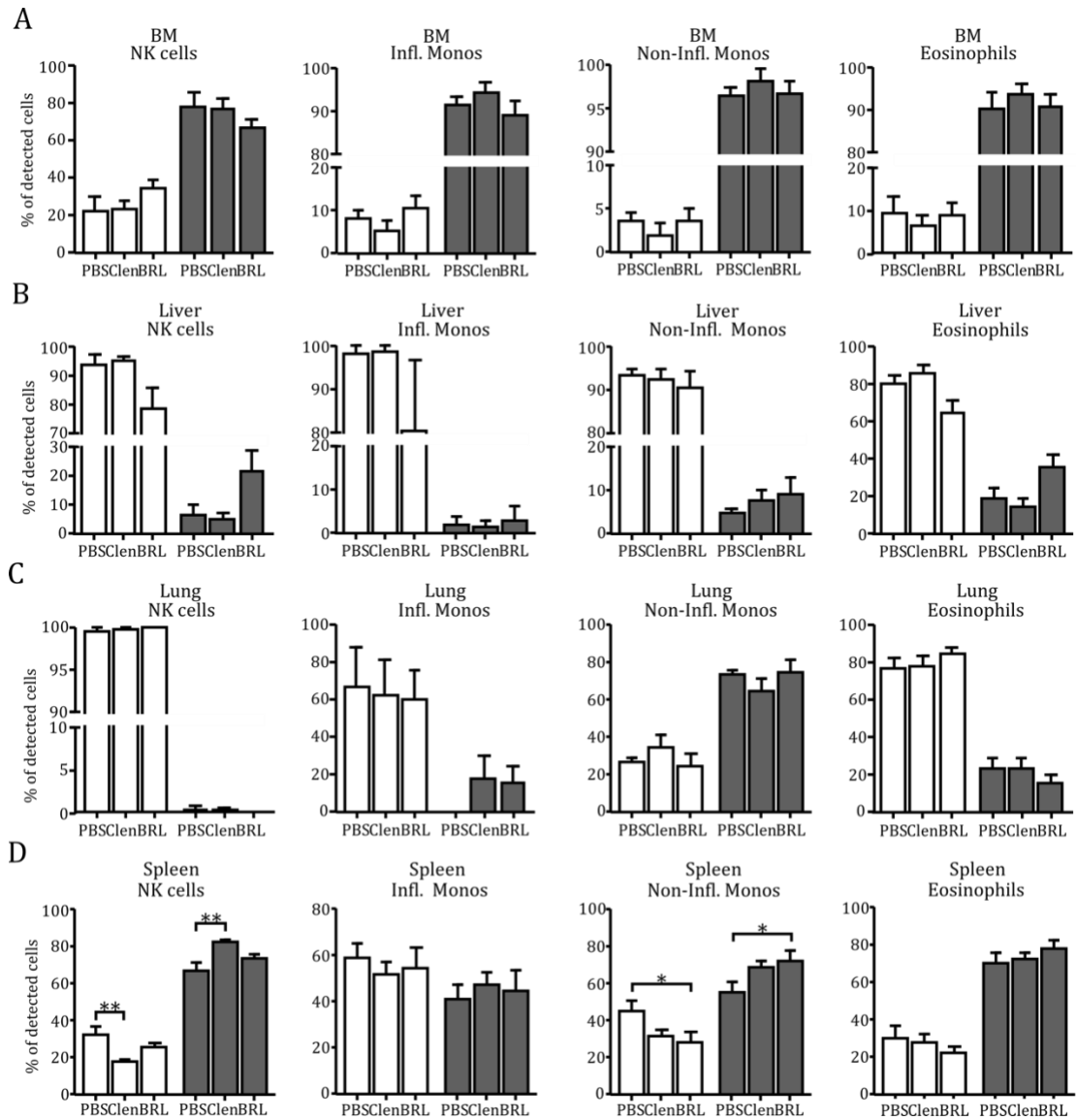


**Figure 6-8: Ratios of intra- and extravascular donor myeloid cells in various organs upon adrenergic stimulation.**

**(A)** Intravascular (white) and extravascular (gray) donor myeloid cells in the bone marrow (BM) as percentage of the detected cells in this organ.  $n = 5-6$ , two-way ANOVA, Dunnett's test. **(B)** Intravascular (white) and extravascular (gray) donor myeloid cells in the liver as percentage of the detected cells in this organ.  $n = 5-6$ , two-way ANOVA, Dunnett's test. **(C)** Intravascular (white) and extravascular (gray) donor myeloid cells in the lung as percentage of the detected cells in this organ.  $n = 5-6$ , two-way ANOVA, Dunnett's test. **(D)** Intravascular (white) and extravascular (gray) donor myeloid cells in the spleen as percentage of the detected cells in this organ.  $n = 5-6$ , two-way ANOVA, Dunnett's test. NK cells = Natural Killer cells, Infl. Monos = Inflammatory Monocytes, Non-Infl. Monos = Non-Inflammatory Monocytes.

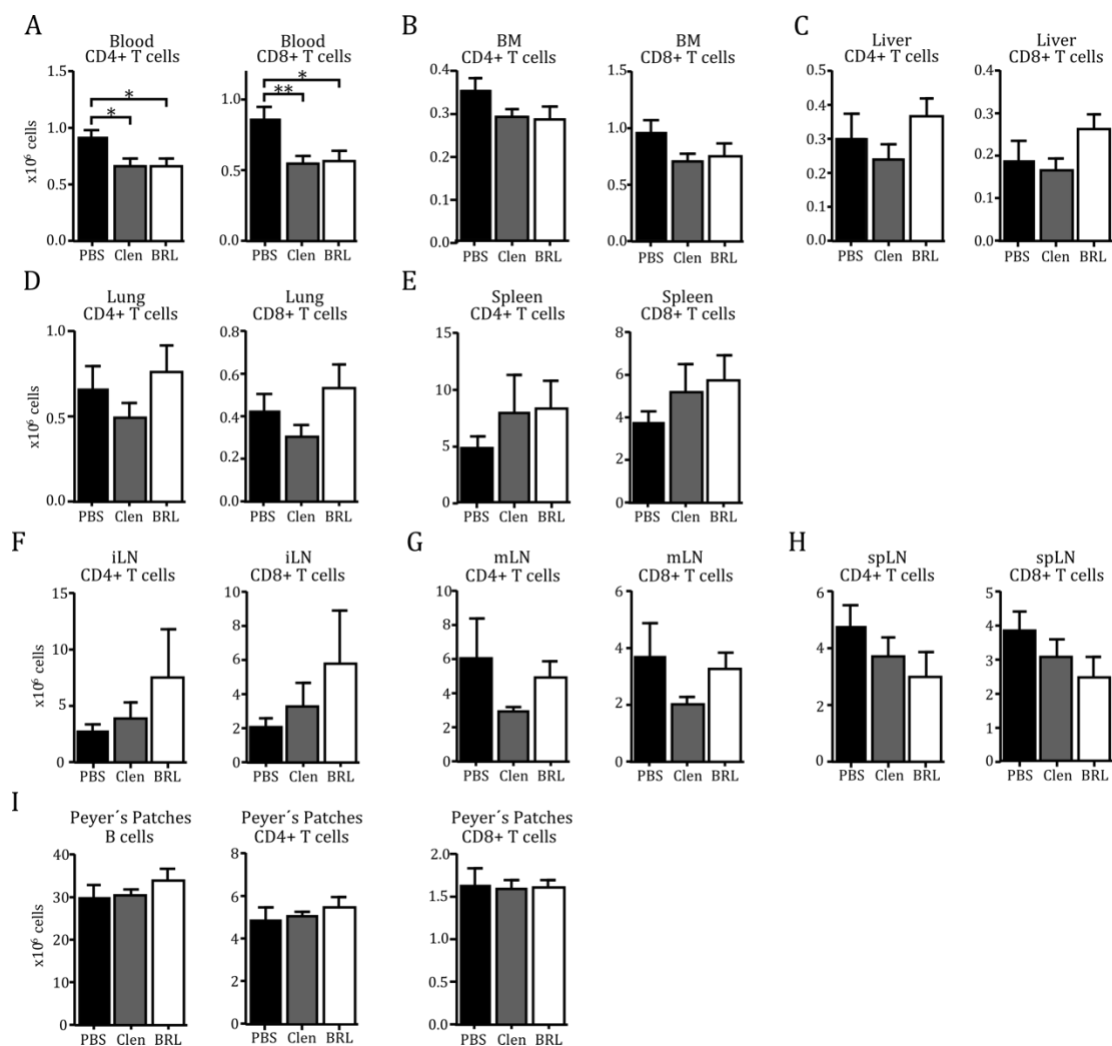


**Figure 6-9: Endogenous lymphoid cell numbers in various organs upon adrenergic stimulation.**

**(A)** Endogenous lymphoid cell counts in blood, 2 hrs after stimulation with Clenbuterol (Clen) or BRL37344 (BRL).  $n = 36-39$ , one-way ANOVA, Dunnett's test. **(B)** Endogenous lymphoid cell counts in the bone marrow (BM), 2 hrs after stimulation with Clen or BRL.  $n = 11-12$ , one-way ANOVA, Dunnett's test. **(C)** Endogenous lymphoid cell counts in the liver, 2 hrs after stimulation with Clen or BRL.  $n = 11-12$ , one-way ANOVA, Dunnett's test. **(D)** Endogenous lymphoid cell counts in the lung, 2 hrs after stimulation with Clen or BRL.  $n = 11-12$ , one-way ANOVA, Dunnett's test. **(E)** Endogenous lymphoid cell counts in the spleen, 2 hrs after stimulation with Clen or BRL.  $n = 5-6$ , one-way ANOVA, Dunnett's test. **(F)** Endogenous lymphoid cell counts in two iLNs, 2 hrs after stimulation with Clen or BRL.  $n = 8-9$ , one-way ANOVA, Dunnett's test. **(G)** Endogenous lymphoid cell counts in the mLN, 2 hrs after stimulation with Clen or BRL.  $n = 5-6$ , one-way ANOVA, Dunnett's test. **(H)** Endogenous lymphoid cell counts in two spLNs, 2 hrs after stimulation with Clen or BRL.  $n = 5-6$ , one-way ANOVA, Dunnett's test. **(I)** Endogenous lymphoid cell counts in pooled Peyer's Patches, 2 hrs after stimulation with Clen or BRL.  $n = 6$ , one-way ANOVA, Dunnett's test. iLN = inguinal lymph node, mLN = mesenteric lymph node, spLN = superficial parotid lymph node.

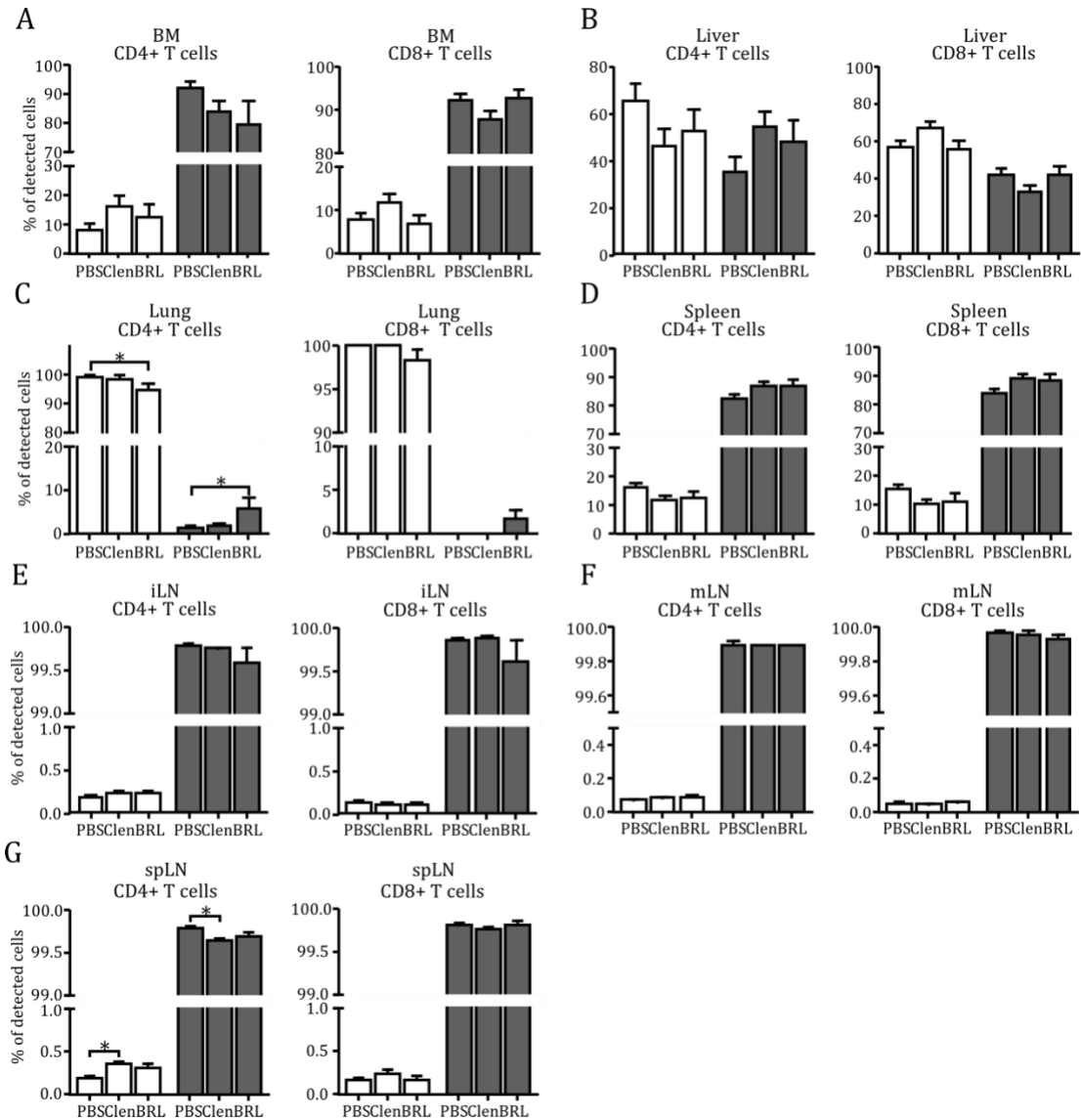


**Figure 6-10: Ratios of intra- and extravascular endogenous lymphoid cells in various organs upon adrenergic stimulation.**

**(A)** Intravascular (white) and extravascular (gray) endogenous lymphoid cells in the BM as percentage of the detected cells in this organ.  $n = 5-6$ , two-way ANOVA, Dunnett's test. **(B)** Intravascular (white) and extravascular (gray) endogenous lymphoid cells in the liver as percentage of the detected cells in this organ.  $n = 5-6$ , two-way ANOVA, Dunnett's test. **(C)** Intravascular (white) and extravascular (gray) endogenous lymphoid cells in the lung as percentage of the detected cells in this organ.  $n = 5-6$ , two-way ANOVA, Dunnett's test. **(D)** Intravascular (white) and extravascular (gray) endogenous lymphoid cells in the spleen as percentage of the detected cells in this organ.  $n = 5-6$ , two-way ANOVA, Dunnett's test. **(E)** Intravascular (white) and extravascular (gray) endogenous lymphoid cells in two iLN as percentage of the detected cells in this organ.  $n = 5-6$ , two-way ANOVA, Dunnett's test. **(F)** Intravascular (white) and extravascular (gray) endogenous lymphoid cells in the mLN as percentage of the detected cells in this organ.  $n = 5-6$ , two-way ANOVA, Dunnett's test. **(G)** Intravascular (white) and extravascular (gray) endogenous lymphoid cells in two spLNs as percentage of the detected cells in this organ.  $n = 5-6$ , two-way ANOVA, Dunnett's test. BM = bone marrow, iLN = inguinal lymph node, mLN = mesenteric lymph node, spLN = superficial parotid lymph node.

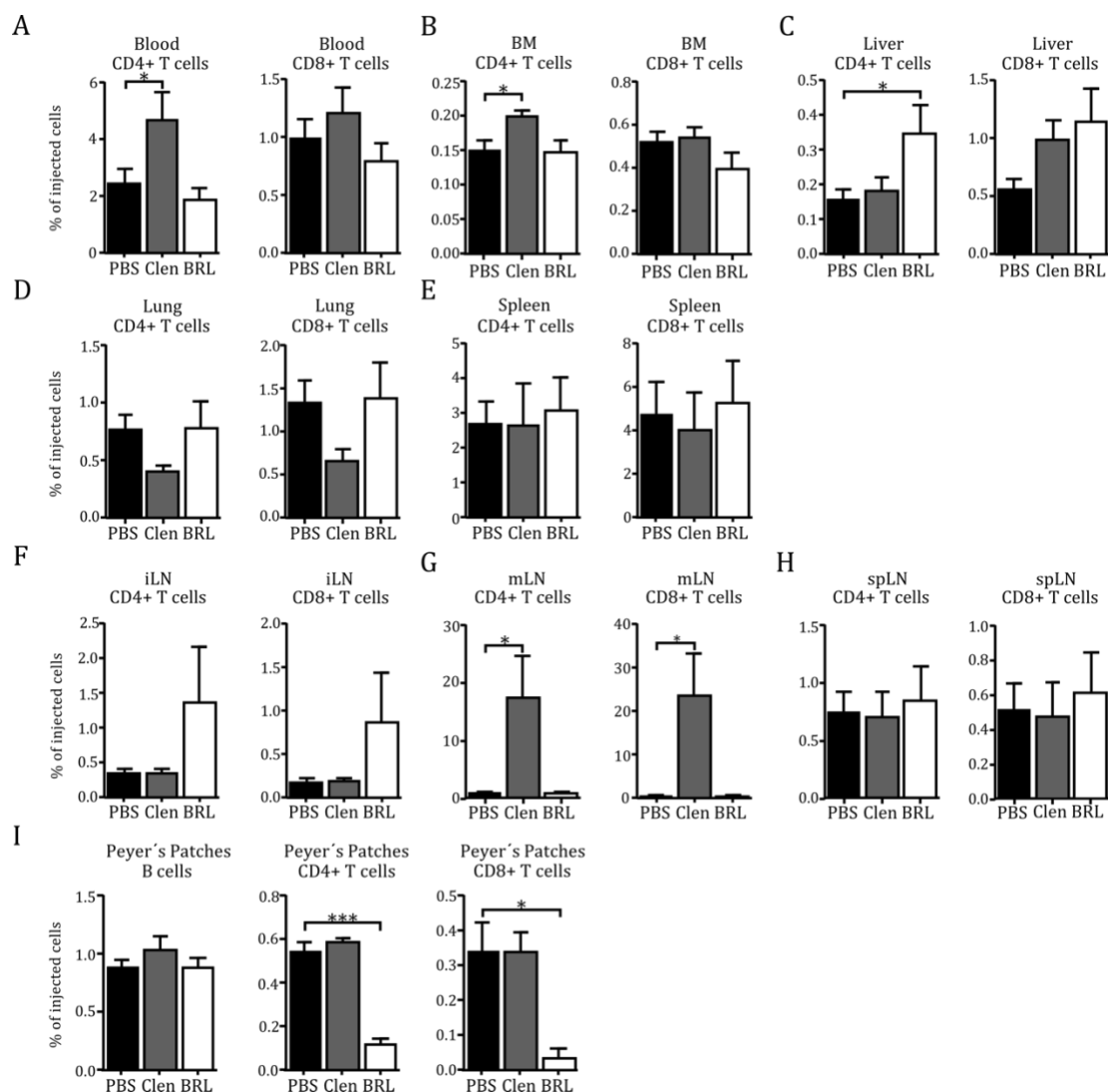


**Figure 6-11: Donor lymphoid cell numbers in various organs upon adrenergic stimulation.**

**(A)** Donor lymphoid cell counts in blood, 2 hrs after stimulation with Clenbuterol (Clen) or BRL37344 (BRL).  $n = 5-6$ , one-way ANOVA, Dunnett's test. **(B)** Donor lymphoid cell counts in the BM, 2 hrs after stimulation with Clen or BRL.  $n = 5-6$ , one-way ANOVA, Dunnett's test. **(C)** Donor lymphoid cell counts in the liver, 2 hrs after stimulation with Clen or BRL.  $n = 5-6$ , one-way ANOVA, Dunnett's test. **(D)** Donor lymphoid cell counts in the lung, 2 hrs after stimulation with Clen or BRL.  $n = 5-6$ , one-way ANOVA, Dunnett's test. **(E)** Donor lymphoid cell counts in the spleen, 2 hrs after stimulation with Clen or BRL.  $n = 5-6$ , one-way ANOVA, Dunnett's test. **(F)** Donor lymphoid cell counts in two iLNs, 2 hrs after stimulation with Clen or BRL.  $n = 5-6$ , one-way ANOVA, Dunnett's test. **(G)** Donor lymphoid cell counts in the mLN, 2 hrs after stimulation with Clen or BRL.  $n = 5-6$ , one-way ANOVA, Dunnett's test. **(H)** Donor lymphoid cell counts in two spLNs, 2 hrs after stimulation with Clen or BRL.  $n = 5-6$ , one-way ANOVA, Dunnett's test. **(I)** Donor lymphoid cell counts in pooled Peyer's Patches, 2 hrs after stimulation with Clen or BRL.  $n = 3$ , one-way ANOVA, Dunnett's test. BM = bone marrow, iLN = inguinal lymph node, mLN = mesenteric lymph node, spLN = superficial parotid lymph node.

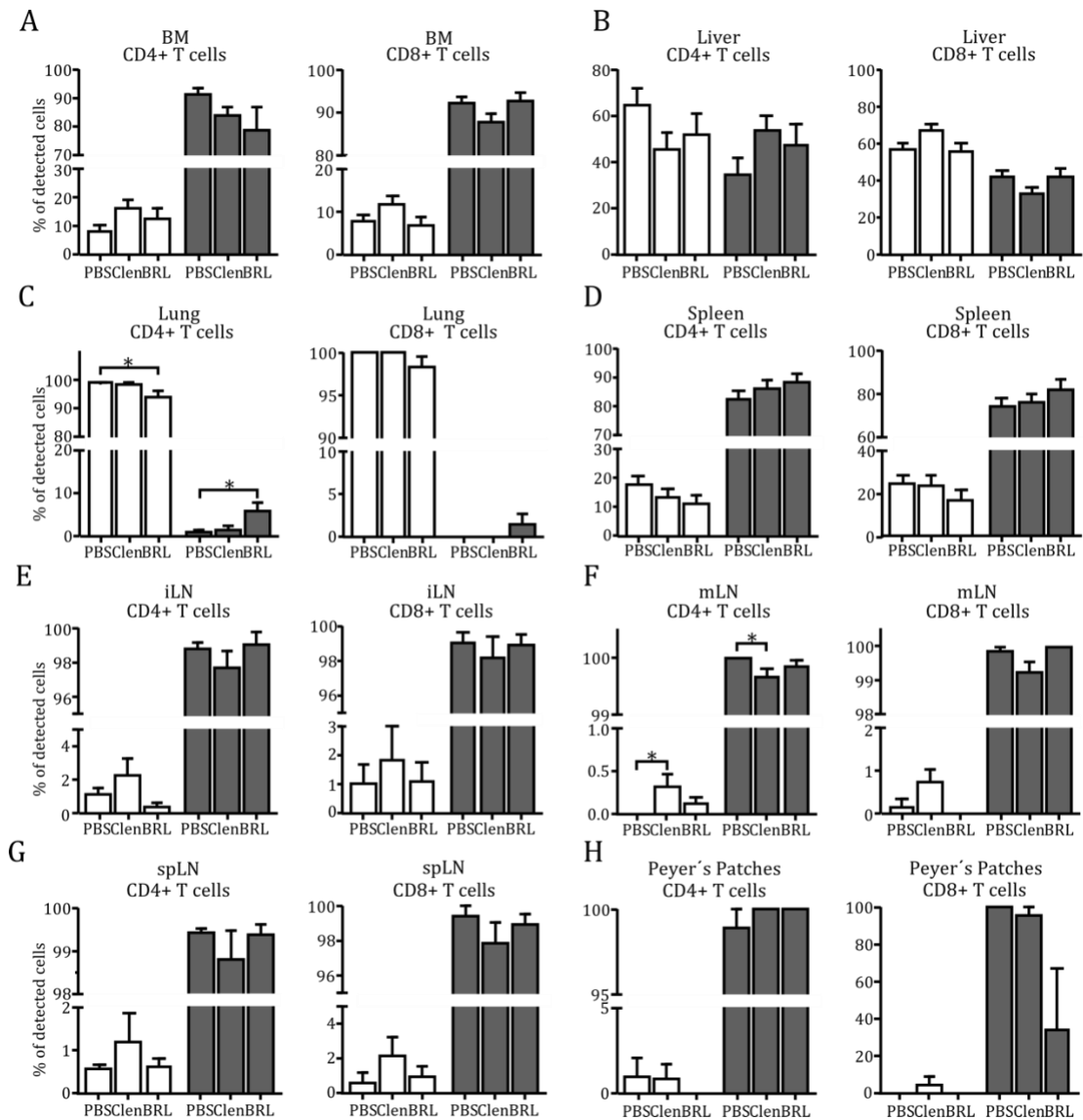


**Figure 6-12: Ratios of intra- and extravascular donor lymphoid cells in various organs upon adrenergic stimulation.**

**(A)** Intravascular (white) and extravascular (gray) donor lymphoid cells in the BM as percentage of the detected cells in this organ.  $n = 5-6$ , two-way ANOVA, Dunnett's test. **(B)** Intravascular (white) and extravascular (gray) donor lymphoid cells in the liver as percentage of the detected cells in this organ.  $n = 5-6$ , two-way ANOVA, Dunnett's test. **(C)** Intravascular (white) and extravascular (gray) donor lymphoid cells in the lung as percentage of the detected cells in this organ.  $n = 5-6$ , two-way ANOVA, Dunnett's test. **(D)** Intravascular (white) and extravascular (gray) donor lymphoid cells in the spleen as percentage of the detected cells in this organ.  $n = 5-6$ , two-way ANOVA, Dunnett's test. **(E)** Intravascular (white) and extravascular (gray) donor lymphoid cells in two iLNs as percentage of the detected cells in this organ.  $n = 5-6$ , two-way ANOVA, Dunnett's test. **(F)** Intravascular (white) and extravascular (gray) donor lymphoid cells in the mLN as percentage of the detected cells in this organ.  $n = 5-6$ , two-way ANOVA, Dunnett's test. **(G)** Intravascular (white) and extravascular (gray) donor lymphoid cells in two spLNs as percentage of the detected cells in this organ.  $n = 5-6$ , two-way ANOVA, Dunnett's test. **(H)** Intravascular (white) and extravascular (gray) donor lymphoid cells in pooled Peyer's Patches as percentage of the detected cells in this organ.  $n = 3$ , two-way ANOVA, Dunnett's test. BM = bone marrow, iLN = inguinal lymph node, mLN = mesenteric lymph node, spLN = superficial parotid lymph node.

Clen-induced effects on cell numbers	Endo	Blood	BM	Liver	Lung	LN	Spleen	Peyer's Patches
	Donor							
■ increased	CD4+	■	■		■	■		
■ decreased	CD8+	■				■		
□ no change	NK	■	■			■		
■ not tested	Infl. Monos					■		
	Non-Infl. Monos					■	■	■
	Eos	■			■	■	■	■

**Figure 6-13: Summary of cell distributions upon Clenbuterol administration.**

Increased, decreased or unchanged endogenous and donor cell numbers of CD4+ T cells, CD8+ T cells, NK cells, inflammatory monocytes, non-inflammatory monocytes and eosinophils in various organs 2 hrs after injection of Clenbuterol (Clen). BM = bone marrow, LN = lymph nodes, Endo = endogenous, CD4+ = CD4+ T cells, CD8+ = CD8+ T cells, NK = Natural Killer cells, Infl. Monos = Inflammatory Monocytes, Non-Infl. Monos = Non-Inflammatory Monocytes, Eos = Eosinophils.

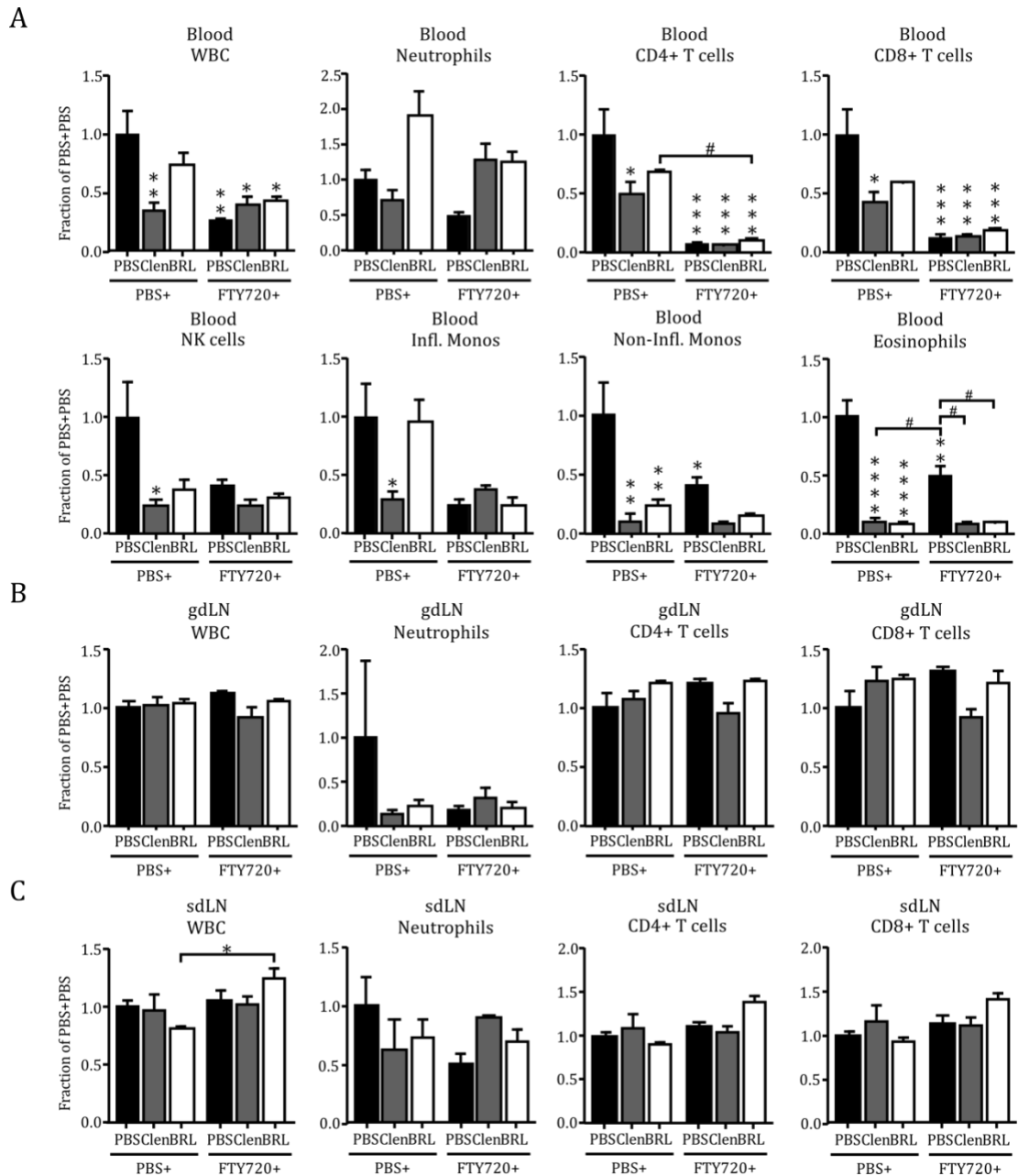


**Figure 6-14: Leukocyte numbers in blood and lymph nodes upon egress block.**

**(A)** Fraction of leukocytes in blood after egress block with FTY720 and adrenergic stimulation. WT mice were intraperitoneally injected with PBS or FTY720 and directly afterwards with PBS, Clen or BRL. At 12 pm blood was harvested and processed for flow cytometry.  $n = 3$ , two-way ANOVA, Tukey's test; \* test against PBS+PBS, # test against indicated group. **(B)** Fraction of leukocytes in gut-draining lymph node after egress block with FTY720 and adrenergic stimulation. WT mice were intraperitoneally injected with PBS or FTY720 and directly afterwards with PBS, Clen or BRL. At 12 pm, the mesenteric lymph node was harvested and processed for flow cytometry  $n = 3$ , two-way ANOVA, Tukey's test. **(C)** Fraction of leukocytes in skin-draining lymph nodes after egress block with FTY720 and adrenergic stimulation. WT mice were intraperitoneally injected with PBS or FTY720 and directly afterwards with PBS, Clen or BRL. At 12 pm, eight sdLNs were harvested, pooled and processed for flow cytometry.  $n = 3$ , two-way ANOVA, Tukey's test. gdLN = gut-draining lymph node, sdLN = skin-draining lymph node, WBC = White blood cells, NK cells = Natural Killer cells, Infl. Monos = Inflammatory Monocytes, Non-Infl. Monos = Non-Inflammatory Monocytes.

## 6.2 Affidavit

Weber, Jasmin  
Großhaderner Str. 9  
82152 Pnalegg-Martinsried  
Germany

I hereby declare, that the submitted thesis entitled

### **Control of Leukocyte Trafficking by the Sympathetic Nervous System**

is my own work. I have only used the sources indicated and have not made unauthorized use of services and a third party. Where the work of others has been quoted or reproduced, the source is always given. I further declare that the submitted thesis or parts thereof have not been presented as part of an examination degree to any other university.

Munich, 02.03.21

*Place, date*

Jasmin Weber

*Signature doctoral candidate*

### 6.3 List of publications

- 01/2019 Ince LM, **Weber J**, Scheiermann C: Control of Leukocyte Trafficking by Stress-Associated Hormones, *Frontiers in Immunology*, 11(9): 3143
- 12/2018 He W, Holtkamp S, Hergenhan SM, Kraus K, de Juan A, **Weber J**, (...) Scheiermann C: Circadian Expression of Migratory Factors Establishes Lineage-Specific Signatures that Guide the Homing of Leukocyte Subsets to Tissues, *Immunity*, 49(6): 1175-1190
- 09/2018 Moretti FA, Klapproth S, Ruppert R, Margraf A, **Weber J**, (...) Moser M: Differential requirement of kindlin-3 for T cell progenitor homing to the non-vascularized and vascularized thymus, *Elife*, 7: e35816

## **6.4 Confirmation of congruency between printed and electronic version of the doctoral thesis**

Weber, Jasmin  
Großhaderner Str. 9  
82152 Planegg-Martinsried  
Germany

I hereby declare that the electronic version of the submitted thesis entitled

### **Control of Leukocyte Trafficking by the Sympathetic Nervous System**

is congruent with the printed version, both in content and format.

Munich, 02.03.21

*Place, date*

Jasmin Weber

*Signature doctoral candidate*